Université de Montréal

Synthèse en phase solide de pyrrolo[3,2-e][1,4]diazépin-2-ones modulateurs du système urotensinergétique

par

Julien Dufour-Gallant

Département de Chimie

Faculté des arts et des sciences

Université de Montréal

Mémoire présenté à la Faculté des études supérieures et postdoctorales en vue de l'obtention du grade de maître ès sciences (M.Sc.) en chimie

Avril, 2016

Résumé

Les pyrrolodiazépinones ont des activités biologiques intéressantes sur différents récepteurs biologiques, ce qui en font une cible de choix pour développer de nouvelles petites molécules biologiquement actives. Une méthodologie en solution a été développée pour synthétiser des pyrrolo[3,2-*e*][1,4]diazépin-2-ones, qui utilise la réaction de Pictet-Spengler pour former le cycle diazépinone, comme réaction clé. Il a été démontré que le pyrrolo[3,2-*e*][1,4]diazépin-2-one mime un tour-γ inverse par l'analyse de cristaux par rayon X. Cette méthodologie a été transposée sur trois types de support, soit la résine de Merrifield, de Wang et un support soluble (TAP).

Le système urotensinergétique joue un rôle dans certaines pathologies du système cardiovasculaire, comme l'hypertension artérielle, l'insuffisance cardiaque et l'athérosclérose. Le système urotensinergétique est exprimé dans le système circulatoire, extractoire et le système nerveux central et comprend l'UII, l'URP et le récepteur UT. L'UII et l'URP humains sont composés respectivement des séquences d'acides aminés : H-Glu-Thr-Pro-Asp-*c*[Cys-Phe-Trp-Lys-Tyr-Cys]-Val-OH et H-Ala-*c*[Cys-Phe-Trp-Lys-Tyr-Cys]-Val-OH. L'UII est le peptide vasoconstricteur le plus puissant connu à ce jour, dont l'URP est son isoforme. Les deux peptides ont des effets biologiques différents et on peut supposer qu'ils jouent un rôle distinct dans certaines pathologies. Il a été démontré que la partie active de l'UII est composée du tripeptide : Trp-Lys-Tyr. Dans l'URP, il a été démontré que ce tripeptide forme un tour-γ inverse, ce qui fait du récepteur UT une bonne cible biologique pour tester une librairie de pyrrolo[3,2-*e*][1,4]diazépin-2-ones, reprenant le tripeptide Trp-Lys-Tyr. Dernièrement, l'équipe du professeur David Chatenet a mis au point un peptide, l'urocontrin en remplaçant le segment Trp par un groupement biphénylalanine, qui a démontré un comportement spécifique comme antagoniste du récepteur UT.

La Librairie de pyrrolo[3,2-*e*][1,4]diazépin-2-ones est basée sur la séquence Trp-Lys-Tyr de l'UII et de l'URP et de la séquence Trp-Lys-Bip de l'urocontrin. La synthèse de la librairie est faite sur la résine de Wang. La chaîne latérale de Tyr est mimée en utilisant la tyramine, Lys et Orn sont utilisés et la chaîne latérale de Trp a été reproduite

en utilisant le biphényle (comme dans l'urocontrin), le 1-naphthyle et le 2-naphthyle, sont introduits en employant les aldéhydes respectifs dans la réaction de Pictet-Spengler, ce qui donne les pyrrolo[3,2-*e*][1,4]diazépin-2-ones insaturés et les saturés *S*- et *R*-.

L'évaluation de l'activité biologique des pyrrolo[3,2-*e*][1,4]diazépin-2-ones obtenues sur le récepteur UT se fait par des tests *in vitro* et *ex vivo*. Les tests *in vitro* consistent en un essai de liaisons sur des cellules CHO exprimant le récepteur UT en employant hUII-^{125}I, comme contrôle radiomarqé. Les tests ex vivo sont effectués sur des aortes de rats pour mesurer la capacité à induire des contractions ou de moduler les contractions induites par hUII et URP.

Certains *R*-pyrrolo[3,2-*e*][1,4]diazépin-2-ones causent une réduction de 50% du signal radioactivité du hUII-^{125}I. Les pyrrolo[3,2-*e*][1,4]diazépin-2-ones ne montrent guère d'activité *ex vivo*, mais ils ont la capacité de moduler les contractions induites par l'hUII et l'URP. Par exemple, l'analogue Lys *R*-saturé avec le biphényle inhibe toutes les contractions de l'aorte à 14 μM avec un pKb de 5,54 à 4 μM, sans influencer les contractions de l'aorte induites par l'URP. Les pyrrolo[3,2-*e*][1,4]diazépin-2-ones ont une sélectivité pour le système urotensinergétique et sont inactifs sur le récepteur de l'endotheline-1. Les pyrrolo[3,2-*e*][1,4]diazépin-2-ones sont les premières petites molécules qui peuvent moduler l'activité biologique de l'UII et URP et offrir un potentiel intéressant comme outil pour étudier le système urotensinergétique.

Mots-clés : Mimes peptidiques, Structure privilégiée, Pyrrolo[3,2-*e*][1,4]diazépin-2-one, Tour-γ inverse, Chimiothèque, Phase solide, Résine de Wang, Urotensine II, URP, Système urotensinergétique, *in vitro*, *ex vivo*.

Abstract

The pyrrolodiazepinones have interesting biological activities on various biological receptors, which makes them a prime target for developing new biologically active small molecules. A methodology in solution had been developed for synthesizing pyrrolo[3,2-*e*][1,4]diazepin-2-ones, which utilized the Pictet-Spengler condensation as the key reaction to form the diazepinone ring. Pyrrolo[3,2-*e*][1,4]diazepin-2-ones were found to mimic an inverse γ-turn conformation by X-ray crystallographic analysis. The methodology was subsequently implemented on three types of support: Merrifield resin, Wang resin and the soluble TAP support.

The urotensinergic system plays a role in certain diseases of the cardiovascular system, such as hypertension, heart failure and atherosclerosis. The urotensinergic system is expressed in the circulatory system, excretory and central nervous systems and includes the endogenous ligands urotensin II (UII) and urotensin II-related peptide (URP), and the urotensin receptor UT. The ligands UII and human URP are composed of the respective amino acid sequences: H-Glu-Thr-Pro-Asp-*c*[Cys-Phe-Trp-Lys-Tyr-Cys]-Val-OH and H-Ala-*c*[Cys-Phe-Lys-Tyr-Trp-Cys]-Val-OH. The peptide UII is the most potent vasoconstrictor known to date. The two peptides have different biological effects and may exhibit distinct roles in certain diseases. Their common Trp-Lys-Tyr sequence is believed to play an important role in the activity of UII and URP, and has been suggested to adopt an inverse γ-turn conformation. Notably, the laboratory of Professor David Chatenet developed the UT receptor antagonist peptide urocontrin by replacing the Trp residue by biphenylalanine (Bip) in URP. A library of pyrrolo[3,2-*e*][1,4]diazepin-2-one analogs was thus designed to mimic the inverse γ-turn sequence and targeted against UT.

The pyrrolo[3,2-*e*][1,4]diazepin-2-one library was designed based on the Trp-Lys-Tyr sequence of UII and URP, and Trp-Lys-Bip sequence of urocontrin. The synthesis of the pyrrolo[3,2-*e*][1,4]diazepin-2-one library was achieved on Wang resin. The side chain of Tyr was mimicked using tyramine, Lys and Orn were used as the basic amino acid component, and the side chain of Trp was replicated using biphenyl (as in urocontrin) 1-naphthyl and 2-naphthyl groups that were introduced by employing their respective

aldehydes in a Pictet-Spengler reaction, which furnished unsaturated and saturated *S*- and *R*-pyrrolo[3,2-*e*][1,4]diazepin-2-ones.

Evaluation of the biological activity of the pyrrolo[3,2-*e*][1,4]diazepin-2-ones on the UT receptor was performed *in vitro* and *ex vivo*. Tests *in vitro* measured binding in CHO-cells which expressed UT by employing hUII-^{125}I as radiolabeled control. In rat aorta, *ex vivo* tests measured capacity to induce contraction, or modulate the contractions induced by hUII and URP.

Certain *R*-pyrrolo[3,2-*e*][1,4]diazepin-2-ones caused an up to 50% reduction of the radioactive signal of hUII-^{125}I. Pyrrolo[3,2-*e*][1,4]diazepin-2-ones exhibited little activity *ex vivo*; however, they modulated contractions induced by hUII and URP. For example, the saturated *R*-analog possessing lysine and a biphenyl side chain inhibited completely hUII-induced contractions of the aorta at 14 μM with a pKb of 5.54 at 4 μM, without influencing URP-induced contractions. Pyrrolo[3,2-*e*][1,4]diazepin-2-ones were selective for the urotensinergic system and inactive on the related receptor endothelin-1. Pyrrolo[3,2-*e*][1,4]diazepin-2-ones represent the first small molecules that can differently modulate the biological activities of UII and URP, and offer interesting potential as tools for studying the urotensinergic system.

Keywords : Peptide mimic, Privileged structure, Pyrrolo[3,2-*e*][1,4]diazepin-2-one, Reverse γ-turn, Chemical library, Wang resin, Urotensin II, URP, Urotensinergic system, *in vitro*, *ex vivo*.

Note

Ce mémoire se consacra principalement sur l'article publié dans le *Journal of Medicinal Chemistry* et non sur tout le cheminement pour en venir à cette publication. En se focalisant sur la synthèse de pyrrolo[3,2-*e*][1,4]diazépin-2-ones modulateurs du système urotensinergétique que j'ai fait sur la résine de Wang et des essaies biologiques in vitro et ex vivo que j'ai effectué.

Table de matières

Liste des Figures

Liste des Schémas

Liste des tableaux

Abréviation

Ac	Acétyle
ACE	Enzyme de conversion de l'angiotensine
ADP	Adénosine diphosphate
ADN	Acide désoxyribonucléique
Ar	Aryle
Bip	Biphénylalanine
Bn	Benzyle
Boc	*tert*-Butyloxycarbonyle
BTC	(bis(trichlorométhyl) carbonate
Btz	Benzothiazole
CCK	Cholécystokinine
CCM	Chromatographie sur couche mince
δ	Déplacement chimique en ppm en RMN
CHO	Cellule d'ovaire de hamster géant
DCE	1,2-Dichloroéthane
DCM	Dichlorométhane
DIBAL	Hydrure de diisobutylaluminium
DIC	*N,N'*-Diisopropylcarbodiimide
DIEA	*N,N*-Diisopropyléthylamine
DMSO	Diméthylsulfoxyde

DMF	*N*,*N*-Diméthylformamide
DVB	Divinylbenzène
EC_{50}	Concentration efficace médiane
EL	Boucle extracellulaire
Et	Éthyle
ET-1	Endotheline-1
éq	Équivalent
FA	Formic acid
Fmoc	Fluorénylméthyloxycarbonyle
GABA	Acide γ-aminobutyrique
hET-1	Endotheline-1 humaine
HMQC	*Heteronuclear Multiple-Quantum Correlation*
HOBt	Hydroxybenzotriazole
HPLC	*High performance liquid chromatography*
HRMS	*High resolution mass spectrometry*
hUII	Urotensine II humain
IC_{50}	Concentration inhibitrice médiane
IR	Infrarouge
LCMS	*Liquid chromatography mass spectroscopy*
LFA	Antigène-1 associé à la fonction du lymphocyte
Me	Méthyle

MHz	Mégahertz
mRNA	Acide ribonucléique messager
NMR	*Nuclear magnetic resonance*
NOESY	*Nuclear overhausser effect spectroscopy*
PARP-1	Poly(ADP-ribose)polymérase-1
Pen	*β*,*β*-dimethylcystéine
Pep	phényléthynyl)phénylalanine
PhF	9-(9-Phényl)fluorenyle
ppm	Partie par million
PIFA	Iodure de phényle (III) bis(trifluoroacétate)
RCPG	Récepteurs couplés aux protéines G
RMN	Résonnance magnétique nucléaire
ROESY	*Rotating frame nuclear Overhauser effect spectroscopy*
RP	*Reverse phase*
R*t*	*Retention time*
TAP	Tétraarylphosphonium
THF	Tétrahydrofuranne
TFA	Acide tétrafluroacétique
TLC	*Thin layer chromatography*
TMR	Récepteur transmembranaire
TM	Transmembranaire
p-TsOH	Acide p-toluènesulfonique

t_R	retention time
UII	Urotensine II
URP	UII *related peptide*
UT	Récepteur urotensine II
VIH	Virus de l'immudéficience humaine
VIH-RT	Virus de l'immudéficience humaine rétrotranscriptase

Remerciement

Tout d'abord, je tiens à remercier particulièrement mon directeur de recherche, le Professeur William D. Lubell de m'avoir donné la possibilité de me joindre à son magnifique groupe de recherche, de m'avoir confié ce projet de recherche et de m'avoir donné la possibilité de poursuivre ce projet suite à des premiers composés inactifs sur le système urotensinergétique et de le pousser jusqu'à des composés actifs, qui sont des mimes de l'urocontrin. En poussant ce projet, cela m'a permis de développer les premières petites molécules modulatrices du système urotensinergétique. Je le remercie pour tous ses judicieux conseils et pour nos échanges.

Je tiens à remercier mon collaborateur le Professeur David Chatenet (INRS/Institut Armand-Frappier) et son équipe, plus particulièrement Myriam Létourneau pour m'avoir montré les procédures pour effectuer les tests biologiques. Je tiens également à remercier le Professeur David Chatenet pour m'avoir donné la chance de vivre mes premières expériences en pharmacologie en testant moi-même les pyrrolo[3,2-e][1.4]diazépin-2-ones me permettant ainsi de me familiariser avec de nouvelles techniques.

Je remercie également Dr Nicolas Boutard pour l'encadrement au début de ce projet, pour tout ce qu'il m'a montré sur la synthèse en phase solide ainsi que la méthodologie se rapportant à ce projet et pour notre collaboration même si les composés étaient inactifs.

Je remercie Dre Carine Bourget pour l'accueil dans le groupe, l'aide apportée lors de la synthèse du matériel de départ, dont la protection de l'hydroxyproline avec le groupement 9-(9-phénylfluorényle) et pour les révisions de mon manuscrit. Je remercie ma collègue de laboratoire Aurélie Dörr de m'avoir enduré tout au long de ma maitrise dans le laboratoire qu'on partageait toutes ses années, pour nos échanges, son aide et pour la révision de mon manuscrit.

Je remercie l'équipe du centre régional de spectrométrie de masse (Dre Alexandra Fürtos, Karine Venne et Marie-Christine Tang) pour toutes les analyses HRMS, du centre

régional de RMN (Dr Minh Tan Phan Viet, Sylvie Bilodeau, Antoine Hamel et Cédric Malveau) pour toutes les analyses des pyrrolodiazépinones finaux aux 700 Mhz et du laboratoire de diffraction des rayons X (Françine Bélanger) pour son aide pour la cristallisation et pour les analyses aux rayons X du cristal.

Je remercie également la faculté des études supérieures et postdoctorales (FESP) pour le soutien financier.

Je remercie affectueusement toute ma famille et tous mes amis proches pour leur soutien indéfectible.

1.CHAPITRE 1 : Introduction

1.1. Tours et mimes peptidiques

1.1.1. Tours peptidiques

Les protéines et les peptides jouent des rôles essentiels dans l'homéostasie des organismes vivants. Composés d'une série d'acides aminés liés entre eux par des liaisons amides, les protéines et les peptides adoptent des conformations très spécifiques. Ils peuvent adopter diverses conformations soient des structures secondaires engendrées par les chaînes peptidiques lorsqu'elles se replient ou tournent pour économiser de l'énergie en formant des ponts d'hydrogènes, soit les hélices α, les feuillets β et les tours (α, β et γ).[1-6] L'étude des conformations de certaines protéines connues par rayon X a permis de déterminer les intervalles de valeurs des angles dièdres (ψ et ϕ) des différents types de tours, pour être considéré comme un « tour idéal » (Tableau 1.1).[1, 3, 5]

Figure 1.1 : Représentation des différents tours peptidiques.

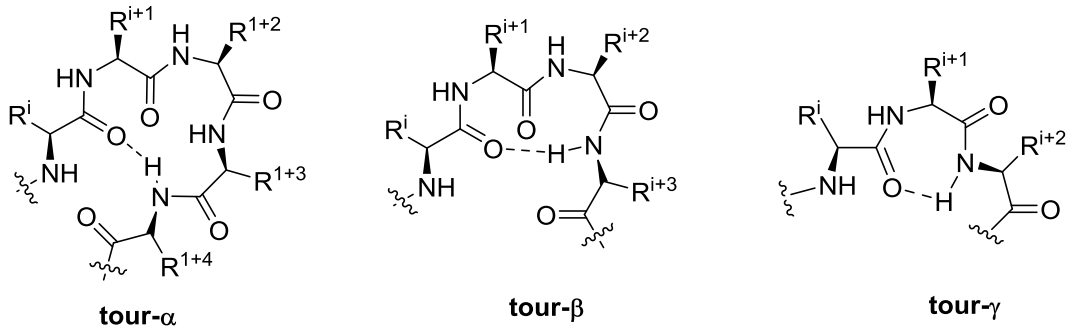

Tableau 1.1 : Résultats des angles dièdres d'un tour-γ idéal et tour-γ inverse idéal, du 1-4-diazépinone **1** et du pyrrolodiazépin-2-one **2**.

#	Ψ	Φ
tour-γ[1]	-60 à 70°	70 à 85°
tour-γ inverse ideal[1]	60° à 70°	–70° à –85°
1,4-diazépinones (**1**)[7]	67°	–83°
pyrrolodiazépin-2-one (**2**)[8]	72°	–93°

Les tours-γ sont les moins communs des tours peptidiques et sont composés d'un cycle peptidique à sept membres formés par un pont d'hydrogène avec le carbonyle du

résidu de l'acide aminé *i* et l'amide NH du résidu de l'acide aminé *i*+2, donc le tour-γ parcourt trois résidus (Figure 1.1). Les angles dièdres ϕ et ψ du résidu *i*+1 pour le tour-γ sont entre 70 et 85° et –60 et –70° respectivement et pour le tour-γ inverse entre –70 et –85° et 60 et 70° (Tableau 1.1).[1] Les tours inverses sont décrits comme étant une image miroir du tour correspondant, mais tout en conservant la chiralité du C^{α}.[5, 9] Selon l'orientation de la chaîne latérale du résidu *i*+1 est en position axiale ou équatoriale, le tour est décrit comme étant classique ou inverse respectivement.[10] Les tours inverses sont très abondants dans les protéines globulaires et se situent généralement à la surface.

La géométrie du tour-γ joue un rôle dans les interactions avec certains récepteurs biologiques et dans la reconnaissance moléculaire des processus biologiques protéine-protéine, d'interaction protéine-ADN et de repliement des peptides.[11, 12] Pour illustrer le rôle essentiel de la conformation du tour-γ dans l'activité biologique des peptides et dans les bons fonctionnements des organismes, voici quelques peptides endogènes, qui forme un tour-γ dans leur conformation biologiquement active : l'urotensine II[13, 14], l'angiotensine[15], la vasopressine[16, 17], la bradykinine[18], la somatostatine[19] et l'ocytocine[20]. Le tour-γ présent dans la vitronectine contribue à la reconnaissance spécifique du récepteur intégrine αvβ3 qui joue un rôle dans l'adhésion cellulaire tumorale, l'angiogenèse et l'ostéoporose.[12] Les tours-γ inverse ont eux aussi leurs activités biologiques propres. Les études de relations de structure-activité de plusieurs peptides, qui interagissent avec différents récepteurs couplés aux protéines G (RCPG), suggèrent que ses peptides prennent une conformation de tour inverse lorsqu'ils se lient aux récepteurs.[21] Il a été démontré que certains peptides cycliques avec un tour-γ inverse ont la propriété d'agir comme antagoniste de plusieurs RCPG.[21, 22]

1.1.2. Mimes peptidiques

En général, les peptides peuvent être utilisés comme drogue, mais leurs applications sont limitées, car ils ont souvent une faible biodisponibilité due à leur sensibilité à la protéolyse lors de l'administration orale.[23] Afin de résoudre ce problème, des mimes peptidiques ont été conçus reproduisant les angles dièdres des tours

peptidiques, offrant une plus grande stabilité métabolique et ayant des activités similaires aux peptides naturels.[1, 16, 24, 25]

Certains mimes peptidiques ont la capacité de reproduire les angles dièdres des tours peptidiques.[1, 16, 24, 25] Dans certains cas, comme les aza-peptides, les lactames, et les N-amino-imidazolin-2-ones,[26, 27] ils sont intégrés directement dans le peptide original. Dans d'autres cas, comme les diazépinones et les benzodiazépinones,[26-31]une petite molécule peut servir à simuler une structure secondaire du peptide. Ces modifications permettent d'améliorer grandement l'efficacité pharmacologique du peptide initiale. Les mimes peptidiques peuvent être utilisés directement comme agent thérapeutique en remplaçant le peptide et sont formés principalement à partir d'une structure dite « privilégiée ».[32]

Dans le passé, l'étude par rayon X d'un cristal du 1,4-diazepin-2-one **1** a permis de confirmer que les valeurs des angles dièdres mesurés correspondent aux valeurs d'un tour-γ inverse idéal (Tableau 1.1).[7] Malgré l'ajout de différents substituants, le 1,4-diazepin-2-one garde la conformation d'un tour-γ inverse. Les études aux rayons X des cristaux du pyrrolo[3,2-*e*][1,4]diazépin-2-one **2** (Figure 1.2)[8], et du pyrrolo[1,2-*d*][1,4]benzodiazépin-6-one[33] ont démontré que le résidu de l'acide α-aminé du diazépinone a des angles dièdres qui correspondent aux valeurs d'un tour-γ inverse. La conformation du tour-γ inverse du pyrrolo[3,2-*e*][1,4]diazépin-2-one et du pyrrolobenzodiazépinone en font des candidats idéals pour le mimétisme de peptides d'intérêts.[8, 33]

Figure 1.2 : Représentation du tour-γ inverse du 1,4-diazépinone et du pyrrolodiazépin-2-one.

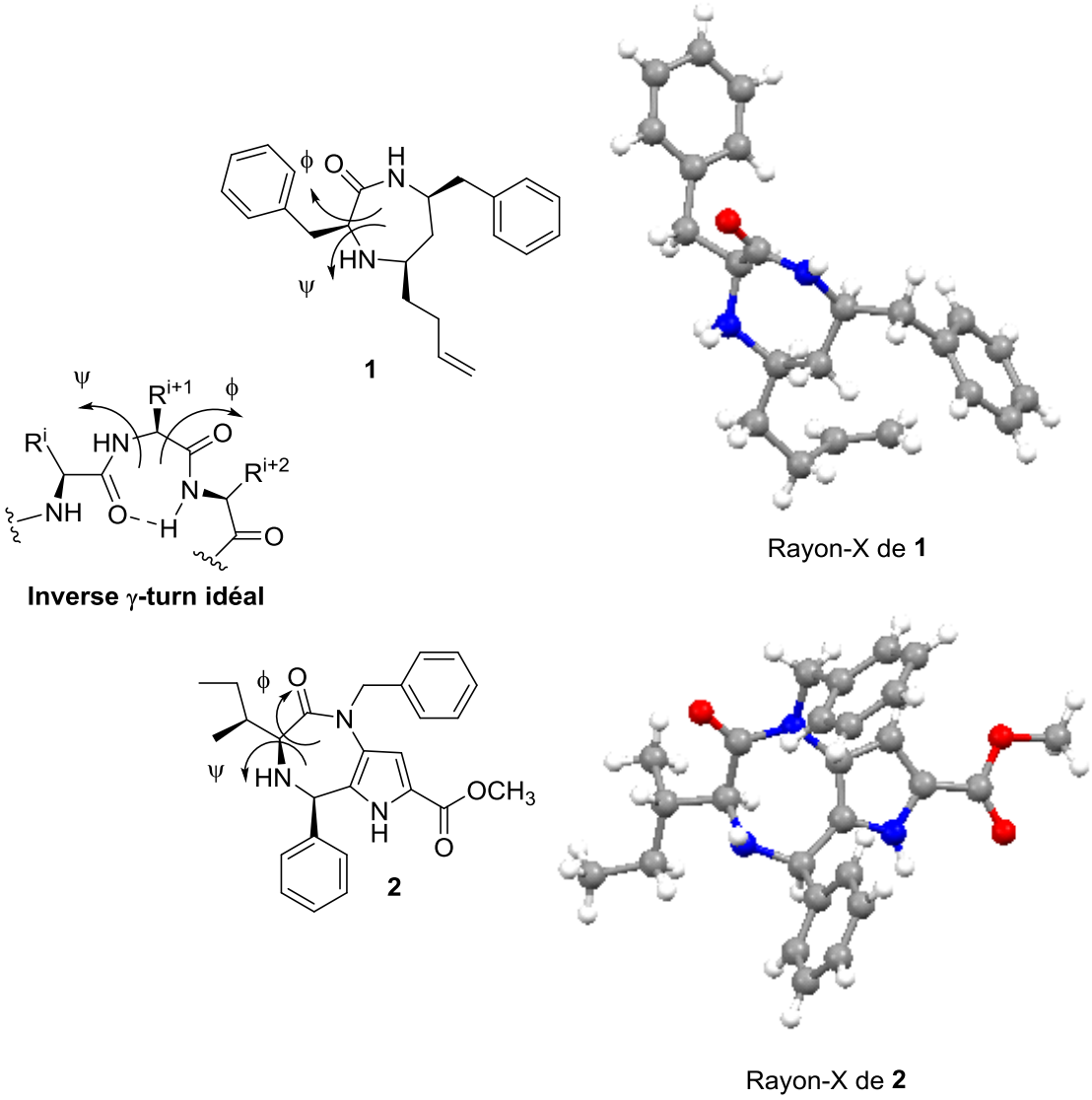

1.2. Structures privilégiées

En chimie médicinale, il y a des structures qui sont reconnues pour se lier à une multitude de récepteurs biologiques avec une haute affinité.[34, 35] Elles sont appelées « structures privilégiées »,[34] un terme introduit pour la première fois par l'équipe d'Evans en 1988, lorsqu'ils ont démontré que la 1,4-benzodiazepin-2-one **4** est capable de se lier à plus d'un récepteur : le récepteur de la cholecystokinine (CCK), le récepteur de la gastrine et le récepteur de la benzodiazépine.[36] La liste de structures dites privilégiées est

assez vaste de même que leur potentiel biologique, allant du simple composé aux plus complexes, tel que les 1,4-dihydropyridines, les indoles, les benzopyranes, les biphényles et les purines.[34] Dans ce vaste choix de structure, c'est plus particulièrement les diazépinones qui nous intéressent. Comme mentionné, les diazépinones présentent des qualités pour mimer des tours peptidiques et dont les activités peuvent être très variées, tel que montré avec l'inhibiteur LFA-1 **5**,[7, 37] et l'antagoniste du récepteur GABA **6**[34, 38, 39] (Figure 1.3).

Figure 1.3 : Quelques exemples de structures privilégiées et leurs dérivées biologiquement actives.

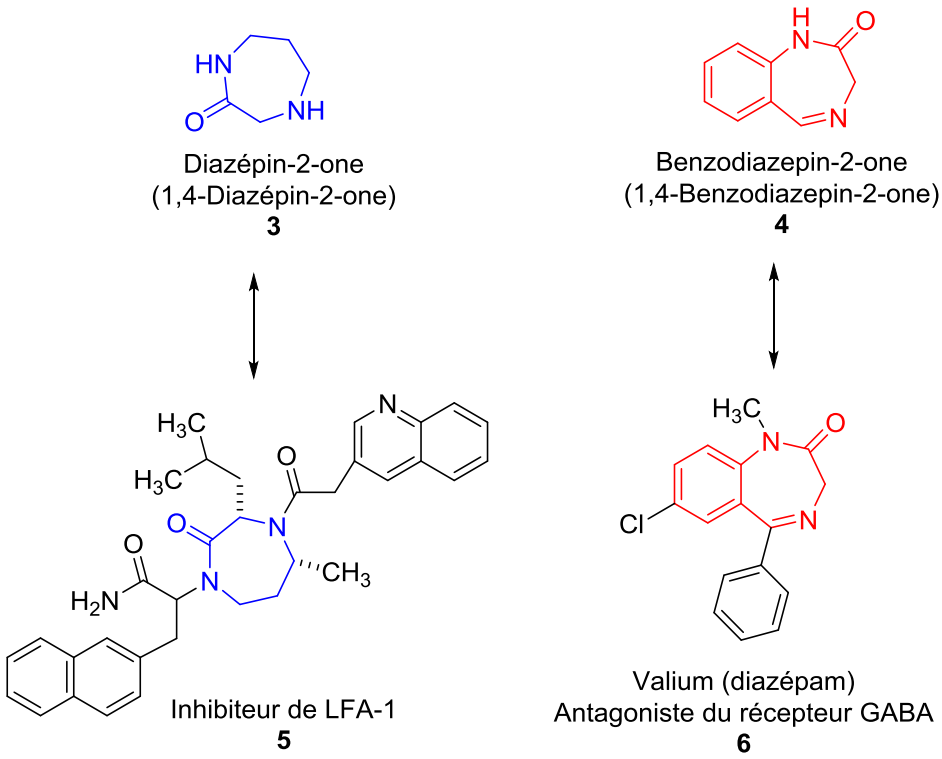

1.3. Diazépinones

La diazépinone est un hétérocycle à sept membres qui contient deux azotes et un carbonyle. Il existe plusieurs versions de la structure de l'hétérocycle du diazépinone, tel que les cycles 1,4-diazépin-2-one, 1,3-diazépin-2-one, 1,2-diazépin-3-one et 1,4-diazépin-4-one.[7, 40-42] Présent dans plusieurs composés actifs biologiquement, il peut se lier à une multitude de récepteurs biologiques. La diversité de l'échafaudage de l'hétérocycle diazépinone, en fait d'excellents outils en chimie médicinale et comme agents thérapeutiques.

1.3.1. Aryldiazépinones

Les composés formés d'un aryldiazépin-2-one sont souvent actifs biologiquement (Figures 1.4-1.5). Ils ont la capacité de se lier à plusieurs récepteurs biologiques avec une haute affinité. Les aryldiazépin-2-ones sont une des classes de composés les plus représentatifs de la notion de « structures privilégiées ». En plus de leur potentiel en chimie médicinale, les aryldiazépin-2-ones peuvent être diversifiés, en utilisant divers substituants, en allant des halogènes à d'autres types d'hétérocycles.[43-46] Avec cette gamme de diversification possible, l'éventail de composés testés biologiquement peut-être considérable, ce qui peut mener rapidement à des composés actifs.

1.3.1.1. Benzodiazépinones

L'activité des benzodiazépinones sur le système nerveux central comme la diminution de l'anxiété, la relaxation musculaire ainsi qu'une activité anticonvulsivant, est connue depuis les années 60.[38, 39, 47] Ils peuvent se lier à plusieurs récepteurs dans le système nerveux central, mais aussi à d'autres récepteurs présents dans l'organisme. L'activité du benzodiazépinone est probablement causée par leur capacité à mimer différents repliements peptidiques tels que le tour β[28, 44, 48] ou tour γ[29, 49-51], ce qui leur confrère la capacité à inhiber la prolifération des cellules cancéreuses[52], une activité antivirale[53], un effet analgésique et anti inflammatoire[54] et la capacité à bloquer le canal du sodium dans le traitement de la douleur neuropathique[55]. Le diazépam **6** est un antagoniste du récepteur de l'acide γ-aminobutyrique (GABA)[38, 39] (Figure 1.3). En plus

de l'activité sur le récepteur GABA, les benzodiazépinones sont des antagonistes du récepteur du fibrinogène **7**[56], du récepteur neurokinin-1 **8**[57], du récepteur de l'endotheline[43], du récepteur RCPG [58], activateur de la protéine kinase C[59], inhibiteur de la prolifération des cellules cancéreuses **9**[60], inhibiteur de la caspase-3 **10**[61] (Figure 1.4). En ayant la capacité de mimer le tour γ et tour β, certains benzodiazepinones ont été intégrés dans certains peptides afin de maintenir le tour du peptide initial, comme dans l'angiotensine II (Ang II, Asp-Arg-Val-Tyr-Ile-His-Pro-Phe)**,** en remplaçant Val-Tyr-Ile par un benzodiazépinone, ce qui a permis de former des analogues actifs **11**.[28, 29, 51]

Figure 1.4: Quelques exemples de benzodiazépinones biologiquement actifs.

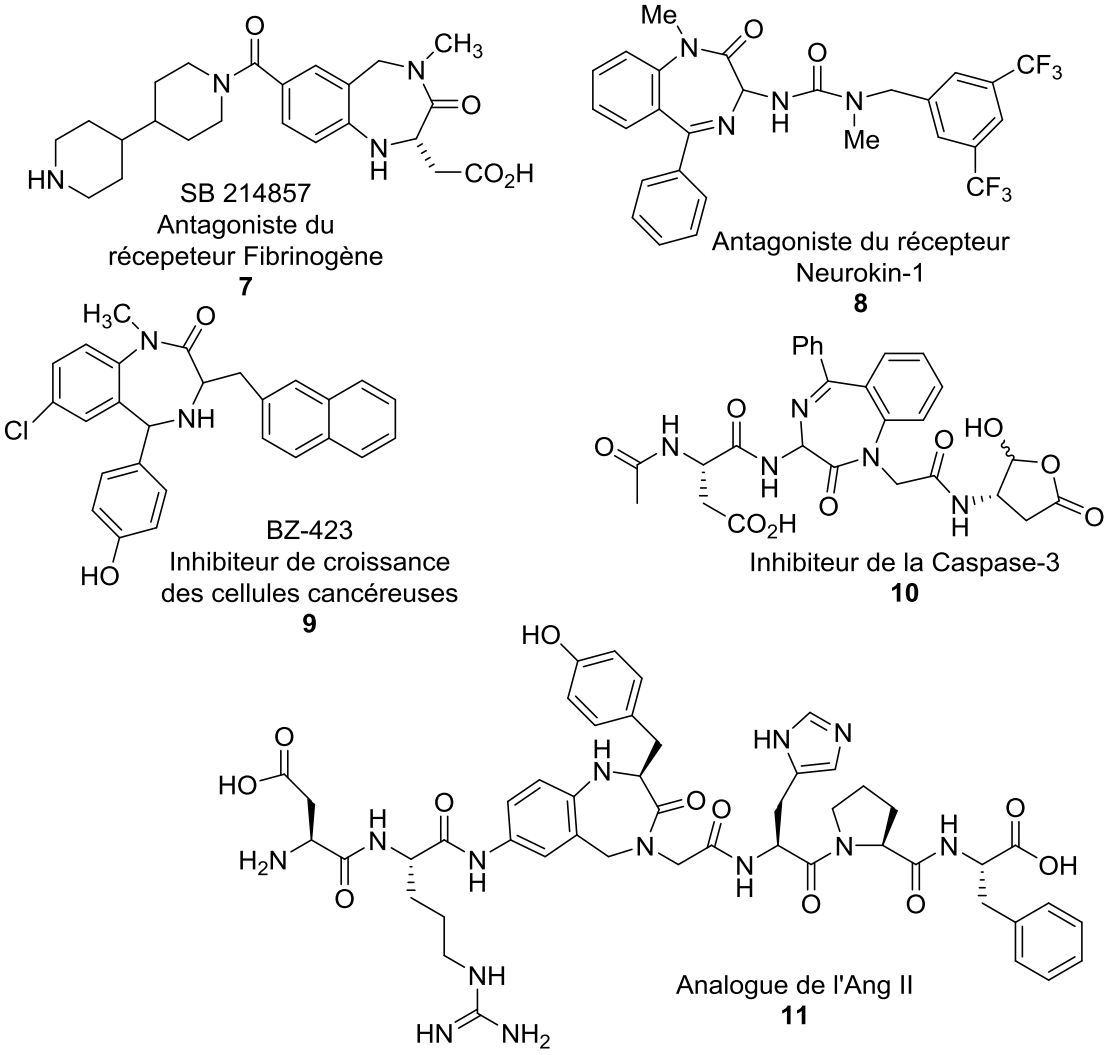

1.3.1.1.1. Synthèse de benzodiazépinones

Les benzodiazépinones sont la classe de molécules la plus représentative des aryldiazépinones. Au cours des années, plusieurs méthodes de synthèses ont été développées pour former le cycle du diazépinone, par exemple en utilisant des métaux de transition ainsi que différents types de précurseurs permettant d'accéder à une variété de squelettes de benzodiazépinones.[62-65]

Dans la littérature, la plupart des synthèses de benzodiazépinones ont en commun une cyclisation intramoléculaire comme illustrée au schéma 1.1. Le précurseur **13** est préparé en utilisant une réaction de Buchwald sur la 2-halogenobenzophénone (Schéma 1.1).[62] Cette méthode permet d'accéder à différents types d'hétérocycles difficiles à obtenir ainsi qu'à des nouveaux comme la pyridazinodiazépin-2-one.[62]

Schéma 1.1: Synthèse du 1,4-benzodiazépin-2-one par déprotection/cyclisation.

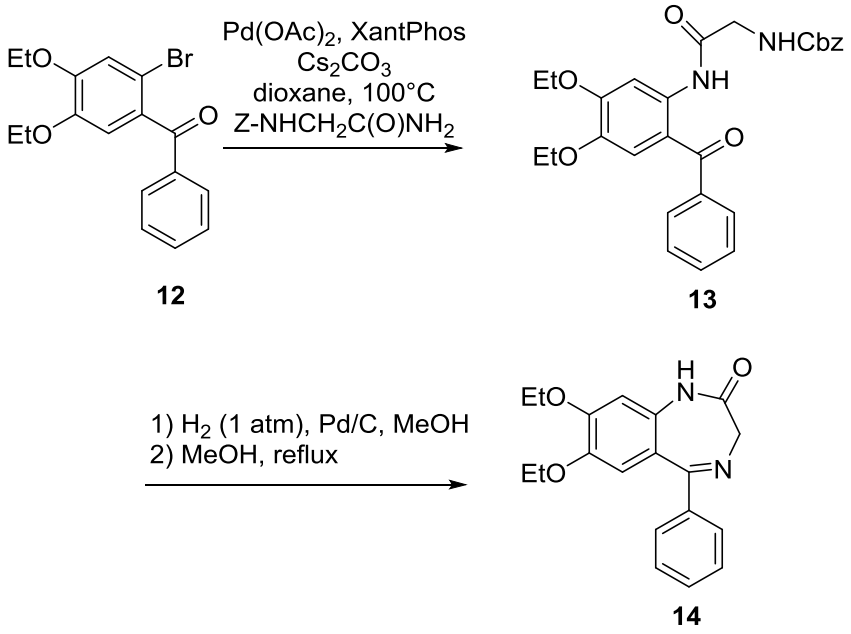

Les benzodiazépinones peuvent être synthétisées en utilisant une réaction intermoléculaire suivie d'une réaction intramoléculaire comme dans le schéma 1.2. La construction du cycle benzodiazépinone par des réactions intermoléculaires a permis de développer des benzodiazépinones pouvant servir à l'imagerie médicale, comme la 1,5-benzodiazépin-2-one **17** est un agent d'imagerie pour le récepteur métabotrope au

glutamate 2.[66] Le 1,2-diaminobenzène **15** est couplé avec le β-céto ester **16** par chauffage dans le toluène et la cyclisation est provoquée par du TFA pour donner la 1,5-benzodiazépin-2-one **17** (Schéma 1.2).

Schéma 1.2: Synthèse du 1,5-benzodiazépin-2-one ayant la capacité d'être des agents d'imagerie.

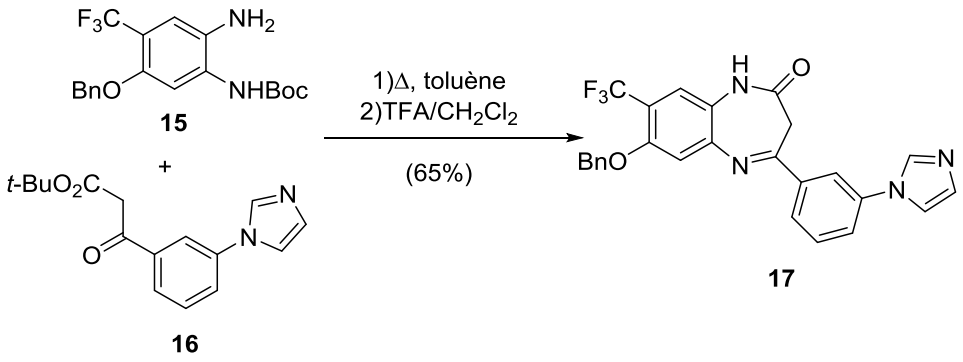

Le développement de nouvelles méthodes synthèses de benzodiazépinones a amené à transposer les synthèses en phase solide, ce qui en fait les premières petites molécules à être synthétisées sur support solide.[67] Depuis cette première synthèse, les méthodologies de synthèses sur support solide de benzodiazépinones ont évolué avec de nouvelles méthodologies et l'utilisation de différentes résines en utilisant principalement une cyclisation intramoléculaire.

Schéma 1.3: Synthèse du 1,4-benzodiazépin-2-one sur support solide.

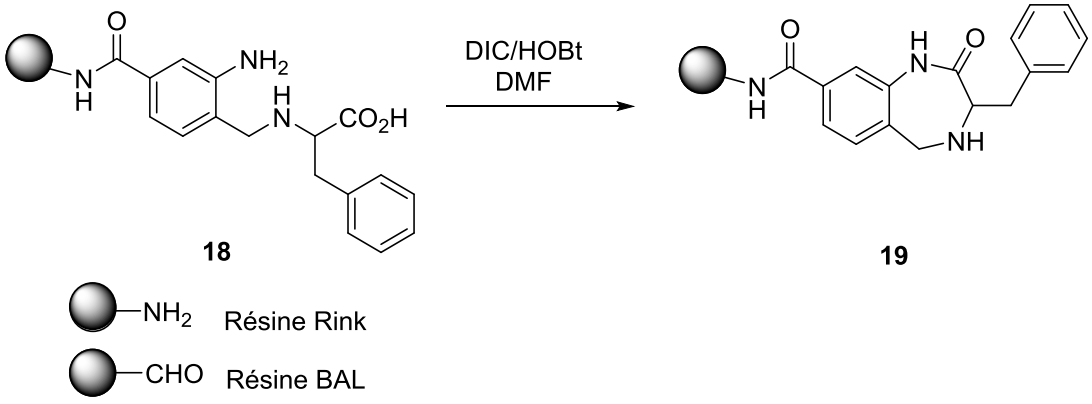

La synthèse du 1,4-benzodiazépin-2-one **19** sur support solide peut se faire sur la résine Rink ou sur la résine BAL.[68] La construction du 1,4-benzodiazépin-2-one **19** a été

obtenu par une cyclisation intramoléculaire effectuée en présence de *N*,*N*'-diisopropylcarbodiimide (DIC) et hydroxybenzotriazole (HOBt) (Schéma 1.3).[68] En utilisant la cyclisation avec un mélange DIC/HOBt, le 3,4,5-substitué 1,5-benzodiazépin-2-one est synthétisé à partir de l'acide 4-fluoro-3-nitrobenzoïque sur résine Rink.[69]

1.3.1.2. Pyrrolodiazépinones

Les pyrrolodiazépinones sont aussi des composés qualifiés de « structures privilégiées », mais beaucoup moins approfondies comparativement aux benzodiazépinones. Par contre, leur potentiel biologique est semblable à celles des benzodiazépinones, car ils peuvent interagir avec une multitude de récepteurs biologiques (Figure 1.5).

Le produit naturel, l'anthramycine (**20**, Figure 1.5) est le premier exemplaire dans la littérature de pyrrolobenzodiazépinones à avoir été identifié. Isolé du *Streptomyces rufuineus*,[70] l'anthramycine (**20)** est une pyrrolo[2,1-c][1,4]benzodiazépinone connue pour son activité antibiotique et antitumorale, due à sa capacité à se lier avec l'ADN de façon sélective.[71-77] Dans la littérature, il y a aussi d'autres produits naturels similaires à l'anthramycine comme la limazépine A à F **21**[46, 78], la tomamycine[79], la chicamycine[80] et la sibiromycine[81] qui ont aussi une activité antibiotique et antitumorale. Les pyrrolobenzodiazépinones sont conçus naturellement pour lier l'ADN, ce qui leur donne leur potentiel en tant qu'antibiotique et antitumoral.[73, 75, 77, 82-84] Le pyrrolobenzodiazépinone **22** est capable d'inhiber la poly(ADP-ribose)polymérase-1 (PARP-1) qui constitue une cible dans la mise au point de traitement du cancer, car la PARP-1 joue un rôle dans la réplication de l'ADN.[85] Le pyrrolothienodiazépinone **23** présente une activité antiproliférative envers les cellules leucémiques.[86] Le pyrrolobenzodiazépinone **24** a une activité antivirale contre VIH-1 en inhibant la transcriptase inverse du VIH (VIH-RT avec un IC_{90} de 0,8 μM).[87] Certains pyrrolodiazépinones ont aussi une activité antifongique envers les dermatophytes spécifiquement[88] et d'autres pyrrolodiazépinones ont une activité antibiotique[78]. Le pyrrolodiazépinone **25** a une activité inhibitrice de l'enzyme de conversion de l'angiotensine (ACE), une peptidase jouant un rôle dans l'activité cardiovasculaire,

comme l'hypertension.[89] Comme les benzodiazépinones, les pyrrolodiazépinones ont aussi une activité sur le système nerveux central[90-92], dont une activité sédative, antiépileptique[93] et une action analgésique[94]. Le pyrrolodiazépinone **26** a démontré une activité antimuscarinique.[95] Le pyrrolodiazépinone **27** est un antagoniste du récepteur GABA, d'où une activité anticonvulsante et anxiolytique.[96, 97]

Figure 1.5 : Quelques exemples de pyrrolodiazépinones actives biologiquement.

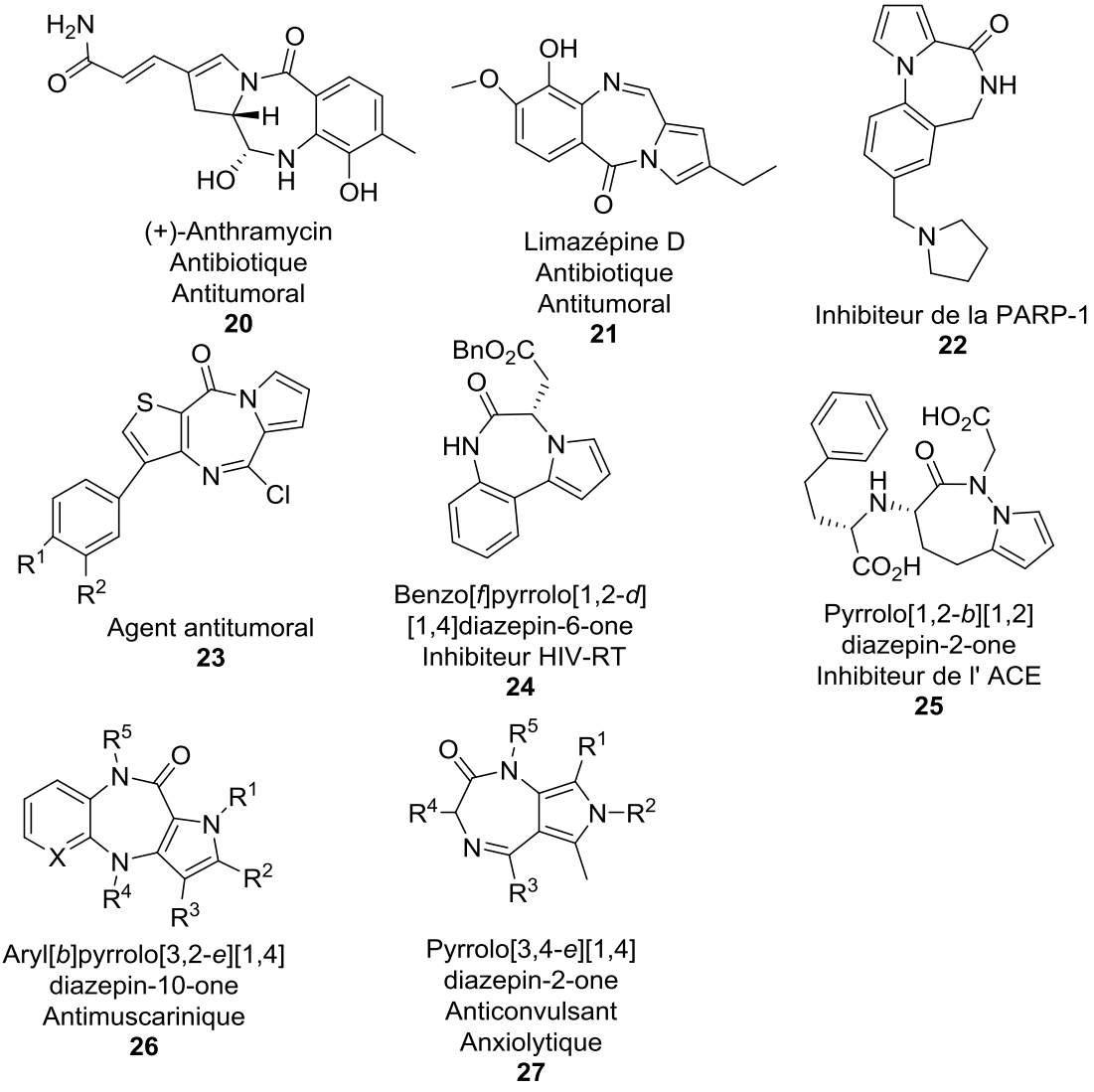

Comme illustrées dans la figure 1.5, les activités biologiques des pyrrolodiazépinones sont très diverses. Cette grande diversité s'expliquerait par la capacité du pyrrolodiazépinone à mimer la géométrie des tours peptidiques le tour-γ

inverse[8]. Cette capacité en fait d'excellents candidats pour être de futurs agents thérapeutiques pour traiter diverses pathologies.

1.3.1.2.1. Synthèse de pyrrolodiazépinones

Dans la littérature, il existe aussi des pyrrolodiazépinones formés sans le cycle benzénique, soit composés uniquement d'un pyrrole et d'un cycle diazépinone, mais ils sont moins fréquents. Comme dans la plupart des synthèses du cycle diazépinone, la formation de ce cycle passe par une cyclisation intramoléculaire à partir d'un précurseur dont le pyrrole sert de point d'ancrage, comme illustré au schéma 1.4.[98]

Schéma 1.4: Synthèse du 1,4-pyrrolo[2,3-*f*]diazépin-2-one **30**.

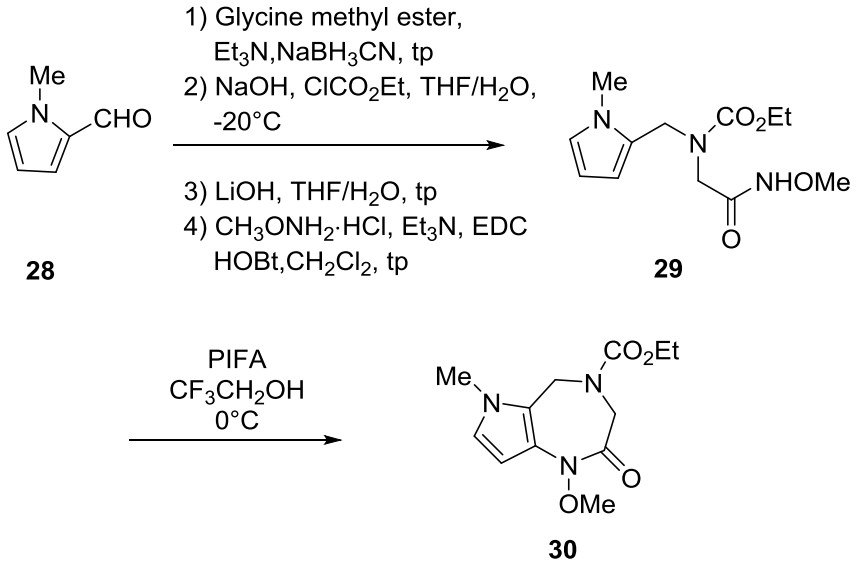

PIFA = l'iodure de phényle (III) bis(trifluoroacétate)

La construction de la structure diazépinone se fait à partir du Gly-OMe ou d'un dérivé de l'alanine. L'ester méthylique de la glycine réagit avec le composé **28** pour former l'aminoester, qui est protégé pour être ensuite hydrolysé et transformé en amide **29** (Schéma 1.4). La cyclisation intramoléculaire pour former le cycle diazépinone se fait via la formation d'ions *N*-acylnitrénium par l'utilisation de l'iodure de phényle (III) bis(trifluoroacétate) (PIFA) qui est piégé par l'anneau nucléophilique pour compléter la réaction d'amidation aromatique et former le 1,4-pyrrolo[2,3-*f*]diazépin-2-one **30** (Schéma 1.4).[98, 99] La cyclisation par ion *N*-acylnitrénium est la réaction clé de cette

synthèse et ne cause pas de racémisation durant la cyclisation lorsque le précurseur **29** est énantiomériqment pur. Avec cette méthodologie, il est possible aussi de synthétiser d'autres types d'aryldiazépinones, telles que le 1,4-thiéno[2,3-*f*]diazépin-2-one.[98, 99]

La grande majorité des synthèses de pyrrolobenzodiazépinones (PBD) et de pyrrolodiazépinones sont faites à partir de cyclisations intramoléculaires comme réactions clés, mais les pyrrolodiazépinones peuvent être accessibles à partir de réactions à plusieurs composants, comme illustré au schéma 1.5.[100]

Schéma 1.5 : Synthèse du pyrazolo[4,3-*f*]pyrrolo[1,2-*a*][1,4]diazépinone **33** par condensation de type Ugi à 4 composants.

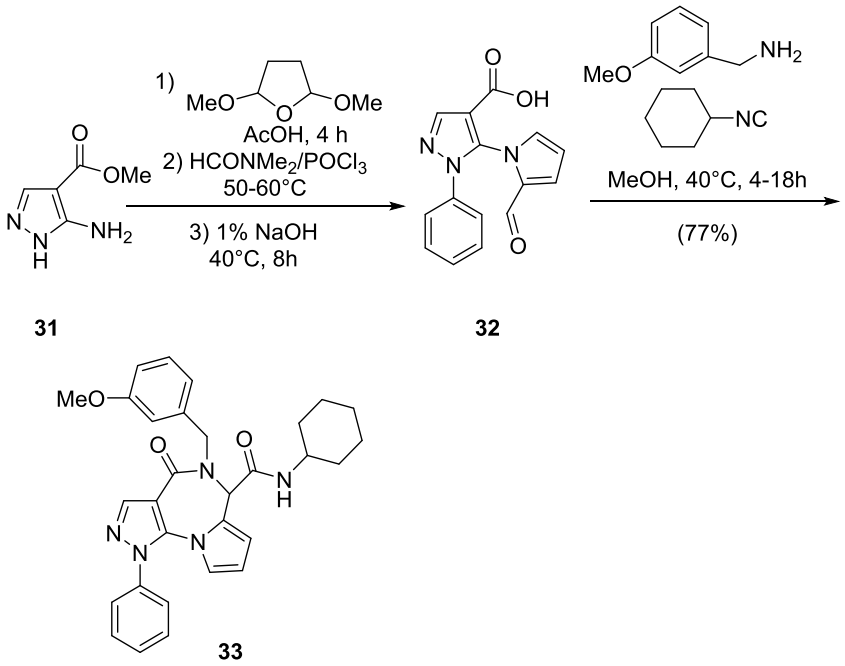

Les réactions d'Ugi peuvent servir à construire le squelette du diazépinone comme démontré par la synthèse du benzodiazépinones qui utilise la réaction Imide-Ugi intramoléculaire.[64, 100, 101] Le pyrazolo[4,3-*f*]pyrrolo[1,2-*a*][1,4]diazépinone **33** est accessible en utilisant une condensation de type Ugi à quatre composants comme réaction clé (Schéma 1.5).[100] La condensation d'Ugi à plusieurs composés est comme une réaction d'Ugi classique, l'intermédiaire imine qui est attaquée par l'isonitrile pour former l'intermédiaire nitrilium menant à la cyclisation intramoléculaire. Pour cette méthodologie, il est possible de varier les groupements aromatiques à la place du

pyrazole, comme le benzothiényle pour former le benzothiéno[4,3-*f*]pyrrolo[1,2-*a*][1,4] diazépinone.[100]

Une autre stratégie possible pour former les divers échafaudages du pyrrolodiazépinone, qui n'utilise qu'un pyrrole ou d'autres hétérocycliques, comme point d'ancrage pour la cyclisation, emploie une cyclisation intramoléculaire à partir d'un intermédiaire linéaire (schéma 1.6). Également, les pyrrolodiazépinones peuvent être aussi accessibles par un réarrangement du cyclopropylkétimine.[102, 103]

Schéma 1.6: Synthèse du pyrrolo[1,2-*g*][1,4]diazépin-4-one **35** et du 5-méthyl pyrrolo[1,2-*g*][1,4]diazépin-4-one **37** par condensation de Paal-Knorr intramoléculaire.

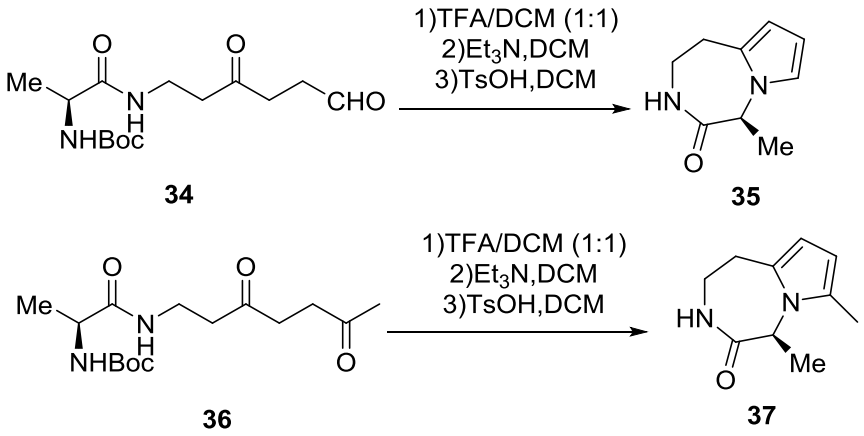

Lors de la synthèse des 1,4-diazépinones,[7] il a été démontré qu'il est possible de former les pyrrolo[1,2-*g*][1,4]diazépin-4-ones **35** et **37** en utilisant une cyclisation par la condensation de Paal-Knorr intramoléculaire (Schéma 1.6).[7]

Pour former le pyrrolo[1,2-*d*][1,4]diazépinone **40**, le précurseur linéaire **39** provient de l'ouverture du furane **38**.[104] Cette stratégie a été déjà utilisée pour donner le pyrrolo[1,2-*d*][1,4]benzodiazépin-6-one.[104] L'ouverture du furane **38** se fait en présence de HCl et d'acide acétique pour former l'intermédiaire dicétone **39**, qui cyclise ensuite pour former le pyrrolodiazépinone **40** (Schéma 1.7).

Schéma 1.7: Synthèse du pyrrolo[1,2-*d*][1,4]diazépinone **40**.

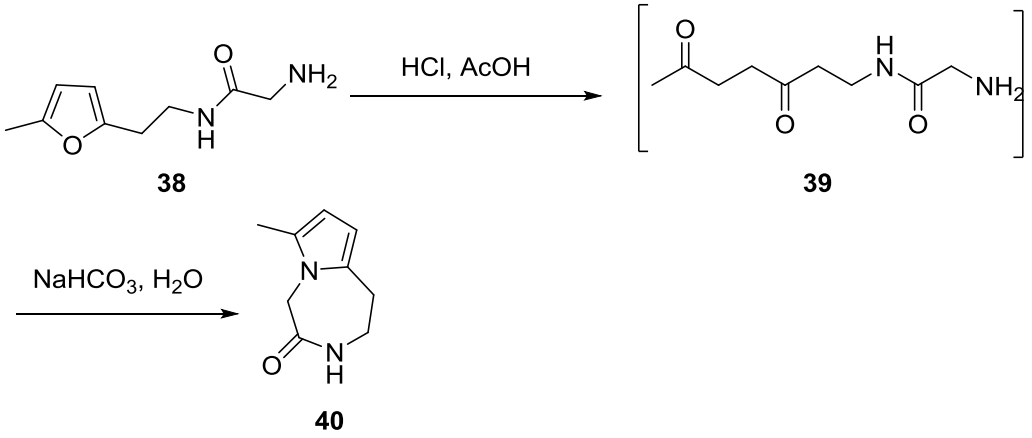

38 **39** **40**

1.3.1.3. Synthèse en phase solide de pyrrolodiazépinones

Comme les benzodiazépinones, les pyrrolobenzodiazépinones et les pyrrolodiazépinones peuvent être synthétisés sur support solide. La synthèse sur support solide serait très avantageuse puisqu'elle permettrait d'avoir accès à un plus grand nombre de molécules plus rapidement pour un criblage à haut débit.[73] Dans la littérature, c'est principalement les pyrrolobenzodiazépinones qui sont synthétisés sur support solide en utilisant 4 points de liaisons possibles entre le matériel de départ et le support solide, soit par un lien ester, thioester ou amide au C-11[105-107] (schéma 1.8), par un lien carbamate au N-10[71], sur le cycle benzénique par lien éther[108] ou par un lien éther au C-2[109]. Les synthèses en phase solide des pyrrolobenzodiazépinones **43** et **46** ont utilisé l'acide azidobenzoïque ou nitrobenzoïque comme matériel de départ.[71, 105-107, 110]

Schéma 1.8 : Synthèse de pyrrolobenzodiazépinones sur support solide liés au C-11 par un lien ester et thioester.

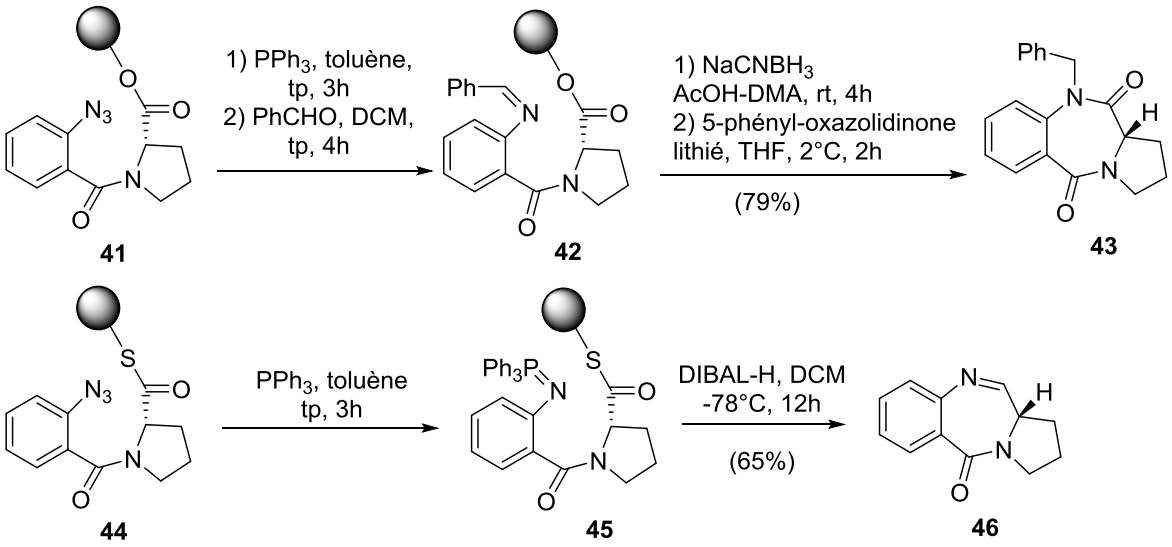

La réaction d'aza-Wittig a déjà servi pour synthétiser des pyrrolobenzodiazépinones en solution, il a été transposé sur support solide pour la synthèse de pyrrolobenzodiazépinones dilactame **43** et imine **46**. L'azoture **41** est traité avec de la triphénylphosphine pour former l'intermédiaire iminophosphorane suivi d'une condensation d'un aldéhyde, tel que le benzaldéhyde pour former l'intermédiaire imine **42**. L'imine formée est réduite chimiosélectivement avec du cyanoborohydrure de sodium suivi d'une cyclisation provoquée par le traitement avec le 5-phényl-oxazolidinone lithié pour former **43** (Schéma 1.8).[106] La cyclisation intramoléculaire entraine le clivage du diazépinone du support solide. L'avantage de cette méthode est qu'elle permet de fonctionnaliser la position N-10 du diazépinone.[73, 106] Il est possible aussi d'accrocher au C-11 par un lien thioester à la résine de Wang. L'utilisation d'un lien thioester avec la résine permet une méthodologie impliquant une cyclisation intramoléculaire aza-Wittig engendrée par un clivage réducteur en utilisant le DIBAL-H pour former l'imine **46** (Schéma 1.8).[110]

1.3.2. Synthèse en solution et sur phase solide du pyrrolo[3,2-*e*][1,4]diazépin-2-one

Le pyrrolo[3,2-*e*][1,4]diazépin-2-one **2** a été développé par une méthode en solution en utilisant la réaction de Pictet-Spengler[111] comme réaction clé pour former le cycle du diazépin-2-one (Schéma 1.9).[8] En général la réaction de Pictet-Spengler consiste en une condensation sur un analogue de la tryptamine avec un aldéhyde ou une cétone pour former un β-carboline.[112] Toutefois, cette cyclisation intramoléculaire via un ion iminium intermédiaire est accomplie avec une variété d'amines et d'hétérocycles et de plus le pyrrole peut être utilisé comme un nucléophile dans la réaction de Pictet-Spengler.[113-117] Dans la littérature, il y a quelques exemples de synthèses qui utilisent le pyrrole comme nucléophile dans les réactions de Pictet-Spengler, comme pour la synthèse de pyrimido[4,5-*b*][1,4]benzodiazépines[118] et celle de pyrrolo[3,2-*e*]pyrimidines[117]. Au moment de cette synthèse, il n'y avait pas de synthèse de pyrrolodiazépinones utilisant la réaction de Pictet-Spengler pour la cyclisation.[113] Plus tard, la réaction de Pictet-Spengler par un 7-endo trig cyclisation à donner une librairie de 46 benzopyrrolodiazépinones.[46]

Le pyrrolo[3,2-*e*][1,4]diazépin-2-one **2** est accessible après 3 étapes à partir du 4-oxo-N-(PhF)proline **48**, qui est préparé à partir du 4-hydroxyproline **47**, en utilisant une protection par le groupe 9-(9-phénylfluorényle) (PhF), suivi d'une estérification.[8, 119] L'amidopyrrole **50** est préparé en faisant réagir le 4-oxo-*N*-(PhF)proline **48** avec la benzylamine en présence d'un catalyseur acide, l'acide *p*-toluène sulfonique, pour former le 4-aminopyrrole **49**,[120] suivi d'une aminoacylation en utilisant divers acides aminés.[121] À partir de l'amidopyrrole **50**, les pyrrolodiazépin-2-ones **2** voulus sont formés par la réaction de divers aldéhydes dans le toluène, en présence de l'acide trifluoroacétique (TFA), dans un tube scellé et chauffé à 70 °C dans un bain d'huile, pendant 48 h (Schéma 1.9).[8]

Schéma 1.9 : Synthèse en solution du pyrrolo[3,2-*e*][1,4]diazépin-2-one.

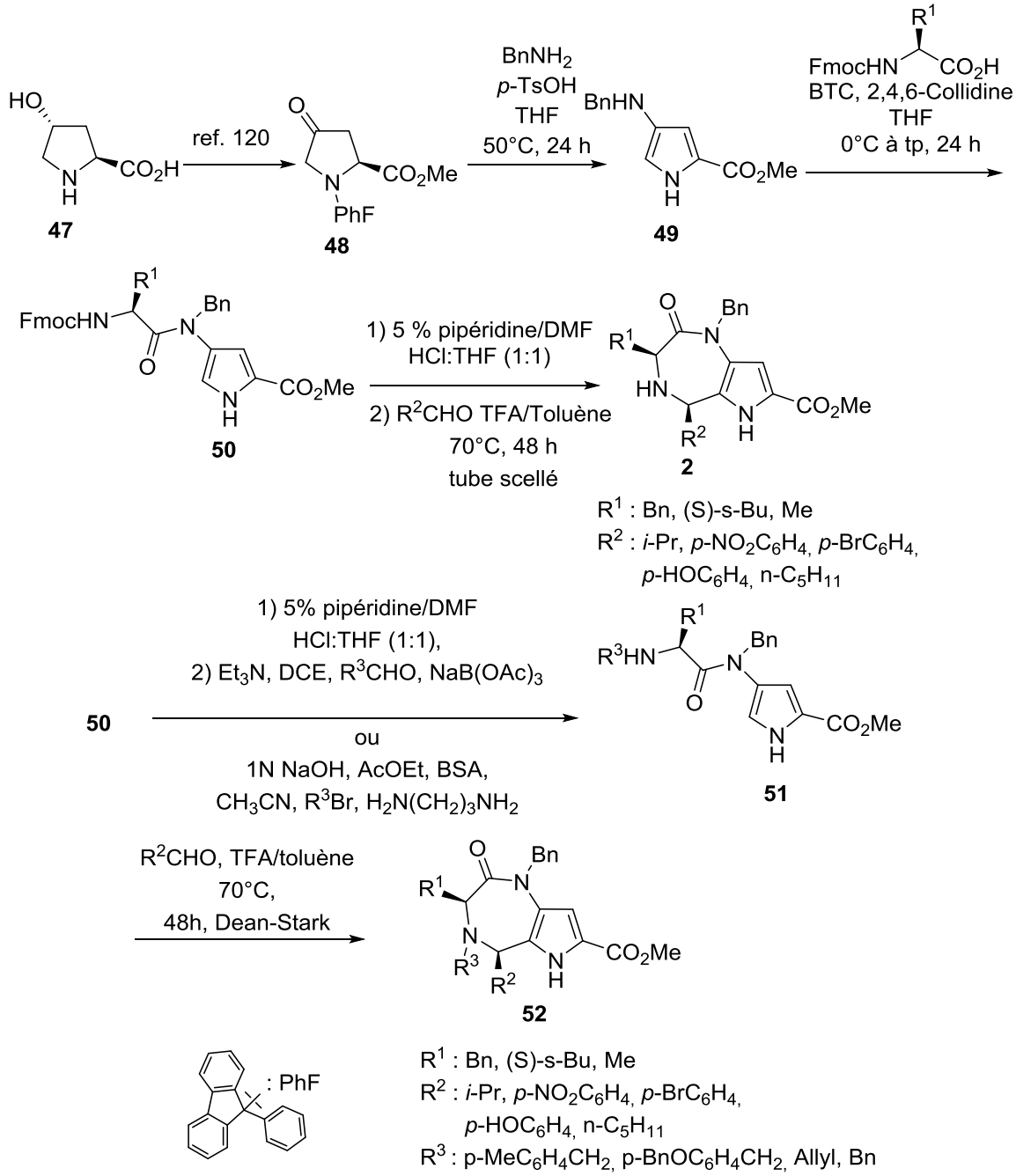

La plupart des synthèses de pyrrolodiazépinones dans la littérature permettent d'obtenir une insaturation entre le N-4 et C-5, mais l'utilisation de la réaction Pictet-Spengler pour la cyclisation par des ions iminiums permet d'introduire un centre stéréogénique en position C-5 et en ayant une *cis* diastéréosélective. Le mécanisme de

cette sélectivité est basé sur une attaque endo de l'ion *E*-iminium, qui engendre un état de transition préférant une conformation équilatérale avec la chaîne latérale de l'acide aminé.[8, 122] La stéréochimie *cis* est assignée par l'analyse du spectre NOESY (effet par l'interaction entre le C-5 et C-3. De plus, il n'y a aucune racémisation de la chaîne latérale de l'acide aminé durant la réaction de Pictet-Spengler.[8] Le cristal du pyrrolo[3,2-*e*][1,4]diazépin-2-one **2b** a été analysé par rayon X et confirme que les angles dièdres du pyrrolo[3,2-*e*][1,4]diazépin-2-one miment le tour-γ inverse (Figure 1.2).

Cette méthodologie a été employée pour synthétiser huit pyrrolo[3,2-*e*][1,4]diazépin-2-ones **2** (Figure 1.6).[123] La cyclisation par réaction de Pictet-Spengler peut se faire aussi sur une amine secondaire, mais en utilisant un Dean-Stark à reflux à partir de l'amidopyrrole **51** dont l'amine a été alkylée par amination réductrice ou par un intermédiaire sillylamide pour donner le 4,5-disubstitué pyrrolo[3,2-*e*][1,4]diazépin-2-one **52** (Schéma 1.9). Sur les amines secondaires, il y a une perte de stéréosélectivité lors de la cyclisation, pour donner un mélange de (5*R*)- et (5*S*)-diastéréisomères avec un ratio de 5:1 ou 8:1.

Figure 1.6: Quelques exemples de pyrrolo[3,2-*e*][1,4]diazépin-2-ones obtenus par la réaction de Pictet-Spengler.

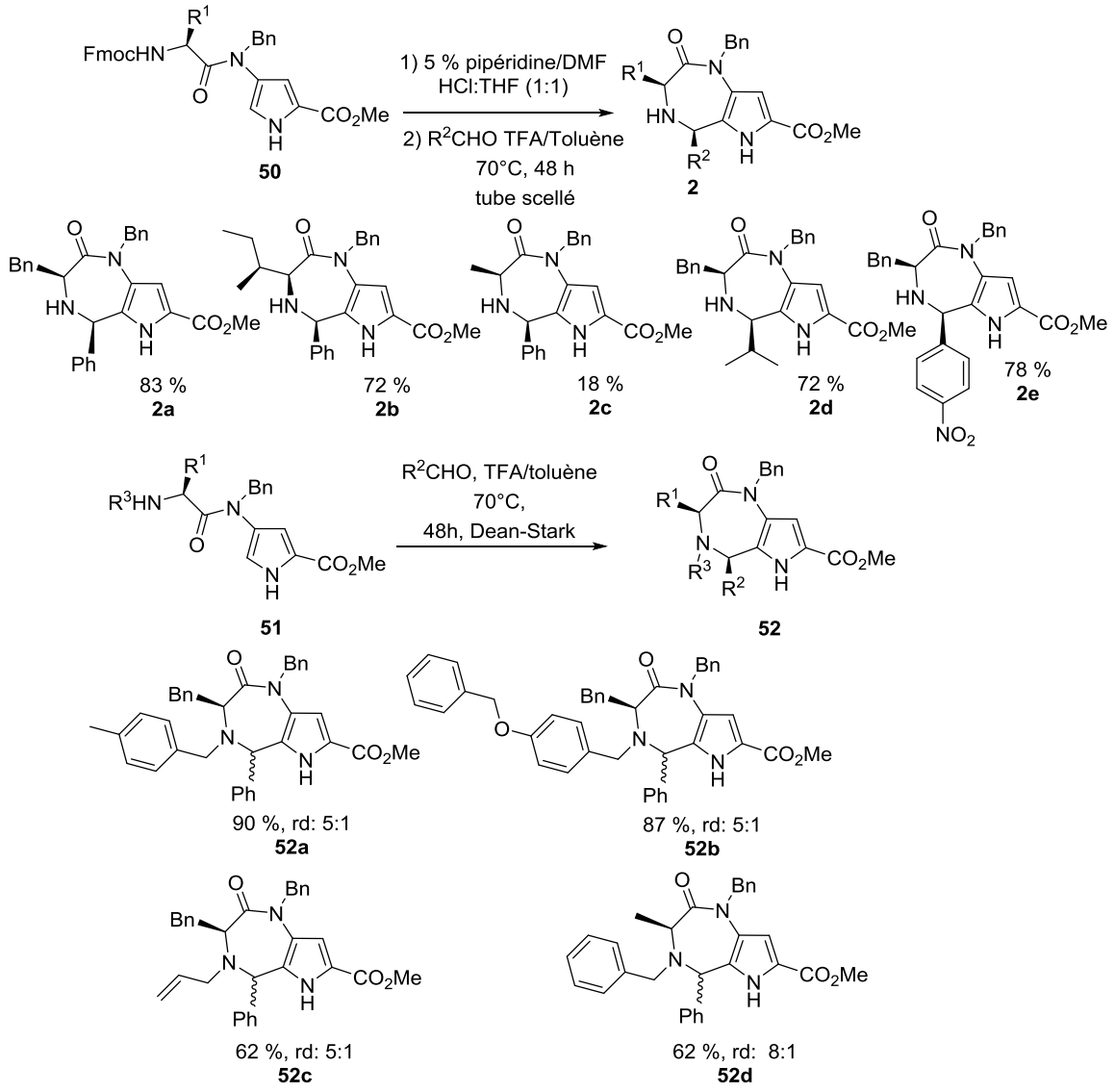

La comparaison de trois différents supports a été faite pour transférer la méthodologie en solution sur support solide: soit la résine de Merrifield, la résine de Wang et un support soluble TAP (Schéma 1.10).[8] Dans la littérature, les résines de Merrifield et de Wang sont fréquemment utilisées pour la synthèse d'hétérocycles et de peptides.[73, 124-126] La résine de Merrifield est une résine de polystyrène chlorométhylée et réticulée avec 1 % de divinylbenzène (DVB). La résine de Wang est une résine de polystyrène 4-hydroxybenzyle d'alcool et réticulée avec 1 % DVB. Le support soluble

TAP, qui correspond au sel de (4'-bromométhyl)-[1,1'-biphényl]-4-yl)triphénylphosphonium[127] est une variante soluble de la résine de Merrifield.[127-129]

Un résumé de cette étude sera présenté si bas et l'article sera mis en annexe pour plus d'informations. La synthèse du pyrrolo[3,2-*e*][1,4]diazépin-2-one sur support solide se fait en général comme pour la synthèse en solution, avec le matériel de départ 4-hydroxy-*N*-(PhF)proline (schéma 1.10).[123]

Schéma 1.10 : Synthèse de pyrrolo[3,2-*e*][1,4]diazépin-2-ones sur trois différents supports.

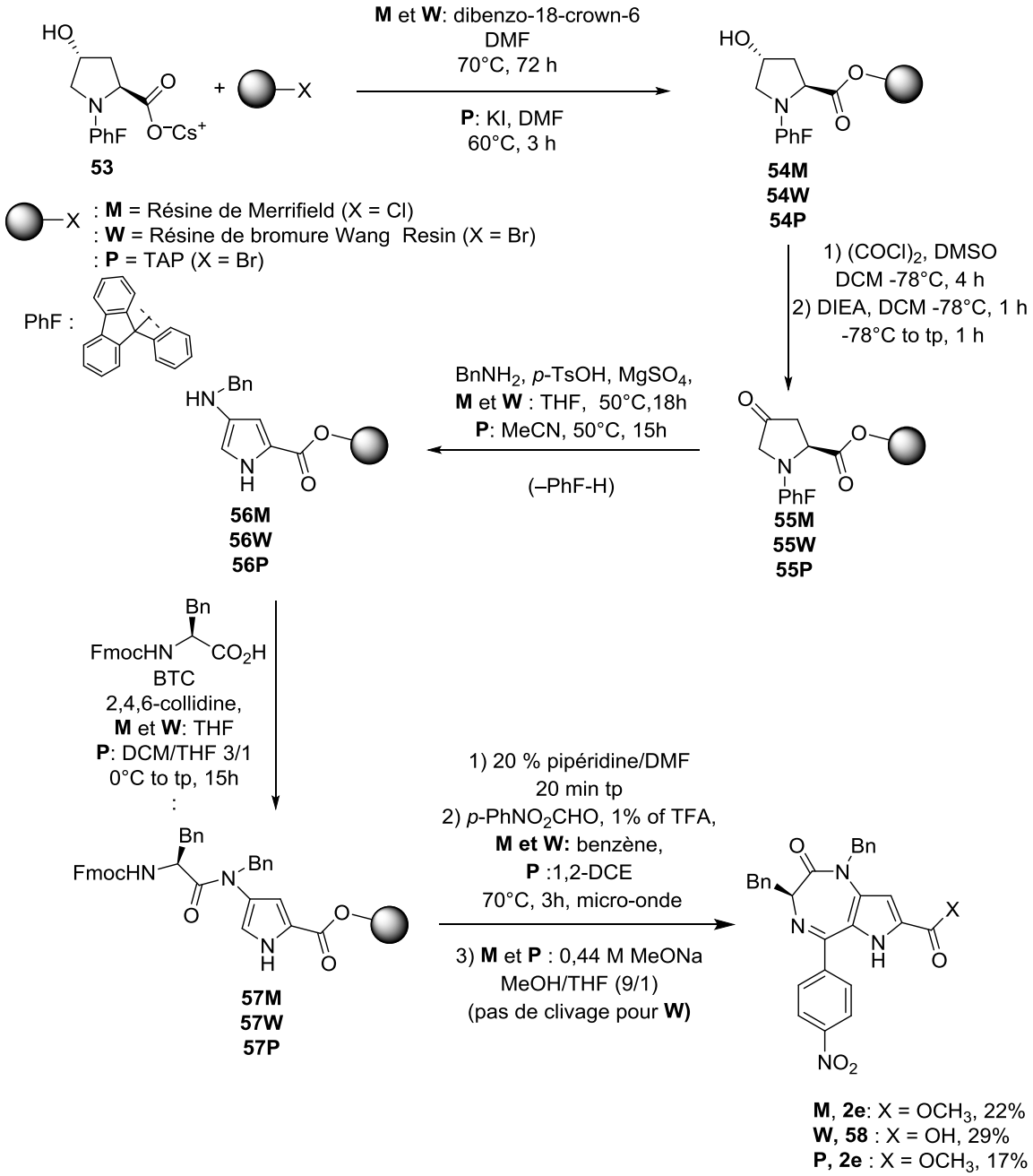

La réaction de Pictet-Spengler se fait dans le micro-onde en utilisant le *p*-nitrobenzaldéhyde avec 1 % de TFA dans le benzène ou 1,2-dichloroéthane, à 70°C durant 3h. (Schéma 1.10). La réaction de Pictet-Spengler sur la résine de Wang est particulière, car la cyclisation en condition acide entraîne la rupture du lien avec la résine

pour former le pyrrolo[3,2-*e*][1,4]diazépin-2-one acide carboxylique **58**. Pour libérer le pyrrolo[3,2-*e*][1,4]diazépin-2-one de la résine de Merrifield et du support TAP, il faut procéder à une étape de clivage en utilisant par exemple une solution de 0,44 M méthoxyde de sodium (NaOMe) dans une solution de THF/MeOH (9:1), qui donne le pyrrolo[3,2-*e*][1,4]diazépin-2-one ester méthylique **2e**. La présence du groupe nitrophényle à la position C-5 favorise la formation d'une insaturation entre C-5 et N-4. Par contre, lorsque le *p*-nitrobenzaldéhyde est remplacé par l'isobutyraldéhyde, il y a présence du pyrrolo[3,2-*e*][1,4]diazépin-2-one insaturé et également des *R*- et *S*-pyrrolo[3,2-*e*][1,4]diazépin-2-ones saturés.

1.4. Urotensine II

1.4.1. Découverte de l'urotensine et de l'URP

À la fin des années 60, l'urotensine II (UII) fut identifié pour la première fois dans l'urophyse d'un poisson-téléostéen sur la base de son activité spasmogénique sur le rectum de la truite.[130-134] L'UII de Gobie est une hormone dodécapeptidique cyclique, le cycle étant formé par un pont disulfure entre les deux cystéines, dont la séquence d'acides aminés est la suivante : H-Ala-Gly-Thr-Ala-Asp-c**[Cys-Phe-Trp-Lys-Tyr-Cys]-**Val-OH (Tableau 1.2). En raison d'homologie de séquence, mais également de similitude structurale avec la somatostatine (Tableau 1.2), l'UII fut initialement baptisée «somatostatin-like peptide».[130]

Pendant longtemps, l'UII fut considérée comme un peptide uniquement présent chez les poissons. L'intérêt pour l'UII a donc considérablement augmenté lorsqu'il a été démontré que ce peptide provoquait la relaxation des muscles anococcygien de souris et la contraction de l'aorte de rat.[135, 136] Cette découverte mena ainsi à l'identification et la caractérisation d'isoforme de l'UII dans diverses espèces de vertébrés et notamment les poissons (comme la truite, l'esturgeon, la carpe et le chien de mer)[137-143], les amphibiens [144, 145] et les mammifères incluant l'homme[142, 143, 146-149] (Tableau 1.2). Chez l'humain, ce peptide est retrouvé au niveau du tronc cérébral et dans la moelle épinière ainsi que dans

des tissus périphériques comme le cœur, la rate, le foie, le pancréas et la prostate.[133, 150, 151]

Tableau 1.2: Comparaison de la structure de l'UII et URP chez différentes espèces animales.

	Séquence d'acide aminé	Ref
Somatostatine	H-Ala-Gly- *c*[Cys-Lys-Asn-Phe-Phe-Trp-Lys-Thr-Phe-Ser-Cys]-OH	130
Espèce	UII	
Gobies	H-Ala-Gly-Thr-Ala-Asp-*c*[Cys-Phe-Trp-Lys-Tyr-Cys]-Val-OH	130, 131
Truite	H-Gly-Gly-Asn-Ser-Glu-c[Cys-Phe-Trp-Lys-Tyr-Cys]-Val-OH	138
Grenouille	H-Ala-Gly-Asn-Leu-Ser-Glu- *c*[Cys-Phe-Trp-Lys-Tyr-Cys]-Val-OH	144, 145
Souris	<Gln-His-Lys-Gln-His-Gly-Ala-Ala-Pro-Glu-*c*[Cys-Phe-Trp-Lys-Tyr-Cys]-Ile-OH	143, 146
Rat	<Gln-His-Gly-Thr-Ala-Pro-Glu-*c*[Cys-Phe-Trp-Lys-Tyr-Cys]-Ile-OH	143, 146
Singe	H-Glu-Thr-Pro-Asp-*c*[Cys-Phe-Trp-Lys-Tyr-Cys]-Val-OH	143
Humain (**59**)	H-Glu-Thr-Pro-Asp-*c*[Cys-Phe-Trp-Lys-Tyr-Cys]-Val-OH	143, 150
URP		
Rat	H- Ala-*c*[Cys-Phe-Trp-Lys-Tyr-Cys]-Val-OH	143, 147
Souris	H- Ala-*c*[Cys-Phe-Trp-Lys-Tyr-Cys]-Val-OH	143
Chimpanzé	H- Ala-*c*[Cys-Phe-Trp-Lys-Tyr-Cys]-Val-OH	143
Humain (**60**)	H- Ala-*c*[Cys-Phe-Trp-Lys-Tyr-Cys]-Val-OH	143

L'ensemble des isoformes d'UII comprennent entre 11 et 17 acides aminés avec une séquence *N*-terminal hautement variable d'une espèce à l'autre. En revanche, tous possèdent une région cyclique strictement invariable au niveau du domaine C-terminal (Tableau 1.2). La présence d'un tel motif, conservé dans chaque isoforme d'UII, suggère que ce segment était essentiel pour son activité biologique ce qui fut démontré ultérieurement.[152-155] Enfin, l'acide aminé adjacent le cycle est généralement porteur d'une fonction acide, soit Asp ou Glu, alors que le dernier acide aminé de la séquence est un acide aminé neutre, généralement Val ou à l'occasion Ile. Au début du 21e siècle, un

paralogue de l'UII, nommé « urotensin II-related peptide » (URP), fut isolé dans le cerveau de rat par l'équipe Sugo.[147] L'URP (H-Ala-*c*(Cys-Phe-Trp-Lys-Tyr-Cys)-Val-OH), considéré comme la seule forme immunoréactive dans le cerveau de rat, conserve la région cyclique caractéristique aux UII (Figure 1.7 et Tableau 1.2).[143, 147, 156] Plusieurs isoformes de l'URP ont ainsi été identifiés et contrairement à l'UII, ces derniers présentent strictement la même séquence avec notamment une très courte région *N*-terminale.

Figure 1.7 : Représentation de l'UII humaine (hUII) et d'URP.

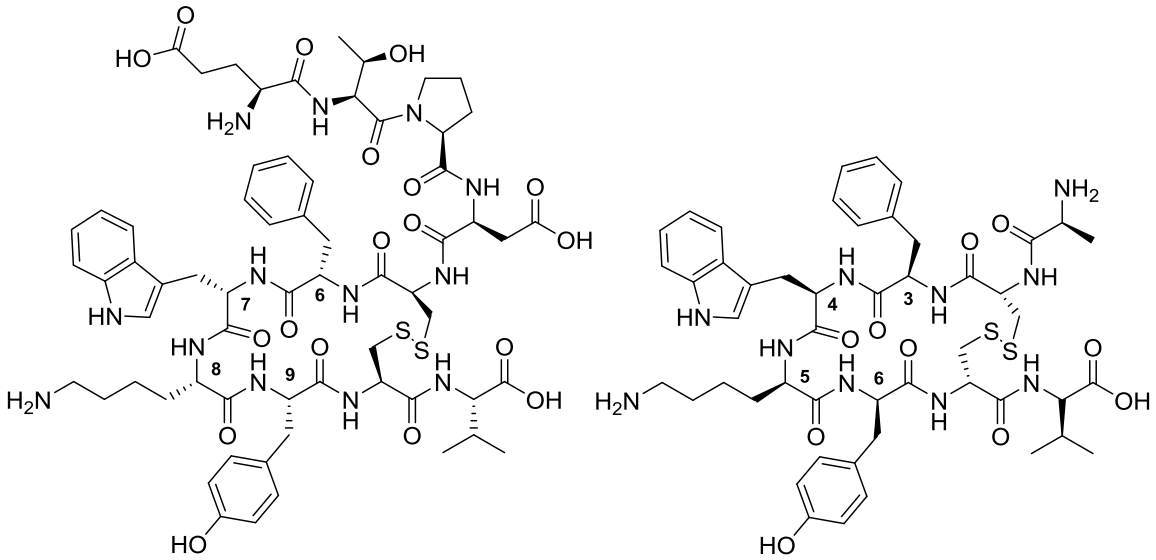

59
UII humain (hUII)

60
URP

1.4.2. Activités biologiques associées à l'UII et à l'URP

Initialement caractérisé à la fin des années 80 pour sa capacité à provoquer la relaxation des muscles anococcygiens de souris et la contraction de l'aorte de rat,[135, 136, 152] l'UII est également capable de provoquer des actions spasmogéniques, prolifération, angiogénique et myotropique.[157, 158] Notamment, différentes études *ex vivo* ont clairement démontré que l'UII était le plus puissant vasoconstricteur jamais identifié.[159, 160] Ce dernier est en effet 10 à 100 fois plus puissant que l'endothéline sur les mêmes tissus.[159,

[160] L'injection d'UII *in vivo* à divers mammifères conscients provoque des actions hypotensives pouvant conduire à un collapse cardio-respiratoire.[135, 136, 146, 158] D'autres effets ont également été rapportés sur le pancréas avec notamment une inhibition de la sécrétion d'insuline induite par le glucose, sur le coeur avec des effets inotropiques et hypertrophiques ou encore sur les reins avec une régulation des processus osmorégulateurs.[161] Au niveau du système nerveux central, l'administration d'UII par voie intracérébroventriculaire provoque des effets cardiovasculaires, ainsi que des actions endocrines et comportementales (stress et anxiété).[162-165]

1.4.3. Récepteur UT

L'UII et l'URP sont les deux ligands endogènes d'un récepteur couplés aux protéines G (famille 1A des RCPG initialement connu sous le terme GPR14 et récemment rebaptisé UT).[166] Le récepteur UT humain et de singe sont composés de 389 résidus contrairement aux récepteurs murins qui n'en comportent que 386.[149] Ce récepteur, comme tous ceux appartenant à la classe A des 7TMRs (famille de*s récepteurs apparentés à la rhodopsine*), est constitué d'un segment *N*-terminal court (54 acides aminés chez l'homme), d'un résidu Asp dans le TM2 essentiel dans l'interaction avec le ligand, d'un motif D/ERY à la jonction entre TM3 et IL2 responsables du « ionic lock » et de multiples sites possibles de phosphorylation Ser/Thr dans IL3 et le segment *C*-terminal. Il existe également un pont disulfure entre Cys^{123} et Cys^{119} reliant EL1 et EL2 ainsi que deux sites de glycosylations dans le segment *N*-terminal au niveau des Asn^{29} et Asn^{33} [167]. Chez l'homme, le récepteur UT est, comme ses ligands, exprimé dans le système nerveux central ainsi que dans les systèmes cardiovasculaire, hépatique et rénal.[159, 166, 168, 169] Récemment, et comme pour l'angiotensine et l'endothéline, des récepteurs fonctionnels UT ont été décrits dans l'environnement périnucléaire des cellules nerveuses et cardiaques.[170, 171]

1.4.4. Rôle du système urotensinergétique

Le système urotensinergique joue un rôle déterminant dans la régulation de divers processus physiologiques au niveau du système cardiovasculaire, du système nerveux central et du système endocrine..[143, 157, 165, 166, 172, 173]

De par ces vastes actions pléiotropes, ce système apparait comme une cible privilégiée pour certaines pathologies[165, 174], dont le diabète[165], les dysfonctions rénaux[175], mais surtout les pathologies cardiovasculaires. En effet, l'UII joue un grand rôle dans l'homéostasie cardiovasculaire, l'hypertrophie des cardiomyocytes, l'insuffisance cardiaque[176], l'athérosclérose[177, 178], la fibrose cardiaque[179] et d'autres maladies cardiovasculaires.[143, 170, 180] En accord avec ces observations, des taux circulants d'UII et d'URP élevés ont été mesurés chez des patients atteints d'hypertension.[181] De façon similaire, lors d'insuffisances cardiaques ou rénales ou encore chez des patients atteints de diabète de type 2, les taux plasmatiques d'UII et URP combinés sont très élevés.[165, 182]

Au niveau du système nerveux central, le système urotensinergétique pourrait être impliqué dans le contrôle de la fonction cardiaque, mais également de troubles psychologiques. En effet, concernant ce dernier point, l'UII est en effet capable de stimuler la production de norépinephrine, sur des coupes cérébrocorticales.[164] Cependant, peu d'études ont été consacrées aux rôles joués par ce système au niveau du système nerveux central.

Depuis sa découverte, l'URP a toujours été considéré comme un peptide redondant de ce système dont l'expression serait restreinte à certains organes. Cependant, il fut récemment suggéré que l'UII et l'URP en se liant à leur récepteur UT pourraient induire une sélectivité fonctionnelle au niveau de leur signalisation qui pourrait résulter en une implication différente de ces deux peptides en conditions physiologiques, mais surtout physiopathologiques.[159, 183] Le système urotensinergique semble jouer un rôle important dans la mise en place et la progression de diverses pathologies dont l'athérosclérose[177], le diabète de type II[184] ou encore certains cancers[185-187]. Dans toutes ces pathologies, une élévation des concentrations plasmatiques associées à une immunoréactivité de type UII a été relevée. Il est important de noter que les concentrations d'UII sont détectées par immunofluorescence en employant des anticorps incapables de discerner l'UII de l'URP résultant ainsi en une mesure globale[181]. Afin de séparer UII et URP, les auteurs ont développé une méthode de séparation chromatographique de ces deux peptides qui a permis de démontrer que les taux circulant d'UII et d'URP, chez des patients atteints d'insuffisance cardiaque sévère, étaient chacun

significativement plus élevés chez les patients atteints d'insuffisance cardiaque, et que chez ces patients la concentration d'URP était 10 fois supérieure à celle d'UII[181]. Il est également important de noter que l'UII mais pas l'URP est capable (1) de stimuler *in vitro* la prolifération d'astrocytes de rats, ce que n'entraîne pas l'URP[188], (2) de réduire la contractilité du ventricule gauche de cœurs de rats ischémiés[189] et (3) d'augmenter l'activité transcriptionnelle sur des noyaux isolés de cardiomyocytes[190]. L'ensemble de ces observations supporte un rôle biologique distinct de ces deux peptides et suggère l'importance de comprendre et de contrôler les voies de signalisation spécifiquement activées par ces peptides. Pour cette raison, il est important de développer des antagonistes capables de moduler sélectivement les activités biologiques associées à chaque peptide.[191]

1.4.5. Étude de relations de structure-activité

Le développement de composés à des fins pharmacologiques et/ou thérapeutiques repose initialement sur des études de relations structure-activité afin de bien comprendre les mécanismes essentiels responsables de l'interaction et de l'activation d'UT par ces ligands endogènes UII et URP. Ce type d'études commence généralement par la réalisation d'un « Ala-scan », et d'un « $_D$-scan » qui consistent à remplacer chacun des acides aminés par une alanine (afin d'évaluer l'impact des chaînes latérales de chaque acide aminé sur le mode d'action) ou par l'isomère D de l'acide aminé étudié (influence de la configuration).[153] Ces nouveaux analogues de l'hUII et URP ont alors été testés pour leur capacité à se lier au récepteur UT humain et pour leur capacité à induire la contraction d'anneaux d'aorte de rat. Les résultats ont ainsi démontré l'importance des résidus intracycliques de l'UII et URP dans la liaison et l'activation d'UT.[153, 192] Au cours de ces études, il fut démontré que le remplacement de la Lys à la position 8 par une ornithine dans UII permettait d'accéder à des antagonistes de ce système. Toutefois, dépendamment du modèle cellulaire utilisé, ce composé s'est avéré posséder une activité résiduelle consistante avec le profil d'un agoniste partiel.[153, 154, 193,182, 194] La conclusion de ses études de relations structure-activité suggère que le centre névralgique de l'activité

biologique de l'hUII et de l'URP est la triade intracyclique Trp-Lys-Tyr avec la Lys comme axe central de l'interaction avec UT.[154]

Les analyses de conformations de l'UII lors de l'interaction avec le récepteur UT démontre que la liaison avec la région *N*-terminal de l'UII provoque un changement de conformation du récepteur UT, pour accueillir la partie *C*-terminal du peptide, ce qui suggère que le cycle adopte un β-tour à l'intérieur de la poche de liaison.[195] Pour la liaison au récepteur, l'URP semble agir différemment, dû à l'absence de la région *N*-terminal et ce qui suggère que l'URP adopte un tour-γ dans le cycle.[13, 183] L'étude de conformations par spectroscopie RMN en milieux aqueux de l'URP et l'hUII a démontré que le segment Trp-Lys-Tyr adopte un tour-γ inversé (Figure 1.8).[13, 14, 196]

Figure 1.8: Représentation du tour-γ inverse entre Trp-Lys-Tyr de l'hUII.

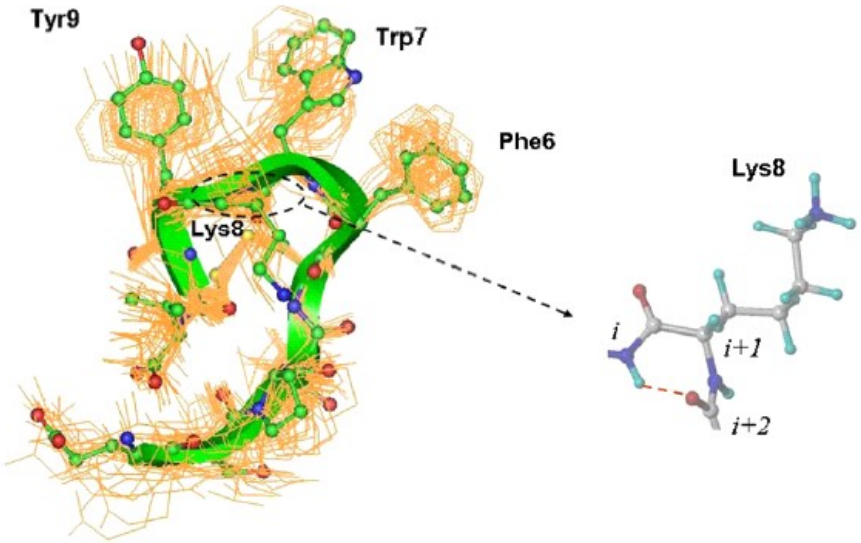

1.4.6. Agoniste

Les études précédentes ont ainsi permis le développement de quelques agonistes peptidiques par exemple le dérivé P5U **61** caractérisé par le remplacement de la Cys à la position 5 de l'UII(4-11) par une pénicillamine (Pen; *β*,*β*-dimethylcystéine): H-Asp-c**[Pen-Phe-Trp-Lys-Tyr-Cys]**-Val-OH (Figure 1.9).[197] Cet agoniste a un pK_i de 9.6 et un pEC_{50} de 9.6 (comparé à l'UII 9.1 et 8.3), déterminé des essais de contraction sur des aortes de rat, ce qui leur confrère une bonne affinité et une activité intrinsèque pour le récepteur UT. [27,50,69,70] L'analyse par spectroscopie RMN de P5U en combinaison à la

modélisation a permis de déterminer qu'il mime de près la conformation liée au récepteur du naturel ligand.[197] Les premiers agonistes non peptidiques, initialement identifiés par screening de chimiothèque, ont été mis au point, par Acadia Pharmaceuticals et sont caractérisés par la présence d'une lactone (Figure 1.9).[198] Dans la littérature, c'est le AC7954 **62** qui s'est démarqué, dont la forme racémique a un pEC_{50} de 6.5 et plus particulièrement, l'énantiomère (+)-AC7954 **62** avec pEC_{50} de 6.6, comparativement à 11.3 pour UII humain, les essais sont déterminés sur des cellules exprimant le récepteur UT humain.[27,50,67,69,70] La découverte de ces premiers agonistes non peptidiques a ainsi mené au développement de nouvelles molécules dont le composé (+)-FL104 **63** lequel présente un pEC_{50} de 7,49 avec une efficacité de 116 % (Figure 1.9).[199] Plusieurs autres agonistes du récepteur UT ont été développés, en se basant sur AC7954 et de FL104.[14, 200]

Figure 1.9: Quelques exemples peptidiques et non peptiques d'agonistes de l'UII.

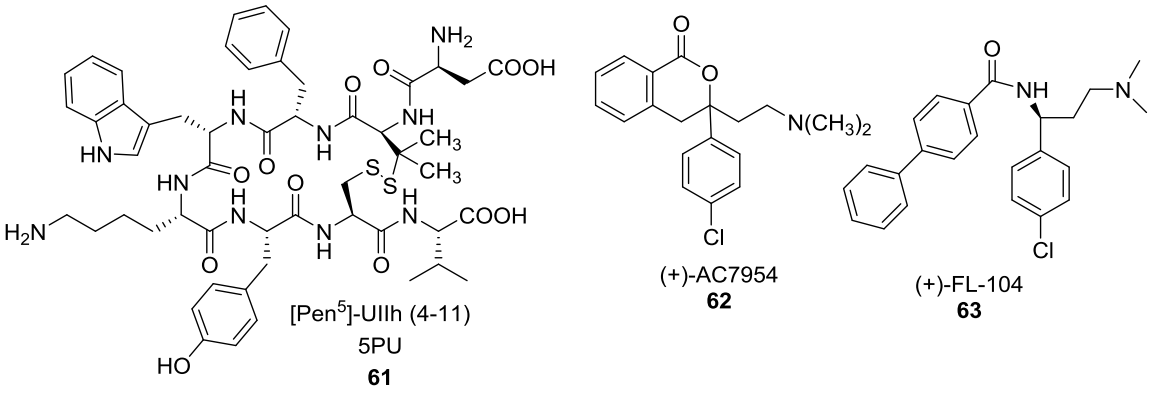

1.4.7. Antagoniste

Le développement d'un antagoniste peptidique ou non peptidique est plus fastidieux et à ce jour peu d'antagonistes efficaces du système urotensinergique sont disponibles.[191] Plusieurs raisons, incluant la complexité de la pharmacologie de ce système, mais surtout les différences d'efficacité inter-espèces observées, sont responsables de cette situation.[172, 189, 201] Malgré tout, quelques composés peptidiques et non peptidiques présentent tout de même un certain attrait.

Notamment, l'antagoniste peptidique dénommé urantide (**64**; Asp-*c*[Pen-Phe-*D*-Trp-Orn-Tyr-Cys]-Val-OH) est capable, de l'ordre du nanomolaire, de bloquer des concentrations dans divers modèles *in vitro* les différentes actions provoquées par l'interaction de l'UII avec UT (Figure 1.10).[153, 202, 203] L'urantide s'est avéré tout aussi capable de bloquer les actions induites par l'activation du système urotensinergique *in vivo*, dans des modèles murins d'athérosclérose ou d'hypertension artérielle pulmonaire.[204-207]

Le palosuran (ACT-058362; **65**) est un antagoniste non peptidique possédant une bonne affinité (IC_{50} = 67 nM) pour le récepteur UT humain (Figure 1.10).[208, 209] En revanche, bien que présentant un excellent potentiel *in vitro*, ce composé s'est avéré incapable d'améliorer la condition de patients atteints de néphropathie diabétique dans le cadre d'un essai en phase clinique II mené par Actelion Pharmaceuticals.[175, 208, 210, 211] À ce jour, le palosuran **65** est le seul antagoniste non peptidique à avoir atteint la phase II dans des études cliniques.[191] GlaxoSmithKline a également développé quelques antagonistes non peptidiques[182, 208, 212], dont le GSK1440115 **66**[213] (Figure 1.10) et le GSK1562590[213], qui présentent une excellente sélectivité et affinité (K_i de 8,38 et de 9,46, respectivement) pour le récepteur UT. Le GSK1440115 **66** été évalué, sans succès, au cours d'un essai clinique de phase I comme traitement potentiel de l'asthme.[191] À partir du GSK1440115, le composé GSK1562590 a été développé et présente un profil unique en son genre puisque ce dernier est caractérisé par une très lente dissociation du récepteur UT, provoquant ainsi une réduction de l'efficacité de contractions pouvant se prolonger jusqu'à 24 heures, mais sans aucune étude clinique à ce jour.[213] Takeda Chemical Industries a également développé en utilisant une structure de type benzazepine **67** antagoniste non peptidique très affin pour l'isoforme humaine de l'UT avec un IC_{50} de 2 nM (Figure 1.10).[14, 157, 214] Malheureusement, aucun essai clinique n'a été rapporté à ce jour.

Figure 1.10: Quelques exemples peptidiques et non peptiques d'agonistes et d'antagonistes de l'urotensin II.

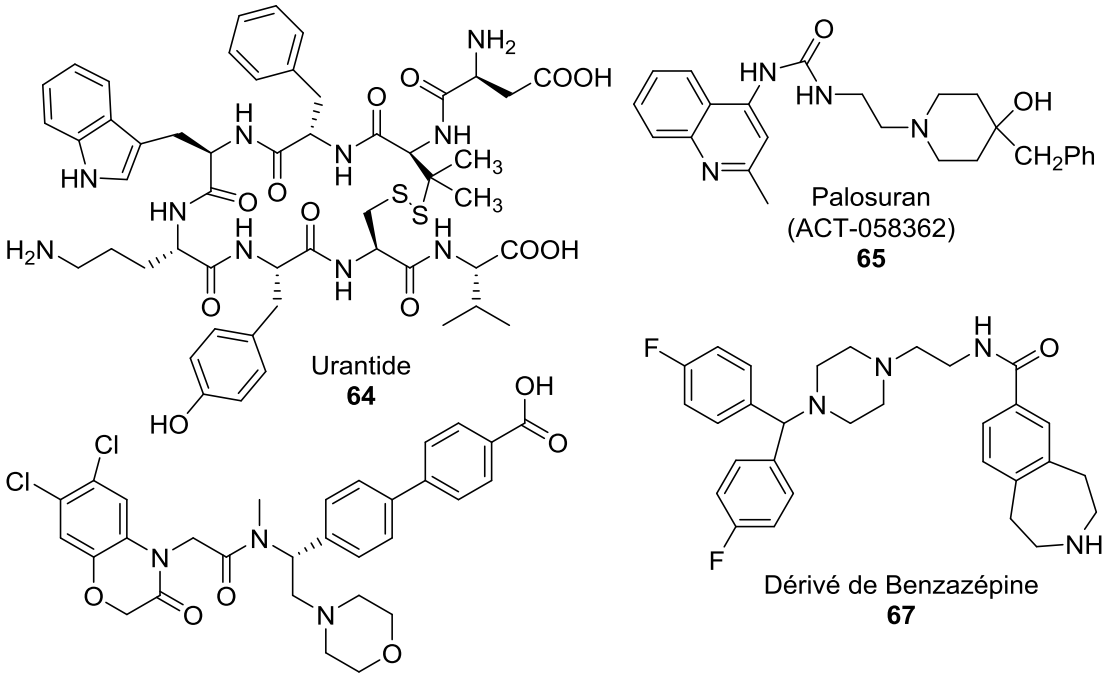

Aux meilleurs de nos connaissances, les composés agonistes et antagonistes, peptidiques et non peptiques, **61** à **67**, agissent comme des ligands orthostériques du récepteur UT puisqu'ils semblent se lier dans la même poche orthostérique que le ligand naturel, l'UII. De plus, aucun de ces dérivés ne fut testé quant à leur capacité à bloquer les effets de l'URP. En ne faisant aucune différenciation entre l'UII et l'URP lors des tests biologiques, ils ratent des informations importantes, puisque l'UII et l'URP jouent des rôles distincts dans certaines pathologies, dont l'hypertension, ce qui pourraient expliquer les résultats obtenus lors des essaies cliniques.

1.4.8. Urocontrine et Urocontine A

Contrairement aux ligands orthostériques, les dérivés allostériques se lient habituellement sur des sites éloignés du site de liaison naturelle, ce qui affecte la

conformation du récepteur et modifie par la même les interactions avec les ligands naturels et les protéines effectrices requises pour l'activation des voies de signalisation intracellulaire.[216, 217] Ce type de modulateur devrait présenter, d'un point de vue théorique, une grande sélectivité vis-à-vis du récepteur d'intérêt et des effets secondaires réduits.[216, 218] En considérant que l'UII et l'URP peuvent induire une fonctionnalité sélective, ils pourraient donc contribuer de façon différente au développement et à la progression de certaines maladies cardiovasculaires.[183, 191] Par conséquent, et en rapport avec les pathologies décrites précédemment, la modulation sélective des signaux activés par UII et/ou URP pourrait représenter une voie prometteuse pour le traitement de l'athérosclérose et l'hypertension artérielle pulmonaire.[157, 165, 178, 179, 204, 207, 219]

Au cours des 5 dernières années, deux peptides agissants comme des modulateurs allostériques, l'urocontrine ([Bip^4]URP) **68** et l'urocontrin A ([Pep^4]URP) **69**, ont été développés (Figure 1.11).[183, 191, 215, 220] Sur les aortes de rats, l'urocontrine et l'urocontrine A sont capables de réduire l'efficacité des contractions induites par l'hUII sans moduler celles provoquées par l'URP.[183, 215]

Figure 1.11: Urocontrine et Urocontrine A.

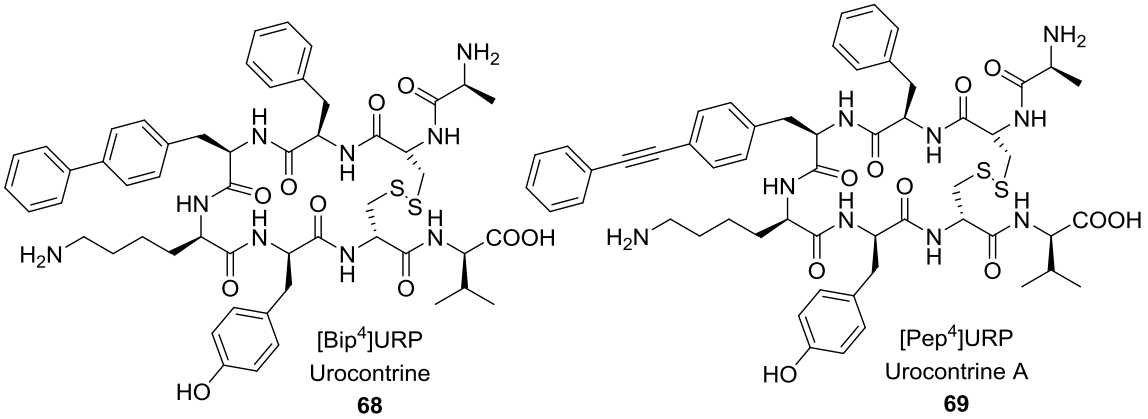

Dans la littérature, il n'existe à ce jour aucune petite molécule reconnue comme modulateur allostérique du système urotensinergique. Le pharmacophore de ces dérivés de type urocontrin étant très proche de celui de l'UII et de l'URP, nous avons émis l'hypothèse qu'il serait possible d'accéder à des modulateurs allostériques en utilisant un mime du tour-γ inverse ainsi que certains pharmacophores de la triade Trp-Lys-Tyr. Sur

la base des dérivés peptidiques décrits dans la littérature, nous avons également supposé que le remplacement du Trp par un résidu de type Bip ou Pep pourrait représenter une voie d'accès à ce type de modulateur.

1.4.9. Méthodologie

L'évaluation des composés peptidiques et non peptidiques du système urotensinergique inclut généralement des tests *in vitro* et *ex vivo*. Les tests *in vitro* sont effectués sur des cellules humaines ou animales, qui expriment le récepteur UT humain de façon endogène ou alors après transfection par exemple les cellules CHO-hUT, HEK293-hUT ou SJRH30.[13, 194, 209, 213, 215] L'interaction entre l'activité et l'affinité de récepteur UT cellulaire et le composé testé peuvent se mesurer par le dosage du calcium par fluorométrie, car l'hUII augmente le calcium intracellulaire, ou par un test de liaisons entre le composé testé, hUII radiomarqué avec ^{125}I et le récepteur UT.[194, 209, 215] Les essais de liaisons par compétitivité permet d'évaluer l'affinité du composé pour le récepteur UT, soit en empêchant la liaison de l'hUII radiomarqué au récepteur UT ou en favorisant la liaison de l'hUII radiomarqué au récepteur UT, tout en comparant à la liaison spécifique de l'hUII.

L'évaluation par *ex vivo* des composés développés se fait généralement sur les aortes de rat, afin de vérifier s'ils peuvent provoquer la contraction de l'aorte, ce qui démontrait une activité agoniste, ou s'ils peuvent empêcher les contractions provoquées par l'hUII, ce qui démontrait une activité antagoniste. De plus, l'activité modulation allostérique est vérifiée s'ils peuvent modifier le profil de vasoconstriction de l'hUII et de l'URP, présenté à la figure 1.12.

Figure 1.12: Courbe dose-réponse de vasocontraction pour l'hUII et l'URP sur l'aorte de rats.

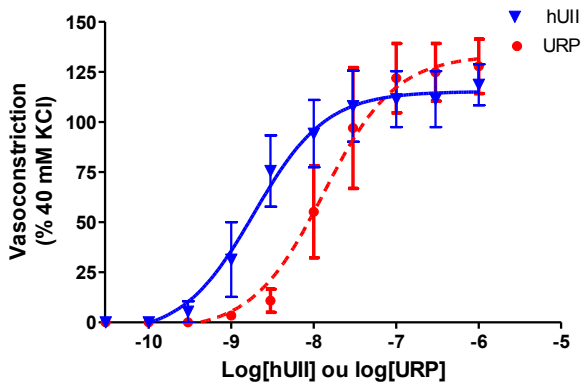

Contraction de l'aorte (hUII)				Contraction de l'aorte (URP)			
n	E_{max} (%)	EC_{50} (nM)	pEC_{50}	n	E_{max} (%)	EC_{50} (nM)	pEC_{50}
4	115 ± 3	1.89	8.72 ± 0.09	3	133 ± 5	13	7.88 0.09

Les modulateurs allostériques sont typiquement des ligands non compétitifs qui se lient à un site différent de celui du ligand endogène, et peuvent ainsi modifier la fonction du récepteur. L'affinité (pKb) d'un antagoniste non compétitif est déterminée en utilisant la méthode de Gaddum, dans laquelle les concentrations égales-actives de l'agoniste en l'absence et en présence de l'antagoniste non compétitif ont été comparés en utilisant une régression linéaire.[221]

1.5. But

Initialement, le projet de maîtrise consistait à développer une librairie de pyrrolo[3,2-*e*][1,4]diazépin-2-ones sur la résine de Wang et de les tester *in vivo* et *ex vivo* pour leur activité biologique sur une cible biologique qui restait à déterminer. La librairie était constituée de différentes amines, acide aminé et d'aldéhyde pour construire le pyrrolo[3,2-*e*][1,4]diazépin-2-one. Finalement, la cible biologique fut déterminée, le système urotensinergique. Le système urotensinergique semble être une bonne cible pour tester les pyrrolo[3,2-*e*][1,4]diazépin-2-ones puisque les pyrrolo[3,2-*e*][1,4]diazépin-2-

ones miment le tour-γ inverse et que la partie active UII forme également un tour-γ inverse. Pour cette première librairie, les résultats des tests biologiques n'ont donné rien de guère intéressant.

Suite à ces résultats, le projet de maîtrise a été poussé aux développements de mimes de l'UII et de l'urocontrin, un peptide développé par l'équipe de David Chatenet, où le tryptophane est remplacé par le 4,4'-biphenylalanine et qui a une activité reconnue sur le système urotensinergique. Cette nouvelle librairie pourra vérifier le postulat qu'en mimant la géométrie et les substituants de la partie active de l'UII, les pyrrolo[3,2-*e*][1,4]diazépin-2-ones pourraient moduler le système urotensinergique. Cette nouvelle librairie sera composée de la tyramine, pour mimer la tyrosine, de la lysine et de l'ornithine, et de la biphényl-4-carboxaldéhyde, du 1- et 2-naphthylaldéhyde pour mimer le 4,4'-biphenylalanine. Pour la synthèse de cette nouvelle librairie, la résine de Wang est envisagée, car il permet d'éviter les problèmes de clivage rencontré sur la résine de Merrifield. Ces nouveaux pyrrolo[3,2-*e*][1,4]diazépin-2-ones mimes de l'urocontrin seront testés *ex vivo* et *in vivo* par moi dans les laboratoires à l'IRNS de l'équipe de David Chatenet.

2. Chapitre 2 : De novo conception of small molecule modulators based on endogenous peptide ligands. Pyrrolodiazepin-2-one γ-turn mimics that differentially modulate urotensin II receptor-mediated vasoconstriction ex vivo

De novo conception of small molecule modulators based on endogenous peptide ligands. Pyrrolodiazepin-2-one γ-turn mimics that differentially modulate urotensin II receptor-mediated vasoconstriction *ex vivo*

Julien Dufour-Gallant[a,b], David Chatenet[b]*, William D. Lubell[a]*

[a] Département de Chimie, Université de Montréal, C.P. 6128, Succursale Centre-Ville, Montréal, Québec H3C 3J7, Canada, [b] INRS – Institut Armand-Frappier, Groupe de Recherche en Ingénierie des Peptides et en Pharmacothérapie (GRIPP), Université du Québec, Ville de Laval, Québec, Canada

2.1. Abstract

A proof-of-concept library of pyrrolodiazepinone small molecules was designed based on the Bip-Lys-Tyr motif found in a recently described modulator of the urotensinergic system. Solid-phase synthesis provided 13 analogs, which were tested for their ability to modulate selectively and differentially the potency (EC_{50}) and the efficacy (E_{max}) of hUII and URP *ex vivo* in a rat aortic ring bioassay. Notably, at 14 µM, pyrrolodiazepinone *R*-**80a** inhibited completely hUII-induced contractions and increased URP-associated vasoconstriction. Pyrrolodiazepinone *R*-**80a** represents to the best of our knowledge the first-in-class small molecule that exerts a probe-dependent effect on hUII and URP biological activities, and proves that UT modulators of the urotensin II receptor (UT) can be rationally designed. The importance of the UT system in the pathogenesis and progression of cardiovascular diseases highlights the utility of pyrrolodiazepinones such as *R*-**80a**, which exhibit promising potential as tools for differentiating the respective roles, signalling pathways and phenotypic outcomes of UII and URP in the UT system.

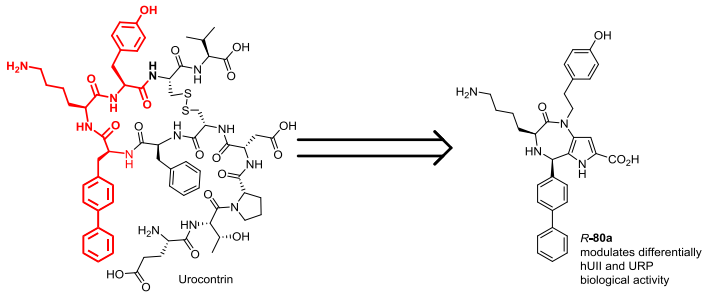

2.2. Introduction

Peptides play essential roles that are crucial for proper body function. Inherent in their native structures are however pharmacokinetic properties, such as short half-life *in vivo* and limited oral availability that restrict their application as drugs. Over the past thirty years, chemists have modified these poly-amides to gain insight and prototypes for developing small-molecule surrogates, so-called peptidomimetics,[30, 35, 222-225] that maintain the attributes of native peptides without their limitations. Although significant efforts have been made respectively to control peptide backbone conformation and to modify side chains with rigid and functional molecular surrogates, few examples have demonstrated success in the rational replacement of the complete peptide structure by a peptidomimetic small molecule. In such cases, an organic scaffold serves typically to orient the side chains necessary for molecular recognition of the peptide. For example, bicyclo[2.2.2]octane (e.g., **70**),[226] cyclohexane (e.g., **71**),[227] and β-D-glucose (e.g., **72**)[228-230] have been respectively employed as scaffolds in mimics of enkephalin, thyrotropin-releasing hormone, and somatostatin (Figure 2.1). In addition, certain molecules, so-called "privileged structures",[35, 36, 231, 232] such as benzodiazepines (e.g., **73**) have exhibited notable affinity for receptors that bind peptides, likely due to their capacity to mimic natural peptide conformations frequently involved in protein recognition.

Figure 2.1: Small molecule peptidomimetics **70-72** and "privileged structure" benzodiazepine **73**.

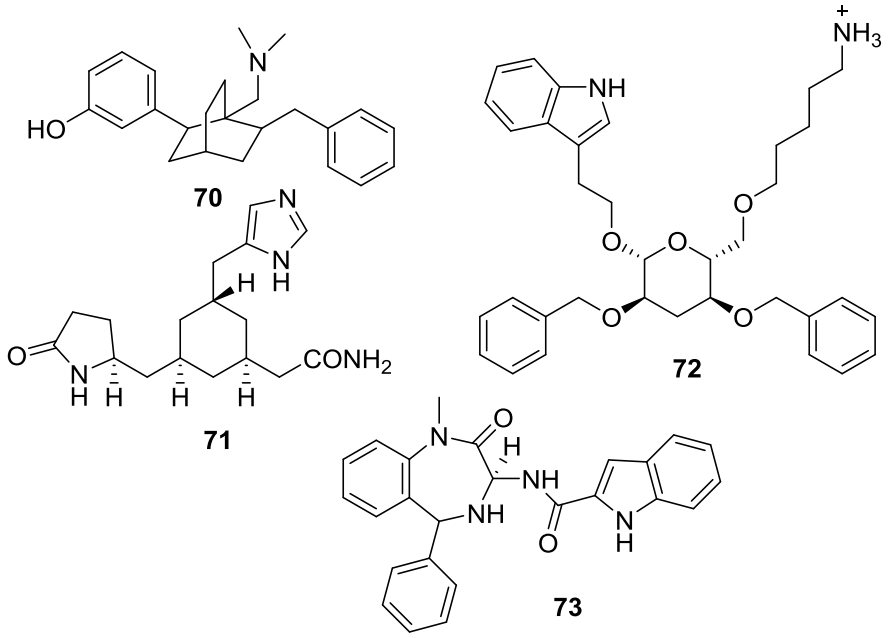

The urotensin II receptor (UT) is a member of the class 1A G protein-coupled receptor (GPCR) family and binds, in humans, two endogenous cyclic peptide ligands: urotensin II (hUII, H-Glu-Thr-Pro-Asp-*c*[Cys-Phe-Trp-Lys-Tyr-Cys]-Val-OH) and urotensin II-related peptide (URP, H-Ala-*c*[Cys-Phe-Trp-Lys-Tyr-Cys]-Val-OH).[143] Expressed in the circulatory, excretory and central nervous systems in humans,[143] the so-called urotensinergic system plays a determining role in the physiological regulation of various organs and tissues, particularly in the cardiovascular system.[172] In the cardiovascular system, both UII and URP have been implicated in various symptoms of hypertension and atherosclerosis, including vasoconstriction,[233] positive inotropic and chronotropic responses,[234, 235] salt and water retention,[236] accumulation of collagen and fibronectin,[237, 238] formation of macrophage foam cell[239] and induction of cardiac and vascular hypertrophy.[240] For example, deletion of the UII gene in an apolipoprotein E

knockout model of atherosclerosis attenuated the initiation and the progression of the disease.[241] Antagonism of UT has conferred vasoprotective action in diabetes-associated atherosclerosis.[242] Moreover, in monocrotaline-induced pulmonary arterial hypertension, UT antagonists have alleviated the sequalae associated with disease progression.[206, 207, 243] Consequently, the UT system exerts crucial roles in the etiology and the progression of cardiovascular and pulmonary diseases, which have only begun to be identified in recent years.[165, 241, 243]

All UIIs and URPs share a conserved C-terminal cyclic hexapeptide, but their *N*-terminal region is variable both in length and sequence. Previous structure-activity relationship (SAR) studies have highlighted the critical role played in both the recognition and activation of UT by the conserved intra-cyclic residues of UII and URP.[153, 244] In particular, the Trp-Lys-Tyr triad has been linked to the molecular pharmacology of both UII and URP. Upon binding of the *N*-terminal region of UII, the receptor may however undergo a conformational change to accommodate the *C*-terminal domain of the peptide, the cycle of which has been suggested to adopt an inverse γ-turn within a specific binding pocket.[245] Receptor binding may likely occur differently for URP, which lacks the *N*-terminal region.[13, 183] Hence, in accordance with the concept that particular ligand-induced receptor conformational changes can lead to the activation of specific signaling pathways, UII and URP have been observed to induce common and divergent physiological actions probably through the recruitment of specific subsets of secondary messengers that are dependent on the ligand-induced UT conformation.[172, 189, 246] For example, UII and URP exert different actions upon transcriptional modulation,[246] cell proliferation,[172] and myocardial contractile activities.[189] Furthermore, distinct

pathophysiological roles for UII and URP in hypertension have been indicated by the specific up-regulation of the mRNA of the latter in the aorta and kidney of spontaneously hypertensive rats.[201] In patients with acute heart failure, both UII and URP plasma levels were observed to increase; however, the concentration of the latter was almost 10 times higher, suggesting distinct processing of their precursor proteins and different roles for each peptide in pathological conditions.[181] Each ligand could thus be functionally selective and differentially participate in the etiology of a specific cardiovascular disease.[183, 247]

Programs targeting UT have led to the development of peptide agonists (e.g., [Pen^5]hUII(4-11)),[157, 182, 197, 248] and antagonists (e.g., [Pen^5, D-Trp^7, Orn^8]hUII(4-11) also termed urantide),[157, 202, 203, 220] as well as non-peptide agonists [e.g., (+)-AC7954],[157, 182, 198] and antagonists (e.g., palosuran, GSK1562590, and GSK1440115).[208,213] Unfortunately, to the best of our knowledge, none among them has been able to discriminate UII- and/or URP-mediated biological activities. Peptide-based allosteric modulators derived from the URP sequence (e.g., urocontrin ([Bip^4]URP) and urocontrin A ([Pep^4]URP), Bip = 4,4'-biphenylalanine; Pep = (phenylethynyl)phenylalanine)) have been recently described.[183, 220] These peptide derivatives possess the striking ability to decrease the maximal contractile response of hUII without significant change in its potency and without noticeable effect on URP-induced vasoconstriction. Hence, a new paradigm in drug discovery focuses on identifying potent and selective non-peptide UT ligands that modulate UII- and/or URP-associated functions.

Pyrrolodiazepinones, initially identified in microorganisms, are a subclass of diazepin-2-ones that exert a wide range of biological activity.[130, 249, 250] X-ray analyses

have shown that the amino acid moiety in the pyrrolo[3,2-*e*][1,4]diazepin-2-one scaffold may adopt dihedral angles corresponding to an ideal inverse γ-turn in the solid state.[1, 8, 251] Considering that γ-turn secondary structures play important roles in the recognition and activation of GPCRs by their endogenous ligands,[22-16] pyrrolodiazepinone activity may stem from mimicry of this natural privileged structure.

In pursuit of small molecule UT ligands, a proof-of-concept library of pyrrolo[3,2-*e*][1,4]diazepin-2-ones was designed to mimic the Bip-Lys-Tyr sequence of urocontrin. Employing a criteria for peptide to peptidomimetic transformation,[4] the pyrrolodiazepin-2-one heterocycle was constructed using tyramine, basic amino acids and aromatic aldehydes to mimic and orient the side chains in the biologically active turn conformation. After synthesis by a solid-phase approach on Wang resin, X-ray crystallographic analysis confirmed the potential of the pyrrolo[3,2-*e*][1,4]diazepin-2-one scaffolds to mimic the γ-turn conformation. The pharmacological profiles of the pyrrolodiazepinones were tested *in vitro* using a competitive binding assay in CHO-*h*UT cells and *ex vivo* using a rat aortic ring bioassay. The results of this examination validate the design strategy, which has provided a set of small-molecules that selectively modulate UII- and URP-associated biological activity.

2.3. Result and Discussion

Pyrrolo[3,2-*e*][1,4]diazepin-2-ones were designed to mimic the Bip-Lys-Tyr sequence and synthesized by employing a solid-phase approach featuring a Pictet-Spengler cyclization and cleavage reaction from Wang resin.[123] Different aromatic aldehydes (e.g., *p*-phenylbenzaldehyde, 1- and 2-naphthaldehyde) were employed to

mimic and explore the chemical space of the biphenyl residue. Lysine and ornithine were respectively used as the basic amino acid component. Tyramine was employed as a tyrosine residue surrogate. The synthesis of the proof-of-concept library began with 4-oxo-*N*-(PhF)proline Wang resin **74** [PhF = 9-(9-phenylfluorenyl)],[123] which was placed in MacroKans™ and treated with an excess of tyramine and a catalytic amount of *p*-TsOH in degassed THF for 24 h at 55°C (Scheme 2.1). After filtration of the resin, evaporation of the filtrate and purification by column chromatography, released PhFH was weighed to determine the resin loading of 4-aminopyrrole **75** (0.89 mmol/g).[119, 120] The quality of 4-aminopyrrole **75** was further characterized after acetylation of an aliquot of resin with acetic anhydride and DIEA in dry DMF at room temperature,[130] by cleavage with a 0.44 M NaOMe in 9:1 THF/MeOH, and RP-HPLC-MS analysis, which demonstrated 4-acetamidopyrrole **81** to be of 93% purity contaminated with 3% of 4-hydroxy-*N*-(PhF)proline (Scheme 2.2).

Scheme 2.1: Synthesis of pyrrolo[3,2-e][1,4]diazepin-2-one on Wang resin.

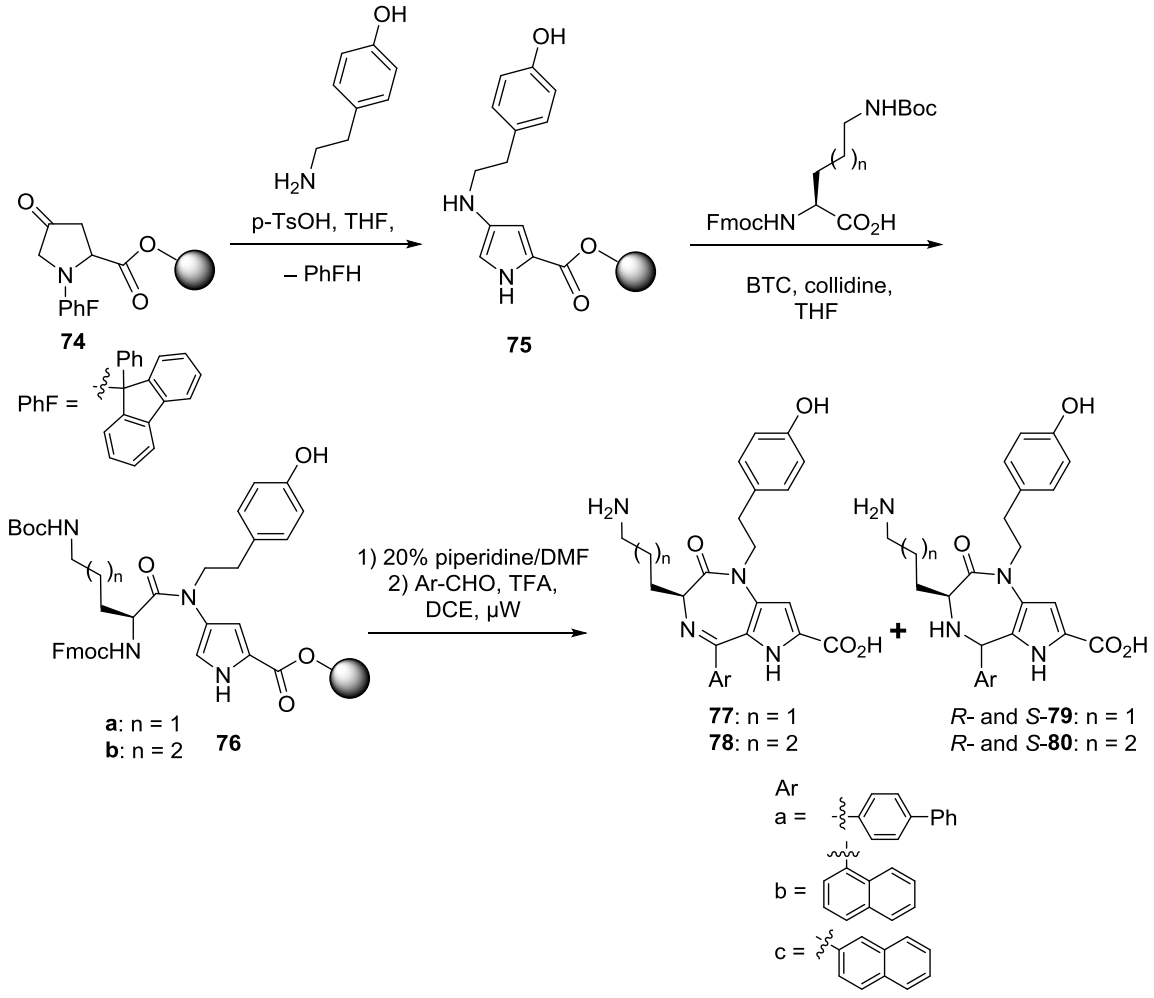

Scheme 2.2: Acetylation and cleavage of aminopyrrole **75** and amidopyrrole **76**.

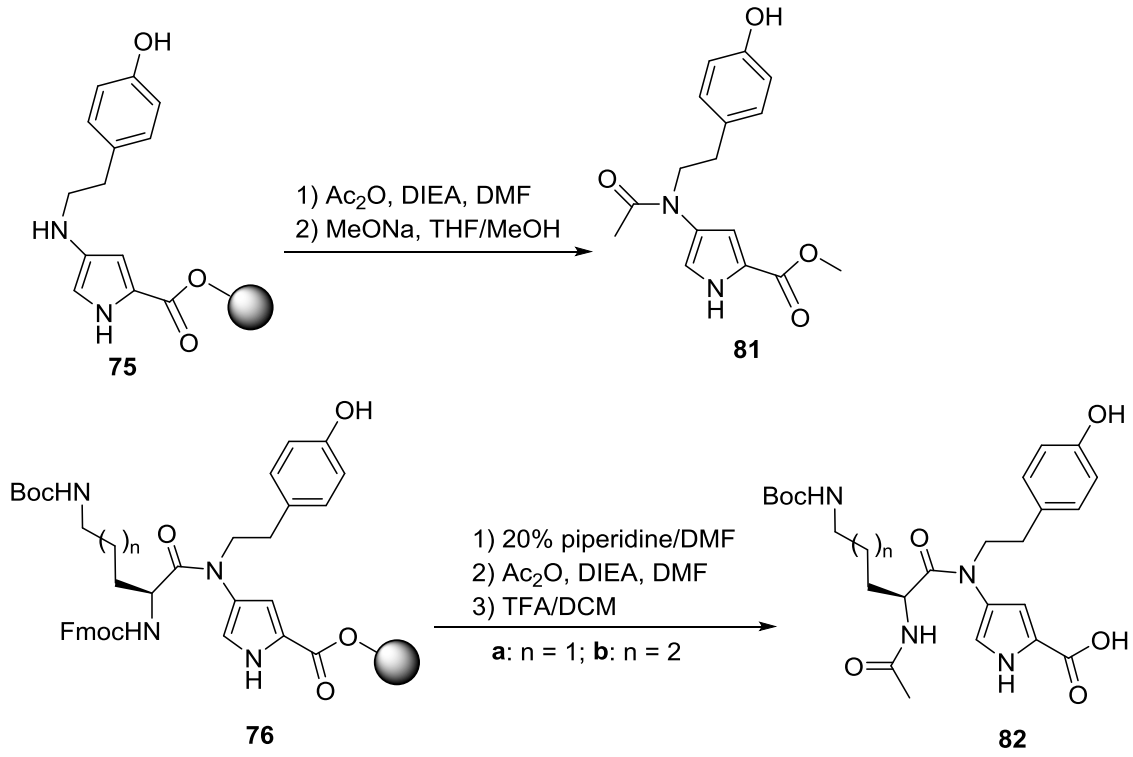

Aminoacylation of 4-aminopyrrole-2-carboxylate resin **75** with Fmoc-Lys(Boc) and Fmoc-Orn(Boc) was respectively performed using BTC and 2,4,6-collidine in THF for 15 h.[121] Coupling efficiency was evaluated after Fmoc removal using 20% piperidine in DMF, acetylation with Ac_2O and DIEA in DMF, resin cleavage using 1:1 TFA/DCM and LC-MS analysis, which found **82a** and **82b** to be of 93% and 92% purity respectively. After Fmoc removal with 20% piperidine in DMF, amidopyrrole resins (100-150 mg) were heated with different aldehydes (20 eq.) and TFA in dichloroethane at 75°C using microwave irradiation for 3.5 h (Scheme 2.1). Excess aldehyde was necessary to convert all amidopyrrole resin to pyrrolo[3,2-*e*][1,4]diazepin-2-one product, which included both saturated pyrrolo[3,2-e][1,4]diazepin-2-ones *R*- and *S*-**79** and *R*- and *S*-**80** and their unsaturated counterparts **77** and **78**. The acid labile Wang resin was cleaved

under the acidic conditions of the Pictet-Spengler reaction.[123] After the Pictet-Spengler reaction, a series of pyrrolo[3,2-e][1,4]diazepin-2-ones were isolated in 3-8% overall yields from Wang resin by preparative RP-HPLC as described in the experimental section (Figure 2.2). Although higher selectivity and yield have been obtained using optimized conditions,[21a, 24] for this proof of concept library, the formation of separable mixtures of analogs was looked at as a favourable means for obtaining a library to study structure-activity relationships.

Figure 2.2: Isolated yields of pyrrolo[3,2-*e*][1,4]diazepin-2-ones from synthesis on Wang resin.

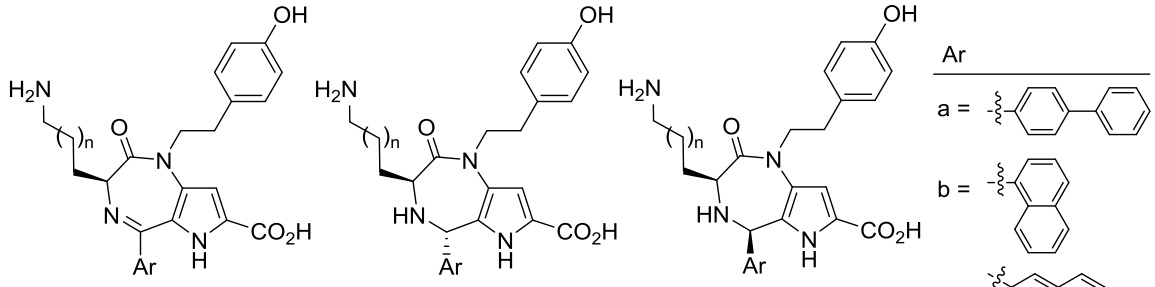

77a: n = 1 (8%)
77b: n = 1 (8%)
77c: n = 1 (8%)
78a: n = 2 (6%)
78b: n = 2 (8%)
78c: n = 2 (6%)

S-**79b**: n = 1 (2%)
S-**80a**: n = 2 (5%)
S-**80c**: n = 2 (2%)

R-**79a**: n = 1 (5%)
R-**79b**: n = 1 (3%)
R-**80a**: n = 2 (5%)
R-**80c**: n = 2 (3%)

The relative stereochemistry of saturated pyrrolo[3,2-*e*][1,4]diazepin-2-ones **80** was assigned based on NOESY experiments on *R*- and *S*-**80a**, in which through-space transfer of magnetization was observed between the protons at C-5 (6.10 ppm) and C-3 (4.27 ppm) for only the *R*-isomer (Figure 2.3). The *S*-isomers had shorter retention times than the *R*-isomers in the RP-HPLC-MS analyses. Moreover, the specific rotations ($[\alpha]^{21}_{D}$) for *R*- and *S*-**79** and **80** exhibited respectively positive and negative values.

Figure 2.3: Assignment of stereochemistry for pyrrolo[3,2-*e*][1,4]diazepin-2-one *R*-**80a** based on observed through-space magnetisation transfer.

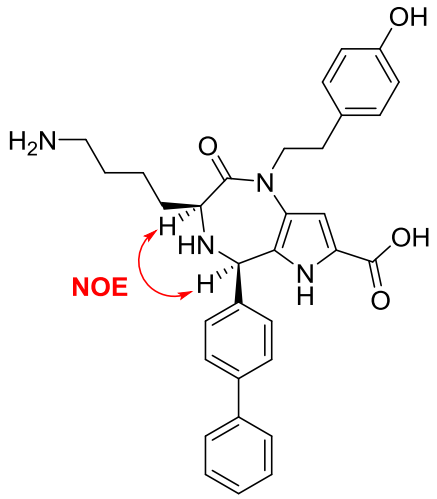

R-**80a**

Crystals of pyrrolo[3,2-*e*][1,4]diazepin-2-one **77a** were grown from MeOH, and examined by X-ray diffraction. The dihedral angles of the amino acid moiety of **77a** (ψ = 74° and ϕ = –79°) were similar to those of the central residue of an ideal inverse γ-turn (ψ = 60° to 70° and ϕ = –70° to –85°, Figure 2.4 and Table 2.1).[1, 8, 251] The ϕ- and ψ-dihedral angle values of unsaturated diazepinone **77a** were respectively significantly closer and slightly further from those of an ideal inverse γ-turn, relative to values observed in the crystal structure of saturated pyrrolo[3,2-*e*][1,4]diazepin-2-one **81**.[8]

Figure 2.4: Dihedral angles of pyrrolo[3,2-*e*][1,4]diazepin-2-one **77a**.

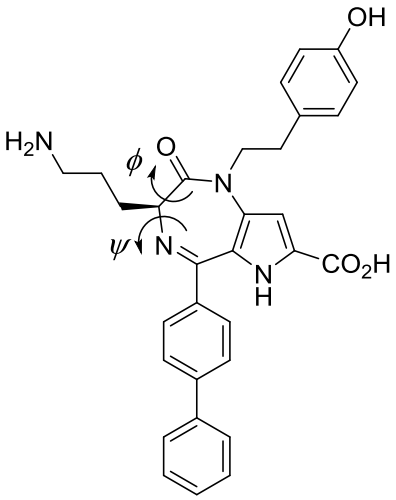

77a

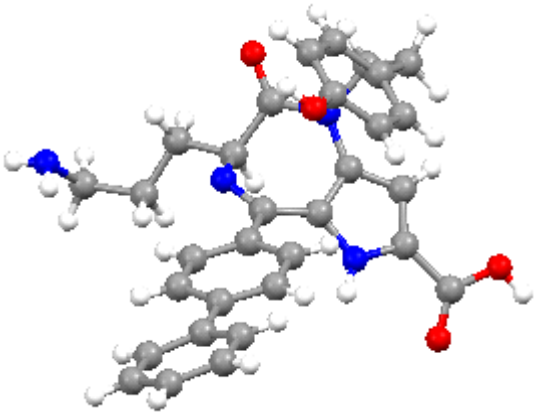

X-ray of **77a**

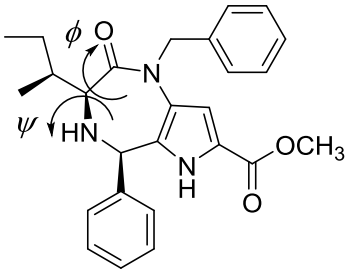

81

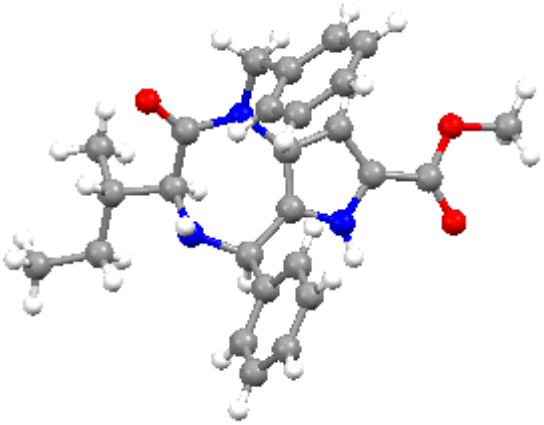

X-Ray of **81**

Table 2.1: Ideal γ-turn and diazepinone ring system dihedral angles.

Structure	ψ	ϕ
Ideal inverse γ-turn[1]	60° to 70°	–70° to –85°
pyrrolo[3,2-*e*][1,4]diazepin-2-one **81**[8]	72°	–93°
pyrrolo[3,2-*e*][1,4]diazepin-2-one **77a**	74°	–79°

2.4. Biology

The urotensin II receptor (UT), formerly called sensory epithelium neuropeptide-like receptor or GPR14, along with its two endogenous ligands (UII and URP), have been studied due to their marked roles in cardiovascular homeostasis and in the etiology of cardiovascular diseases.[143, 219] Recent years have seen new evidence pointing out a functional selectivity of UII and URP.[247] To date, and to the best of our knowledge, none of the available small molecule UT antagonists have exhibited the ability to selectively block UII- or URP-mediated action. With the objective to identify such molecules, the set of abovementioned pyrrolo[3,2-*e*][1,4]diazepin-2-ones was pharmacologically characterized for their ability to bind to the human UT isoform, for their propensity to induce rat aortic ring contractions, and for their ability to modulate hUII- and URP-induced vasoconstriction.

Binding experiments were first performed to identify putative orthosteric agonists and antagonists. Pyrrolo[3,2-*e*][1,4]diazepin-2-ones (100 μM) were tested for their capacity to displace ^{125}I-hUII in a radiolabeled ligand binding assay using stably transfected CHO-*h*UT cells.[13] Although none of the tested derivatives was able to completely displace radioligand binding, pyrrolo[3,2-*e*][1,4]diazepin-2-ones *S*-**79b**, *R*-**79b**, *R*-**80a**, *S*-**80c** and *R*-**80c** all displaced weakly (25-60%) ^{125}I-hUII from the UT

receptor. Notably, pyrrolo[3,2-e][1,4]diazepin-2-one **77a** increased slightly but significantly (117%) the binding of ^{125}I-hUII to the receptor UT. The other derivatives exhibited little to no influence on the binding of ^{125}I-hUII. Although no correlation was observed between the side chain substituents and the binding efficiency, the potential for the pyrrolodiazepinones to serve as allosteric modulators or non-competitive antagonists with weak or no effect on the binding of the radioligand to the receptor was considered, and all compounds were functionally evaluated in a rat aortic ring contraction bioassay.

The pyrrolo[3,2-*e*][1,4]diazepin-2-one derivatives (10 or 100 μM) exhibited no agonist behavior, and were therefore unable to induce rat aortic ring contractions. The propensity of the pyrrolodiazepinones to modulate hUII and URP-associated vasoconstriction was next examined. Thoracic aortic rings were exposed to pyrrolo[3,2-*e*][1,4]diazepin-2-ones for 15 min to establish a binding equilibrium,[252] and then cumulative concentration-responses were respectively measured using increasing concentrations (10^{-10} - $3x10^{-6}$ M) of hUII or URP (Figure 2.4, Table 2.2).

Figure 2.5: Representative modulation of hUII- or URP-mediated vasoconstriction in presence of biphenyl-substituted pyrrolo[3,2-*e*][1,4]diazepin-2-ones.

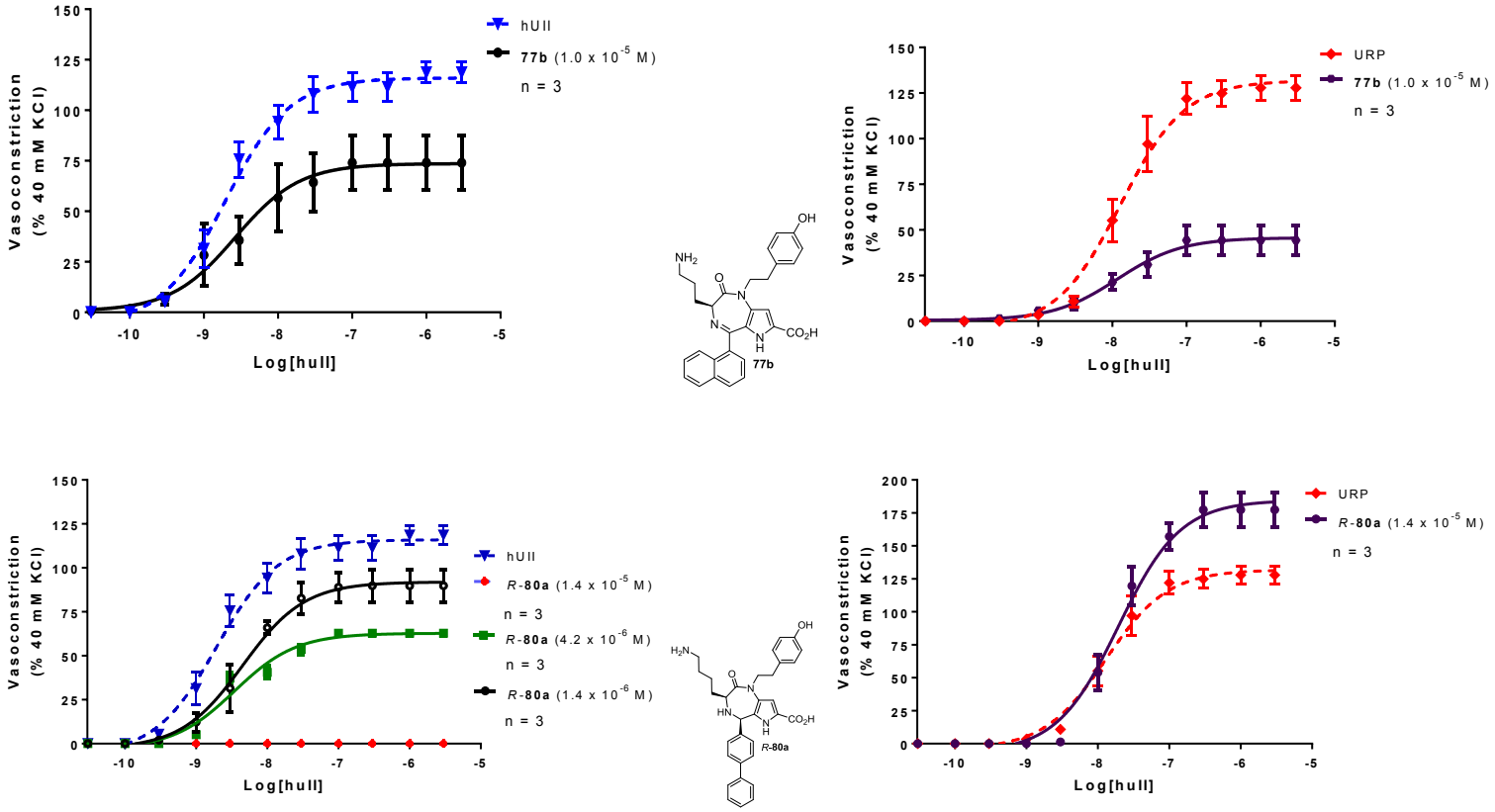

Table 2.2: Comparison of the UII and URP vasoactive profiles obtained in the presence or absence of various pyrrolo[3,2-*e*][1,4]diazepin-2-ones.

Aortic ring contraction (hUII)						Aortic ring contraction (URP)					
#	[ ] µM	N	E_{max} (%)	EC_{50} (nM)	pEC_{50}	#	[ ] µM	n	E_{max} (%)	EC_{50} (nM)	pEC_{50}
hUII	-	4	116 ± 3	1.9	8.71 ± 0.08	**URP**	-	3	132 ± 4	13	7.89 ± 0.08
77a	10	3	97 ± 2*	12.3	7.91 ± 0.06**	**77a**	10	3	93 ± 3**	23.4	7.63 ± 0.07*
77b	10	3	74 ± 5**	2.7	8.58 ± 0.23	**77b**	10	3	46 ± 3***	11.7	7.93 ± 0.17
77c	10	3	70 ± 5**	9.5	8.03 ± 0.19**	**77c**	10	3	142 ± 10	6.8	8.17 ± 0.21
78a	15	4	128 ± 4*	6.6	8.19 ± 0.08**	**78a**	15	4	110 ± 4*	11.9	7.93 ± 0.09
78b	8	4	123 ± 12	7.8	8.11 ± 0.27**	**78b**	8	3	60 ± 6***	5.3	8.27 ± 0.29*
78c	10	4	80 ± 5**	4.	8.33 ±0.18*	**78c**	10	4	51 ± 5***	21.4	7.67 ± 0.26*
***R*-79a**	11	4	162 ± 3***	4.3	8.37 ± 0.06*	***R*-79a**	11	4	139 ± 4	8.1	8.09 ± 0.09
***S*-79b**	10	3	148 ± 6**	4.8	8.32 ± 0.13*	***S*-79b**	10	3	238 ± 6***	3.7	8.44 ± 0.08**
***R*-79b**	10	3	139 ± 5*	5.7	8.25 ± 0.10*	***R*-79b**	10	4	210 ± 6***	4.5	8.34 ± 0.08*
***S*-80a**	14	3	121 ± 4	8.8	8.06 ± 0.09**	***S*-80a**	14	4	113 ± 4*	10.2	7.99 ± 0.10
***R*-80a**	14	3	0***	0	0***	***R*-80a**	14	3	185 ± 6**	19.4	7.71 ± 0.08*
	4	3	63 ± 1**	3.5	8.46 ± 0.07*						
	1	3	92 ± 3*	4.5	8.35 ± 0.11*						
***S*-80c**	10	3	194 ± 11***	1.5	8.81 ± 0.21	***S*-80c**	10	3	107 ± 5**	8.7	8.06 ± 0.13
***R*-80c**	10	3	175 ± 6***	5.0	8.31 ± 0.11*	***R*-80c**	10	3	217 ± 9***	8.2	8.08 0.12

All values are expressed as mean ± SEM. Statistical comparisons for both pEC_{50} and E_{max} values were performed using the unpaired Student's t-test analysis where *P < 0.05, **P < 0.01, and ***P < 0.001 versus vehicle control values.

Among the unsaturated analogs, Lys-bearing derivatives **78a** (15 μM) and **78b** (8 μM) reduced significantly hUII potency (**78a**: 8.19 ± 0.08, **78b**: 8.11 ± 0.11 *vs* hUII: 8.71 ± 0.08), but were almost unable to affect hUII-induced maximal vasoconstriction (Table 2.2). On the other hand, **78c**, at 10 μM, was able to reduce significantly the pEC_{50} (8.33 ± 0.18 *vs* 8.71 ± 0.08) and the E_{max} (80 ± 5% *vs* 116 ± 3%) of the hUII dose-response curve. Although the biphenyl analog **78a** was only able to modulate moderately URP-mediated vasoconstriction (110 ± 4% *vs* 132 ± 4%), naphthyl-containing analogs **78b** and **78c** reduced significantly URP efficacy (around 50% at 10^{-5}M). Ornithine analogs **77a-c** exhibited a more pronounced pharmacological profile compared to their Lys-bearing counterparts. For example, biphenyl analog **77a** (10 μM) demonstrated slight but significant ability to reduce both UII (97 ± 2% *vs* 116 ± 3%) and URP (93 ± 3% *vs* 132 ± 4%) contractile efficacy (Table 2.2). Naphthyl analogs **77b** (10 μM) and **77c** (10 μM) also diminished significantly (by almost 60%) UII contractile efficacy (Table 2.2). Although **77a** and **77c** reduce the potency of hUII-induced contraction (**77a**: 7.91 ± 0.06, **77c**: 8.03 ± 0.19 *vs* hUII: 8.71 ± 0.08), **77b** has no impact on hUII contractile force (8.33 ± 0.18 *vs* 8.71 ± 0.08). Although 2-naphthyl analog **77c** caused no change in URP-induced contractility (142 ± 10% *vs* 132 ± 4%), its 1-naphthyl counterpart **77b** blocked significantly (more than 65% of the total URP response) URP contractile efficacy (Table 2.2). Notably, 2-naphthyl analog **77c** may represent a putative allosteric modulator that exerts probe-dependent effects on UII and URP. In the unsaturated series, the ornithine side chain appeared to be required to influence UII-mediated contraction. The combination of the length of the amine bearing side-chain and shape of the aromatic side chain seem to both mediate the effects on observed URP contractile efficacy.

In the case of saturated lysine analogs, *S*-diastereomer *S*-**80a** (15 μM) was unable to influence the efficacy of hUII (121 ± 4% *vs* 116 ± 3%) and the pEC_{50} of URP (7.99 ± 0.10 *vs* 7.89 ± 0.08), albeit it modified slightly but significantly the pEC_{50} of hUII (8.06 ± 0.09 *vs* 8.71 ± 0.08) and the efficacy of URP (113 ± 4% *vs* 132 ± 4%) (Table 2.2). The *R*-diastereomer *R*-**80a** (4 μM) diminished slightly the pEC_{50} of hUII (8.46 ± 0.07 *vs* 8.71 ± 0.08), but caused a significant concentration-dependent reduction of the hUII maximum contractile response (63 ± 1% *vs* 116 ± 3%), which was abolished at 14 μM (Figure 2.4, Table 2.2). Alternatively, *R*-**80a** (14 μM) potentiated the maximal contractile efficacy of URP (185 ± 6% *vs* 132 ± 4%) and slightly decreased its potency (7.71 ± 0.08 *vs* 7.89 ± 0.08. Duality in modulation of hUII- and URP-mediated vasoconstriction may be due to an allosteric effect. The affinity (pK_b) of the non-competitive antagonist *R*-**80a** was subsequently determined using the method of Gaddum and the slope was used to calculate the equilibrium constant K_b.[221] Consistent with non-competitive antagonism, the double reciprocal plot of equally active concentrations of agonist in the presence and absence of *R*-**80a** (4 μM) gave a linear slope of 2.46 ± 0.09, equating to a pK_b value of 5.54 (Figure 2.5). The selectivity of *R*-**80a** for UT was evaluated by testing its impact on endothelin-1-mediated contraction (hET-1), and *R*-**80a** was found to be unable to modulate the vasocontractile action of hET-1 (Annexe 3). Owing to the high structural homology between UII, URP, and somatostatin ligands, *R*-**80a** could potentially act on somatostatin receptors ligands; however, this is unlikely because *R*-**80a** was unable to potentiate ET-1-induced effects in the rat aorta (a phenomenon closely connected to somatostatin receptor affinity).[253]

Figure 2.6: The double reciprocal plot of equally active concentrations of hUII in absence (A) and presence (A′) of 4.2 x 10^{-6} M *R*-**80a** is linear and consistent with non-competitive antagonism.

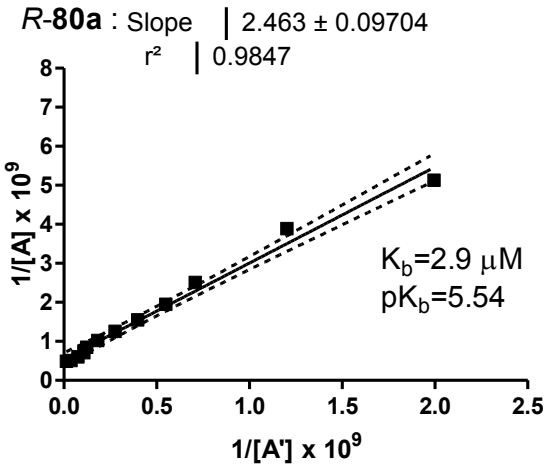

In the case of the saturated 2-naphthyl analogs, and in contrast to the activity of biphenyl analog *R*-**80a**, the efficacy of UII contraction was increased (175 ± 6% *vs* 116 ± 3%) significantly by *R*-**80c** (10 μM), which similarly improved the observed effect of URP (217 ± 9% *vs* 132 ± 4%). The *S*-diastereomer *S*-**80c** (10 μM) improved similarly UII contractile efficiency (194 ± 11% *vs* 116 ± 3%), but significantly reduces the URP-mediated vasoconstriction (107 ± 5% *vs* 132 ± 4%; Table 2.2).

In the case of the saturated ornithine analogs, as described above, only *R*-diastereomer *R*-**79a**, and *R*- and *S*-**79b** were isolated from our synthetic procedure (Figure 2.2). Biphenyl analog *R*-**79a** improved the efficiency of contraction of UII (E_{max} = 162% vs 116%), yet had no effect on URP vasoactive profile. Hence, the shift from a Lys to Orn moiety completely reversed the effect induced on hUII by its Lys-counterpart. In contrast to the saturated analog **78b**, which was able to reduce both hUII and URP

vasoconstriction, unsaturated diastereomer *R*-**79b** and *S*-**79b** increased the contraction efficiency of UII and URP.

2.5. Conclusion

Considering that a turn conformation is adopted by UII and URP during the activation of their cognate receptor, a series of pyrrolo[3,2-*e*][1,4]diazepin-2-ones were prepared, in which side chain homologs of the Bip-Lys-Tyr triad were grafted onto a heterocyclic scaffold. Pyrrolodiazepinones were synthesized by a solid-phase method on Wang resin employing a Pictet-Spengler cyclization, isolated by HPLC and their pharmacological profile evaluated using a competitive binding assay and an *ex vivo* rat aortic ring contraction bioassay. Crystals of pyrrolo[3,2-*e*][1,4]diazepin-2-one **77a** were examined by X-ray diffraction and shown to adopt dihedral angle values characteristic of an ideal reverse γ-turn conformation about the ornithine residue. Pyrrolodiazepinone **77b** and *R*-**80a** can differentially modulate the vasoconstriction induced by hUII and URP. They modulate selectively hUII- or URP-induced contraction while leaving unaffected the other endogenous ligand. Although their relatively low potency has limited our initial efforts to assess their mechanism of action, their probe-dependence points toward an allosteric mechanism of action for receptor modulation by the pyrrolo[3,2-*e*][1,4]diazepin-2-ones. Moreover, their potential to discriminate hUII- and URP-associated signalling pathways make these non-peptide modulators valuable tools for probing the selective roles of the endogenous ligands in the physiology and associated pathologies of the urotensinergic system.

2.6. Acknowledgement

This research was supported by the Natural Sciences and Engineering Research Council of Canada (NSERC). We thank Dr. Nicolas Boutard for helpful discussions. We are grateful to Marie-Christine Tang and Karine Venne from the Université de Montréal Mass Spectrometry Facility for MS analyses, to Sylvie Bilodeau and Cédric Malveau from the Université de Montréal High Field NMR Regional Laboratory for 500 and 700 MHz NMR spectra, and to Francine Bélanger-Gariépy from the Université de Montréal for X-ray crystal analyses. Myriam Létourneau from IRNS-Institut-Armand is thanked for her technical support during the biological assays and their analysis.

3. Chapitre 3 : Perspective et Conclusion

3.1. Perspective

Suite à ces résultats prometteurs, les produits secondaires obtenus lors de la réaction de Pictet-Spengler sont plus investigués. L'analyse par HRMS, l'ion moléculaire de **81a** montre bien l'ajout de deux aldéhydes et le modèle de fragmentation du *N-p*-phénylbenzylpyrrolodiazépinone **81a** montre la perte d'un groupement aryle méthyle et un ion moléculaire qui correspond au $[M+H]^+$ de l'insaturé pyrrolo[3,2-*e*][1,4]diazépin-2-one **77a**. L'analyse sur CCM avec de la ninhydrine du *N-p*-phénylbenzylpyrrolodiazépinone **81a** montre une tache pourpre de Ruhemann ce qui démontre la présence d'une amine primaire. Le spectre RMN ^{1}H du *N-p*-phénylbenzylpyrrolodiazépinone **81a** est similaire à son correspondant insaturé **77a**, avec l'ajout de neuf protons dans la région des aromatiques et l'addition d'un singulet à 4.32 ppm, qui correspond à deux protons. Le spectre RMN ^{13}C montre l'apparition d'un nouveau carbone aliphatique à 50.6 ppm. Dans le spectre ROESY du **81a**, le singulet à 4.32 ppm transfère l'aimantation à la chaîne latérale de l'Orn à 2.03 ppm et 3.24 ppm et les protons aromatiques à 7.66 ppm (Figure 3.1). Dans le spectre HMQC du **81a**, le signal du carbone à 50.6 ppm est corrélé à la chaine latérale de l'Orn à 3.24 ppm et les protons du cycle aromatique à 7.66 ppm. Le proton singulet à 4.32 ppm a corrélé avec le carbone vinylique à 162.9 ppm.

Figure 3.1: Caractérisation par ROE du *N*-*p*-phénylbenzylpyrrolodiazépinone **81a**.

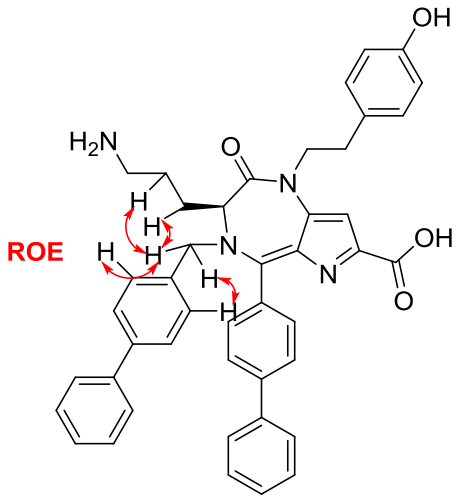

81a

La formation du *N*-*p*-phénylbenzylpyrrolodiazépinone **81b** est due à une double addition de l'aldéhyde sur le pyrrolo[3,2-*e*][1,4]diazépin-2-one saturé *R*-**80b** et non sur le saturé pyrrolo[3,2-*e*][1,4]diazépin-2-one **78a**, qui est non réactif, comme illustré dans le schéma 3.1.

Schéma 3.1: Synthèse du pyrrolo[3,2-*e*][1,4]diazépin-2-one *N*-*p*-phénylbenzyle **81b** à partir du *R*-**80b**.

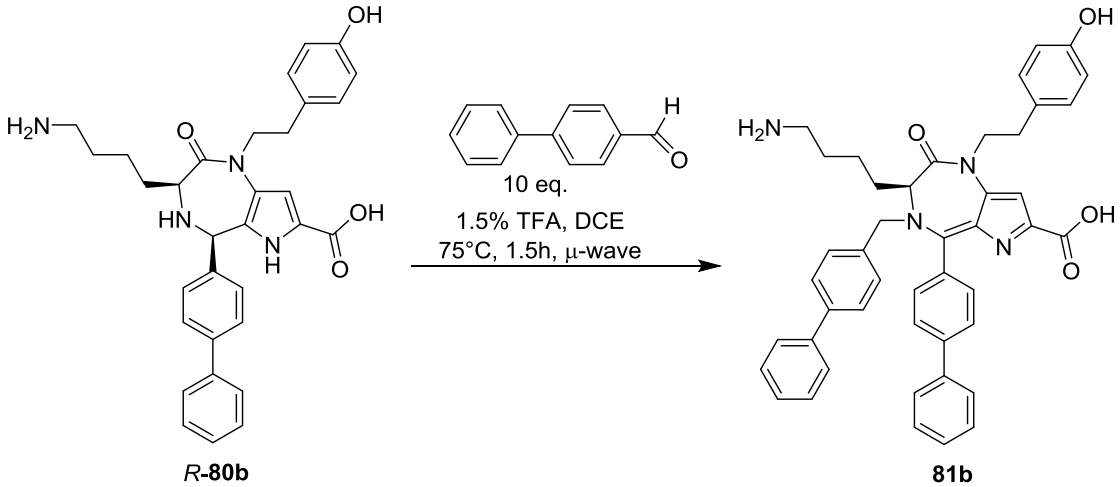

R-**80b** **81b**

Dans le cas de la réaction Pictet-Spengler avec 1- et 2-naphthaldéhyde, il y a formation d'un mélange d'atropisomères. La purification du mélange d'atropisomères est

difficile, car seulement un des atropisomères a été isolé pour les analogues avec Orn et dans le cas des analogues de Lys, la séparation des atropisomères a été inefficace.

Figure 3.2 : Pyrrolo[3,2-*e*][1,4]diazépin-2-ones *N*-substitués.

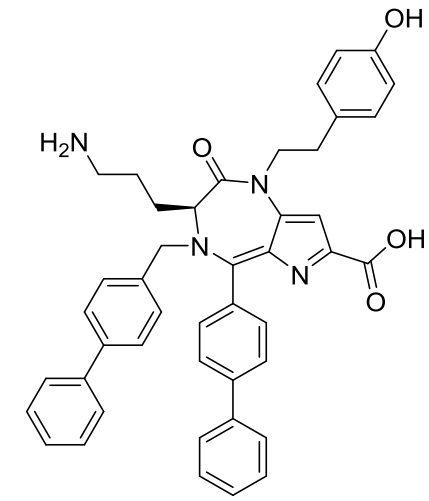

81a

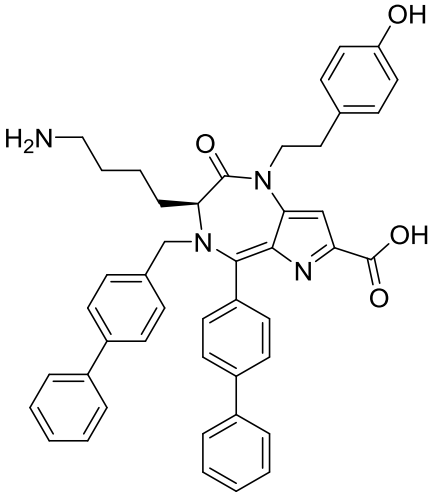

81b

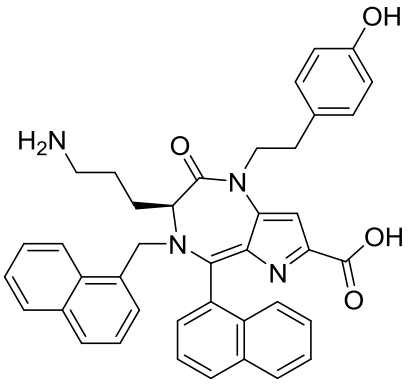

81c

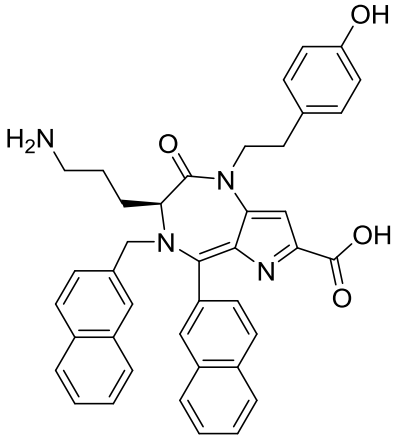

81d

Figure 3.3: Représentation des modulations des vasoconstrictions induites par hUII ou par URP en présence de pyrrolo[3,2-*e*][1,4]diazépin-2-ones *N*-substitués.

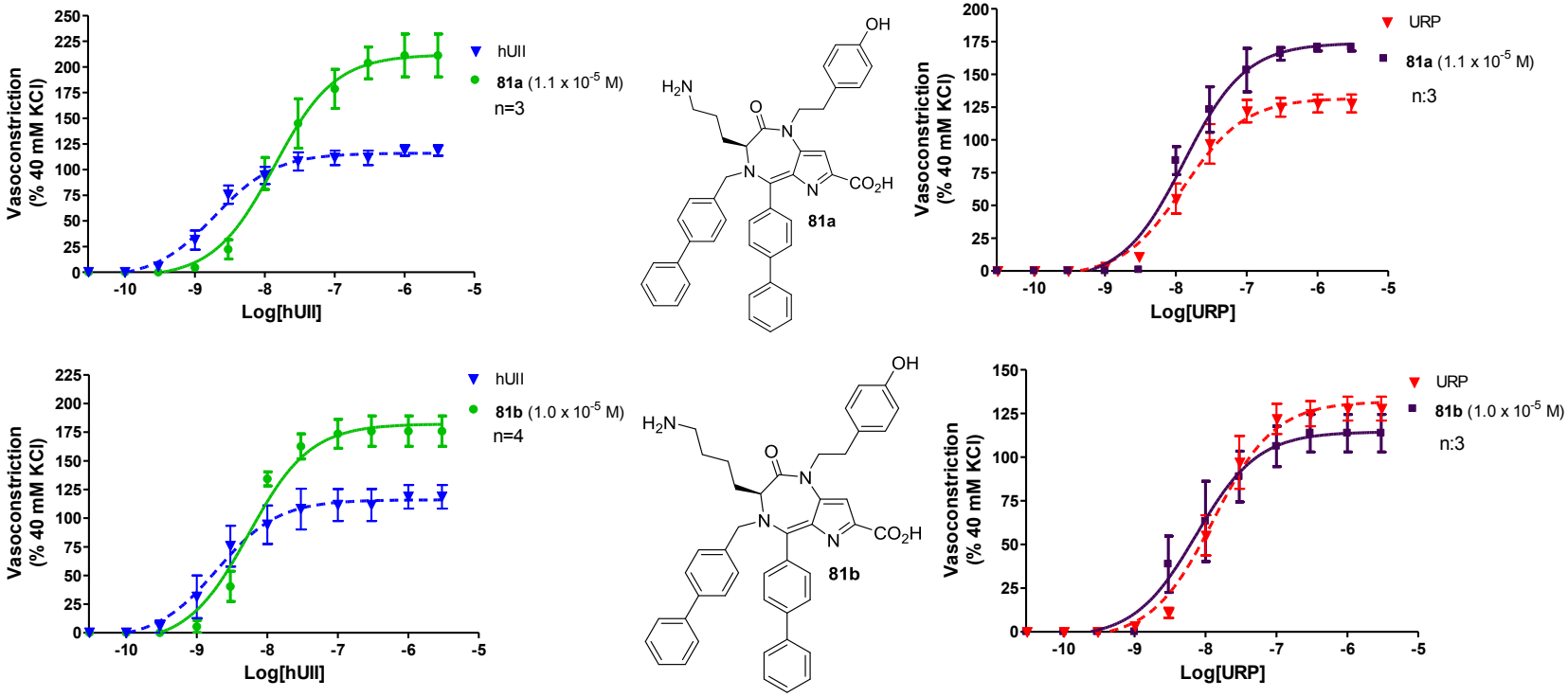

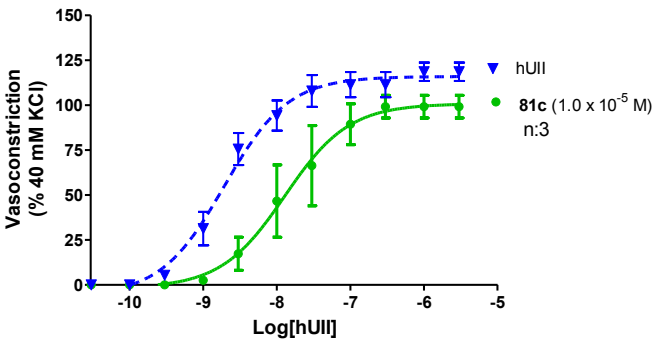
Vasoconstriction (% 40 mM KCl)
Log[hUII]
hUII
81c (1.0 x 10-5 M)
n:3

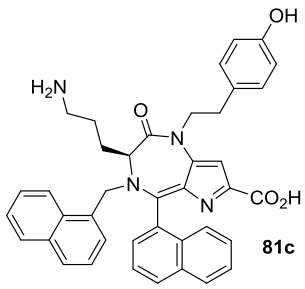
OH
H2N
O
N
N
N
CO2H

81c

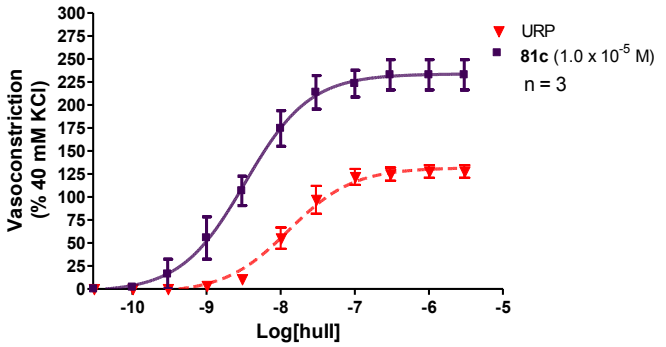
Vasoconstriction (% 40 mM KCl)
Log[hull]
URP
81c (1.0 x 10-5 M)
n = 3

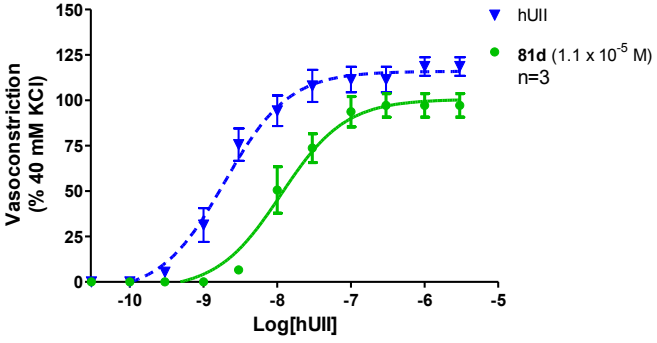
Vasoconstriction (% 40 mM KCl)
Log[hUII]
hUII
81d (1.1 x 10-5 M)
n=3

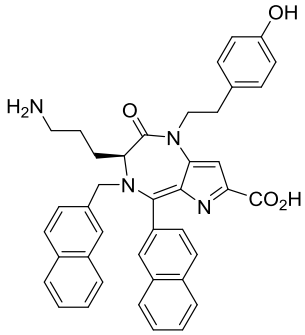
OH
H2N
O
N
N
N
CO2H

81d

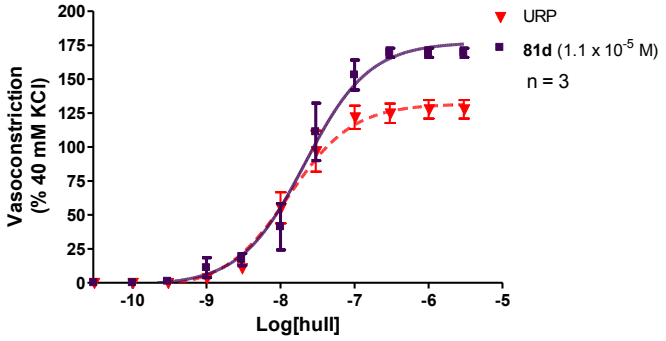
Vasoconstriction (% 40 mM KCl)
Log[hull]
URP
81d (1.1 x 10-5 M)
n = 3

Tableau 3.1 : Comparaison des profiles vasoactifs de l'hUII et l'URP obtenue en présence ou en absence de pyrrolo[3,2-*e*][1,4]diazépin-2-ones *N*-substitués.

Aortic ring contraction (hUII)						Aortic ring contraction (URP)					
#	[ ] µM	n	E_{max} (%)	EC_{50} (nM)	pEC_{50}	#	[ ] µM	n	E_{max} (%)	EC_{50} (nM)	pEC_{50}
hUII	-	4	116 ± 3	1.93	8.71 ± 0.08	**URP**	-	3	132 ± 4	12.9	7.89 ± 0.08
81a	11	3	212 ± 8 ***	13.7	7.86 ± 0.09	**81a**	11	3	174 ± 5 ***	13.0	7.89 ± 0.08
81b	10	4	182 ± 5 ***	5.45	8.26 ± 0.08	**81b**	10	3	115 ± 5 *	7.4	8.13 ± 0.14
81c	10	3	101 ± 5 *	12.9	7.90 ± 0.14 **	**81c**	10	3	234 ± 7 ***	3.3	8.48 ± 0.09 ***
81d	11	3	101 ± 3 *	11.3	7.95 ± 0.09 **	**81d**	11	3	177 ± 5 ***	21	7.67 ± 0.08 *

Toutes les valeurs sont exprimées en moyenne ± SEM. Les statistique de comparaisons pEC_{50} et E_{max} ont été effectués en utilisant le test-t de Student où que *P < 0.05, **P < 0.01, and ***P < 0.001 versus les valeurs de control.

Comme pour le cas des pyrrolo[3,2-*e*][1,4]diazépin-2-ones insaturés et saturés, les *N*-substitués dérivés ont aussi la capacité de moduler les vasoconstrictions induites par l'hUII ou l'URP (Tableau 3.1 et figure 3.3). Le pyrrolo[3,2-*e*][1,4]diazépin-2-one insaturé **77a** diminue les contractions de l'aorte provoquée par l'hUII et l'URP ainsi qu'un léger déplacement de la courbe dose-réponse de l'hUII et l'URP, contrairement au diastéréoisomère *R*-**79a** qui a la capacité d'augmenter les contractions de l'aorte provoquée par l'hUII et n'a aucun effet sur l'URP. La version insaturée lysine **78a** et le diastéréoisomère *S*-**80a** ne sont guère actifs sur l'hUII et l'URP, par contre le diastéréoisomère *R*-**80a** est capable d'inhiber totalement les contractions de l'aorte induite par l'hUII. Comme pour le diastéréoisomère *R*-**79a**, le pyrrolo[3,2-*e*][1,4]diazépin-2-one *N*-*p*-phénylbenzyle **81a** et l'analogue lysine **81b** ont la capacité d'augmenter la force des contractions de l'aorte provoquée par l'hUII (212 ± 8% vs 116% ± 3 et 182 ± 5% vs 116 ± 3% respectivement) mais uniquement le pyrrolo[3,2-*e*][1,4]diazépin-2-one *N*-*p*-phénylbenzyle **81a** a une activité sur l'URP en augmentant les contractions de l'aorte (174 ± 5% vs 132 ± 4%).

La substitution du biphényle par 1-naphthyle ou 2-naphthyle engendre aussi des pyrrolo[3,2-*e*][1,4]diazépin-2-ones *N*-substitués modulateurs de l'hUII et l'URP. Le pyrrolo[3,2-*e*][1,4]diazépin-2-one *N*-1-naphthyle **81c** et le pyrrolo[3,2-*e*][1,4]diazépin-2-one *N*-2-naphthyle **81d** ont la capacité de réduire légèrement les contractions de l'aorte induite par l'hUII (101 ± 5% vs 116 ± 3% et 101 ± 3% vs 116 ± 3% respectivement) et l'effet est contraire sur l'URP, les contractions de l'aorte induite par l'URP augmentent en puissance (234 ± 7% vs 132 ± 4% et 177 ± 5% vs 132 ± 4% respectivement).

La synthèse de cette librairie de pyrrolo[3,2-*e*][1,4]diazépin-2-ones sera transférée sur la résine de Merrifield, cela permettrait de faire une diversification à la position 7 sur le pyrrolo[3,2-*e*][1,4]diazépin-2-one par diverses méthodes de clivages afin de voir l'effet que peuvent avoir cette diversification sur l'activité du système urotensinergique.

De nouveaux analogues ont été pensés, suite à une récente publication de l'équipe de Grieco[254], où la tyrosine a été remplacée par des acides aminés aromatiques non naturels, tels que 4-cyanophénylalanine ((*p*CN)Phe) et 4-nitrophénylalanine ((*p*NO_2)Phe), qui rendent l'urantide **64** comme pur antagoniste et le benzothiazolylalanine (BtzPhe) et le 3,4-dichlorophénylalanine ((3,4-Cl)Phe), qui rendent l'urantide superagoniste. Suite à ces informations, la future librairie de pyrrolo[3,2-*e*][1,4]diazépin-2-ones serait construite sur résine de Wang et de Merrifield, en remplaçant la tyramine par 2-(3,4-dichlorophényl)éthanamine, 2-(benzo[*d*]thiazol-2-yl)éthan-1-amine, tryptamine, 4-cyanophényléthanamine et 4-(2-aminoéthyl)benzonitrile, tout en gardant la lysine et le biphényle.

3.2. Conclusion

La synthèse de pyrrolo[3,2-*e*][1,4]diazépin-2-ones sur support solide est relativement efficace avec 5 étapes à partir du 4-hydroxy-*N*-(PhF)proline. La méthodologie employée permet rapidement d'accéder à des diversifications sur le pyrrolo[3,2-*e*][1,4]diazépin-2-one. La réaction clé de cette synthèse donne plusieurs produits, soient insaturés et saturés *R*- et *S*-diastéréoisomères, ainsi que des pyrrolo[3,2-*e*][1,4]diazépin-2-ones *N*-substitués, ce qui est avantageux pour les études de relations

structure-activité. L'analyse par rayon X de cristaux de pyrrolo[3,2-*e*][1,4]diazépin-2-ones synthétisés confirme leur capacité à mimer un tour-γ inverse.

On a fait se postulat comme le fait de mimer le tour-γ inverse et en reprenant les parties actives de l'UII, Trp-Lys-Tyr, peut mener à des composés actifs. Ce postulat a été confirmé avec les résultats obtenus lors des tests *ex vivo*, sur les aortes de rats en provoquant des contractions avec l'hUII ou l'URP. La plupart des pyrrolodiazépinones testés ont démontré des activités modulatrices du système urotensinergique. Le pyrrolodiazépinone *R*-**80a** a démontré la meilleure activité de tous les pyrrolodiazépinones en inhibant toutes les contractions de l'aorte provoquée par l'hUII à 14 μM avec un pK_b de 5.54 à 4 μM. La majorité des pyrrolodiazépinones *N*-substittués ont la capacité d'accroitre les contractions de l'hUII et/ou URP. Le pyrrolo[3,2-*e*][1,4]diazépin-2-one *N*-*p*-phénylbenzyle **81a** double les contractions de l'hUII et pour le pyrrolo[3,2-*e*][1,4]diazépin-2-one *N*-*p*-1-naphthyl **81c** double presque les contractions provoquées par l'URP avec un E_{max} de 234%..

Avec les résultats obtenus, le pyrrolodiazépinone est une excellente structure pour poursuivre l'investigation au développement d'un petit composé actif sur le système urotensinergique, car ils peuvent moduler l'hUII et l'URP de façon différente. De plus, Le pyrrolo[3,2-*e*][1,4]diazépin-2-one a aussi démontré une sélectivité envers le récepteur UT, puisqu'il est inactif sur l'*h*ET-1.

Les concentrations nécessaires pour avoir une activité biologique sont quand même élevées, se situant aux alentours de 10 μM, ce qui limite les essais *in vitro* pour déterminer le mode d'action sur le récepteur UT. À première vue selon les résultats, les pyrrolo[3,2-*e*][1,4]diazépin-2-ones agissent comme modulateur sur du récepteur UT avec un mécanisme allostérique du fait qu'il peut différencier l'hUII et l'URP.

Ce mémoire récapitule les balbutiements du développement d'une petite molécule modulatrice du récepteur UT et les premières études de relations structure-activité. Avec ces premières pistes, il serait possible d'améliorer l'efficacité des pyrrolo[3,2-*e*][1,4]diazépin-2-ones sur le récepteur UT, puisqu'il y a cinq positions possibles pour diversifier le pyrrolo[3,2-*e*][1,4]diazépin-2-one. De plus, les pyrrolo[3,2-*e*][1,4]diazépin-

2-ones peuvent être de bons outils pour étudier sélectivement les rôles des peptides endogènes dans le système urotensinergique et de mieux les comprendre.

4. Bibliographie

1. Rose, G. D.; Glerasch, L. M.; Smith, J. A. Turns in peptides and proteins. In *Adv. Protein Chem.*, C.B. Anfinsen, J. T. E.; Frederic, M. R., Eds. Academic Press: 1985; Vol. *37*, pp 1-109.
2. Moore, M. L. G., G. Peptide Design Considerations, Synthetic Peptides: A user's guide. *Peptide Design Considerations, Synthetic Peptides: A user's guide, New-York, Freeman, W. H. and Co. Editions.* **1993**.
3. Shepherd, N. E.; Hoang, H. N.; Abbenante, G.; Fairlie, D. P. Single turn peptide alpha helices with exceptional stability in water. *Journal of the American Chemical Society* **2005,** 127, 2974-2983.
4. Ramachan.Gn; Venkatac.Cm; Krimm, S. Stereochemical criteria for polypeptide and protein chain condormations .3. helical and hydrogen-bonded polypeptide chains. *Biophys. J.* **1966,** 6, 849-&.
5. Venkatac.Cm. Stereochemical criteria for polypeptides and proteins .V. conformation of a system of 3 linked peptide units. *Biopolymers* **1968,** 6, 1425-&.
6. Richardson, J. S. The anatomy and taxonomy of protein structure. *Advances in protein chemistry* **1981,** 34, 167-339.
7. Iden, H. S.; Lubell, W. D. 1,4-Diazepinone and pyrrolodiazepinone syntheses via homoallylic ketones from cascade addition of vinyl grignard reagent to α-aminoacyl-β-amino esters. *Organic Letters* **2006,** 8, 3425-3428.
8. Deaudelin, P.; Lubell, W. D. Diastereoselective Pictet-Spengler approach for the synthesis of pyrrolo[3,2-e][1,4]diazepin-2-one peptide turn mimics. *Organic Letters* **2008,** 10, 2841-2844.
9. Smith, J. A.; Pease, L. G. Reverse turns in peptides and proteins. *CRC Critical Reviews in Biochemistry* **1980,** 8, 315-399.
10. Milnerwhite, E. J. Situations of gamma-turns in proteins - their relation to alpha-helices, beta-Sheets and ligand-binding sites. *Journal of Molecular Biology* **1990,** 216, 385-397.
11. Milon, A.; Miyazawa, T.; Higashijima, T. Transferred nuclear overhauser effect analyses of membrane-bound enkephalin analogs by H-1 nuclear magnetic-resonance - correlation between activities and membrane-bound conformations. *Biochemistry* **1990,** 29, 65-75.
12. Haubner, R.; Gratias, R.; Diefenbach, B.; Goodman, S. L.; Jonczyk, A.; Kessler, H. Structural and functional aspects of RGD-containing cyclic pentapeptides as highly potent and selective integrin alpha(v)beta(3) antagonists. *Journal of the American Chemical Society* **1996,** 118, 7461-7472.
13. Chatenet, D.; Dubessy, C.; Leprince, K.; Boularan, C.; Carlier, L.; Segalas-Milazzo, I.; Guilhaudis, L.; Oulyadi, H.; Davoust, D.; Scalbert, E.; Pfeiffer, B.; Renard, P.; Tonon, M. C.; Lihrmann, I.; Pacaud, P.; Vaudry, H. Structure-activity relationships and structural conformation of a novel urotensin II-related peptide. *Peptides* **2004,** 25, 1819-1830.
14. Lescot, E.; Bureau, R.; Rault, S. Nonpeptide Urotensin-II receptor agonists and antagonists: Review and structure-activity relationships. *Peptides* **2008,** 29, 680-690.
15. Bleich, H. E.; Galardy, R. E.; Printz, M. P. Conformationof angiotensin-II in aqueous-solution - evidence for gamma-turn model. *Journal of the American Chemical Society* **1973,** 95, 2041-2042.

16. Hedenstrom, M.; Yuan, Z. Q.; Brickmann, K.; Carlsson, J.; Ekholm, K.; Johansson, B.; Kreutz, E.; Nilsson, A.; Sethson, I.; Kihlberg, J. Conformations and receptor activity of desmopressin analogues, which contain gamma-turn mimetics or a Psi CH2O isostere. *J. Med. Chem.* **2002,** 45, 2501-2511.
17. Schmidt, J. M.; Ohlenschlager, O.; Ruterjans, H.; Grzonka, Z.; Kojro, E.; Pavo, I.; Fahrenholz, F. Conformation of 8-arginine vasopressin and V1 antagonists in dimethyl-sulfoxide solutionderived from 2-dimensional NMR-spectroscopy and molecular dynamics simulation. *European Journal of Biochemistry* **1991,** 201, 355-371.
18. Sato, M.; Lee, J. Y. H.; Nakanishi, H.; Johnson, M. E.; Chrusciel, R. A.; Kahn, M. Design, synthesis and conformational analysis of gamma -turn peptide mimetics of bradykinin. *Biochemical and Biophysical Research Communications* **1992,** 187, 999-1006.
19. Wynants, C.; Sugg, E.; Hruby, V. J.; Van Binst, G. Conformational study of a somatostatin analog by high-field NMR spectroscopy, in aqueous solution. *International Journal of Peptide and Protein Research* **1987,** 30, 541-7.
20. Yuan, Z. Q.; Blomberg, D.; Sethson, I.; Brickmann, K.; Ekholm, K.; Johansson, B.; Nilsson, A.; Kihlberg, J. Synthesis and pharmacological evaluation of an analogue of the peptide hormone oxytocin that contains a mimetic of an inverse gamma-turn. *Journal of Medicinal Chemistry* **2002,** 45, 2512-2519.
21. Marshall, G. R. Peptide interactions with G-protein coupled receptors. *Biopolymers* **2001,** 60, 246-277.
22. Porcelli, M.; Casu, M.; Lai, A.; Saba, G.; Pinori, M.; Cappelletti, S.; Mascagni, P. Cyclic pentapeptides of chiral sequence DLDDL as scaffold for antagonism of G-protein coupled receptors: Synthesis, activity and conformational analysis by NMR and molecular dynamics of ITF 1565 a substance P inhibitor. *Biopolymers* **1999,** 50, 211-219.
23. Pauletti, G. M.; Gangwar, S.; Siahaan, T. J.; Aube, J.; Borchardt, R. T. Improvement of oral peptide bioavailability: Peptidomimetics and prodrug strategies. *Advanced Drug Delivery Reviews* **1997,** 27, 235-256.
24. Grauer, A.; Koenig, B. Peptidomimetics - A Versatile Route to Biologically Active Compounds. *European Journal of Organic Chemistry* **2009**, 5099-5111.
25. Ahn, J.-M.; Boyle, N. A.; MacDonald, M. T.; Janda, K. D. Peptidomimetics and peptide backbone modifications. *Mini reviews in medicinal chemistry* **2002,** 2, 463-73.
26. Proulx, C.; Sabatino, D.; Hopewell, R.; Spiegel, J.; Ramos, Y. G.; Lubell, W. D. Azapeptides and their therapeutic potential. *Future Medicinal Chemistry* **2011,** 3, 1139-1164.
27. Proulx, C.; Lubell, W. D. N-Amino-imidazolin-2-one Peptide Mimic Synthesis and Conformational Analysis. *Organic Letters* **2012,** 14, 4552-4555.
28. Rosenstrom, U.; Skold, C.; Lindeberg, G.; Botros, M.; Nyberg, F.; Karlen, A.; Hallberg, A. Design, synthesis, and incorporation of a beta-turn mimetic in angiotensin II forming novel pseudopeptides with affinity for AT(1) and AT(2) receptors. *Journal of Medicinal Chemistry* **2006,** 49, 6133-6137.
29. Rosenstrom, U.; Skold, C.; Lindeberg, G.; Botros, M.; Nyberg, F.; Karlen, A.; Hallberg, A. A selective AT(2) receptor ligand with a gamma-turn-like mimetic replacing the amino acid residues 4-5 of angiotensin II. *Journal of Medicinal Chemistry* **2004,** 47, 859-870.
30. Jamieson, A. G.; Boutard, N.; Sabatino, D.; Lubell, W. D. Peptide scanning for studying structure-activity relationships in drug discovery. *Chem. Biol. Drug Des.* **2013,** 81, 148-165.
31. Verdie, P.; Subra, G.; Feliu, L.; Sanchez, P.; Berge, G.; Garcin, G.; Martinez, J. On-line synthesis of pseudopeptide library incorporating a benzodiazepinone turn mimic: Biological evaluation on MC1 receptors. *Journal of Combinatorial Chemistry* **2007,** 9, 254-262.

32. Welsch, W. E.; Snyder, S. A.; Stockwell, B. R. Privileged Scaffolds for Library Design and Drug Discovery *Curr. Opin. Chem. Biol.* **2010,** 14, 347-361.
33. Dorr, A. A.; Lubell, W. D. γ-Turn Mimicry with Benzodiazepinones and Pyrrolobenzodiazepinones Synthesized from a Common Amino Ketone Intermediate. *Organic Letters* **2015,** 17, 3592-3597.
34. Horton, D. A.; Bourne, G. T.; Smythe, M. L. The Combinatorial Synthesis of Bicyclic Privileged Structures or Privileged Substructures. *Chemical Reviews* **2003,** 103, 893-930.
35. Patchett, A. A.; Nargund, R. P. Chapter 26. Privileged structures -- An update. In *Annu. Rep. Med. Chem.*, Academic Press: 2000; Vol. *35*, pp 289-298.
36. Evans, B. E.; Rittle, K. E.; Bock, M. G.; DiPardo, R. M.; Freidinger, R. M.; Whitter, W. L.; Lundell, G. F.; Veber, D. F.; Anderson, P. S. Methods for drug discovery: development of potent, selective, orally effective cholecystokinin antagonists. *Journal of Medicinal Chemistry* **1988,** 31, 2235-2246.
37. Wattanasin, S.; Kallen, J.; Myers, S.; Guo, Q.; Sabio, M.; Ehrhardt, C.; Albert, R.; Hommel, U.; Weckbecker, G.; Welzenbach, K.; Weitz-Schmidt, G. 1,4-Diazepane-2,5-diones as novel inhibitors of LFA-1. *Bioorganic & Medicinal Chemistry Letters* **2005,** 15, 1217-1220.
38. Sternbach, L. H. 1,4-Benzodiazepines. Chemistry and Some Aspects of the Structure-Activity Relationship. *Angewandte Chemie, International Edition* **1971,** 10, 34-43.
39. Sternbach, L. H. The benzodiazepine story. *Journal of Medicinal Chemistry* **1979,** 22, 1-7.
40. Ludek, O. R.; Schroeder, G. K.; Liao, C.; Russ, P. L.; Wolfenden, R.; Marquez, V. E. Synthesis and Conformational Analysis of Locked Carbocyclic Analogues of 1,3-Diazepinone Riboside, a High-Affinity Cytidine Deaminase Inhibitor. *Journal of Organic Chemistry* **2009,** 74, 6212-6223.
41. Wan, W.; Hou, J.; Jiang, H. Z.; Wang, Y. L.; Zhu, S. Z.; Deng, H. M.; Hao, J. Concise synthesis of omega-fluoroalkylated ketoesters. A building block for the synthesis of six-, seven-, and eight-membered fluoroalkyl substituted 1,2-diaza-3-one heterocycles. *Tetrahedron* **2009,** 65, 4212-4219.
42. Shen, S. L.; Shao, J. H.; Luo, J. Z.; Liu, J. T.; Miao, J. Y.; Zhao, B. X. Novel chiral ferrocenylpyrazolo 1,5-a 1,4 diazepin-4-one derivatives - Synthesis, characterization and inhibition against lung cancer cells. *European Journal of Medicinal Chemistry* **2013,** 63, 256-268.
43. Bolli, M. H.; Marfurt, J.; Grisostomi, C.; Boss, C.; Binkert, C.; Hess, P.; Treiber, A.; Thorin, E.; Morrison, K.; Buchmann, S.; Bur, D.; Ramuz, H.; Clozel, M.; Fischli, W.; Weller, T. Novel Benzo[1,4]diazepin-2-one Derivatives as Endothelin Receptor Antagonists. *Journal of Medicinal Chemistry* **2004,** 47, 2776-2795.
44. Im, I.; Webb, T. R.; Gong, Y.-D.; Kim, J.-I.; Kim, Y.-C. Solid-Phase Synthesis of Tetrahydro-1,4-benzodiazepine-2-one Derivatives as a β-Turn Peptidomimetic Library. *Journal of Combinatorial Chemistry* **2004,** 6, 207-213.
45. Araujo, A. C.; Rauter, A. P.; Nicotra, F.; Airoldi, C.; Costa, B.; Cipolla, L. Sugar-Based Enantiomeric and Conformationally Constrained Pyrrolo 2,1-c 1,4 -Benzodiazepines as Potential GABA(A) Ligands. *Journal of Medicinal Chemistry* **2011,** 54, 1266-1275.
46. Sharma, S. K.; Mandadapu, A. K.; Kumaresan, M., K.; Arora, A.; Kundu, B. Efficient Synthesis of Congeners based on a Naturally occurring Skeleton 5−7−6 Tricyclic Pyrrolo[2,1-c][1,4]Benzodiazepin-5-one via π-cyclization. *Synthesis* **2010**, 4087-4095.
47. Hadjipavloulitina, D.; Hansch, C. Quantitative structure-activity-relationships of the benzodiazepines - a review and reevaluation. *Chemical Reviews* **1994,** 94, 1483-1505.
48. Ripka, W. C.; Delucca, G. V.; Bach, A. C.; Pottorf, R. S.; Blaney, J. M. Protein beta-turn mimetics .1. design, synthesis, and evaluation in model cyclic-peptides. *Tetrahedron* **1993,** 49, 3593-3608.

49. Keenan, R. M.; Callahan, J. F.; Samanen, J. M.; Bondinell, W. E.; Calvo, R. R.; Chen, L. C.; DeBrosse, C.; Eggleston, D. S.; Haltiwanger, R. C.; Hwang, S. M.; Jakas, D. R.; Ku, T. W.; Miller, W. H.; Newlander, K. A.; Nichols, A.; Parker, M. F.; Southhall, L. S.; Uzinskas, I.; Vasko-Moser, J. A.; Venslavsky, J. W.; Wong, A. S.; Huffman, W. F. Conformational preferences in a benzodiazepine series of potent nonpeptide fibrinogen receptor antagonists. *Journal of Medicinal Chemistry* **1999,** 42, 545-559.
50. Ku, T. W.; Ali, F. E.; Barton, L. S.; Bean, J. W.; Bondinell, W. E.; Burgess, J. L.; Callahan, J. F.; Calvo, R. R.; Chen, L. Direct design of a potent non-peptide fibrinogen receptor antagonist based on the structure and conformation of a highly constrained cyclic RGD peptide. *Journal of the American Chemical Society* **1993,** 115, 8861-8862.
51. Schmidt, B.; Lindman, S.; Tong, W. M.; Lindeberg, G.; Gogoll, A.; Lai, Z. N.; Thornwall, M.; Synnergren, B.; Nilsson, A.; Welch, C. J.; Sohtell, M.; Westerlund, C.; Nyberg, F.; Karlen, A.; Hallberg, A. Design, synthesis, and biological activities of four angiotensin II receptor ligands with gamma-turn mimetics replacing amino acid residues 3-5. *Journal of Medicinal Chemistry* **1997,** 40, 903-919.
52. Dourlat, J.; Liu, W.-Q.; Gresh, N.; Garbay, C. Novel 1,4-benzodiazepine derivatives with antiproliferative properties on tumor cell lines. *Bioorganic & Medicinal Chemistry Letters* **2007,** 17, 2527-2530.
53. Dennison, H.; Warne, J.; Spencer, K.; Cockerill, G.; Lumley, J. Benzodiazepine derivatives for treating hepatitis c infection. WO2007034127, 2007.
54. Najafi, N. P., M.; Dowlatabadi, R.; Bagheri, M.; Rastkari, N.; Abdollahi, M. *Pharm. Chem.* **2005,** 39, 641-643.
55. Hoyt, S. B.; London, C.; Gorin, D.; Wyvratt, M. J.; Fisher, M. H.; Abbadie, C.; Felix, J. P.; Garcia, M. L.; Li, X.; Lyons, K. A.; McGowan, E.; MacIntyre, D. E.; Martin, W. J.; Priest, B. T.; Ritter, A.; Smith, M. M.; Warren, V. A.; Williams, B. S.; Kaczorowski, G. J.; Parsons, W. H. Discovery of a novel class of benzazepinone Na(v)1.7 blockers: Potential treatments for neuropathic pain. *Bioorganic & Medicinal Chemistry Letters* **2007,** 17, 4630-4634.
56. Miller, W. H.; Ku, T. W.; Ali, F. E.; Bondinell, W. E.; Calvo, R. R.; Davis, L. D.; Erhard, K. F.; Hall, L. B.; Huffman, W. F.; Keenan, R. M.; Kwon, C.; Newlander, K. A.; Ross, S. T.; Samanen, J. M.; Takata, D. T.; Yuan, C. K. Enantiospecific synthesis of SB 214857, a potent, orally active, nonpeptide fibrinogen receptor antagonist. *Tetrahedron Letters* **1995,** 36, 9433-9436.
57. Armour, D. R.; Aston, N. M.; Morriss, K. M. L.; Congreve, M. S.; Hawcock, A. B.; Marquess, D.; Mordaunt, J. E.; Richards, S. A.; Ward, P. 1,4-Benzodiazepin-2-one derived neurokinin-1 receptor antagonists. *Bioorganic & Medicinal Chemistry Letters* **1997,** 7, 2037-2042.
58. Burgey, C. S.; Stump, C. A.; Nguyen, D. N.; Deng, J. Z.; Quigley, A. G.; Norton, B. R.; Bell, I. M.; Mosser, S. D.; Salvatore, C. A.; Rutledge, R. Z.; Kane, S. A.; Koblan, K. S.; Vacca, J. P.; Graham, S. L.; Williams, T. M. Benzodiazepine calcitonin gene-related peptide (CGRP) receptor antagonists: Optimization of the 4-substituted piperidine. *Bioorganic & Medicinal Chemistry Letters* **2006,** 16, 5052-5056.
59. Ma, D. W.; Wang, G. Q.; Wang, S. M.; Kozikowski, A. P.; Lewin, N. E.; Blumberg, P. M. Synthesis and protein kinase C binding activity of benzolactam-V7. *Bioorganic & Medicinal Chemistry Letters* **1999,** 9, 1371-1374.
60. Boitano, A.; Ellman, J. A.; Glick, G. D.; Opipari, A. W. The proapoptotic benzodiazepine Bz-423 affects the growth and survival of malignant B cells. *Cancer Research* **2003,** 63, 6870-6876.

61. Micale, N.; Vairagoundar, R.; Yakovlev, A. G.; Kozikowski, A. P. Design and Synthesis of a Potent and Selective Peptidomimetic Inhibitor of Caspase-3. *Journal of Medicinal Chemistry* **2004,** 47, 6455-6458.
62. Salome, C.; Schmitt, M.; Bourguignon, J.-J. Novel access to 1,4-benzodiazepin-2-ones via the Buchwald reaction and application to the synthesis of novel heterocyclics. *Tetrahedron Letters* **2012,** 53, 1033-1035.
63. Wang, H. X.; Jiang, Y. W.; Gao, K.; Ma, D. W. Facile synthesis of 1,4-benzodiazepin-3-ones from o-bromobenzylamines and amino acids via a cascade coupling/condensation process. *Tetrahedron* **2009,** 65, 8956-8960.
64. Mossetti, R.; Saggiorato, D.; Tron, G. C. Exploiting the Acylating Nature of the Imide-Ugi Intermediate: A Straightforward Synthesis of Tetrahydro-1,4-benzodiazepin-2-ones. *Journal of Organic Chemistry* **2011,** 76, 10258-10262.
65. Liu, J.; Cheng, A. C.; Tang, H. L.; Medina, J. C. Benzodiazepinone Derivatives as CRTH2 Antagonists. *Acs Medicinal Chemistry Letters* **2011,** 2, 515-518.
66. Gilfillan, L.; Blair, A.; Morris, B. J.; Pratt, J. A.; Schweiger, L.; Pimlott, S.; Sutherland, A. Synthesis and biological evaluation of novel 2,3-dihydro-1H-1,5-benzodiazepin-2-ones; potential imaging agents of the metabotropic glutamate 2 receptor. *Medchemcomm* **2013,** 4, 1118-1123.
67. Bunin, B. A.; Ellman, J. A. A general and expedient method for the solid-phase synthesis of 1,4-benzodiazépine derrivatives. *Journal of the American Chemical Society* **1992,** 114, 10997-10998.
68. Zhang, J. F.; Goodloe, W. P.; Lou, B. L.; Saneii, H. Solid-phase synthesis of tetrahydro-1,4-benzodiazepin-2-one derivatives. *Molecular Diversity* **2000,** 5, 127-130.
69. Lee, J.; Gauthier, D.; Rivero, R. A. Solid-phase synthesis of 3,4,5-substituted 1,5-benzodiazepin-2-ones. *Journal of Organic Chemistry* **1999,** 64, 3060-3065.
70. Leimgruber, W.; Stefanović, V.; Schenker, F.; Karr, A.; Berger, J. Isolation and Characterization of Anthramycin, a New Antitumor Antibiotic. *J. Am. Chem. Soc.* **1965,** 87, 5791-5793.
71. Berry, J. M.; Howard, P. W.; Thurston, D. E. Solid-phase synthesis of DNA-interactive pyrrolo 2,1-c 1,4 benzodiazepines. *Tetrahedron Letters* **2000,** 41, 6171-6174.
72. Thurston, D. E. Advances in the study of pyrrolo[2,1-*c*][1,4]benzodiazepine (PBD) antitumor antibiotics. In *Molecular Aspects of Anticancer Drug-DNA Interactions*, Neidle, S.; Waring, M., Eds. MacMillan: London, UK, 1993; Vol. 1, pp 54-88.
73. Antonow, D.; Thurston, D. E. Synthesis of DNA-Interactive Pyrrolo 2,1-c 1,4 benzodiazepines (PBDs). *Chemical Reviews* **2011,** 111, 2815-2864.
74. Kaneko, T.; Wong, H.; Doyle, T. W.; Rose, W. C.; Bradner, W. T. Bicyclic and tricyclic analogs of anthramycin. *Journal of Medicinal Chemistry* **1985,** 28, 388-392.
75. Hopton, S. R.; Thompson, A. S. Nuclear Magnetic Resonance Solution Structures of Inter- and Intrastrand Adducts of DNA Cross-Linker SJG-136. *Biochemistry* **2011,** 50, 4720-4732.
76. Hurley, L. H.; Reck, T.; Thurston, D. E.; Langley, D. R.; Holden, K. G.; Hertzberg, R. P.; Hoover, J. R. E.; Gallagher, G.; Faucette, L. F.; Mong, S. M.; Johnson, R. K. Pyrrolo 1,4 benzodiazepine antitumor antibiotics - relationship of DNA alkylation and sequence specificity to the biological - activity of natural and synthetic compounds. *Chemical Research in Toxicology* **1988,** 1, 258-268.
77. Fabis, F.; Santos, J. S. D.; Fouchet-Jolivet, S.; Rault, S. An expedient route to aromatic pyrrolo 2,1-c 1,4 benzodiazepines and a study of their reactivity. *Tetrahedron Letters* **2001,** 42, 5183-5185.

78. Fotso, S.; Zabriskie, T. M.; Proteau, P. J.; Flatt, P. M.; Santosa, D. A.; Sulastri; Mahmud, T. Limazepines A-F, Pyrrolo 1,4 benzodiazepine Antibiotics from an Indonesian Micrococcus sp. *Journal of Natural Products* **2009,** 72, 690-695.
79. Arima, K.; Kosaka, M.; Tamura, G.; Imanaka, H.; Sakai, H. Studies on tomaymycin, a new antibiotic. I. Isolation and properties of tomaymycin. *The Journal of antibiotics* **1972,** 25, 437-44.
80. Konishi, M.; Hatori, M.; Tomita, K.; Sugawara, M.; Ikeda, C.; Nishiyama, Y.; Imanishi, H.; Miyaki, T.; Kawaguchi, H. Chicamycin, a new antitumor antibiotic .1. production, isolation and properties. *Journal of Antibiotics* **1984,** 37, 191-199.
81. Giessen, T. W.; Kraas, F. I.; Marahiel, M. A. A Four-Enzyme Pathway for 3,5-Dihydroxy-4-methylanthranilic Acid Formation and Incorporation into the Antitumor Antibiotic Sibiromycin. *Biochemistry* **2011,** 50, 5680-5692.
82. Schmidt, A.; Shilabin, A. G.; Namyslo, J. C.; Nieger, M.; Hemmen, S. Pyrimidine-annulated pyrrolobenzodiazepines. A new ring system related to Aspergillus alkaloids. *European Journal of Organic Chemistry* **2005**, 1781-1789.
83. Rohtash Kumar, J. W. L. Recent developments in novel pyrrolo[2,1-c][1,4]benzodiazepine conjugates: synthesis and biological evaluation. *Mini Rev. Med. Chem.* **2003,** 17, 323-339.
84. Kluczyk, A.; Rudowska, M.; Stefanowicz, P.; Szewczuk, Z. Microwave-assisted TFA cleavage of peptides from Merrifield resin. *Journal of Peptide Science* **2010,** 16, 31-39.
85. Miyashiro, J.; Woods, K. W.; Park, C. H.; Liu, X.; Shi, Y.; Johnson, E. F.; Bouska, J. J.; Olson, A. M.; Luo, Y.; Fry, E. H.; Giranda, V. L.; Penning, T. D. Synthesis and SAR of novel tricyclic quinoxalinone inhibitors of poly(ADP-ribose)polymerase-1 (PARP-1). *Bioorganic & Medicinal Chemistry Letters* **2009,** 19, 4050-4054.
86. Lisowski, V.; Fabis, F.; Pierre, A.; Caignard, D. H.; Renard, P.; Rault, S. Synthesis of new aromatic pyrrolo 2,1-c 1,4 benzodiazepines and pyrrolo 1,2-a thieno 3,2-e 1,4 diazepines as anti-tumoral agents. *J. Enzyme Inhib. Med. Chem.* **2002,** 17, 403-407.
87. De Lucca, G. V.; Otto, M. J. Synthesis and anti-HIV activity of pyrrolo-[1,2-d]-(1,4)-benzodiazepin-6-ones. *Bioorganic & Medicinal Chemistry Letters* **1992,** 2, 1639-1644.
88. Meerpoel, L.; Van Gestel, J.; Van Gerven, F.; Woestenborghs, F.; Marichal, P.; Sipido, V.; Terence, G.; Nash, R.; Corens, D.; Richards, R. D. Pyrrolo 1,2-a 1,4 benzodiazepine: A novel class of non-azole anti-dermatophyte anti-fungal agents. *Bioorganic & Medicinal Chemistry Letters* **2005,** 15, 3453-3458.
89. Bolos, J.; Perez, A.; Gubert, S.; Anglada, L.; Sacristan, A.; Ortiz, J. A. Asymmetric synthesis of pyrrolo[1,2-b][1,2]diazepine derivatives as potential antihypertensive drugs. *Journal of Organic Chemistry* **1992,** 57, 3535-3539.
90. Corelli, F.; Massa, S.; Pantaleoni, G. C.; Palumbo, G.; Fanini, D. Heterocyclic - systems .5. synthesis and activity on the CNS of derivatives of 6H-pyrrolo 1,2-a 1,4 benzodiazepine. *Farmaco-Edizione Scientifica* **1984,** 39, 707-717.
91. Massa, S.; Artico, M.; Mai, A.; Corelli, F.; Botta, M.; Tafi, A.; Pantaleoni, G. C.; Giorgi, R.; Coppolino, M. F.; Cagnotto, A.; Skorupska, M. Pyrrolobenzodiazepines and related systems .2. synthesis and biological properties of isonoraptazepine derivatives. *Journal of Medicinal Chemistry* **1992,** 35, 4533-4541.
92. Hara T; Kayama Y; Mori T; Itoh K; Fujimori H; Sunami T; Hashimoto Y; S., I. Diazepines. 5. Synthesis and biological action of 6-phenyl-4H-pyrrolo[1,2-a][1,4]benzodiazepines. *Mini Rev. Med. Chem.* **1978,** 21, 263.
93. Hara, T.; Shikayama, Y.; Ito, K.; Mori, T.; Fujimori, H.; Sunami, T.; Hashimoto, Y.; Ishimoto, Y. JP 61001433, 1986.

94. Saito, S.; Umemiya, H.; Suga, Y.; Sato, M.; Kawashima, N. Spiro-Ring Compound WO 2003095427, 2003.
95. Doods, H.; Eberlein, W.; Engel, W.; Entzeroth, M.; Mihm, G.; Rudolf, K.; Ziegler, H. Condensed diazepinones, process for their preparation and compositions containing them for the treatment of the central nervous system and to enhance cerebral perfusion. . EP0508370 (A1), 19920407., 1992.
96. Mariani, L.; Tarzia, G. 1,7-Dihydropyrrolo[3,4-e][1,4]diazepin-2(3H)-one derivatives, and their use as anticonvulsant and antianxiety agents. EP0102602 (A1) 19830827., 1984.
97. Mariani, L.; Tarzia, G. 3,7-Dihydropyrrolo[3,4-e][1,4]diazepin-2(1H)-one derivatives. EP0066762 (A2) 19820522., 1982.
98. Correa, A.; Herrero, M. T.; Tellitu, I.; Dominguez, E.; Moreno, I.; SanMartin, R. An alternative approach towards novel heterocycle-fused 1,4-diazepin-2-ones by an aromatic amidation protocol. *Tetrahedron* **2003,** 59, 7103-7110.
99. Correa, A.; Tellitu, I.; Dominguez, E.; Moreno, I.; SanMartin, R. An efficient, PIFA mediated approach to benzo-, naphtho-, and heterocycle-fused pyrrolo 2,1-c 1,4 diazepines. An advantageous access to the antitumor antibiotic DC-81. *Journal of Organic Chemistry* **2005,** 70, 2256-2264.
100. Ilyn, A. P.; Trifilenkov, A. S.; Kuzovkova, J. A.; Kutepov, S. A.; Nikitin, A. V.; Ivachtchenko, A. V. New Four-Component Ugi-Type Reaction. Synthesis of Heterocyclic Structures Containing a Pyrrolo[1,2-a][1,4]diazepine Fragment. *J. Org. Chem.* **2005,** 70, 1478-1481.
101. Van den Bogaert, A. M.; Nelissen, J.; Ovaere, M.; Van Meervelt, L.; Compernolle, F.; De Borggraeve, W. M. Synthesis of Pyridodiazepinediones by Using the Ugi Multicomponent Reaction. *European Journal of Organic Chemistry* **2010**, 5397-5401.
102. Belov, V. N.; Funke, C.; Labahn, T.; Es-Sayed, M.; de Meijere, A. Cyclopropyl building blocks in organic synthesis, 50 - An easy access to bicyclic peptides with an octahydro 2H pyrazino 1,2-a pyrazine skeleton. *European Journal of Organic Chemistry* **1999**, 1345-1356.
103. Funke, C.; Es-Sayed, M.; de Meijere, A. Facile Preparation of Hexahydropyrrolo[3,2-e][1,4]diazepine- 2,5-diones and Tetrahydrofuro[1H][3,2-e][1,4]diazepine- 2,5-diones by Rearrangements of Cyclopropylketimines and Cyclopropylketones. *Organic Letters* **2000,** 2, 4249-4251.
104. Nevolina, T. A.; Shcherbinin, V. A.; Serdyuk, O. V.; Butin, A. V. Furan Ring Opening-Pyrrole Ring Closure: A New Route to Pyrrolo 1,2-d 1,4 benzodiazepin-6-ones. *Synthesis-Stuttgart* **2011**, 3547-3551.
105. Mayer, J. P.; Zhang, J. W.; Bjergarde, K.; Lenz, D. M.; Gaudino, J. J. Solid phase synthesis of 1,4-benzodiazepine-2,5-diones. *Tetrahedron Letters* **1996,** 37, 8081-8084.
106. Kamal, A.; Reddy, K. L.; Devaiah, V.; Shankaraiah, N.; Reddy, G. S. K.; Raghavan, S. Solid-phase synthesis of a library of pyrrolo 2,1-c 1,4 benzodiazepine-5,11-diones with potential antitubercular activity. *Journal of Combinatorial Chemistry* **2007,** 9, 29-42.
107. Ohlmeyer, M. H. J. Combinatorial 1,4-Benzodiazepin-2,5-dione Library. WO2007034127, 1999.
108. Kamal, A.; Reddy, G. S. K.; Reddy, K. L. Efficient reduction of aromatic nitro/azido groups on solid support employing indium: synthesis of pyrrolo 2,1-c 1,4 benzodiazepine-5,11-diones. *Tetrahedron Letters* **2001,** 42, 6969-6971.
109. Kamal, A.; Reddy, G. S. K.; Reddy, K. L.; Raghavan, S. Efficient solid-phase synthesis of DNA-interactive pyrrolo 2,1-c 1,4 benzodiazepine antitumour antibiotics. *Tetrahedron Letters* **2002,** 43, 2103-2106.

110. Kamal, A.; Reddy, K. L.; Devaiah, V.; Shankaraiah, N.; Reddy, Y. N. A new approach for the solid-phase synthesis of pyrrolo 2,1-c 1,4 benzodiazepines involving reductive cleavage. *Tetrahedron Letters* **2004,** 45, 7667-7669.
111. Pictet, A.; Spengler, T. Über die Bildung von Isochinolin-derivaten durch Einwirkung von Methylal auf Phenyl-äthylamin, Phenyl-alanin und Tyrosin. *Berichte der deutschen chemischen Gesellschaft* **1911,** 44, 2030-2036.
112. Cox, E. D.; Cook, J. M. The Pictet-Spengler condensation - a new direction for an old reaction. *Chemical Reviews* **1995,** 95, 1797-1842.
113. Xiang, J.; Zheng, L.; Chen, F.; Dang, Q.; Bai, X. A cascade reaction consisting of Pictet-Spengler-type cyclization and Smiles rearrangement: Application to the synthesis of novel pyrrole-fused dihydropteridines. *Organic Letters* **2007,** 9, 765-767.
114. Rousseau, J. F.; Dodd, R. H. Synthesis of 3-deaza-beta-hydroxyhistidine derivatives and their use for the preparation of substituted pyrrolo 2,3-c pyridine-5-carboxylates via the Pictet-Spengler reaction. *Journal of Organic Chemistry* **1998,** 63, 2731-2737.
115. Raiman, M. V.; Pukin, A. V.; Tyvorskii, V. I.; De Kimpe, N.; Kulinkovich, O. G. A convenient approach to the synthesis of 2-(2-aminoethyl)pyrroles and their heterocyclization into hydrogenated pyrrolopyridines and related pyrroloindolizines. *Tetrahedron* **2003,** 59, 5265-5272.
116. Raheem, I. T.; Thiara, P. S.; Jacobsen, E. N. Regio- and enantioselective catalytic cyclization of pyrroles onto N-acyliminium ions. *Organic Letters* **2008,** 10, 1577-1580.
117. Fridkin, G.; Lubell, W. D. 2-vinylpyrroles and pyrrolo 3,2-d pyrimidines from direct addition of aldehydes to 4-amino-pyrrole-2-carboxylate derivatives. *Organic Letters* **2008,** 10, 849-852.
118. Duncton, M. A. J.; Smith, L. M.; Burdzovic-Wizeman, S.; Burns, A.; Liu, H.; Mao, Y. Y.; Wong, W. C.; Kiselyov, A. S. Preparation of substituted pyrimido 4,5-b -1,4-benzoxazepines, thiazepines, and diazepines via a Pictet-Spengler cyclization. *Journal of Organic Chemistry* **2005,** 70, 9629-9631.
119. Blanco, M. J.; Sardina, F. J. Entiospecific and stereoselective synthesis of polyhydroxylated pyrrolidines and indolizidines from trans-4-hydroxy-L-proline. *Journal of Organic Chemistry* **1996,** 61, 4748-4755.
120. Marcotte, F.-A.; Lubell, W. D. An effective new synthesis of 4-aminopyrrole-2-carboxylates. *Organic Letters* **2002,** 4, 2601-2603.
121. Falb, E.; Yechezkel, T.; Salitra, Y.; Gilon, C. In situ generation of Fmoc-amino acid chlorides using bis(trichloromethyl) carbonate and its utilization for difficult couplings in solid-phase peptide synthesis. *J. Pept. Res.* **1999,** 53, 507-517.
122. Royer, J.; Bonin, M.; Micouin, L. Chiral heterocycles by iminium ion cyclization. *Chemical Reviews* **2004,** 104, 2311-2352.
123. Boutard, N.; Dufour-Gallant, J.; Deaudelin, P.; Lubell, W. D. Pyrrolo 3,2-e 1,4 diazepin-2-one synthesis: A head-to-head comparison of soluble versus insoluble supports. *Journal of Organic Chemistry* **2011,** 76, 4533-4545.
124. Brouillette, Y.; Rombouts, F. J. R.; Lubell, W. D. Solid-phase synthesis of 3-aminopyrrole-2,5-dicarboxylate analogues. *Journal of Combinatorial Chemistry* **2006,** 8, 117-126.
125. Iden, H. S.; Lubell, W. D. 1,3,5-tri- and 1,3,4,5-tetra-substituted 1,4-diazepin-2-one solid-phase synthesis. *Journal of Combinatorial Chemistry* **2008,** 10, 691-699.
126. Albericio, F. *Solid-Phase Synthesis: A Practical Guide*. CRC Press: 2000.
127. Stazi, F.; Marcoux, D.; Poupon, J. C.; Latassa, D.; Charette, A. B. Tetraarylphosphonium salts as soluble supports for the synthesis of small molecules. *Angewandte Chemie, International Edition* **2007,** 46, 5011-5014.

128. Ginisty, M.; Roy, M. N.; Charette, A. B. Tetraarylphosphonium-supported carbodiimide reagents: Synthesis, structure optimization and applications. *Journal of Organic Chemistry* **2008,** 73, 2542-2547.
129. Poupon, J. C.; Boezio, A. A.; Charette, A. B. Tetraarylphosphonium salts as solubility-control groups: Phosphonium-supported triphenylphosphine and azodicarboxylate reagents. *Angewandte Chemie, International Edition* **2006,** 45, 1415-1420.
130. Pearson, D.; Shively, J. E.; Clark, B. R.; Geschwind, II; Barkley, M.; Nishioka, R. S.; Bern, H. A. Urotensin II: A somatostatin-like peptide in the caudal neurosecretory system of fishes. *Proc. Natl. Acad. Sci. U. S. A.* **1980,** 77, 5021-5024.
131. Bern, H.; Lederis, K. A reference preparation for the study of active substances in the caudal neurosecretory system of teleosts. *J. Endochinol.* **1969,** 45, Suppl:xi–xii.
132. Fridberg, G.; Bern, H. A. The urophysis and the caudal neurosecretory system of fishes. *Biological in Review* **1968**, 175-199.
133. Coulouarn, Y.; Lihrmann, I.; Jegou, S.; Anouar, Y.; Tostivint, H.; Beauvillain, J. C.; Conlon, J. M.; Bern, H. A.; Vaudry, H. Cloning of the cDNA encoding the urotensin II precursor in frog and human reveals intense expression of the urotensin II gene in motoneurons of the spinal cord. *Proceedings of the National Academy of Sciences of the United States of America* **1998,** 95, 15803-15808.
134. Bern, H. A.; Pearson, D.; Larson, B. A.; Nishioka, R. S. Neurohormones from fish tails: the caudal neurosecretory system. I. "Urophysiology" and the caudal neurosecretory system of fishes. *Recent Progress in Hormone Research* **1985,** 41, 533-52.
135. Gibson, A.; Bern, H. A.; Ginsburg, M.; Botting, J. H. Neuropeptide-induced contraction and relaxation of the mouse anococcygeus muscle. *Proceedings of the National Academy of Sciences of the United States of America-Biological Sciences* **1984,** 81, 625-629.
136. Gibson, A. Complex effects of gillichthys urotensin-II on rat aortic strips. *British Journal of Pharmacology* **1987,** 91, 205-212.
137. McMaster, D.; Belenky, M. A.; Polenov, A. L.; Lederis, K. Isolation and amino-acid-sequence of urotensin-II from the sturgeon acipenser-ruthenus. *General and Comparative Endocrinology* **1992,** 87, 275-285.
138. Waugh, D.; Conlon, J. M. Purification and characterization of urotensin-II from the brain of a teleost (trout, oncorhynchus-mykiss) and an elasmobranch (skate, raja rhina). *General and Comparative Endocrinology* **1993,** 92, 419-427.
139. Ichikawa, T.; Lederis, K.; Kobayashi, H. Primary structures of multiple forms of urotensin-II in the urophysis of the carp, cyprinus-carpio. *General and Comparative Endocrinology* **1984,** 55, 133-141.
140. Ohsako, S.; Ishida, I.; Ichikawa, T.; Deguchi, T. Cloning and sequence - analysis of CDNAS encoding precursors of urotensin-II-alpha and urotensin-II-gamma. *Journal of Neuroscience* **1986,** 6, 2730-2735.
141. Conlon, J. M.; Arnoldreed, D.; Balment, R. J. Posttranslational processing of prepro-urotensin-II. *FEBS Letters* **1990,** 266, 37-40.
142. Conlon, J. M. "Liberation" of urotensin II from the teleost urophysis: An historical overview. *Peptides* **2008,** 29, 651-657.
143. Vaudry, H.; Do Rego, J. C.; Le Mevel, J. C.; Chatenet, D.; Tostivint, H.; Fournier, A.; Tonon, M. C.; Pelletier, G.; Conlon, J. M.; Leprince, J. Urotensin II, from fish to human. *Ann N Y Acad Sci* **2010,** 1200, 53-66.
144. Conlon, J. M.; Oharte, F.; Smith, D. D.; Tonon, M. C.; Vaudry, H. Isolation and primary structure of urotensin-II from the brain of a tetrapod the frog rana-ridibunda. *Biochemical and Biophysical Research Communications* **1992,** 188, 578-583.

145. Chartrel, N.; Conlon, J. M.; Collin, F.; Braun, B.; Waugh, D.; Vallarino, M.; Lahrichi, S. L.; Rivier, J. E.; Vaudry, H. Urotensin II in the central nervous system of the frog Rana ridibunda: Immunohistochemical localization and biochemical characterization. *Journal of Comparative Neurology* **1996,** 364, 324-339.
146. Coulouarn, Y.; Jegou, S.; Tostivint, H.; Vaudry, H.; Lihrmann, I. Cloning, sequence analysis and tissue distribution of the mouse and rat urotensin II precursors. *FEBS Letters* **1999,** 457, 28-32.
147. Sugo, T.; Murakami, Y.; Shimomura, Y.; Haradam, M.; Abe, M.; Ishibashi, Y.; Kitada, C.; Miyajima, N.; Suzuki, N.; Mori, M.; Fujino, M. Identification of urotensin II-related peptide as the urotensin II-immunoreactive molecule in the rat brain. *Biochemical and Biophysical Research Communications* **2003,** 310, 860-868.
148. Mori, M.; Sugo, T.; Abe, M.; Shimomura, Y.; Kurihara, M.; Kitada, C.; Kikuchi, K.; Shintani, Y.; Kurokawa, T.; Onda, H.; Nishimura, O.; Fujino, M. Urotensin II is the endogenous ligand of a G-protein-coupled orphan receptor, SENR (GPR14). *Biochemical and Biophysical Research Communications* **1999,** 265, 123-129.
149. Elshourbagy, N. A.; Douglas, S. A.; Shabon, U.; Harrison, S.; Duddy, G.; Sechler, J. L.; Ao, Z. H.; Maleeff, B. E.; Naselsky, D.; Disa, J.; Aiyar, N. V. Molecular and pharmacological characterization of genes encoding urotensin-II peptides and their cognate G-protein-coupled receptors from the mouse and monkey. *British Journal of Pharmacology* **2002,** 136, 9-22.
150. Chartrel, N.; Leprince, J.; Dujardin, C.; Chatenet, D.; Tollemer, H.; Baroncini, M.; Balment, R. J.; Beauvillain, J. C.; Vaudry, H. Biochemical characterization and immunohistochemical localization of urotensin II in the human brainstem and spinal cord. *Journal of Neurochemistry* **2004,** 91, 110-118.
151. Onan, D.; Hannan, R. D.; Thomas, W. G. Urotensin II: the old kid in town. *Trends in Endocrinol. Metab.* **2004,** 15, 175-182.
152. Itoh, H.; McMaster, D.; Lederis, K. Functional receptors for fish neuropeptide urotensin-II in major rat arteries. *European Journal of Pharmacology* **1988,** 149, 61-66.
153. Leprince, J.; Chatenet, D.; Dubessy, C.; Fournier, A.; Pfeiffer, B.; Scalbert, E.; Renard, P.; Pacaud, P.; Oulyadi, H.; Segalas-Milazzo, I.; Guilhaudis, L.; Davoust, D.; Jonon, M.-C.; Vaudry, H. Structure-activity relationships of urotensin II and URP. *Peptides* **2008,** 29, 658-673.
154. Flohr, S.; Kurz, M.; Kostenis, E.; Brkovich, A.; Fournier, A.; Klabunde, T. Identification of nonpeptidic urotensin II receptor antagonists by virtual screening based on a pharmacophore model derived from structure-activity relationships and nuclear magnetic resonance studies on urotensin II. *Journal of Medicinal Chemistry* **2002,** 45, 1799-1805.
155. Labarrere, P.; Chatenet, D.; Leprince, J.; Marionneau, C.; Loirand, G.; Tonon, M. C.; Dubessy, C.; Scalbert, E.; Pfeiffer, B.; Renard, P.; Calas, B.; Pacaud, P.; Vaudry, H. Structure-activity relationships of human urotensin II and related analogues on rat aortic ring contraction. *Journal of Enzyme Inhibition and Medicinal Chemistry* **2003,** 18, 77-88.
156. Sugo, T.; Mori, M. Another ligand fishing for G protein-coupled receptor 14 - Discovery of urotensin II-related peptide in the rat brain. *Peptides* **2008,** 29, 809-812.
157. Douglas, S. A.; Dhanak, D.; Johns, D. G. From 'gills to pills': urotensin-II as a regulator of mammalian cardiorenal function. *Trends in Pharmacological Sciences* **2004,** 25, 76-85.
158. Conlon, J. M.; Yano, K.; Waugh, D.; Hazon, N. Distribution and molecular forms of urotensin II and its role in cardiovascular regulation in vertebrates. *Journal of Experimental Zoology* **1996,** 275, 226-238.
159. Kinney, W. A.; Almond, H. R.; Qi, J. S.; Smith, C. E.; Santulli, R. J.; de Garavilla, L.; Andrade-Gordon, P.; Cho, D. S.; Everson, A. M.; Feinstein, M. A.; Leung, P. A.; Maryanoff, B. E.

Structure-function analysis of urotensin II and its use in the construction of a ligand-receptor working model. *Angewandte Chemie-International Edition* **2002,** 41, 2940-2944.
160. Maguire, J. J.; Davenport, A. P. Is urotensin-II the new endothelin? *British Journal of Pharmacology* **2002,** 137, 579-588.
161. Silvestre, R.; Egido, E. M.; Hernandez, R.; Leprince, J.; Chatenet, D.; Tollemer, H.; Chartrel, N.; Vaudry, H.; Marco, J. Urotensin-II is present in pancreatic extracts and inhibits insulin release in the perfused rat pancreas. *European Journal of Endocrinology* **2004,** 151, 803-809.
162. Gartlon, J.; Parker, F.; Harrison, D. C.; Douglas, S. A.; Ashmeade, T. E.; Riley, G. J.; Hughes, Z. A.; Taylor, S. G.; Munton, R. P.; Hagan, J. J.; Hunter, J. A.; Jones, D. N. C. Central effects of urotensin-II following ICV administration in rats. *Psychopharmacology* **2001,** 155, 426-433.
163. Lu, Y.; Zou, C. J.; Huang, D. W.; Tang, C. S. Cardiovascular effects of urotensin II in different brain areas. *Peptides* **2002,** 23, 1631-1635.
164. Kawaguchi, Y.; Ono, T.; Kudo, M.; Kushikata, T.; Hashiba, E.; Yoshida, H.; Kudo, T.; Furukawa, K.; Douglas, S. A.; Hirota, K. The Effects of Benzodiazepines on Urotensin II-Stimulated Norepinephrine Release from Rat Cerebrocortical Slices. *Anesthesia and Analgesia* **2009,** 108, 1177-1181.
165. Ross, B.; McKendy, K.; Giaid, A. Role of urotensin II in health and disease. *American Journal of Physiology-Regulatory Integrative and Comparative Physiology* **2010,** 298, R1156-R1172.
166. Ames, R. S.; Sarau, H. M.; Chambers, J. K.; Willette, R. N.; Alyar, N. V.; Romanic, A. M.; Louden, C. S.; Foley, J. J.; Sauermelch, C. F.; Coatney, R. W.; Ao, Z. H.; Disa, J.; Holmes, S. D.; Stadel, J. M.; Martin, J. D.; Liu, W. S.; Glover, G. I.; Wilson, S.; McNulty, D. E.; Ellis, C. E.; Elshourbagy, N. A.; Shabon, U.; Trill, J. J.; Hay, D. W. P.; Ohlstein, E. H.; Bergsma, D. J.; Douglas, S. A. Human urotensin-II is a potent vasoconstrictor and agonist for the orphan receptor GPR14. *Nature* **1999,** 401, 282-286.
167. Onan, D.; Hannan, R. D.; Thomas, W. G. Urotensin II: the old kid in town. *Trends Endocrinol Metab* **2004,** 15, 175-82.
168. Clark, S. D.; Nothacker, H. P.; Wang, Z.; Saito, Y.; Leslie, F. M.; Civelli, O. The urotensin II receptor is expressed in the cholinergic mesopontine tegmentum of the rat. *Brain Research* **2001,** 923, 120-127.
169. Liu, Q. Y.; Pong, S. S.; Zeng, Z. Z.; Zhang, Q.; Howard, A. D.; Williams, D. L.; Davidoff, M.; Wang, R. P.; Austin, C. P.; McDonald, T. P.; Bai, C.; George, S. R.; Evans, J. F.; Caskey, C. T. Identification of urotensin II as the endogenous ligand for the orphan G-protein-coupled receptor GPR14. *Biochemical and Biophysical Research Communications* **1999,** 266, 174-178.
170. Doan, N. D.; Nguyen, T. T.; Letourneau, M.; Turcotte, K.; Fournier, A.; Chatenet, D. Biochemical and pharmacological characterization of nuclear urotensin II binding sites in rat heart. *Br J Pharmacol* **2011,** 166, 243-257.
171. Nguyen, T. T. M.; Letourneau, M.; Chatenet, D.; Fournier, A. Presence of urotensin-II receptors at the cell nucleus: Specific tissue distribution and hypoxia-induced modulation. *International Journal of Biochemistry & Cell Biology* **2012,** 44, 639-647.
172. Jarry, M.; Diallo, M.; Lecointre, C.; Desrues, L.; Tokay, T.; Chatenet, D.; Leprince, J.; Rossi, O.; Vaudry, H.; Tonon, M. C.; Prezeau, L.; Castel, H.; Gandolfo, P. The vasoactive peptides urotensin II and urotensin II-related peptide regulate astrocyte activity through common and distinct mechanisms: involvement in cell proliferation. *Biochemical Journal* **2010,** 428, 113-124.

173. Matsushita, M.; Shichiri, M.; Imai, T.; Iwashina, M.; Tanaka, H.; Takasu, N.; Hirata, Y. Co-expression of urotensin II and its receptor (GPR14) in human cardiovascular and renal tissues. *Journal of Hypertension* **2001,** 19, 2185-2190.
174. Gruson, D.; Ginion, A.; Decroly, N.; Lause, P.; Vanoverschelde, J. L.; Ketelslegers, J. M.; Bertrand, L.; Thissen, J. P. Urotensin II induction of adult cardiomyocytes hypertrophy involves the Akt/GSK-3 beta signaling pathway. *Peptides* **2010,** 31, 1326-1333.
175. Totsune, K.; Takahashi, K.; Arihara, Z.; Sone, M.; Murakami, O.; Ito, S.; Kikuya, M.; Ohkubo, T.; Hashimoto, J.; Imai, Y. Elevated plasma levels of immunoreactive urotensin II and its increased urinary excretion in patients with type 2 diabetes mellitus: association with progress of diabetic nephropathy. *Peptides* **2004,** 25, 1809-1814.
176. Watanabe, T.; Katagiri, T.; Pakala, R.; Benedict, C. R. Synergistic effect of urotensin II with serotonin on vascular smooth muscle cell proliferation. *American Journal of Hypertension* **2003,** 16, 170A-171A.
177. Bousette, N.; Patel, L.; Douglas, S. A.; Ohlstein, E. H.; Giaid, A. Increased expression of urotensin II and its cognate receptor GPR14 in atherosclerotic lesions of the human aorta. *Atherosclerosis* **2004,** 176, 117-123.
178. Watanabe, T.; Arita, S.; Shiraishi, Y.; Suguro, T.; Sakai, T.; Hongo, S.; Miyazaki, A. Human Urotensin II Promotes Hypertension and Atherosclerotic Cardiovascular Diseases. *Current Medicinal Chemistry* **2009,** 16, 550-563.
179. Tzanidis, A.; Hannan, R. D.; Thomas, W. G.; Onan, D.; Autelitano, D. J.; See, F.; Kelly, D. J.; Gilbert, R. E.; Krum, H. Direct actions of urotensin II on the heart - Implications for cardiac fibrosis and hypertrophy. *Circulation Research* **2003,** 93, 246-253.
180. Desai, N.; Sajjad, J.; Frishman, W. H. Urotensin II: a new pharmacologic target in the treatment of cardiovascular disease. *Cardiol Rev* **2008,** 16, 142-53.
181. Jani, P. P.; Narayan, H.; Ng, L. L. The differential extraction and immunoluminometric assay of Urotensin II and Urotensin-related peptide in heart failure. *Peptides* **2013,** 40, 72-76.
182. McDonald, J.; Batuwangala, M.; Lambert, D. G. Role of urotensin II and its receptor in health and disease. *Journal of Anesthesia* **2007,** 21, 378-389.
183. Chatenet, D.; Letourneau, M.; Nguyen, Q. T.; Doan, N. D.; Dupuis, J.; Fournier, A. Discovery of new antagonists aimed at discriminating UII and URP-mediated biological activities: insight into UII and URP receptor activation. *British Journal of Pharmacology* **2013,** 168, 807-821.
184. Totsune, K.; Takahashi, K.; Arihara, Z.; Sone, M.; Ito, S.; Murakami, O. Increased plasma urotensin II levels in patients with diabetes mellitus. *Clin Sci (Lond)* **2003,** 104, 1-5.
185. Shenouda, A.; Douglas, S. A.; Ohlstein, E. H.; Giaid, A. Localization of urotensin-II immunoreactivity in normal human kidneys and renal carcinoma. *J. Histochem. Cytochem.* **2002,** 50, 885-9.
186. Grieco, P.; Franco, R.; Bozzuto, G.; Toccacieli, L.; Sgambato, A.; Marra, M.; Zappavigna, S.; Migaldi, M.; Rossi, G.; Striano, S.; Marra, L.; Gallo, L.; Cittadini, A.; Botti, G.; Novellino, E.; Molinari, A.; Budillon, A.; Caraglia, M. Urotensin II Receptor Predicts the Clinical Outcome of Prostate Cancer Patients and Is Involved in the Regulation of Motility of Prostate Adenocarcinoma Cells. *Journal of Cellular Biochemistry* **2011,** 112, 341-353.
187. Grieco, P.; Caraglia, M.; Addeo, S. R.; Budillon, A.; Franco, R.; Marra, M.; Molinari, A.; Campiglia, P.; Novellino, E. Uratensin-II receptor: A new diagnostic marker and therapeutic target in human prostate adenocarinoma. *Biopolymers* **2007,** 88, 629-629.
188. Jarry, M.; Diallo, M.; Lecointre, C.; Desrues, L.; Tokay, T.; Chatenet, D.; Leprince, J.; Rossi, O.; Vaudry, H.; Tonon, M. C.; Prezeau, L.; Castel, H.; Gandolfo, P. The vasoactive peptides

urotensin II and urotensin II-related peptide regulate astrocyte activity through common and distinct mechanisms: involvement in cell proliferation. *Biochem J* **2010,** 428, 113-24.
189. Prosser, H. C. G.; Forster, M. E.; Richards, A. M.; Pemberton, C. J. Urotensin II and urotensin II-related peptide (URP) in cardiac ischemia-reperfusion injury. *Peptides* **2008,** 29, 770-777.
190. Doan, N. D.; Nguyen, T. T.; Letourneau, M.; Turcotte, K.; Fournier, A.; Chatenet, D. Biochemical and pharmacological characterization of nuclear urotensin-II binding sites in rat heart. *Br J Pharmacol* **2012,** 166, 243-57.
191. Chatenet, D. N., TT.; Létourneau, M.; Fournier, A. *Frontiers in Endocrinology* **2013,** 3, 1-13.
192. Chatenet, D.; Dubessy, C.; Boularan, C.; Scalbert, E.; Pfeiffer, B.; Renard, P.; Lihrmann, I.; Pacaud, P.; Tonon, M. C.; Vaudry, H.; Leprince, J. Structure-activity relationships of a novel series of urotensin II analogues: Identification of a urotensin II antagonist. *Journal of Medicinal Chemistry* **2006,** 49, 7234-7238.
193. Guerrini, R.; Camarda, V.; Marzola, E.; Arduin, M.; Calo, G.; Spagnol, M.; Rizzi, A.; Salvadori, S.; Regoli, D. Structure-activity relationship study on human urotensin II. *Journal of Peptide Science* **2005,** 11, 85-90.
194. Camarda, V.; Guerrini, R.; Kostenis, E.; Rizzi, A.; Calo, G.; Hattenberger, A.; Zucchini, M.; Salvadori, S.; Regoli, D. A new ligand for the urotensin II receptor. *British Journal of Pharmacology* **2002,** 137, 311-314.
195. Carotenuto, A.; Grieco, P.; Campiglia, P.; Novellino, E.; Rovero, P. Unraveling the active conformation of urotensin II. *J Med Chem* **2004,** 47, 1652-61.
196. Boivin, S.; Guilhaudis, L.; Milazzo, I.; Oulyadi, H.; Davoust, D.; Fournier, A. Characterization of urotensin-II receptor structural domains involved in the recognition of U-II, URP, and urantide. *Biochemistry* **2006,** 45, 5993-6002.
197. Grieco, P.; Carotenuto, A.; Campiglia, P.; Zampelli, E.; Patacchini, R.; Maggi, C. A.; Novellino, E.; Rovero, P. A new, potent urotensin II receptor peptide agonist containing a pen residue at the disulfide bridge. *Journal of Medicinal Chemistry* **2002,** 45, 4391-4394.
198. Croston, G. E.; Olsson, R.; Currier, E. A.; Burstein, E. S.; Weiner, D.; Nash, N.; Severance, D.; Allenmark, S. G.; Thunberg, L.; Ma, J. N.; Mohell, N.; O'Dowd, B.; Brann, M. R.; Hacksell, U. Discovery of the first nonpeptide agonist of the GPR14/urotensin-II receptor: 3-(4-chloropheny)-3-(2-(dimethylamino)ethyl)isochroman-1-one (AC-7954). *Journal of Medicinal Chemistry* **2002,** 45, 4950-4953.
199. Lehmann, F.; Pettersen, A.; Currier, E. A.; Sherbukhin, V.; Olsson, R.; Hacksell, U.; Luthman, K. Novel potent and efficacious nonpeptidic urotensin II receptor agonists. *Journal of Medicinal Chemistry* **2006,** 49, 2232-2240.
200. Lehmann, F.; Currier, E. A.; Olsson, R.; Ma, J.-N.; Burstein, E. S.; Hacksell, U.; Luthman, K. Optimization of isochromanone based urotensin II receptor agonists. *Bioorganic & Medicinal Chemistry* **2010,** 18, 4844-4854.
201. Hirose, T.; Takahashi, K.; Mori, N.; Nakayama, T.; Kikuya, M.; Ohkubo, T.; Kohzuki, M.; Totsune, K.; Imai, Y. Increased expression of urotensin II, urotensin II-related peptide and urotensin II receptor mRNAs in the cardiovascular organs of hypertensive rats: Comparison with endothelin-1. *Peptides* **2009,** 30, 1124-1129.
202. Grieco, P.; Carotenuto, A.; Campiglia, P.; Gomez-Monterrey, I.; Auriemma, L.; Sala, M.; Marcozzi, C.; Bianca, R. D. D.; Brancaccio, D.; Rovero, P.; Santicioli, P.; Meini, S.; Maggi, C. A.; Novellino, E. New insight into the binding mode of peptide ligands at urotensin-II receptor: structure-activity relationships study on P5U and urantide. *Journal of Medicinal Chemistry* **2009,** 52, 3927-3940.

203. Patacchini, R.; Santicioli, P.; Giuliani, S.; Grieco, P.; Novellino, E.; Rovero, P.; Maggi, C. A. Urantide: an ultrapotent urotensin II antagonist peptide in the rat aorta. *British Journal of Pharmacology* **2003,** 140, 1155-1158.
204. Zhao, J.; Yu, Q. X.; Kong, W.; Gao, H. C.; Sun, B.; Xie, Y. Q.; Ren, L. Q. The urotensin II receptor antagonist, urantide, protects against atherosclerosis in rats. *Experimental and Therapeutic Medicine* **2013,** 5, 1765-1769.
205. Zhang, J. Y.; Chen, Z. W.; Yao, H. Protective effect of urantide against ischemia-reperfusion injury via protein kinase C and phosphtidylinositol 3 '-kinase - Akt pathway. *Canadian Journal of Physiology and Pharmacology* **2012,** 90, 637-645.
206. Mei, Y.; Jin, H.; Tian, W.; Wang, H.; Wang, H.; Zhao, Y.; Zhang, Z.; Meng, F. Urantide alleviates monocrotaline induced pulmonary arterial hypertension in Wistar rats. *Pulmonary Pharmacology & Therapeutics* **2011,** 24, 386-393.
207. Onat, A. M.; Pehlivan, Y.; Turkbeyler, I. H.; Demir, T.; Kaplan, D. S.; Ceribasi, A. O.; Orkmez, M.; Tutar, E.; Taysi, S.; Sayarlioglu, M.; Kisacik, B. Urotensin Inhibition with Palosuran Could Be a Promising Alternative in Pulmonary Arterial Hypertension. *Inflammation* **2013,** 36, 405-412.
208. Maryanoff, B. E.; Kinney, W. A. Urotensin-II receptor modulators as potential drugs. *Journal of Medicinal Chemistry* **2010,** 53, 2695-2708.
209. Clozel, M.; Binkert, C.; Birker-Robaczewska, M.; Boukhadra, C.; Ding, S. S.; Fischli, W.; Hess, P.; Mathys, B.; Morrison, K.; Muller, C.; Muller, C.; Nayler, O.; Qiu, C. B.; Rey, M.; Scherz, M. W.; Velker, J.; Weller, T.; Xi, J. F.; Ziltener, P. Pharmacology of the urotensin-II receptor antagonist palosuran (ACT-058362; 1- 2-(4-benzyl-4-hydroxy-piperidin-1-yl)-ethyl -3-(2-methyl-quinolin-4-y l)-urea sulfate salt): First demonstration of a pathophysiological role of the urotensin system. *Journal of Pharmacology and Experimental Therapeutics* **2004,** 311, 204-212.
210. Clozel, M.; Hess, P.; Qiu, C. B.; Ding, S. S.; Rey, M. The urotensin-II receptor antagonist palosuran improves pancreatic and renal function in diabetic rats. *Journal of Pharmacology and Experimental Therapeutics* **2006,** 316, 1115-1121.
211. Behm, D. J.; McAtee, J. J.; Dodson, J. W.; Neeb, M. J.; Fries, H. E.; Evans, C. A.; Hernandez, R. R.; Hoffman, K. D.; Harrison, S. M.; Lai, J. M.; Wu, C.; Aiyar, N. V.; Ohlstein, E. H.; Douglas, S. A. Palosuran inhibits binding to primate UT receptors in cell membranes but demonstrates differential activity in intact cells and vascular tissues. *British Journal of Pharmacology* **2008,** 155, 374-386.
212. Douglas, S. A.; Behm, D. J.; Aiyar, N. V.; Naselsky, D.; Disa, J.; Brooks, D. P.; Ohlstein, E. H.; Gleason, J. G.; Sarau, H. M.; Foley, J. J.; Buckley, P. T.; Schmidt, D. B.; Wixted, W. E.; Widdowson, K.; Riley, G.; Jin, J.; Gallagher, T. F.; Schmidt, S. J.; Ridgers, L.; Christmann, L. T.; Keenan, R. M.; Knight, S. D.; Dhanak, D. Nonpeptidic urotensin-II receptor antagonists I: in vitro pharmacological characterization of SB-706375. *British Journal of Pharmacology* **2005,** 145, 620-635.
213. Behm, D. J.; Aiyar, N. V.; Olzinski, A. R.; McAtee, J. J.; Hilfiker, M. A.; Dodson, J. W.; Dowdell, S. E.; Wang, G. Z.; Goodman, K. B.; Sehon, C. A.; Harpel, M. R.; Willette, R. N.; Neeb, M. J.; Leach, C. A.; Douglas, S. A. GSK1562590, a slowly dissociating urotensin-II receptor antagonist, exhibits prolonged pharmacodynamic activity ex vivo. *British Journal of Pharmacology* **2010,** 161, 207-228.
214. Tarui, N.; Santo, T.; Watanabe, H.; Aso, K.; Ishihara, Y. Preparation of 2,3,4,5-tetrahydro-1H-3-benzazepine derivatives as GPR14 antagonists. *Takeda Chemical Industries, PCT Int Appl.* **2002,,** WO2002002530.

215. Chatenet, D.; Nguyen, Q. T.; Letourneau, M.; Dupuis, J.; Fournier, A. Urocontrin, a novel UT receptor ligand with a unique pharmacological profile. *Biochemical Pharmacology* **2012,** 83, 608-615.
216. Christopoulos, A.; May, L. T.; Avlani, V. A.; Sexton, P. M. G-protein-coupled receptor allosterism: the promise and the problem(s). *Biochemical Society Transactions* **2004,** 32, 873-877.
217. Terrillon, S.; Bouvier, M. Roles of G-protein-coupled receptor dimerization - From ontogeny to signalling regulation. *Embo Reports* **2004,** 5, 30-34.
218. Changeux, J. P.; Edelstein, S. J. Allosteric mechanisms of signal transduction. *Science* **2005,** 308, 1424-1428.
219. Desai, N.; Sajjad, J.; Frishman, W. H. Urotensin II A New Pharmacologic Target in the Treatment of Cardiovascular Disease. *Cardiology in Review* **2008,** 16, 142-153.
220. Chatenet, D.; Nguyen, Q. T.; Létourneau, M.; Dupuis, J.; Fournier, A. Urocontrin, a novel UT receptor ligand with a unique pharmacological profile. *Biochemical Pharmacology* **2012,** 83, 608-615.
221. Kenakin, T.; Jenkinson, S.; Watson, C. Determining the potency and molecular mechanism of action of insurmountable antagonists. *Journal of Pharmacology and Experimental Therapeutics* **2006,** 319, 710-723.
222. Hirschmann, R. Medicinal chemistry in the golden-age of biology – Lessons from steroid and peptide research. *Angew. Chem., Int. Ed. Engl.* **1991,** 30, 1278-1301.
223. Khashper, A.; Lubell, W. D. Design, synthesis, conformational analysis and application of indolizidin-2-one dipeptide mimics. *Org. Biomol. Chem.* **2014,** 12, 5052-5070.
224. Hruby, V. J.; Cai, M. Y. Design of peptide and peptidomimetic ligands with novel pharmacological activity profiles. In *Annu. Rev. Pharmacol. Toxicol., Vol 53, 2013*, Insel, P. A., Ed. 2013; Vol. *53*, pp 557-580.
225. Ko, E.; Liu, J.; Burgess, K. Minimalist and universal peptidomimetics. *Chem. Soc. Rev.* **2011,** 40, 4411-4421.
226. Belanger, P. C. D., C.; . Preparation of exo-6-benzyl-exo-2-(m-hydroxyphenyl)-l-dimethylaminomethylbicyclo[2.2.2.]octane. A non-peptide mimic of enkephalins. *Can. J. Chem.* **1986,** 64, 1514-1520.
227. Olson, G. L.; Bolin, D. R.; Bonner, M. P.; Bos, M.; Cook, C. M.; Fry, D. C.; Graves, B. J.; Hatada, M.; Hill, D. E.; Kahn, M.; Madison, V. S.; Rusiecki, V. K.; Sarabu, R.; Sepinwall, J.; Vincent, G. P.; Voss, M. E. Concepts and progression in the development of peptide mimetics. *J. Med. Chem.* **1993,** 36, 3039-3049.
228. Hirschmann, R.; Nicolaou, K. C.; Pietranico, S.; Leahy, E. M.; Salvino, J.; Arison, B.; Cichy, M. A.; Spoors, P. G.; Shakespeare, W. C.; Sprengeler, P. A.; Hamley, P.; Smith, A. B.; Reisine, T.; Raynor, K.; Maechler, L.; Donaldson, C.; Vale, W.; Freidinger, R. M.; Cascieri, M. R.; Strader, C. D. De novo design and synthesis of somatostatin non-peptide peptidomimetics utilizing beta-D-glucose as a novel scaffolding. *Journal of the American Chemical Society* **1993,** 115, 12550-12568.
229. Hirschmann, R.; Nicolaou, K. C.; Pietranico, S.; Salvino, J.; Leahy, E. M.; Sprengeler, P. A.; Furst, G.; Smith, A. B.; Strader, C. D.; Cascieri, M. A.; Candelore, M. R.; Donaldson, C.; Vale, W.; Maechler, L. Nonpeptidal peptidomimetics with a beta-D-glucose scaffolding – A partial somatostatin agonist bearing a close structural relationship to a potent, selective substance P antagonist. *Journal of the American Chemical Society* **1992,** 114, 9217-9218.
230. Hirschmann, R. F.; Nicolaou, K. C.; Angeles, A. R.; Chen, J. S.; Smith, A. B., III. The beta-D-Glucose Scaffold as a beta-Turn Mimetic. *Accounts of Chemical Research* **2009,** 42, 1511-1520.

231. Evans, B. E.; Bock, M. G.; Rittle, K. E.; Dipardo, R. M.; Whitter, W. L.; Veber, D. F.; Anderson, P. S.; Freidinger, R. M. Design of potent, orally effective, nonpeptidal antagonists of the peptide hormone cholecystokinin. *Proceedings of the National Academy of Sciences of the United States of America* **1986,** 83, 4918-4922.
232. Evans, B. E.; Rittle, K. E.; Bock, M. G.; Dipardo, R. M.; Freidinger, R. M.; Whitter, W. L.; Lundell, G. F.; Veber, D. F.; Anderson, P. S.; Chang, R. S. L.; Lotti, V. J.; Cerino, D. J.; Chen, T. B.; Kling, P. J.; Kunkel, K. A.; Springer, J. P.; Hirshfield, J. Methods for drug discovery: development of potent, selective, orally effective cholecystokinin antagonists. *Journal of Medicinal Chemistry* **1988,** 31, 2235-2246.
233. Kaye, D. M.; Krum, H. Drug discovery for heart failure: a new era or the end of the pipeline? *Nature Reviews Drug Discovery* **2007,** 6, 127-139.
234. Quaile, M. P.; Kubo, H.; Kimbrough, C. L.; Douglas, S. A.; Margulies, K. B. Direct inotropic effects of exogenous and endogenous urotensin-II divergent actions in failing and nonfailing human myocardium. *Circulation-Heart Failure* **2009,** 2, 39-46.
235. Watson, A. M. D.; Lambert, G. W.; Smith, K. J.; May, C. N. Urotensin II acts centrally to increase epinephrine and ACTH release and cause potent inotropic and chronotropic actions. *Hypertension* **2003,** 42, 373-379.
236. Song, W.; Abdel-Razik, A. E. S.; Lu, W.; Ao, Z.; Johns, D. G.; Douglas, S. A.; Balment, R. J.; Ashton, N. Urotensin II and renal function in the rat. *Kidney International* **2006,** 69, 1360-1368.
237. Dai, H.-Y.; Kang, W.-Q.; Wang, X.; Yu, X.-J.; Li, Z.-H.; Tang, M.-X.; Xu, D.-L.; Li, C.-W.; Zhang, Y.; Ge, Z.-M. The involvement of transforming growth factor-beta 1 secretion in Urotensin II-induced collagen synthesis in neonatal cardiac fibroblasts. *Regulatory Peptides* **2007,** 140, 88-93.
238. Zhang, Y.-G.; Li, J.; Li, Y.-G.; Wei, R.-H. Urotensin II induces phenotypic differentiation, migration, and collagen synthesis of adventitial fibroblasts from rat aorta. *Journal of Hypertension* **2008,** 26, 1119-1126.
239. Shiraishi, Y.; Watanabe, T.; Suguro, T.; Nagashima, M.; Kato, R.; Hongo, S.; Itabe, H.; Miyazaki, A.; Hirano, T.; Adachi, M. Chronic urotensin II infusion enhances macrophage foam cell formation and atherosclerosis in apolipoprotein E-knockout mice. *Journal of Hypertension* **2008,** 26, 1955-1965.
240. Papadopoulos, P.; Bousette, N.; Giaid, A. Urotensin-II and cardiovascular remodeling. *Peptides* **2008,** 29, 764-769.
241. You, Z.; Genest, J., Jr.; Barrette, P.-O.; Hafiane, A.; Behm, D. J.; D'Orleans-Juste, P.; Schwertani, A. G. Genetic and pharmacological manipulation of urotensin II ameliorate the metabolic and atherosclerosis sequalae in mice. *Arterioscler, Thromb, Vasc Biol* **2012,** 32, 1809-1816.
242. Watson, A. M. D.; Olukman, M.; Koulis, C.; Tu, Y.; Samijono, D.; Yuen, D.; Lee, C.; Behm, D. J.; Cooper, M. E.; Jandeleit-Dahm, K. A. M.; Calkin, A. C.; Allen, T. J. Urotensin II receptor antagonism confers vasoprotective effects in diabetes associated atherosclerosis: studies in humans and in a mouse model of diabetes. *Diabetologia* **2013,** 56, 1155-1165.
243. Gao, S.; Oh, Y.-B.; Shah, A.; Park, W. H.; Chung, M. J.; Lee, Y.-H.; Kim, S. H. Urotensin II receptor antagonist attenuates monocrotaline-induced cardiac hypertrophy in rats. *American Journal of Physiology-Heart and Circulatory Physiology* **2010,** 299, H1782-H1789.
244. Carotenuto, A.; Auriemma, L.; Merlino, F.; Limatola, A.; Campiglia, P.; Gomez-Monterrey, I.; Bianca, R. D. D.; Brancaccio, D.; Santicioli, P.; Meini, S.; Maggi, C. A.; Novellino, E.; Grieco, P. New insight into the binding mode of peptides at urotensin-II receptor by Trp-constrained analogues of P5U and urantide. *Journal of Peptide Science* **2013,** 19, 293-300.

245. Lescot, E.; Santos, J. S. D.; Dubessy, C.; Oulyadi, H.; Lesnard, A.; Vaudry, H.; Bureau, R.; Rault, S. Definition of new pharmacophores for nonpeptide antagonists of human urotensin-II. Comparison with the 3D-structure of human urotensin-II and URP. *Journal of Chemical Information and Modeling* **2007,** 47, 602-612.
246. Doan, N. D.; Nguyen, T. T. M.; Letourneau, M.; Turcotte, K.; Fournier, A.; Chatenet, D. Biochemical and pharmacological characterization of nuclear urotensin-II binding sites in rat heart. *British Journal of Pharmacology* **2012,** 166, 243-257.
247. Chatenet, D. N., TT.; Létourneau, M.; Fournier, A. Update on the urotensinergic system: new trends in receptor localization, activation, and drug design. *Frontiers in Endocrinology* **2013,** 3, 1-13.
248. Lavecchia, A.; Cosconati, S.; Novellino, E. Architecture of the human urotensin II receptor: Comparison of the binding domains of peptide and non-peptide urotensin II agonists. *Journal of Medicinal Chemistry* **2005,** 48, 2480-2492.
249. Thurston, D. E. Advances in the study of pyrrolo[2,1-*c*][1,4]benzodiazepine (PBD) antitumor antibiotics. In *Mol. Aspects Anticancer Drug-DNA Interact.*, Neidle, S.; Waring, M., Eds. MacMillan: London, UK, 1993; Vol. 1, pp 54-88.
250. De Lucca, G. V.; Otto, M. J. Synthesis and anti-HIV activity of pyrrolo-[1,2-d]-(1,4)-benzodiazepin-6-ones. *Biorg. Med. Chem. Lett.* **1992,** 2, 1639-1644.
251. Iden, H. S.; Lubell, W. D. 1,4-Diazepinone and pyrrolodiazepinone syntheses via homoallylic ketones from cascade addition of vinyl grignard reagent to α-aminoacyl-β-amino esters. *Org. Lett.* **2006,** 8, 3425-3428.
252. Rossowski, W. J.; Cheng, B. L.; Taylor, J. E.; Datta, R.; Coy, D. H. Human urotensin II-induced aorta ring contractions are mediated by protein kinase C, tyrosine kinases and Rho-kinase: inhibition by somatostatin receptor antagonists. *Eur J Pharmacol* **2002,** 438, 159-70.
253. Behm, D. J.; Herold, C. L.; Ohlstein, E. H.; Knight, S. D.; Dhanak, D.; Douglas, S. A. Pharmacological characterization of SB-710411 (Cpa-c[D-Cys-Pal-D-Trp-Lys-Val-Cys]-Cpa-amide), a novel peptidic urotensin-II receptor antagonist. *Br J Pharmacol* **2002,** 137, 449-458.
254. Carotenuto, A.; Auriemma, L.; Merlino, F.; Youssif, A. M.; Marasco, D.; Limatola, A.; Campiglia, P.; Monterrey-Gomez, I.; Santicioli, P.; Meini, S.; Maggi, C. A.; Novellino, E.; Griecio, P. Lead optimization of P5U and Urantide: Discovery of noval potent ligands at the urotensin-II receptor. *J. Med. Chem.* **2014,** 57, 5965-5974.
255. Cann, J. R.; London, R. E.; Stewart, J. M.; Matwiyoff, N. A. Effect of temperature upon the circular dichroism of bradykinin. *International Journal of Peptide and Protein Research* **1979,** 14, 388-92.
256. Stadler, A.; Kappe, C. O. High-speed couplings and cleavages in microwave-heated, solid-phase reactions at high temperatures. *European Journal of Organic Chemistry* **2001**, 919-925.
257. Kaiser, E.; Colescott, R. L.; Bossinger, C. D.; Cook, P. I. Color test for detection of free terminal amino groups in the solid-phase synthesis of peptides. *Analytical Biochemistry* **1970,** 34, 595-598.
258. Zoller, T.; Ducep, J. B.; Hibert, M. Efficient synthesis of benzylic bromides under neutral conditions on solid support. *Tetrahedron Lett.* **2000,** 41, 9985-9988.
259. Blanco, M.-J.; Sardina, F. J. Enantiospecific and Stereoselective Synthesis of Polyhydroxylated Pyrrolidines and Indolizidines from trans-4-Hydroxy-L-proline. *Journal of Organic Chemistry* **1996,** 61, 4748-4755.
260. Armarego, W.; Chai, C. *Purification of laboratory chemicals*. Butterworth-Heinemann, Oxford: 2003.

261. Still, W. C.; Kahn, M.; Mitra, A. Rapid chromatographic technique for preparative separations with moderate resolution. *Journal of Organic Chemistry* **1978,** 43, 2923-2925.
262. Brkovic, A.; Hattenberger, A.; Kostenis, E.; Klabunde, T.; Flohr, S.; Kurz, M.; Bourgault, S.; Fournier, A. Functional and binding characterizations of urotensin II-related peptides in human and rat urotensin II-receptor assay. *J Pharmacol Exp Ther* **2003,** 306, 1200-1209.

Annexe 1 : L'article de comparaisons entre trois résines pour la synthèse de pyrrolo[3,2-e][1,4]diazépin-2-ones

Pyrrolo[3,2-e][1,4]diazepin-2-one Synthesis: A Head-to-Head Comparison of Soluble versus Insoluble Supports.

*Nicolas Boutard, Julien Dufour-Galland, Philippe Deaudelin†, and William D. Lubell**

Chemistry department, Université de Montréal, C.P. 6128, Succursale Centre-Ville, Montreal, Quebec H3C 3J7, Canada.

william.lubell@umontreal.ca

† present address: Galderma Production Canada Inc. 19400 Route Transcanadienne, Baie d'Urfé, Quebec, H9X 3S4, Canada

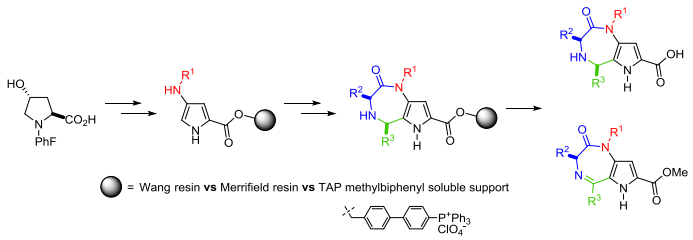

ABSTRACT: Aryldiazepin-2-ones are known as “privileged structures”, because they bind to multiple receptor types with high affinity. Towards the development of a novel class of aryldiazepin-2-one scaffolds, the supported synthesis of pyrrolo[3,2-*e*][1,4]diazepin-2-ones was explored starting from *N*-(PhF)-4-hydroxyproline featuring an acid catalyzed Pictet-Spengler reaction to form the diazepine ring. Three supports [Wang resin, tetraarylphosphonium (TAP) soluble support and Merrifield resin] were examined in the synthesis of the heterocycle and exhibited different strengths and weaknesses. Wang resin proved effective for exploratory optimization of the synthesis, due to effective identification of intermediates after resin cleavage under mild conditions; however, the acidic conditions of the Pictet-Spengler reaction caused premature loss of resin-bound material. Direct monitoring of reactions by TLC, RP-HPLC-MS and in certain cases NMR spectroscopy was possible with the TAP support, which facilitated purification of intermediates by precipitation; however, incomplete precipitation of material led to lower overall yields than the solid-phase approaches on resin. Merrifield resin proved stable to the conditions for the synthesis of the pyrrolo[3,2-*e*][1,4]diazepin-2-one targets and would be amenable to “split-and-mix” chemistry; however, relatively harsh conditions were necessary for final product cleavage. Perspective for the application of supported approaches in heterocycle library synthesis was thus obtained by demonstration of the respective utility of the three supports for preparation of pyrrolo[3,2-*e*][1,4]diazepin-2-one.

KEYWORDS: Pyrrolo[3,2-*e*][1,4]diazepin-2-one, heterocycle, solid support, soluble support

Introduction

Aryldiazepin-2-ones, such as [1,4]benzodiazepin-2-ones, are considered as "privilegedstructures",[1] because of their affinity for multiple receptor targets. Their ability to bind protein receptors and elicit interesting biological activity may be due to their potential to mimic peptide turn secondary structures.[2] The aryldiazepin-2-one scaffold[3] achieved popularity first in the 1960s as a component of GABA receptor antagonists (i.e., Diazepam® and Valium®)[3d,e38, 39] for treating CNS-related conditions. The platform was later shown to interact with various hormone receptors[1b,4] and has been used in enzyme inhibitors[5] as well as in inhibitors of protein-DNA interactions.[6]

Pyrrolodiazepin-2-ones have been reported less often in the literature; however, they similarly display remarkable biological activities. For example, the DNA-binding pyrrolo[2,1-*c*][1,4]benzodiazepine natural product, anthramycin (**96**, Figure A1.1) is an antitumor antibiotic.[771, 72] Pyrrolodiazepin-2-ones **97** and **98** are respectively inhibitors of angiotensin converting enzyme (ACE)[8] and HIV reverse transcriptase (HIV-RT).[9] In addition, pyrrolodiazepin-2-one scaffolds **99** and **100** have been reported in the patent literature to exhibit respectively antimuscarinic[10] and GABA antagonist properties.[11]

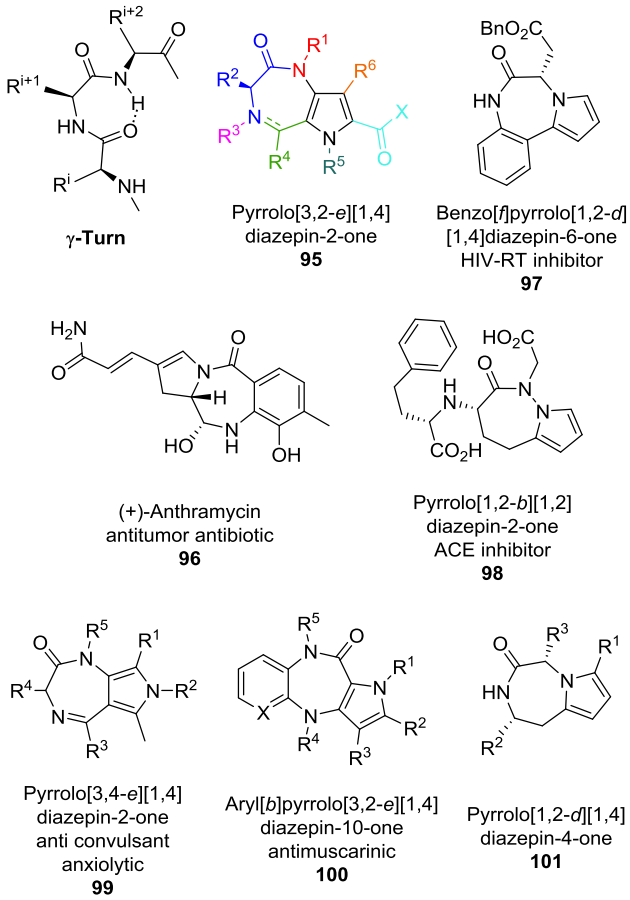

Figure A1.1. Representative pyrrolodiazepinones.

Their notable activities and opportunity for novel structural diversity have made the development of methods for constructing and functionalizing pyrrolodiazepinone scaffolds a promising subject for medicinal chemistry research. Recent examples have key steps featuring the use of the multicomponent Ugi-type condensation,[12] phenyliodine(III)bis-(trifluoroacetate)-mediated intramolecular *N*-acylnitrenium ion reaction,[13] and cyclization *via* Schmidt thermolysis of acylazides.[14] In addition, the intramolecular Paal-Knorr reaction has provided pyrrolo[1,2-*d*][1,4]diazepin-4-ones **101** (Figure A1.1).[2b]

A solution-phase synthesis of the pyrrolo[3,2-*e*][1,4]diazepin-2-one scaffold **2** was recently achieved starting from (2*S*,4*R*)-4-hydroxproline (Scheme A1.10).[15] Key for introducing structural diversity in this approach was the synthesis of 4-*N*-substituted-amino-pyrrole-2-carboxylates **49** on treatment of methyl (*S*)-4-oxo-1-(9-phenyl-9*H*-fluoren-9-yl)prolinate **48** with different primary amines in the presence of catalytic *p*-TsOH, which caused pyrrole formation and concomitant loss of the 9-phenyl-9*H*-fluorene (PhF-H) group.[16,17] Compounds **50** were obtained by 4-aminoacylation with various Fmoc-aminoacids and deprotection with piperidine. Ring closure was accomplished by Pictet-Spengler condensation with aldehydes, giving the pyrrolo[3,2-*e*][1,4]diazepin-2-ones with a *cis* relative stereochemistry for the major compounds. The stereoselective outcome of the reaction favored an *endo* attack of the *E* iminium ion in a transition state having the amino acid side chain in an equatorial orientation. Aromatic aldehydes, especially those bearing electron-withdrawing groups, gave generally better yields than aliphatic aldehydes.

Scheme A1.1. Solution-phase synthesis of pyrrolo[3,2-*e*][1,4]diazepin-2-ones.[15]

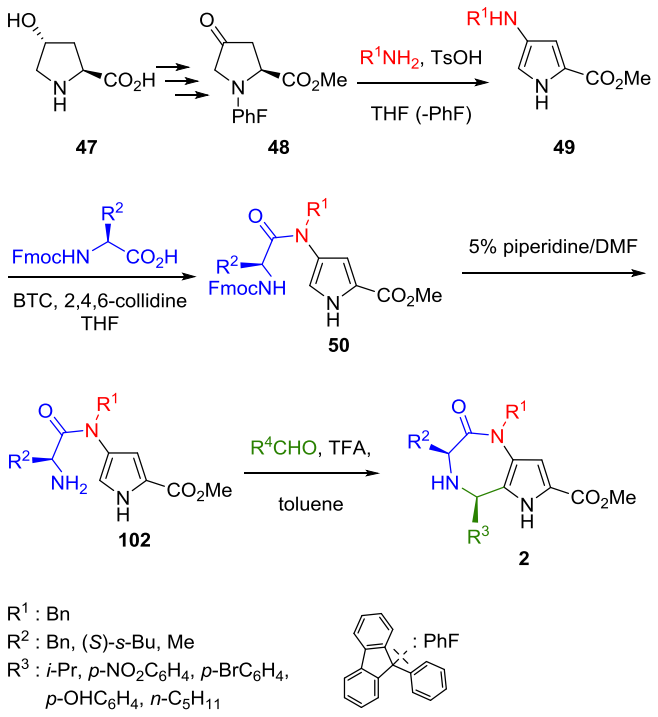

In addition to offering a modular approach for making the bicyclic ring system, crystals of pyrrolo[3,2-e][1,4]diazepin-2-one **2** (Figure A1.1, R^1 = Bn, R^2 = (*S*)-*s*-Bu, R^3 = Ph, R^5 = R^6 = H) were isolated and subjected to X-ray analysis, which demonstrated that the dihedral angles of the diazepinone α-amino acid residue (ϕ = 71°, ψ = –93°) compared favorably with those of an ideal reverse γ-turn (ϕ = 60° to 70°, ψ = –70° to –85°).[15]

Considering the importance of γ-turn conformations for the biological activity of various peptides, such as enkephalin,[18] angiotensin,[19] bradykinin,[2018, 255] vasopressin,[21] substance P,[22] somatostatin,[23] and oxytocin,[24] we are developing a diversity-oriented methodology for modular construction of pyrrolo[3,2-*e*][1,4]diazepin-2-one libraries.

Herein is reported the examination of three different supports to provide the desired scaffold without purification of intermediates by chromatography.

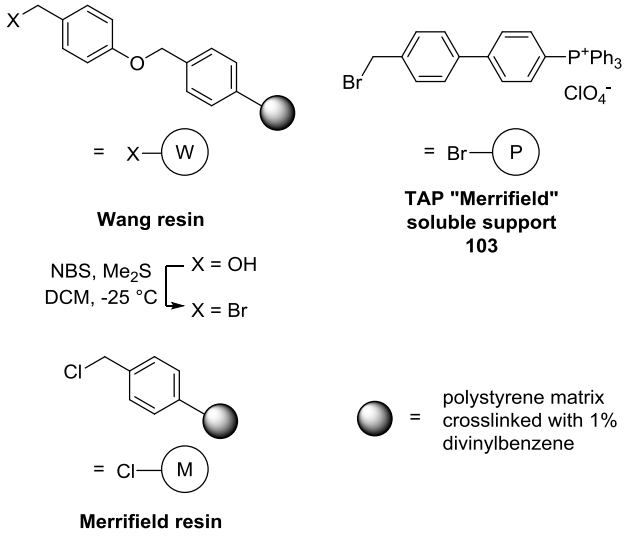

Figure A1.2. Supports used for the synthesis of pyrrolo[3,2-*e*][1,4]diazepin-2-one.

Wang resin (Figure A1.2) was tried because of previous success in the solid-phase synthesis of 3-aminopyrrole-2,5-dicarboxylate analogues;[25] however, its labile nature under acidic conditions meant cleavage of product in the Pictet-Spengler cyclization, inhibiting further modification of the pyrrolo[3,2-*e*][1,4]diazepin-2-one scaffold on the support. Merrifield resin was effective for synthesizing the pyrrolo[3,2-*e*][1,4]diazepin-2-one scaffold without resin cleavage, offering an opportunity for further modification of the heterocycle; however, resin cleavage necessitated relatively harsh conditions. The (4'-(bromomethyl)-[1,1'-biphenyl]-4-yl)triphenylphosphonium salt **103**[26] (Figure A1.2), a soluble variant of Merrifield resin, was chosen as a solubility control group (SCG) for its advantages in the preparation of small molecules and peptides,[26,27] because reactions can be performed under homogenous conditions in polar solvent systems prior to purification by precipitation from solvents of low polarity. Precipitation

of the tetraarylphosphonium (TAP) substrates from Et_2O has been shown to be counterion dependant ($Br^- < ClO_4^- < PF_6^-$),[27b] such that the inexpensive perchlorate salt was chosen for our study. In contrast to resins, which required cleavage prior to reaction analysis, substrates were examined directly on the TAP support by TLC, RP-HPLC-MS and NMR spectroscopy. The head-to-head comparison of these three supports in the context of the synthesis of pyrrolo[3,2-*e*][1,4]diazepin-2-one has revealed their strengths and limitations and is guiding efforts towards the development of an effective method for diversity-oriented library synthesis.

Results

4-Amino-pyrrole-2-carboxylate Synthesis

In the synthesis of pyrrolo[3,2-*e*][1,4]diazepin-2-one, the initial unit of diversity was added in the synthesis of the 4-amino-pyrrole-2-carboxylate. In previous syntheses of amino pyrrole on solid support, ester linkage to Wang resin was used to prepare 4-amino pyrrole-2-carboxylates with tertiary 4-amino groups,[25] and a cysteinamine linker to Merrifield resin was used to attach the amino pyrrole to resin as a secondary amine, which was employed in the synthesis of pyrrolopyrimidines.[28] In both cases, a 4-oxo-*N*-(PhF)proline-2-carboxylate served as precursor in the amino pyrrole forming reaction, which has proven applicable using a wide variety of primary and secondary amines in solution.[17] In light of this precedent, benzylamine was the only example employed to form 4-amino pyrrole-2-carboxylate in the comparative study.

To link (2*S*,4*R*)-4-hydroxy-*N*-(PhF)proline (**104**) to the support, the corresponding cesium salt **53** was prepared and reacted with Wang bromide resin [4-(bromomethyl)phenoxymethyl polystyrene, prepared from Wang resin, Figure A1.2]

according to previously published procedures, and loading was ascertained as previously described. (Scheme A1.2).[25,29] Merrifield resin and its soluble TAP variant **103** were employed as obtained from the manufacturer.

Scheme A1.2. Supported synthesis of 4-amino-pyrrole-2-carboxylates.

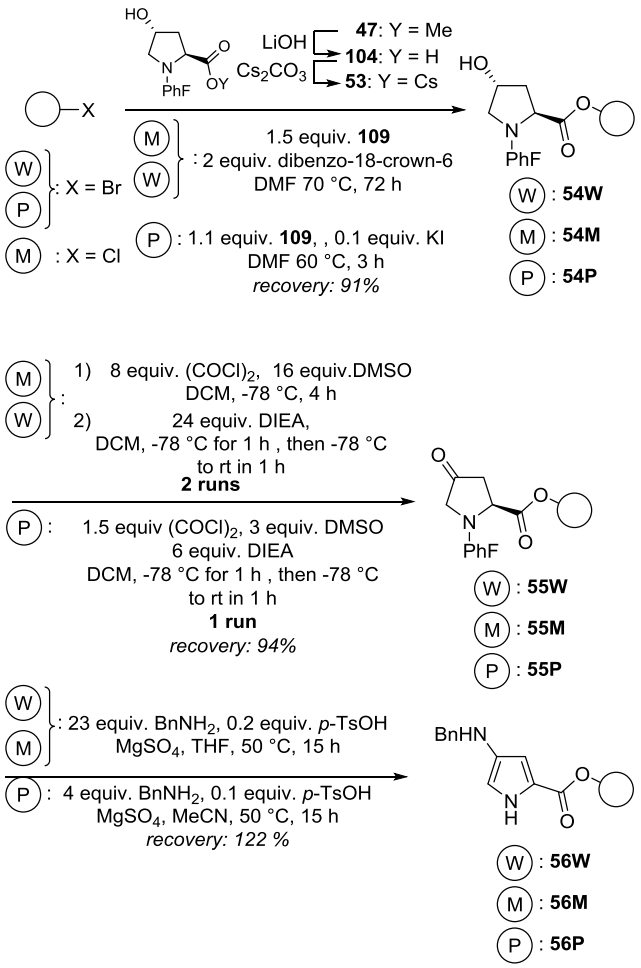

To avoid experimental bias during comparisons of the solid supports, Wang and Merrifield resins were placed in IRORI MacroKans and reacted simultaneously together in the same pot, using magnetic stirring to agitate the Kans without crushing resin. Cesium salt **53** (150 mol%) was respectively reacted with Wang bromide and Merrifield resins in the presence of dibenzo-18-crown-6 in DMF at 70 °C for 48 h.[30] Anchoring efficiency was estimated to be quantitative based on the increase of the resin mass.

Moreover, IR spectroscopy indicated disappearance of the C-Br band at 592 cm^{-1} and appearance of bands at 3448 and 1737 cm^{-1} for the OH and C=O stretches of resin-bound (2*S*,4*R*)-4-hydroxy-*N*-(PhF)proline **54W**.

Soluble support **103** was reacted with cesium salt **53** (110 mol%) in the presence of catalytic potassium iodide in DMF at 60 °C for 3 h, which gave quantitative conversion to the TAP-bound 4-hydroxy-*N*-(PhF)proline **54P** as indicated by TLC (R_f = 0.51, 7.5% MeOH in DCM).[31] After reactions on the TAP support, work-up was completed by a saturated aqueous $LiClO_4$ wash to ensure the presence of the counteranion. Partial purification of TAP-supported material was achieved by dissolving in a minimum volume of CH_2Cl_2 and precipition using a 5-fold volume of Et_2O. For characterization purposes, analytical samples of TAP-supported intermediates were purified by radial chromatography (see Supporting Information).[32]

4-Oxo-*N*-(PhF)prolines **55W** and **55M** were obtained respectively from oxidation of resin-bound alcohols **54W** and **54M** using oxalyl chloride and DMSO at –78 °C for 4 h, followed by treatment with DIEA. In both cases, the oxidation was performed twice for complete conversion to ketone, which was ascertained by the appearance of a second carbonyl band at 1758 cm^{-1} and disappearance of the OH band around 3440-3460 cm^{-1} in the IR spectra of resins **55W** and **55M**. On TAP support, complete oxidation of alcohol **54P** was achieved using similar conditions and less reagent in a single reaction as comfirmed by RP-HPLC-MS; however, ketone **55P** exhibited low stability and was best employed immediately in the following step.

Resin-bound 4-aminopyrroles **56W** and **56M** were respectively prepared by treatment of ketones **55W** and **55M** with excess of benzylamine (2300 mol%), in the

presence of catalytic *p*-TsOH (0.1 equiv.) in dry THF. In individual cases, 4-benzylamino-pyrrole loading was evaluated by the amount of 9-phenyl-9H-fluorene (PhFH) recovered after filtration of the resin, washings, evaporation of the filtrate, and column chromatography (2% Et_2O/hexanes). 4-Amino-pyrrole-2-carboxylate could not be detected by RP-LCMS after resin cleavage with acid (TFA/DCM 1/1) nor methoxide (0.44 M $NaOCH_3$ in THF/MeOH). After *N*-acylation, 4-amidopyrroles (see below, Table A1.1) could however be detected by RP-HPLC-MS analysis after cleavage with sodium methoxide, which caused concomitant Fmoc removal. Accordingly, the PhF group was observed to be retained on 10 to 30% of pyrrole, due to premature aromatization before PhF-H extrusion.[17] This side-reaction was presumed to be due to residual oxygen and avoided by degassing the resin suspended in THF using freeze-thaw cycles of exposure to high vacuum followed by flushing argon, addition of pre-dried $MgSO_4$ (two-fold the weight of dry resin), benzylamine and *p*-TsOH, followed by further degassing by argon bubbling for 30 min before heating the reaction at 50 °C for 15 h. Under these optimized condition, complete conversion to 4-benzylamino-pyrroles **56W** and **56M** was achieved as indicated by the quantitative amounts of PhFH recovered, as well as by RP-HPLC-MS analysis of 4-amido-pyrrole **57W** after resin cleavage with sodium methoxide.

4-Benzylamino-pyrrole **56P** was prepared on the TAP support in acetonitrile instead of THF, because of limited solubility in the latter. Quantitative conversion of TAP-supported ketone **55P** to aminopyrrole **56P** was indicated by RP-HPLC-MS analysis in the same amount of time (15 h) as on resin using less *N*-benzylamine (400 mol%).

Aminoacylation

The scope of *N*-(Fmoc)amino acids which could be employed in the acylation of 2-aminopyrroles was examined on Wang resin **56W** on 0.03 mmol scale using 12 *N*-(Fmoc)amino acids (listed in Table A1.1) and *p*-nitrobenzoic acid (500 mol%, Scheme A1.3). Triphosgene (BTC) was employed as coupling agent in the presence of 2,4,6-collidine in dry THF for 15 h. Efficiency of coupling was ascertained on two resin aliquots, which were first both treated with excess acetyl chloride and DIEA in DMF for 2 h, followed by 20% piperidine in DMF, to respectively, cap excess aminopyrrole and remove the Fmoc group. Subsequently, the resins were respectively cleaved with TFA/DCM 1:1 for 1 h, to give the corresponding acids, or with 0.44 M $NaOCH_3$ in 9:1 THF/MeOH for 3 h to furnish the ester counterparts. Cleaved material was analyzed by RP-HPLC-MS without isolation on a 0.01 mmol scale. Although tertiary amide isomers complicated certain chromatographic analyses, the detection of residual aminopyrrole **56W** was facilitated by conversion to the corresponding acetamide.

Except for *N*-(Fmoc)amino isobutyramide **57Wl**, for which only the cleaved capped starting material **108** and **109** were detected, all desired amides **57W** were produced, with complete consumption of the aminopyrrole starting material. The steric bulk of *N*-(Fmoc)Aib was presumed to inhibit coupling, which also failed using its symmetric anhydride prepared with DIC. Purities were generally higher after the acidic cleavages, which failed only to detect the His and Orn analogues **57Wd** and **57Wk**, which were observed after the methoxide cleavage. The latter, however, was unable to detect the dicarboxylate Asp and Glu analogues **57Wc** and **57Wi**.

Scheme A1.3. Supported aminoacylation of 4-amino-pyrrole-2-carboxylates.

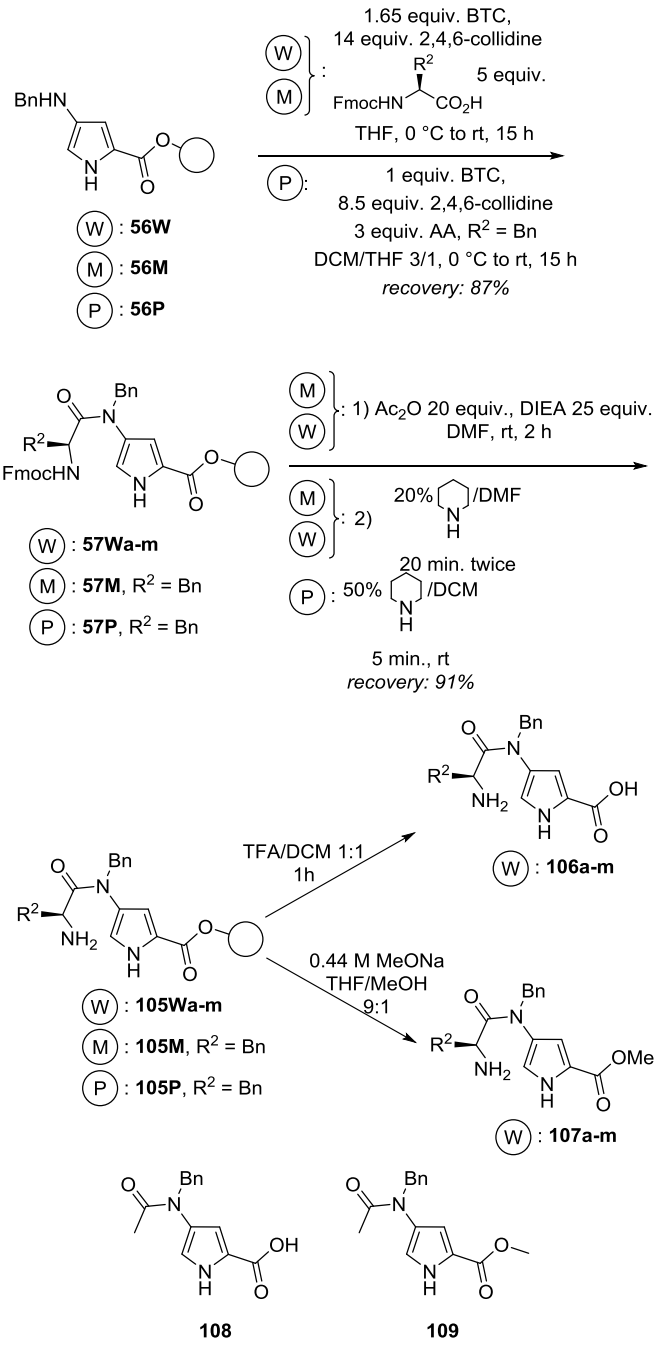

Table A1.1. Amino acylation of 4-benzylaminopyrrole **56W**.

Entry	Acylating agent	Purity after cleavage	
		106 (R_t; $[M+H]^+$)	**107** (R_t; $[M+H]^+$)[b]
a	Fmoc-Phe-OH	82% (18.4; 364.2)[a]	85% (16.6; 378.2)[b]
b	Fmoc-Leu-OH	81% (17.2; 330.2)[a]	93% (15.1; 344.2)[a]
c	Fmoc-Asp(OMe)-OH	76% (16.0; 346.2)[a]	ND
d	Fmoc-His(Trt)-OH	90% (11.9; 354.2)[a]	75% (21.2; 610.2)[b]
e	Fmoc-Ser(OtBu)-OH	87% (11.4; 304.2)[b,c]	83% (16.4; 374.2)[b]
f	Fmoc-Lys(Boc)-OH	82% (12.5; 345.2)[a]	91% (17.6; 459.2)[b]
g	Fmoc-Cys(Trt)-OH	84% (12.8; 320.0)[b,c]	60% (21.2; 576.2)[b]
h	Fmoc-Met-OH	68% (16.7; 348.2)[a]	69% (14.9; 362.2)[b]
i	Fmoc-Glu(OtBu)-OH	74% (12.9; 346.2)[a]	ND
j	Fmoc-Pro-OH	65% (15.8; 314.2)[a]	52% (13.7; 328.2)[b]
k	Fmoc-Orn(Boc)-OH	ND	82% (15.1; 445.2)[b]
l	Fmoc-Aib-OH	32% (11.7; 259.1)[a]	33% (16.2; 273.2)[a]
m	*p*-NO_2PhCO_2H	82% (21.9; 366.2)[b]	37% (23.1; 380.0)[b]

[a] Determined by RP-HPLC-MS [C18 110A column 150 mm × 4.6 mm, 5μm, 5-90% MeOH in H_2O in 20 min. then 90% MeOH for 15 min., 0.1% FA, UV: λ = 254 nm, retention time (R_t) expressed in min.]. [b] Determined by RP-HPLC-MS (C18 110A column 150 mm × 4.6 mm, 5 μm, 5-80% MeOH in H_2O in 20 min. then 90% MeOH for 15 min., 0.1% FA, UV: λ = 254 nm). [c] Several conformers were detected. [d]ND: non-detected.

Phenylalanine was deemed the amino acid of choice for comparative analyses with the other supports, because of its effective coupling as determined by both cleavage methods and utility in subsequent Pictet-Spengler chemistry as described below. On Merrifield resin, the BTC-mediated coupling of Fmoc-Phe (500 mol%) gave amide **105M** in 85% purity, as determined by the methoxide cleavage analysis. On the TAP

support, a DCM/THF 8:2 mixture enhanced solubility in coupling of Fmoc-Phe (300 mol%) with BTC and 2,4,6-collidine to give amide **105P**. Subsequent Fmoc removal was performed respectively with 20% piperidine in DMF twice for 20 min, and with 50% piperidine in DCM once for 10 min on the resin-bound and TAP-supported Fmoc-Phe substrates.

Pictet-Spengler Reaction and Pyrrolo[3,2-*e*][1,4]diazepin-2-one Cleavage

The conditions for the Pictet-Spengler cyclization were initially examined on Wang resin, because parallel chemistry could be conveniently performed and assessed using this support as demonstrated in the amino acylation study above. Conjecturing that the use of strong Brønsted acids might cause premature cleavage of substrate, milder protocols were first explored using $B(OMe)_3$,[33] $Yb(OTf)_3$,[34] LiCl in DCM/hexafluoropropanol,[35] and iodine;[36] however, all had no effect and left the starting material unchanged. A Pictet-Spengler protocol was attempted using an *N*-acyliminium ion (Scheme A1.4),[37] which have previously enhanced such iminium-mediated Mannich-type reactions.[38] On 0.01 mmol scale, ornithine derivative **105Wk** was arbitrarily chosen as substrate and reacted respectively with benzaldehyde and isobutyraldehyde in the presence of methyl orthoformate, as water scavenger, in dry DCM to give imines **110** and **111**, which were treated with *p*-nitrophenyl chloroformate in pyridine to induce Pictet-Spengler cyclization by way of the respective *N*-acyliminiums **112** and **113**. After 18 h at room temperature, resin cleavage with 50% TFA in DCM and analysis RP-HPLC-MS revealed diazepinones **114** and **115** as minor components contaminated with carbamate **116**.

Scheme A1.4. *N*-acylimminium Pictet-Spengler reaction on compound **105Wk**.

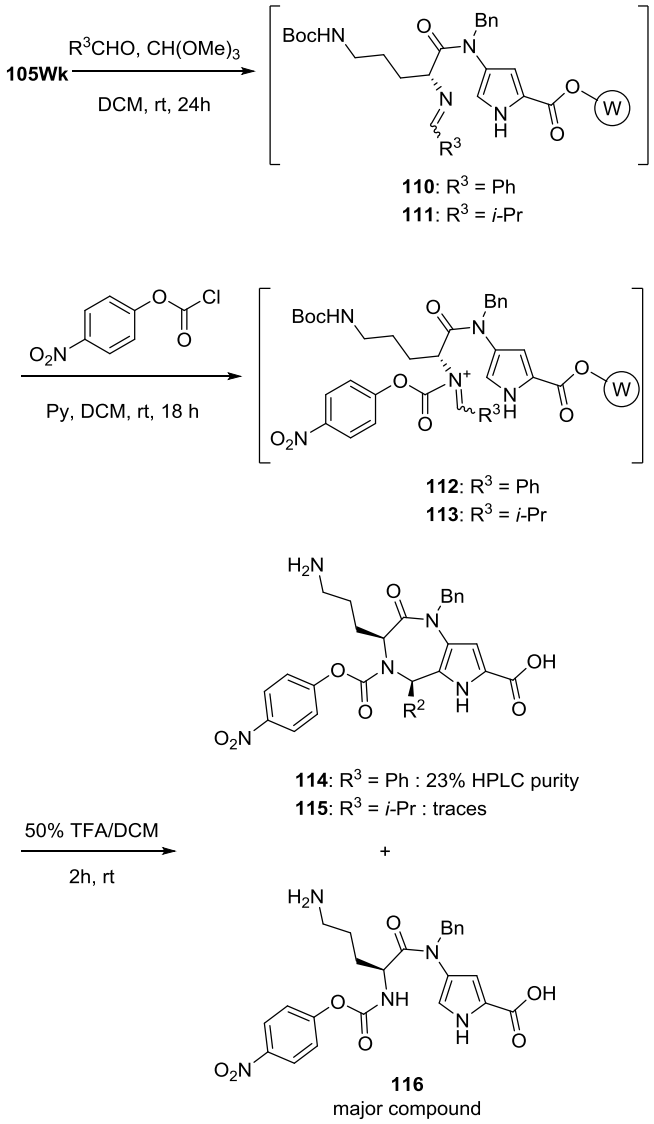

Previous success, in the solution-phase synthesis of pyrrolo[3,2-*e*][1,4]diazepin-2-ones using trifluoroacetic acid as catalyst in the Pictet-Spengler cyclization, compelled study of protic acid conditions on resin. Optimization was performed on Leu amide **105Wb** on 0.01 mmol scale using isobutyraldehyde (1000 mol%) as challenging substrates, by varying the solvent (2 mL), temperature, mode of heating, and TFA concentration (Scheme A1.5).

Scheme A1.5. Pictet-Spengler cyclization of pyrrole **105Wb**.

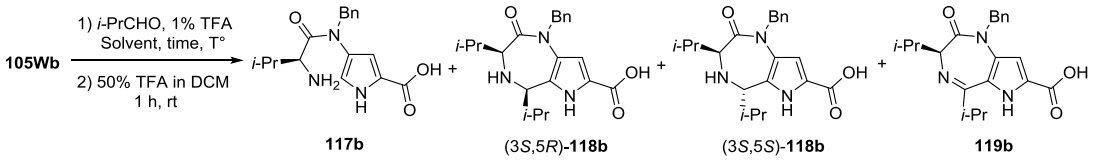

Reaction efficiency was evaluated after resin cleavage with 50% TFA in DCM and RP-HPLC-MS analysis, without product isolation. The conditions were optimized to produce the highest amount of the postulate major stereoisomer (3*S*,5*R*)**-118b** and minimum side-products and starting material (Table A1.2). Unsaturated diazepinone side-product **119** was soon recognized as an inherent product in the synthesis of pyrrolo[3,2-*e*][1,4]diazepin-2-one, which is presumed to be formed by a mechanism as that described for the formation of similar unsaturated carbolines,[39] and could not be avoided by careful degassing using freeze-thaw cycles under vacuum. Moreover, pyrrolo[3,2-*e*][1,4]diazepin-2-ones (3*S*,5*R*)**-118b** and (3*S*,5*S*)**-118b** were observed to convert to their unsaturated counterpart **119b** on standing over time.

Table A1.2. Optimization of the Pictet-Spengler cyclization on compound **105Wb**.

Entry	TFA	T	T	solvent	**117b**[a]	(3*S*,5*R*)-**118b**[a]	(3*S*,5*R*)-**118b**[a]	**119b**[a]
1	1%	RT	24 h	DCM	90%	10%	ND	ND
2	1%	RT	24 h	DCM/TFE 1/1	85%	15%	ND	ND
3	1%	70 °C	24 h	DCM/TFE 1/1	42%	29%	5%	24%
4	1%	60 °C microwave	2 h	DCM/TFE 4/1	67%	23%	3%	7%
5	1%	70 °C Microwave	2 h	DCM/TFE 4/1	17%	73%	3%	7%
6	1%	80 °C Microwave	2 h	DCM/TFE 4/1	11%	65%	9%	15%
7	1%	70 °C Microwave	2 h	$CHCl_3$	8%[b]	55%	4%	18%
9	1%	70 °C Microwave	2 h	THF	13%[b]	9%	ND	61%
9	1%	70 °C Microwave	2 h	Toluene	17%	74%	4%	5%
10	1%	70 °C Microwave	2 h	Benzene	3%	83%	6%	8%
11	0.1 %	70 °C Microwave	2 h	Benzene	23%	45%	6%	26%

[a] Determined by RP-HPLC-MS (C18 110A column 150 mm × 4.6 mm, 5 μm, 0-90% MeOH in H_2O in 20 min. then 90% MeOH for 15 min., 0.1% FA, UV: λ = 254 nm). [b] In these cases, unknown impurities (15-20%) were also detected. ND: non-detected.

Treating Wang resin **105Wb** with 1% TFA in DCM and TFE/DCM 1:1 at rt for 24 h led respectively to 10% and 15% conversion to (3*S*,5*R*)-**118b** (Table A1.2).[40] Heating **105Wb** with 1% TFA in DCM and TFE/DCM 1:1 at 70 °C in a sealed tube for 24 h increased conversion to 29%, albeit with formation of almost equal amounts of

dehydro analogue **119b** and some (3*S*,5*S*)-diastereoisomer. Microwave heating at 70 °C in a sealed reactor in a 4:1 DCM/TFE mixture reduced the reaction time to 2 h, minimized formation of **119b** and improved conversion to (3*S*,5*R*)**-118b** to 73%. Microwave heating at lower temperature (60 °C) decreased the rate of cyclization, and higher temperature (80 °C) promoted formation of (3*S*,5*S*)**-118b** and **119b**. More polar solvents such as THF or $CHCl_3$ increased the amount of **119b** and caused formation of unidentified impurities. Toluene gave similar results as DCM/TFE 4:1. Benzene gave the best results with 83% conversion to (3*S*,5*S*)**-118b** with minimal amounts of (3*S*,5*S*)**-118b** and **119b** (6% and 8%). Further attempts to reduce the amount of TFA in benzene caused a drop in the formation of (3*S*,5*S*)**-118b** and increased the proportion of **119b** (entry 11, Table A1.2).

With optimized Pictet-Spengler conditions in hand, employing a "one-pot" procedure, isobutyraldehyde was reacted with resins **105Wa-j** (0.01 mmol scale) packed in IRORI MicroKans and substrates were cleaved separately using 50% TFA in DCM containing 1% of triethylsilane as scavenger, and analyzed by RP-HPLC-MS, without isolation (Table A1.3, Scheme A1.6).

Scheme A1.6. One-pot Pictet-Spengler cyclization of pyrrole **105Wa-j**.

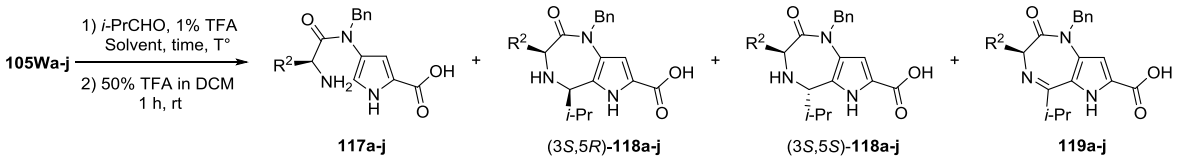

Table A1.3. Pictet-Spengler cyclization with diverse amino acid-derived amidopyrroles **105W**.

Entry	R^2	**117**[a] (R_t; $[M+H]^+$)	(3*S*,5*R*)-**118**[a] (R_t; $[M+H]^+$)	(3*S*,5*S*)-**118**[a] (R_t; $[M+H]^+$)	**119**[a] (R_t; $[M+H]^+$)
A	Bn	27% (12.2; 364.0)	73% (15.1; 418.2)	ND	
B	*i*-Pr	12% (17.3; 330.2)	72% (20.8; 384.4)	5% (19.8; 384.4)	11% (22.6; 382.3)
C	$(CH_2)_2CO_2CH_3$	9% (10.7; 346.2)	63% (14.7; 400.2)	8% (13.4; 400.2)	20% (15.9; 398.3)
d[b]	4-CH_2-1*H*-imidazole	17% (8.8; 354.2)	54% (11.8; 408.3)	29% (11.7; 408.3)	ND
E	CH_2OH	29% (10.7; 304.1)	38% (12.8; 358.2)	8% (12.2; 358.2)	25% (13.3; 356.1)
F	$(CH_2)_4NH_2$	76% (9.0; 345.2)	24% (10.5; 399.2)	ND	
g[b]	CH_2SH	ND			
h[c]	$(CH_2)_2SCH_3$	ND[e]			
i[b]	$(CH_2)_3CO_2H$	ND			
j[b]	pyrrolidine (from Pro)	78% (11.1; 314.2)	ND		

[a] Determined by RP-HPLC-MS (C18 110A column 150 mm × 4.6 mm, 5 μm, 0-90% MeOH in H_2O in 20 min. then 90% MeOH for 15 min., 0.1% FA, UV: λ = 254 nm). [b] In these cases, unknown impurities were also detected. [c] In this case, two isomers with very close retention time were observed. [e] **117h**, **118h** and **119h** products bearing one extra oxygen atom were detected. ND: non-detected.

Substrates bearing simpler alkyl R^2 groups (i.e., *i*-Pr and Bn) gave better conversion, than their heteroalkyl counterparts. Supported *N*-(γ-methyl aspartyl), *N*-(histidyl) and *N*-(serinyl)amidopyrroles **105Wc-e** gave the corresponding (3*S*,5*S*)-pyrrolodiazepinone **118** in reasonable proportions. In the case of **105Wd**, RP-HPLC-MS

analysis indicated peaks with retention times and molecular ions suggesting side-product from Pictet-Spengler reaction with the imidazole ring. *N*-(Lysyl)amidopyrrole **105Wf** furnished the corresponding cyclized product (3*S*,5*R*)**-118f**, albeit in low conversion (18%) with considerable product derived from residual starting material. No desired products were detected from reactions of *N*-(cysteinyl), *N*-(methioninyl), *N*-(glutamyl) and *N*-(prolyl)amidopyrroles **105Wg-j**; however, analysis of the cleaved product from reaction of Met analogue **105Wh** indicated molecular ions for product plus 16 and 32 mass units, suggesting sulfur oxidation under the conditions of the Pictet-Spengler reaction.

Scheme A1.7. Large Scale Pictet-Spengler cyclization on Wang resin.

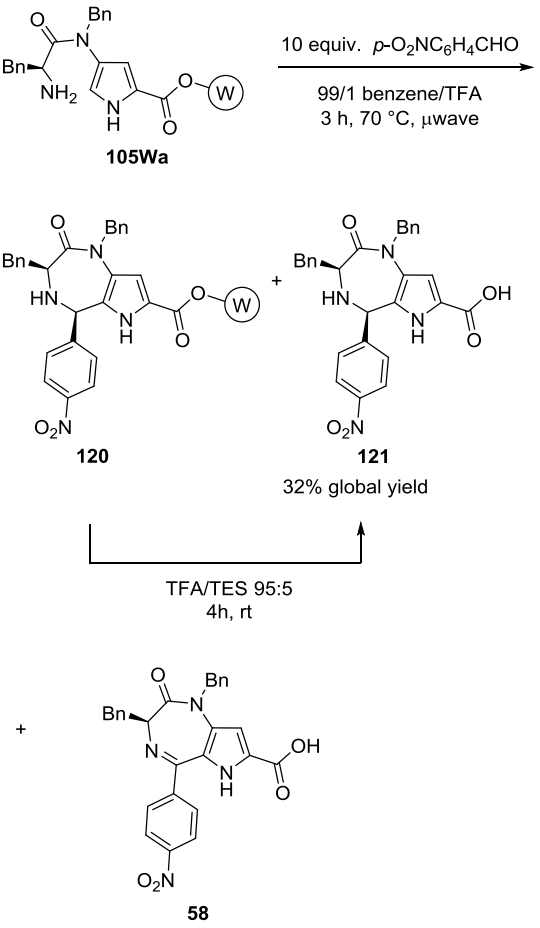

The synthesis of phenylalanine-derived amidopyrrole **105Wa** was repeated on larger scale using 300 mg of starting Wang bromide resin (0.66 mmol) employing IRORI MacroKans in parallel reactions with its Merrifield resin counterpart **105M** (0.37 mmol, 420 mg of resin) in the same pot. For the Pictet-Spengler reaction, resins **105Wa** and **105M** were separately transferred into three IRORI MiniKans (100 mg of resin capacity), which could be fit into the 20 mL Biotage microwave vessel, and respectively reacted with *p*-nitrobenzaldehyde, which had given better yields of diazepinone in the solution-phase synthesis,[15] using optimized conditions (1% TFA in benzene, 1000 mol% aldehyde, 70 °C) for an extended 3 h reaction time to complete conversion (Scheme A1.5).

In the case of Wang resin, after the microwave reaction, the resin and liquid phase were filtered, the resin was washed and the filtrate and washings were evaporated. The resin was cleaved using TFA/DCM 1:1 containing 1% of triethylsilane, filtered and washed and the filtrate and washings were similarly evaporated. Residues from evaporation of the filtrate after Pictet-Spengler reaction and cleavage were separately purified by flash column chromatography[41] (AcOEt/MeOH/MeCN/H_2O 70:10:10:10 as eluent) to yield inseparable 30:70 mixtures of hexahydro pyrrolodiazepinone **121** and tetrahydro pyrrolodiazepinone **58** in 29% (from the Pictet-Spengler) and 3% yields (from resin cleavage). The premature cleavage of around 90% of the Pictet-Spengler cyclization product suggested that substrate may have been cleaved and reacted both in the solid- and solution-phases during the reaction; moreover, it disqualified the use of Wang resin for further modification of the pyrrolo[3,2-*e*][1,4]diazepin-2-one scaffold on support. On the contrary, a similar analysis of the residue from the liquid phase of the

Pictet-Spengler reaction on Merrifield resin **105M** by RP-HPLC-MS revealed the presence of residual *p*-nitrobenzaldehyde without cleaved starting material and only trace amounts of product **58** (less than 1% of the UV signal at λ = 280 nm, Scheme A1.6). Pyrrolo[3,2-*e*][1,4]diazepin-2-one **121** was prone to oxidation even when stored under argon at –10 °C which led to a 1:1 mixture of **121** and unsaturated analogue **58** after a few hours. Compared with the isopropyl analog **118b**, the presence of the electron withdrawing nitrophenyl group may account for the low stability of **121**, because of the increased acidic character of the 5-position proton of the diazepinone ring, Analytical samples were purified by reverse phase preparative HPLC yielding pure **58** and a 9/1 **121**:**58** mixture after freeze-drying.

Scheme A1.8. Pictet-Spengler cyclization on Merrifield resin and TAP Soluble Support.

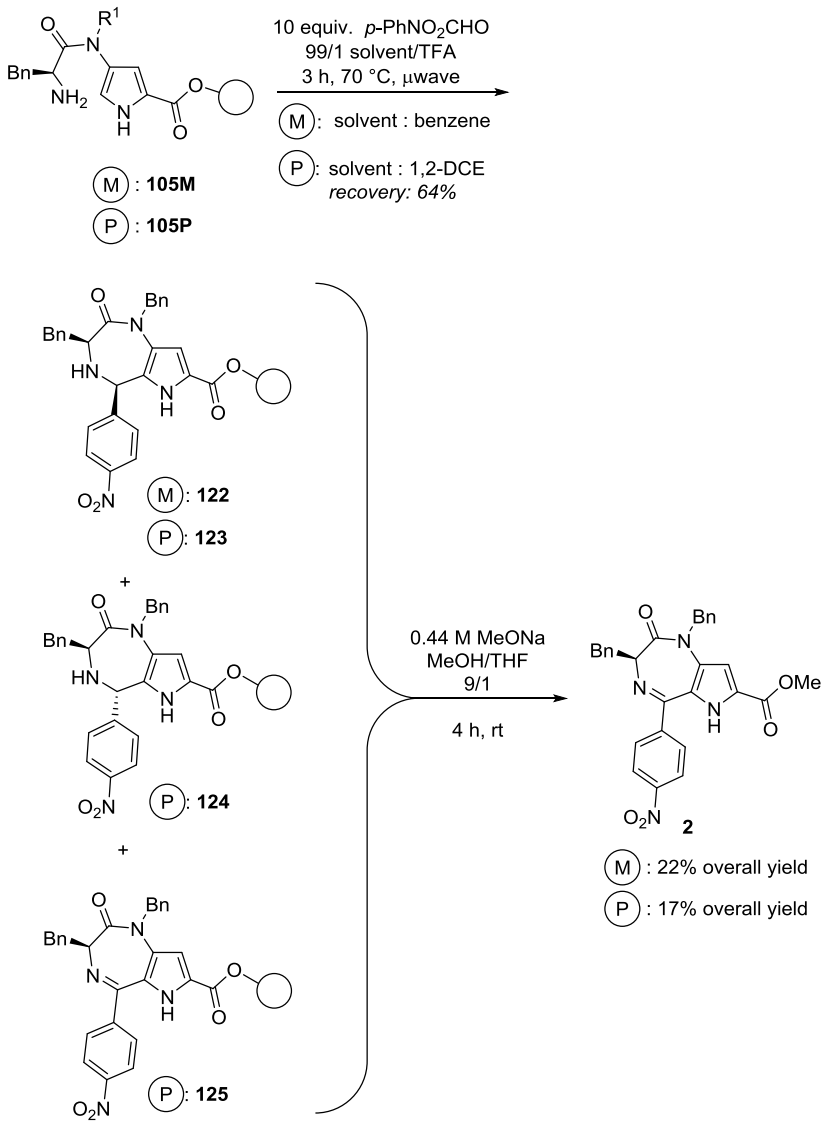

Attempts to cleave pyrrolo[3,2-*e*][1,4]diazepin-2-one from 10 mg aliquots of Merrifield resin using TFA under microwave heating (TFA/TES/H_2O 95:2.5:2.5, 2 mL at 50 °C for 30 min)[4284, 256] gave only enough material for RP-HPLC-MS analysis, which indicated **58** to be 35% pure, contaminated with other degradation products, without any trace of its diastereoisomer or dehydro counterpart **58** nor starting material.

Scheme A1.9. Microwave-assisted TFA cleavage of compound **122**.

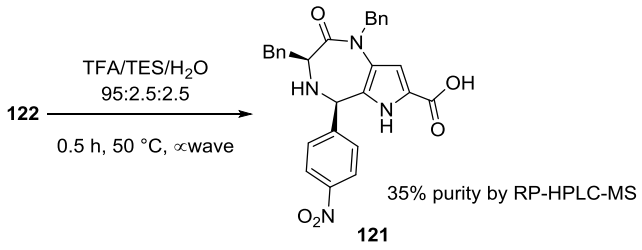

On the TAP support, the Pictet-Spengler reaction was performed using 1% TFA in 1,2-dichloroethane, instead of benzene, to assure solubility of amidopyrrole **105P** during microwave irradiation at 70 °C for 3 h. Analysis by RP-HPLC-MS, after precipitation, indicated no cleavage products in the decanted reaction solution and that the TAP-supported material consisted of 92% (3*S*,5*R*)-**123**, 2% (3*S*,5*S*)-**124** and 6% dehydrogenated product **125** without any starting material **105P**.

Cleavage of compound pyrrolo[3,2-*e*][1,4]diazepin-2-one from both Merrifield resin and the TAP support was effectively accomplished using 0.44 M $NaOCH_3$ in 9:1 THF/MeOH for respectively 4 h and 1 h. Treating the Merrifield resin substrate with methoxide for longer reaction times resulted in significant amounts of degradation. Cleavage provided only tetrahydro diazepinone methyl ester **2** in respectively 22% and 17% overall yields from the Merrifield and TAP supports, after preparative RP-HPLC.

Discussion and Conclusions

All three supports served to provide pyrrolo[3,2-*e*][1,4]diazepin-2-one products. None proved, however, to be ideal for the high criteria of 1) effective monitoring of reaction mixtures, 2) balancing between stability for broad applications and facile cleavage, 3) capacity to minimize the use of excess reagents for obtaining high yield, and 4) utility in split-and-mix[43] experimentations. Nevertheless, each support had benefits.

For example, the solid supports, Wang and Merrifield resin were particularly useful for parallel experiments, because the cross-linked polymers could be conveniently split into independent reactors, which could be employed together in exploratory chemistry in the same pot, before separate cleavages and analyses. The labile nature of Wang resin under both the acid and methoxide cleavage conditions facilitated subsequent analysis by LCMS. The stability of Merrifield resin offers potential for further modifying the pyrrolo[3,2-*e*][1,4]diazepin-2-one scaffold after the Pictet-Spengler cyclization. The soluble TAP support offered the practical advantage of employing homogenous conditions, which resulted in the use of less reagents for driving reactions to completion and quicker reaction times; moreover, chemistry on the soluble TAP support could be conveniently monitored by TLC (using MeOH/CH_2Cl_2 eluents) and RP-HPLC-MS, in addition to, in certain cases, NMR spectroscopy. Although the chemistry on both the solid and soluble supports was similar, in some cases, solvents were changed to comply with the solubility requirements of the TAP-supported compounds.

The recovery of the TAP support by precipitation showed variable efficiency (based on theorical mass) during the course of the synthesis, which amounted to a 43% overall recovery of supported material after 6 steps. Attempts to enhance recovery by additional precipitation of material from filtrates caused often the co-precipitatation of unwanted impurities. For example, after the preparation of aminopyrrole **56P**, precipitation gave a 122% mass recovery due to co-precipitation of impurities, which were not eliminated by additional precipitation. In general, preciptitation performances were contingent on the molecular weight of the supported substrates, with those of lower mass having less solubility in diethyl ether, leading to higher recovery. The monitoring

of TAP-supported substrates during reactions was facilitated by RP-HPLC-MS, because of the relatively high UV absorbance and ion detection of the tetrarylphosphonium group; however, impurities not linked to the TAP support were better detected by ^{1}H NMR spectroscopy. A single purification by silica gel column chromatography of the final pyrrolo[3,2-*e*][1,4]diazepin-2-one was performed after seven steps to isolate pure final ester **2** in 22% overall yield. Although the TAP support was not deemed convenient for "split-and-mix" methodology, the potential for performing synthesis in solution and for examining reactions directly on the support made this method useful for preparing a specific pyrrolo[3,2-*e*][1,4]diazepin-2-one target.

The solid-supports Wang and Merrifield resin and the soluble tetraarylphosphonium support exhibited complementary utilities in the synthesis of pyrrolo[3,2-*e*][1,4]diazepin-2-one. With respect to overall yield, the Wang resin provided pyrrolodiazepinone in a 32 % combined yield for **121** and **58**, albeit product was prematurely cleaved under the acidic conditions used for the Pictet-Spengler cyclization. The overall yields for Merrifield resin and the TAP soluble support **103** were somewhat lower, likely because of the need for vigourous conditions in the final cleavage of the former and incomplete mass recoveries after precipitation of the latter support; however, both were resistant to the acidic conditions of the Pictet-Spengler reaction and could in principle be used for further modification of the scaffold on support. Considering the applicability of the former for split-and-mix chemistry in IRORI Kans, an investigation is currently underway for the construction of pyrrolo[3,2-*e*][1,4]diazepin-2-ones using Merrifield resin and alternative cleavage methods, which will be reported in due course.

Experimental Section

General. Wang resin SS (75-100 mesh, 1.2 mmol/g) and Merrifield resin SS (70-90 mesh, 1.3 mmol/g) were purchased from Advanced Chemtech (Louisville, KY). Wang bromide resin was prepared from Wang resin according to the literature method.[29] TAP soluble support (bromomethylphenyltriphenylphosphonium) was obtained from Soluphase Inc. (Montreal, Quebec, Canada). IRORI MacroKans and MiniKans were from Nexus Biosystems, Inc. (Poway, CA). (2*S*,4*R*)-4-Hydroxy-*N*-1-(PhF)proline was prepared from (2*S*,4*R*)-4-hydroxy-*N*-1-(PhF)proline methyl ester according to references 25 and 16. Fmoc-Orn(Boc) and Fmoc-Asp(OMe) were synthesized according to known procedures.[44] Anhydrous THF, MeCN, DCM, MeOH and DMF were obtained from a Seca Solvent Filtration System (GlassContour Laguna Beach, CA); DMSO was dried over activated 4 Å molecular sieves 24 h prior to use and stored in a tightly sealed bottle under an argon atmosphere.[45] Reactions requiring anhydrous conditions were performed under an atmosphere of dry argon; glassware was flame dried immediately prior to use and allowed to cool under argon atmosphere. Syringes and needles were dried in an oven at 100 °C overnight and were allowed to cool down in desiccators prior to use. Liquid reagents, solutions and solvents were added *via* syringe through rubber septa. Flash column chromatography[41] was performed using SiliaFlashF60 silica (Silicycle, Quebec City). Glass-backed plates precoated with silica gel (SiliaPlate TLC Extra Hard Layer 60 Angstrom F-254, Silicycle, Quebec City) were used for thin layer chromatography (TLC) and were visualized by UV fluorescence or staining with a ninhydrin or a phosphomolybdic acid solution in EtOH prior to heating. Purification by radial chromatography[32] was performed using 2 mm sorbent layers. Sorbent consists in a 2.5/1

silica gel (TLC standard grade, 2-25 μm, pore size 60 Å with fluorescent indicator, Aldrich ref. 288586)/calcium sulfate hemihydrate. Plates were prepared according to ref 32 and elution flow varied between 6 and 8 mL/min. ^{1}H NMR and ^{13}C NMR spectra were recorded on Bruker AV300, ARX400 and AV500 spectrometers with chemical shift values in ppm relative to residual chloroform (δ_H 7.26 & δ_C 77.2), acetone (δ_H 2.05 & δ_C 29.84), or DMSO (δ_H 2.50 & δ_C 39.52) as standards. Coupling constant *J* values are given in Hz, with splitting described as s (singlet), d (doublet), t (triplet), q (quartet), m (multiplet). Mass spectral data and high-resolution mass spectrometry (HRMS, electrospray ionization) were obtained by the Université de Montréal Mass Spectrometry Facility. Specific rotation, $[\alpha]_D$ values are given in units 10^{-1}•deg•cm^2•g^{-1}. Microwave assisted reactions were performed in a Biotage Initiator microwave apparatus (Biotage AB, Uppsala, Sweden) in glass Biotage reaction vessels containing a magnetic stirrer bar and sealed with a septum cap. Analytical RP-HPLC analyses were performed on a C18 column 50 mm × 4.6 mm, 5 μm, (column A) or on a C18 column 150 mm × 4.6 mm, 5 μm (column B) with a flow rate of 0.5 mL/min using a linear gradient of MeOH (0.1% formic acid (FA)) in water (0.1% FA). Retention times (t_R) from analytical RP-HPLC are reported in minutes. Indicated compounds were purified with a C18 column 250 mm × 21mm, 5μm (column C) using a specified linear gradient of MeOH or MeCN (0.1% FA) in water (0.1% FA), with a flow rate of 10.6 mL/min.

Resin swelling in IRORI Kans. Under argon sweeping, resins in Kans and a stirring bar were placed in a flame-dried round-bottom flask, which was exposed to three cycles of vacuum (20 mm Hg) followed by argon, prior to addition of the specified amount of the

appropriate dry solvent. The flask was swept with argon and sealed using a rubber septum and the resin was allowed to swell for 30 minutes under inert atmosphere.

Resin washing in IRORI Kans The Kans were placed together in a Schott Duran glass bottle equipped with a stirring bar, and treated with solvent. The bottle was sealed with a screw cap and shaken by hand for 10 seconds. The Kans were next magnetically stirred for 5 min. The solvent was decanted through a perforated screw cap, then the bottle was shaken vigorously by hand, head down, for 10 seconds. This operation was repeated for as many times and solvents as specified. At the end of the process, residual solvent in Kans was removed by centrifugation, or by subjecting the head of each Kan to vacuum for 1 min using a water aspirator.

(2*S*,4*R*)-4-Hydroxy-*N*-(PhF)proline Wang and Merrifield resins (54W, 54M). In a 200 mL round-bottom flask, a solution of *N*-(PhF)hydroxyproline **104** (1.65 g, 4.44 mmol, 200 mol%, prepared according to ref 25) in MeOH (9 mL) was treated with 1 mL of water, titrated with 20% Cs_2CO_3 to pH 7 (about 2.5 mL), evaporated to dryness, and twice suspended in toluene and evaporated. The residue was ground into a powder by scraping the wall of the flask with a spatula. The round-bottom flask was charged with two IRORI MacroKans containing Wang bromide resin[29] (0.30 g × 2, 1.1 mmol/g, 0.66 mmol) and four IRORI MacroKans containing Merrifield resin (0.30 g, × 4, 1.3 mmol/g, 1.56 mmol). The resins were swollen and cesium salt **53** was dissolved in DMF (100 mL). After treatment with dibenzo-18-crown-6 (1.2 g, 3.33 mmol, 1.5 equiv.), the flask was swept with argon,[46] and the reaction mixture was heated to 70 °C with an oil bath and agitated gently with magnetic stirring for 48 h. The Kans containing resin were transferred together into a 250 mL bottle and washed sequentially with 100 mL volumes

of DCM, MeOH, H_2O, DCM, MeOH, H_2O, MeOH (3 ×) and DCM (3 ×). The beige resins in Kans were dried *in vacuo* and stored usually in desiccators under vacuum or under argon in the refrigerator. Anchoring efficiency of respective resins was evaluated by measuring their mass increase after the reaction. Excess (2*S*,4*R*)-4-hydroxy-*N*-(PhF)proline was recovered as previously described.[25] **54W:** IR (KBr, cm^{-1}): 3448 (OH), 1737 (C=O). The mass increase after reaction was 216 mg and corresponded to a loading of 0.80 mmol/g (98% conversion). **54M:** IR (KBr, cm^{-1}): 3457 (OH), 1732 (C=O). The mass increase after reaction was 501 mg, and corresponded to a loading of 0.88 mmol/g (96% conversion).

(2*S*)-4-Oxo-*N*-(PhF)proline Wang and Merrifield resins (55W, 55M). To a 100 mL round-bottom flask, under argon atmosphere, $(COCl)_2$ (2.20 mL, 25.80 mmol, 12 equiv.) was added drop-wise to a solution of DMSO (3.70 mL, 51,60 mmol, 24 equiv.) in DCM (50 mL) at –78°C, and stirred for 30 min. Into a 200 mL round-bottom flask containing respectively IRORI MacroKans possessing (2*S*,4*R*)-4-hydroxy-*N*-(PhF)proline Wang (**54W**, 0,406 g × 2, 0.80 mmol/g, 0.65 mmol) and Merrifield (**54M**, 0.425 g × 4, 0.88 mmol/g, 1.50 mmol) resins swollen in dry DCM (50 mL) at –78°C, the DMSO mixture was transferred by a double-tipped needle and the Kans were agitated gently with magnetic stirring for 4 h at –78°C. The resins became a light green color, which turned progressively to light brown within 1 h. After 4 h, the resins at –78 °C were treated drop-wise with DIEA (13.50 mL, 77.40 mmol, 36 equiv.) over 1 h, after which time the resins appeared dark brown. The suspension containing the Kans was allowed to warm to room temperature over 1 h and filtered. The Kans were transferred into a 250 mL bottle and washed sequentially with 100 mL volumes of DCM (× 2), MeOH (× 2), DCM (× 2),

MeOH (× 2), DCM (× 2) as described above. The resins in Kans were dried *in vacuo* and the reaction was repeated a second time to assure complete alcohol oxidation as ascertained by the disappearance of the hydroxyl absorption around 3440-3460 cm^{-1} in the IR spectrum. The beige resin was usually stored in desiccators under vacuum or under argon in the refrigerator. **55W**: IR (KBr, cm^{-1}): 1732 and 1758 (C=O). **55M**: IR (KBr, cm^{-1}): 1732 and 1758 (C=O).

4-Benzylamino-1*H*-pyrrole-2-carboxylate Wang resin (56W). In a 100 mL round-bottom flask, two IRORI MacroKans containing (2*S*)-4-oxo-*N*-(PhF)proline Wang resin **55W** (0.405 g × 2, 0.80 mmol/g, 0.65 mmol) were swollen in THF (40 mL). The mixture was degassed by three freeze-thaw cycles, covered with a blanket of argon and treated with anhydrous $MgSO_4$ (0.8 g, dried overnight at 100 °C prior to use), followed by *p*-TsOH•H_2O (25 mg, 0.13 mmol, 0.2 equiv.) and benzylamine (1.60 mL, 14.95 mmol, 23 equiv.). The mixture was purged with argon bubbles for 30 min, and stirred for 18 h at 50 °C in an oil bath under an argon atmosphere. The Kans containing the green resin were transferred to a bottle and washed sequentially with 50 mL volumes of THF, DCM, MeOH, H_2O, DCM, MeOH, H_2O, MeOH (× 2) and DCM (× 3). The light green resin (total weight: 697 mg) was usually stored in desiccators under vacuum or under argon in the refrigerator. The filtrate from the reaction mixture and all washings was combined and evaporated *in vacuo* to a residue, which was partitioned between water (20 mL) and EtOAc (20 mL). The aqueous layer was extracted with EtOAc (2 × 20 mL). The combined organic layers were washed with 10% HCl (2 × 30 mL), $NaHCO_3$ sat. (30 mL) and brine (30 mL), dried over sodium sulfate, filtered and evaporated to a residue, which was purified by column chromatography (2% Et_2O/hexanes). Combination of the

collected fractions and evaporation of the volatiles yield 130 mg of 9,9-phenylfluorene (0.54 mmol, PhF-H, mp 146 °C, litt.[124] mp 148 °C) corresponding to a 0.77 mmol/g loading of aminopyrrole on Wang resin.

4-Benzylamino-1*H*-pyrrole-2-carboxylate Merrifield resin (56M). 4-Benzylamino-1*H*-pyrrole-2-carboxylate Merrifield resin **56M** was synthesized as described above for 4-benzylamino-1*H*-pyrrole-2-carboxylate Wang resin **56W** from **55M** (0.425 g × 4, 0.88 mmol/g, 1.50 mmol) using 4 IRORI MacroKans, 80 mL of THF, 3.77 mL of benzylamine (34.5 mmol, 23 equiv.), 57 mg of *p*-TsOH•H_2O (0.3 mmol, 0.2 equiv.) and 1.2 g of dry $MgSO_4$. After reaction, the Kans containing brownish green resin (total weight: 1.467 g) were usually stored in desiccators under vacuum or under argon in the refrigerator. Purification of the residue from resin filtration and washings as described above yielded 359 mg (1.48 mmol) of PhF-H indicative of an aminopyrrole loading on Merrifield resin of 1.01 mmol/g.

4-[*N*-(9-Fluorenylmethoxycarbonyl)-L-phenylalaninyl]benzylamino-1*H*-pyrrole-2-carboxylate Wang and Merrifield resins (57Wa, 57M). In a 100 mL round-bottom flask under argon atmosphere, Fmoc-Phe (3.971 g, 10.25 mmol, 5 equiv.) was mixed with bis(trichloromethyl)carbonate (0.912 g, 3.38 mmol, 1.65 equiv.) in THF (50 mL) at 0 °C, and treated drop-wise with 2,4,6-collidine (3.8 mL, 28.70 mmol, 14 equiv.) over 5 min. The white suspension was stirred for 10 min at 0 °C and transferred by syringe to a 200 mL round-bottom flask containing IRORI MacroKans filled respectively with 4-benzylamino-1*H*-pyrrole-2-carboxylate Wang (**56W**, 0.348 g × 2, 0.77 mmol/g, 0.54 mmol) and Merrifield (**56M**, 0.368 g × 4, 1.01 mmol/g, 1.48 mmol) resins swollen in THF (50 mL) at 0 °C. The mixture was allowed to warm to room temperature with

stirring for 15 h. The Kans containing resin were transferred to a bottle and washed with 100 mL volumes of DMF (× 3), MeOH (× 3) and DCM (× 3) as described above. The dark green resins (Wang: 0.899 g; Merrifield: 2.005 g) were usually stored in desiccators under vacuum or under argon in the refrigerator. Aliquots (15 mg) of each resin were removed from the Kans, partitioned into two 2 mL plastic filtration tubes equipped with polyethylene frits, swollen respectively in DMF for 20 min and treated twice with a 20% solution of piperidine in DMF for 20 min and filtered. The resins were washed successively with agitation for 1 min and filtered from DMF (3 × 1 mL), MeOH (3 × 1 mL) and DCM (3 × 1 mL). A positive Kaiser test[257] indicated qualitatively the presence of free amine. The resins were respectively treated with acetic anhydride (37 μL, 0.39 mmol, 20 equiv.) and DIEA (85 μL, 0.49 mmol, 25 equiv.) in DMF (1 mL) for 2 h, washed as described above. Afterward, a negative Kaiser test indicated quantitative acylation. In the case of 4-[*N*-(9-fluorenylmethoxycarbonyl)-L-phenylalaninyl]benzylamino-1*H*-pyrrole-2-carboxylate Wang resin **57Wa**, the acylated material was cleaved from the resin using 50% TFA in DCM (1 mL) for 1 h and the filtrate was evaporated to dryness to a residue, which was subjected to RP-LCMS analysis (column A, 0-80% MeOH in H_2O for 10 min. then 90 % MeOH for 5 min., 0.1% FA, UV: λ = 280 nm, t_R 8.76), which indicated >90% purity, with no sign of acylated starting material. In the case of 4-[*N*-(9-fluorenylmethoxycarbonyl)-L-phenylalaninyl]benzylamino-1*H*-pyrrole-2-carboxylate Merrifield resin **57M**, cleavage was performed using a 0.44 M MeONa solution in THF/MeOH (9:1, 1 mL)[48] for 2 h. The sequence of filtration, washing of the resin with EtOAc, and partitioning of the filtrate between EtOAc and saturated aqueous NH_4Cl solution gave an organic layer,

which was filtered through a Pasteur pipette containing a 5 mm high layer of Na_2SO_4, and evaporated to dryness. Analysis of the residue by RP-LCMS (column B, 0-80% MeOH over H_2O in 20 min. then 90% MeOH for 15 min., 0.1% FA, UV: λ = 280 nm, t_r 26.34) demonstrated >82% purity, with no sign of acylated starting material.

4-(*L*-Phenylalaninyl)benzylamino-1*H*-pyrrole-2-carboxylate Wang and Merrifield resins (105Wa, 105M). In a 250 mL bottle, 4-[*N*-(9-fluorenylmethoxycarbonyl)-L-phenylalaninyl]benzylamino-1*H*-pyrrole-2-carboxylate Wang (**57Wa**, 0.442 g × 2, 0.60 mmol/g, 0.53 mmol) and Merrifield (**57M**, 0.497 g × 4, 0.74 mmol/g, 1.47 mmol) resins in IRORI MacroKans were swollen in DMF (100 mL) for 0.5 h, filtered and exposed to a freshly prepared 20% piperidine in DMF solution (100 mL) with gentle magnetic stirring for 20 min. The reaction mixture was decanted and the resin Kans were retreated with the piperidine in DMF solution as before. The resins in Kans were washed with 100 mL volumes of DMF (× 3), MeOH (× 3) and DCM (× 3) as described above. A positive Kaiser test[47] indicated qualitatively the presence of free amines. The resins (**105Wa**: 0.754 g, light brownish orange, **105M**: 1.682 g, light brownish green) were usually stored in desiccators under vacuum or under argon in the refrigerator.

(*S*)-1,3-Dibenzyl-5-(4-nitrophenyl)-2-oxo-1,2,3,6-tetrahydropyrrolo[3,2-*e*][1,4]diazepine-7-carboxylic acid (120). The contents from one MacroKan containing 4-(L-phenylalaninyl)benzylamino-1*H*-pyrrole-2-carboxylate Wang resin (**122a**, 0.377 g, 0.69 mmol/g, 0.26 mmol) were split into three IRORI MiniKans, which were treated with benzene (15 mL) and placed into a 20 mL-Biotage microwave vessel.[67] The vessel was sealed with a conventional rubber septum, and placed under argon atmosphere. After swelling for 20 min, the resin was treated with *p*-nitrobenzaldehyde (0.390 g, 2.58 mmol,

10 equiv.), followed by TFA (150 µL), and stirred with heating under microwave irradiation at 75 °C for 3.5 h. The MiniKans containing resin were transferred to a bottle and sequentially washed with 50 mL volumes of THF (× 3), MeOH (× 3) and DCM (× 3) as described above. The filtrates were evaporated to dryness and the residue (450 mg) was purified by flash silica gel column chromatography using EtOAc/MeOH/MeCN/H_2O (70:10:10:10) as eluent to yield two different fractions, the first one consisting of an inseparable 30/70 mixture of hexahydropyrrolodiazepinone **121** and tetrahydropyrrolodiazepinone **58** (33 mg), and the second one (4 mg) consisting in a 8/92 mixture of **121** and **58** (29% global yield). The resin in Kans was treated with TFA/TES (95:5, 6 mL) for 4h and filtered, washed with 50 mL volumes of THF (× 3), MeOH (× 3) and DCM (× 3) as described above. The filtrate and washings were combined and evaporated to a residue (9 mg), which was purified by chromatography using AcOEt/MeOH/MeCN/H_2O (70:10:10:10) as eluent. Evaporation of the collected fractions gave the same yellow oil consisting of an inseparable 30/70 mixture of hexahydro pyrrolodiazepinone **121** (4 mg, 3% global yield). Pure **58** (2 mg) was obtained by preparative HPLC (column C, 60-90% MeOH in H_2O over 30 min.): $[\alpha]^{21}_D = -47.5$ (*c* = 0.75); ^{1}H NMR (CD_3OD, 300 MHz) δ 3.55 (dd, *J* = 8.0, 13.6 Hz, 1H), δ 3.68 (dd, *J* = 6.0, 13.8 Hz, 1H), 4.08 (dd, *J* = 8.0, 6.0 Hz, 1H), 5.01 (d, *J* = 15.4 Hz, 1H), 5.31 (d, *J* = 15.4 Hz, 1H), 6.69 (s, 1H), 7.09 (dd, *J* = 2.1, 3.5 Hz, 2H), 7.19 (m, H, 4H), 7.30 (t, *J* = 7.3 Hz, 2H), 7.37 (d, *J* = 7.2 Hz, 2H), 7.62 (d, *J* = 8.7 Hz, 2H), 8.23 (d, *J* = 8.7 Hz, 2H), 8.50 (s, 1H); ^{13}C NMR (125 MHz, acetone d_6) δ 38.7 (CH_2), 49.5 (CH_2), 67.0 (CH), 102.7 (CH), 120.2 (C), 123.1 (3CH), 126.0 (C), 126.7 (2CH), 126.9 (CH), 128.0 (2CH), 128.3 (2CH), 129.9 (2CH), 130.1 (2CH), 133.5 (C), 137.6 (C), 139.9 (C), 143.5

(C),148.7 (C), 158.9 (C=O + C=N), 165.5 (C=O); HRMS calcd. for $C_{28}H_{23}N_4O_5$ $[M+H]^+$: 495.1665, found: 495.1663; IR υ_{max}/cm^{-1} (NaCl): 3424 (N-H), 3154 (OH), 3057, 3036, 2942 (C-H), 1674 (C=O acid), 1655 (C=O amide), 1603 ($C=C_{arom}$), 1553 ($C=C_{arom}$), 1520 ($Ar-NO_2$), 1494 ($C=C_{arom}$), 1453 ($C=C_{arom}$), 1434 ($C=C_{arom}$), 1346 (C-H), 1314 (C-O), 1116.

(*S*)-Methyl 1,3-dibenzyl-5-(4-nitrophenyl)-2-oxo-1,2,3,6-tetrahydropyrrolo[3,2-*e*][1,4]diazepine-7-carboxylate from Merrifield resin (2). In IRORI Kans, the Pictet-Spengler reaction was performed on 4-(L-phenylalaninyl)benzylamino-1*H*-pyrrole-2-carboxylate Merrifield resin **105M** using microwave heating as described above for Wang resin **105Wa**. Resin **105M** (0.420 g, 0.88 mmol/g, 0.37 mmol) from one MacroKan was split into three IRORI MiniKans, swollen in benzene (15 mL), treated with *p*-nitrobenzaldehyde (0.559 g, 3.70 mmol, 10 equiv.) and TFA (150 μL) and heated with microwave irradiation. The resin in MiniKans was sequentially washed with 50 mL volumes of THF (× 3), MeOH (× 3) and DCM (× 3) as described above. Evaporation of the combined washing solutions gave a trace amount of (3*S*,5*R*)-1,3-dibenzyl-5-(4-nitrophenyl)-2-oxo-1,2,3,4,5,6-hexahydropyrrolo[3,2-e][1,4]diazepine-7-carboxylic acid **58** as analyzed by RP-HPLC analysis (column A, 10-90% MeOH in H_2O for 20 min. then 90% MeOH for 15 min., 0.1% FA, UV: λ = 280 nm, t_R 24.34, accounting for less than 1% of the UV signal) along with *p*-nitrobenzaldehyde. An aliquot of resin **122** (10 mg) was suspended in TFA/TES/H_2O (95:2.5:2.5, 2 mL) and treated under microwave-assisted cleavage conditions[42a] at 50 °C for 30 min in a V-shaped 2 mL-Biotage vessel with a triangular stirring bar. Filtration of the resin and evaporation of the filtrate gave a residue, which was analyzed by RP-HPLC (column A, 0-80% MeOH in H_2O over 10

min. then 90% MeOH for 5 min., 0.1% FA, UV: λ = 280 nm) and found to contain (3*S*,5*R*)-1,3-dibenzyl-5-(4-nitrophenyl)-2-oxo-1,2,3,4,5,6-hexahydropyrrolo[3,2-*e*][1,4]diazepine-7-carboxylic acid **58** of 35% purity (UV signal at λ = 280 nm, t_R 11.08) without trace of starting 4-(L-phenylalaninyl)benzylamino-1*H*-pyrrole-2-carboxylic acid (t_R 7.05). Product cleavage was performed in a 60 mL filtration tube with a polyethylene frit, by shaking the remaining resin suspended in a 0.44 M MeONa solution in THF/MeOH (9:1, 30 mL) at room temperature for 4 h. The resin was filtered and washed with EtOAc (3 × 30 mL). The filtrate and washings were combined and washed with saturated aqueous NH_4Cl (50 mL). The aqueous phase was extracted with EtOAc (2 × 20 mL) and the combined organic layers were washed with brine (50 mL), dried over anhydrous Na_2SO_4 and evaporated to dryness. Purification of the residue was performed by flash chromatography on a silica gel column (15 to 20% gradient of EtOAc in hexanes) to yield (*S*)-methyl 1,3-dibenzyl-5-(4-nitrophenyl)-2-oxo-1,2,3,6-tetrahydropyrrolo[3,2-*e*][1,4]diazepine-7-carboxylate **2** as a yellow oil (42 mg, 0.084 mmol, 22%). $[\alpha]^{21}_D = -46.4$ (*c* = 0.33,); ^{1}H NMR ($CDCl_3$, 300 MHz) δ 3.68 (dd, *J* = 8.0, 13.5 Hz, 1H), 3.75 (dd, *J* = 5.7, 13.5 Hz, 1H), 3.82 (s, 3H), 4.08 (dd, *J* = 8.0, 5.7 Hz, 1H), 4.96 (d, *J* = 15.4 Hz, 1H), 5.28 (d, *J* = 15.4 Hz, 1H), 6.74 (d, *J* = 2.4 Hz, 1H), 7.08 (dd, *J* = 2.2, 3.5 Hz, 2H), 7.23 (m, 4H), 7.34 (t, *J* = 7.2 Hz, 2H), 7.4 (d, *J* = 7.2 Hz, 2H), 7.62 (d, *J* = 8.8 Hz, 2H), 8.23 (d, *J* = 8.8 Hz, 2H), 8.92 (s, 1H); ^{13}C NMR (125 MHz, $CDCl_3$) δ 38.7 (CH_2), 50.4 (CH_2), 52.5 (CH_3), 67.4 (CH), 106.2 (CH), 122.9 (C), 124.0 (2CH), 124.9 (C), 126.5 (CH), 127.1 (2 CH), 127.6 (CH), 128.4 (2CH), 128.8 (2CH), 130.0 (2CH), 130.1 (2CH), 134.4 (C), 136.6 (C), 139.2 (C), 142.6 (C),149.3 (C),158.5 (C=O),160.8 (C=N),165.6 (C=O); HRMS calcd. for $C_{29}H_{25}N_4O_5$ $[M+H]^+$: 509.1819,

found: 509.1822; IR υ_{max}/cm^{-1} (NaCl): 3423 (N-H), 3064, 3030, 2954, 2929 (C-H), 1718 (C=O ester), 1674 (C=O amide), 1582 ($C=C_{arom}$), 1556 ($C=C_{arom}$), 1521 (arom.-NO_2), 1494 ($C=C_{arom}$), 1453 ($C=C_{arom}$), 1434 ($C=C_{arom}$), 1347 ($C-H_{methyl}$), 1307, 1270 (C-O), 1224 (C-O), 1163, 1107, 1008.

(2*S*,4*R*)-4-Hydroxy-*N*-(PhF)proline TAP (54P). In a 100 mL round-bottom flask, a solution of *N*-(PhF)hydroxyproline **104** (2 g, 5.39 mmol, 1 equiv., prepared according to reference[25]) in MeOH (10 mL) was treated with 1 mL of water, titrated with 20% Cs_2CO_3 to pH 7 (about 3 mL), evaporated to dryness, and twice suspended in toluene and evaporated. The residue was ground into a powder by scraping the wall of the flask with a spatula. The round-bottom flask was charged with (4'-(bromomethyl)-[1,1'-biphenyl]-4-yl)triphenylphosphonium perchlorate **103** (TAP-Br, 2.95 g, 4.85 mmol, 0.9 equiv.), DMF (50 mL) and potassium iodide (90 mg, 0.54 mmol, 10 mol%). The flask was purged with argon,[47] and the reaction mixture was heated to 60 °C with an oil bath and agitated with magnetic stirring for 3 h at which point TLC showed no remaining TAP-Br starting material (R_f = 0.64). The volatiles were removed by sweeping air with stirring for 3 h and the residue was dissolved in DCM (50 mL). The solution was washed with aqueous saturated $NaHCO_3$ (2 × 30 mL), water (30 mL), aqueous saturated $LiClO_4$ (2 × 30 mL), and water (2 × 30 mL), dried (Na_2SO_4), evaporated to a residue which was re-dissolved in DCM (10 mL) and precipitated in ice cold Et_2O (50 mL). The white solid was filtered off, washed with ice cold Et_2O (2 × 20 mL) and dried *in vacuo* to give a white powder, which was stored under argon in the refrigerator (3.09 g, 91% recovery). An analytical sample (90 mg) was purified by radial chromatography (gradient: 0 to 5% MeOH in DCM). After evaporation, the residue was re-dissolved in DCM (2 mL) and

precipitated in ice cold Et_2O (10 mL). The white solid was filtered off, washed with ice cold Et_2O (2 × 5 mL), dried *in vacuo* to give **54P** as a white powder (82 mg). R_f = 0.51 (7.5% MeOH in DCM); $[\alpha]^{21}_D$ = –13.5 (*c* = 0.9,); ^{1}H NMR ($CDCl_3$, 400 MHz) δ 1.80 (m, 2H), 1.99 (dt, *J* = 12.5, 5.5 Hz, 1H), 2.92 (dd, *J* = 5.4, 9.7 Hz, 1H), 3.37 (dd, *J* = 4.7, 9.1 Hz, 1H), 3.59 (dd, *J* = 5.4, 9.7 Hz, 1H), 4.55 (dt, *J* = 5.8, 11.6 Hz, 1H), 4.61 (d, *J* = 12.9 Hz, 1H), 4.81 (d, *J* = 12.9 Hz, 1H), 7.12 (td, *J* = 1.1, 7.5 Hz, 1H), 7.22 (m, 4H), 7.29 (m, 2H), 7.32 (dd, *J* = 1.1, 7.5 Hz, 1H), 7.36 (dt, *J* = 7.5, 0.7 Hz, 1H), 7.42 (td, *J* = 1.1, 7.5 Hz, 1H), 7.56 (m, 3H), 7.61-7.75 (m, 12H), 7.75-7.81 (m, 6H), 7.89 (ttd, *J* = 1.2, 2.0, 6.8 Hz, 3H), 7.97 (ddt, *J* = 1.9, 3.2, 8.5 Hz, 2H); ^{13}C NMR (75 MHz, $CDCl_3$): 2 conformers are observed, signals given by the second conformer are signaled with a *, δ 39.9 (s, $1CH_2$), 56.7 (s, $1CH_2$), 59.5 (s, 1CH), 65.5 (s, $1CH_2$), 70.1 (s, 1CH), 76.2 (s, 1C), 115.6 (d, *J* = 91.5 Hz, 1C), 117.7 (d, *J* = 89.5 Hz, 3C), 119.9 (s, 2CH), 120.2 (s, 2CH*), 126.7 (s, 2CH), 127.2 (s, 1CH*), 127.37 (s, 2CH), 127.41 (s, 2CH), 127.67 (s, 2CH*), 127.75 (s, 2CH*), 128.4 (s, 2CH),128.6 (s, 2CH), 128.7 (s, 4CH), 128.8 (s, 2CH*), 129.1 (s, 2CH), 129.3 (s, 2CH*), 130.8 (d, *J* = 12.9 Hz, 6CH), 134.5 (d, *J* = 10.3 Hz, 6CH), 135.1 (d, *J* = 10.7 Hz, 2CH), 135.8 (d, *J* = 3.0 Hz, 3CH), 137.1 (s, 1C), 137.9 (d, *J* = 1.5 Hz, 1C), 140.0 (s, 1C), 141.4 (s, 2C), 142.8 (s, 2C*), 146.1 (s, 2C), 147.5 (s, 2C*), 147.86 (s, 1C), 147.9 (s, 1C*), 175.4 (s, C=O); HRMS calcd. for $C_{55}H_{45}NO_3P$ $[M]^+$: 798.3140, found: 798.3131; IR υ_{max}/cm^{-1} (NaCl): 3494 (N-H), 3072, 3020, 2927 (C-H), 1736 (C=O ester), 1596 ($C=C_{arom}$), 1486 ($C=C_{arom}$), 1439 ($C=C_{arom}$), 1272 (C-O), 1216 (C-O), 1150 (arom.), 1094 (arom.).

4-Benzylamino-1H-pyrrole-2-carboxylate TAP (56P). A stirred solution of oxalyl chloride (0.42 mL, 5.01 mmol, 1.5 equiv.) in DCM (6 mL) at –78°C was treated with dry DMSO (0.47 mL, 6.68 mmol, 2 equiv.) in DCM (6 mL). After stirring for 20 min, a solution of **54P** (3.0 g, 3.34 mmol, 1 equiv.) in DCM (18 mL) was added dropwise to the mixture which was stirred for 4 h at –78°C, treated with DIEA (3.5 mL, 20.04 mmol, 6 equiv.) over 20 min, stirred at –78 °C for 1 h and allowed to warm to room temperature for 1 h. The mixture was treated with KH_2PO_4 1M (60 mL). The layers were separated and the aqueous phase was extracted with DCM (2 × 30 mL). The organic layers were combined, washed with water (90 mL), aqueous saturated $LiClO_4$ (2 × 90 mL) and water (2 × 90 mL), dried (Na_2SO_4) and evaporated to a residue, which was re-dissolved in DCM (10 mL) and precipitated in ice cold Et_2O (50 mL). The white solid was filtered off, washed with ice cold Et_2O (2 × 20 mL), dried *in vacuo* to give **55P** as a white powder (2.81 g, 94% recovery). Ketone **55P** was directly used in the next step. A stirred solution of **55P** (2.81 g, 3.53 mmol, 1 equiv.) in dry MeCN (80 mL) was degassed by three freeze-thaw cycles. The mixture was treated with $MgSO_4$ (dried overnight prior use, 3 g) swept argon, and treated with benzylamine (1.5 mL, 14.12 mmol, 4 equiv.) and *p*-TsOH (95 mg, 0.35 mmol, 10 mol%) and degassed with bubbling of argon for 30 min. The reaction mixture was warmed to 50 °C, stirred overnight at this temperature and evaporated to a residue, which was partitioned between DCM (60 mL) and water (60 mL). The layers were separated. The aqueous layer was extracted with DCM (2 × 30 mL). The organic layers were combined, washed with aqueous saturated $NaHCO_3$ (2 × 60 mL), water (90 mL), aqueous saturated $LiClO_4$ (2 × 90 mL), and water (2 × 90 mL), dried (Na_2SO_4) and evaporated to a residue, which was re-dissolved in DCM (10 mL)

and precipitated in ice cold Et_2O (50 mL). The white solid was filtered off, washed with ice cold Et_2O (2 × 20 mL), dried *in vacuo* to a white powder and stored under argon in the refrigerator (3.20 g, 122% recovery). An analytical sample (100 mg) was purified by radial preparative chromatography (gradient: 0 to 5% MeOH in DCM). After evaporation of the collected fractions, the residue was re-dissolved in DCM (2 mL) and precipitated in ice cold Et_2O (10 mL). The white solid was filtered off, washed with ice cold Et_2O (2 × 5 mL), and dried *in vacuo* to give **56P** as a white powder (74 mg). R_f: 0.46 (7.5% MeOH in DCM); ^{1}H NMR ($CDCl_3$, 400 MHz) δ 4.14 (s, 2H), 5.27 (s, 2H), 6.45 (t, *J* = 1.9 Hz, 1H), 6.51 (t, *J* = 1.9 Hz, 1H), 7.23 (t, *J* = 7.0 Hz, 1H), 7.29-7.37 (m, 4H), 7.50 (d, *J* = 8.2 Hz, 2H), 7.60-7.72 (m, 10H), 7.77 (td, *J* = 3.6, 7.8 Hz, 6H), 7.88 (dt, *J* = 1.9, 7.8 Hz, 3H), 7.93(dd, *J* = 3.1, 8.4 Hz, 2H); ^{13}C NMR (75 MHz, $CDCl_3$): δ 52.3 (s, 1CH_2), 65.9 (s, 1CH_2), 105.4 (s, 1C), 110.0 (s, 1C), 116.4 (d, *J* = 91.6 Hz, 1C), 118.4 (d, *J* = 88.9 Hz, 1C), 121.0 (s, 1C), 127.9 (s, 1C), 128.49 (s, 2CH), 128.51 (s, 2CH), 129.3 (s, 2CH), 129.6 (s, 2CH), 129.9 (d, *J* = 13.3 Hz, 2CH), 131.6 (d, *J* = 12.8 Hz, 6CH), 135.2 (d, *J* = 12.8 Hz, 6CH), 135.2 (d, *J* = 10.7 Hz, 2CH), 136.6 (d, *J* = 2.9 Hz, 3CH), 137.9 (s, 1C), 138.4 (s, 1C), 138.7 (d, *J* = 1.5 Hz, 1C),140.6 (s, 1C), 148.6 (d, *J* = 3.1 Hz, 1C), 161.4 (C=O); HRMS calcd. for $C_{43}H_{36}N_2O_2P$ $[M]^+$: 643.2517, found: 643.2509; IR υ_{max}/cm^{-1} (NaCl): 3447 (N-H), 3065, 3021, 2925, 2855 (C-H), 1698 (C=O ester), 1596 (C=C_{arom}), 1483 (C=C_{arom}), 1439 (C-P), 1393 (C-N), 1094 (arom.), 998 (C-P).

(*S*)-Methyl 1,3-dibenzyl-5-(4-nitrophenyl)-2-oxo-1,2,3,6-tetrahydropyrrolo[3,2-*e*][1,4]diazepine-7-carboxylate from TAP support (2). A solution of *N*-(Fmoc)-Phe (4.9 g, 12.52 mmol, 3 equiv.) and bis(trichloromethyl)carbonate (BTC, 1.1 g, 4.18 mmol,

1 equiv.) in a 1.7:1 DCM/THF (72 mL) at 0 °C was treated slowly with 2,4,6-collidine (4.7 mL, 35.51 mmol, 8.5 equiv.) yielding a white suspension. After 1-3 min, a solution of aminopyrrole **56P** in DCM (45 mL) was added to the mixture containing the freshly formed acid chloride. The reaction mixture was stirred for 15 h under argon atmosphere and treated with 1N HCl (100 mL). The organic layer was separated and washed with saturated aqueous $NaHCO_3$ (2 × 90 mL), water (90 mL), aqueous saturated $LiClO_4$ (2 × 90 mL), and water (2 × 90 mL), dried (Na_2SO_4), and evaporated to a residue, which was re-dissolved in DCM (10 mL) and precipitated in ice cold Et_2O (50 mL). The white solid was filtered off, washed with ice cold Et_2O (2 × 10 mL), dried *in vacuo* to give **57P** as a beige powder which was stored under argon in the refrigerator [3.7 g, 87% recovery, R_f: 0.45 (5% MeOH in DCM), HRMS: calcd. for $C_{67}H_{55}N_3O_5P$ $[M]^+$: 1012.3874, found: 1012.3894]. Acylaminopyrrole **57P** (0.7 g, 0.63 mmol, 1 equiv.) was dissolved in DCM (5 mL), treated with piperidine (5 mL), stirred for 10 min and added dropwise to a stirring mixture of Et_2O and hexane 1/1 (100 mL). The precipitate was collected by filtration and washed with ice cold Et_2O (2 × 10 mL) and dried *in vacuo*. The beige solid **105P** (499 mg, 89% recovery) was dissolved in dichloroethane (20 mL), transferred to a 20 mL Biotage microwave vessel and treated with trifluoroacetic acid (0.2 mL) and 4-nitrobenzaldehyde (1.2 g, 6.29 mmol, 10 equiv.), sealed and heated at 70 °C under microwave for 3 h. The vessel was cooled to room temperature and treated with aqueous saturated $NaHCO_3$ (20 mL). The phases were separated and the aqueous layer was extracted with DCM (3 × 10 mL). The combined organic layers were washed with aqueous saturated $LiClO_4$ (2 × 50 mL), ans water (50 mL), dried (Na_2SO_4), and evaporated to a residue, which was re-dissolved in DCM (10 mL) and precipitated in ice

cold Et_2O (50 mL). The white solid was filtered off, washed with ice cold Et_2O (2 × 10 mL), dried *in vacuo* to give **124** as a yellow powder [0.41 g, 64% recovery, R_f: 0.43 (5% MeOH in DCM), HRMS: calcd. for $C_{59}H_{48}N_4O_5P$ $[M]^+$: 923.3357, found: 923.3374]. Pyrrolodiazepinone **124** was dissolved in a 0.44 M MeONa solution in THF/MeOH (9:1, 25 mL) at room temperature under argon and the solution was stirred for 1 h, then quenched with saturated aqueous NH_4Cl (50 mL). The aqueous phase was extracted with EtOAc (2 × 50 mL) and the combined organic layers were washed with brine (50 mL), dried (Na_2SO_4) and evaporated a residue which was performed by flash chromatography on a silica gel column (15 to 20% gradient of EtOAc in hexanes) to yield (*S*)-methyl 1,3-dibenzyl-5-(4-nitrophenyl)-2-oxo-1,2,3,6-tetrahydropyrrolo[3,2-*e*][1,4]diazepine-7-carboxylate **2** as a yellow oil (13 mg, 39% yield, 17% overall yield). All the characterization was identical to compound **2** obtained from Merrifield resin.

ACKNOWLEDGMENT

The authors acknowledge financial support from the Natural Sciences and Engineering Research Council of Canada (NSERC), Université de Montréal, Canadian Institutes of Health Research, CIHR-Team in GPCR allosteric regulation (CTiGAR), The Fonds Québécois de la Recherche sur la Nature et les Technologies (FQRNT), The Ministère du Développement Économique, de l'Innovation et de l'Exportation du Québec, and equipment made possible from the Canadian Foundation for Innovation. We thank Marie-Noelle Roy of Soluphase Inc. (Montreal, Canada) for fruitful discussions. We are grateful to Marie- Christine Tang and Karine Venne from the University of Montreal Mass spectrometry facility for MS analyses, and to Cédric Malveau from the University of Montreal High Field NMR Regional Laboratory for 500 MHz NMR analyses.

Supporting Information Available. ^{1}H and ^{13}C NMR spectra of isolated compounds (**58**, **2**, **54P** and **56P**), RP-HPLC-MS traces for aminoacylation and Pictet-Spengler cyclization compounds prepared on Wang Resin.

Reference

(1) (a) Costantino, L.; Barlocco, D. *Curr. Med. Chem.* **2006**, 13, 65 –85. (b) Evans, B. E.; Rittle, K. E.; Bock, M. G.; DiPardo, R. M.; Freidinger, R. M.; Whitter, W. L.; Lundell, G. F.; Veber, D. F.; Anderson, P. S. *J. Med. Chem.* **1988**, 31, 2235–2246. (c) Horton, D. A.; Bourne, G. T.; Smythe, M. L. *Chem. Rev.* **2003**, 103, 893–930. (d) Patchett, A. A.; Nargund, R. P. *Annual Reports in Medicinal Chemistry*; Academic Press: New York, 2000; Vol. 35, pp 289298.

(2) (a) Im, I.; Webb, T. R.; Gong, Y.-D.; Kim, J. -I.; Kim, Y.-C. *J. Comb. Chem*.**2004**, 6, 207–213. (b) Iden, H. S.; Lubell, W. D. *Org. Lett*. **2006**, 8, 3425–3428. (c) Keenan, R. M.; Callahan, J. F.; Samanen, J. M.; Bondinell, W. E.; Calvo, R. R.; Chen, L. C.; DeBrosse, C.; Eggleston, D. S.; Haltiwanger, R. C.; Hwang, S. M.; Jakas, D. R.; Ku, T. W.; Miller, W. H.; Newlander, K. A.; Nichols, A.; Parker, M. F.; Southhall, L. S.; Uzinskas, I.; Vasko-Moser, J. A.; Venslavsky, J. W.; Wong, A. S.; Huffman, W. F. *J. Med. Chem*. **1999**, 42, 545–559. (d) Ku, T. W.; Ali, F. E.; Barton, L.S.;Bean, J. W.;Bondinell,W. E.; Burgess, J. L.; Callahan, J. F.; Calvo, R. R.; Chen, L. *J. Am. Chem. Soc.* **1993**, 115, 8861–8862.

(3) (a) Childress, S.; Gluckman, M. J. *Pharm.Sci*. **1964**, 53, 577–590. (b) Hamor, T. A.; Martin, I. L. *In Progress in Medicinal Chemistry*; Ellis, G. P., West, G. B., Eds.;Elsevier:NewYork, **1983**; Vol. 20, pp 157–223. (c) Spencer, J.; Rathnam, R. P.; Chowdhry, B. Z. *Fut. Med. Chem*. **2010**, 2, 1441–1449. (d) Sternbach, L. H. *Angew. Chem., Int. Ed*. **1971**, 10, 34 –43. (e) Sternbach, L. H. *J. Med. Chem*. **1979**, 22, 1–7.

(4) (a) McDonald, I. M.; Black, J. W.; Buck, I. M.; Dunstone, D. J.; Griffin, E. P.; Harper, E. A.; Hull,R. A. D.; Kalindjian, S. B.; Lilley, E. J.; Linney, I. D.; Pether, M. J.; Roberts, S. P.; Shaxted, M. E.; Spencer, J.; Steel, K. I. M.; Sykes, D. A.; Walker, M. K.; Watt, G. F.; Wright, L.; Wright, P. T.; Xun, W. *J. Med. Chem.* **2007**, 50, 3101–3112. (b) Bock, M. G.; Dipardo, R. M.; Evans, B. E.; Rittle, K. E.; Whitter, W. L.; Veber, D. F.; Anderson, P.S.; Freidinger, R.M. *J. Med. Chem*. **1989**, 32, 13–16. (c) Armour, D. R.; Aston, N. M.; Morriss, K. M. L.; Congreve, M. S.; Hawcock, A. B.; Marquess, D.; Mordaunt, J. E.; Richards, S. A.; Ward, P. *Bioorg. Med. Chem. Lett*. **1997**, 7, 2037–2042. (d) Bolli, M. H.; Marfurt, J.; Grisostomi, C.; Boss, C.; Binkert, C.; Hess, P.; Treiber, A.; Thorin, E.; Morrison, K.; Buchmann, S.; Bur, D.; Ramuz, H.; Clozel, M.; Fischli, W.; Weller, T. *J. Med. Chem.* **2004**, 47, 2776–2795. (e) Burgey, C.S.; Stump, C. A.; Nguyen, D. N.; Deng, J. Z.; Quigley, A. G.; Norton, B. R.; Bell, I.M.; Mosser, S.D.; Salvatore, C.A.; Rutledge, R.Z.; Kane, S.A.; Koblan, K.S.; Vacca, J.P.; Graham, S.L.; Williams,

T.M. *Bioorg. Med. Chem. Lett*. **2006**, 16, 5052–5056. (f) Wood, M. R.; Kim, J. J.; Han, W.; Dorsey, B. D.; Homnick, C. F.; DiPardo, R. M.; Kuduk, S. D.; MacNeil, T.; Murphy, K. L.; Lis, E. V.; Ransom, R. W.; Stump, G. L.; Lynch, J. J.; O'Malley, S. S.; Miller, P.J.; Chen, T. -B.; Harrell, C. M.; Chang, R. S. L.; Sandhu, P.; Ellis, J. D.; Bondiskey, P. J.; Pettibone, D. J.; Freidinger, R. M.; Bock, M. G. *J. Med. Chem.* **2003**, 46, 1803–1806. (g) Wyatt, P. G.; Allen, M. J.; Chilcott, J.; Hickin, G.; Miller, N. D.; Woollard, P.M. *Bioorg. Med. Chem. Lett*. **2001**, 11, 1301–1305.

(5) (a) Churcher, I.; Williams, S.; Kerrad, S.; Harrison, T.; Castro, J. L.; Shearman, M.S.; Lewis, H.D.; Clarke, E.E.; Wrigley, J.D.J.; Beher, D.; Tang, Y. S.; Liu, W. *J. Med. Chem.* **2003**, 46, 2275–2278. (b) Ettari, R.; Micale, N.; Schirmeister, T.; Gelhaus, C.; Leippe, M.; Nizi, E.; Di Francesco, M. E.; Grasso, S.; Zappala, M. *J. Med. Chem*. **2009**, 52, 2157–2160. (c) Guandalini, L.; Cellai, C.; Laurenzana, A.; Scapecchi, S.; Paoletti, F.; Romanelli, M. N. *Bioorg. Med. Chem. Lett*. **2008**, 18, 5071–5074. (d) Merluzzi, V.; Hargrave, K.; Labadia, M.; Grozinger, K.; Skoog, M.; Wu, J.; Shih, C.; Eckner, K.; Hattox, S.; Adams, J.; *Science* **1990**, 250, 1411–1413. (e) Micale, N.; Kozikowski, A. P.; Ettari, R.; Grasso, S.; Zappalà, M.; Jeong, J.-J.; Kumar, A.; Hanspal, M.; Chishti, A. H. *J. Med. Chem*. **2006**, 49, 3064–3067. (f) Proudfoot, J. R. Bioorg. *Med. Chem. Lett*. **1995**, 5, 163–166. (g) Ramdas, L.; Bunnin, B. A.; Plunkett, M. J.; Sun, G.; Ellman, J.; Gallick, G.; Budde, R. J. A. *Arch. Biochem. Biophys*. **1999**, 368, 394–400.

(6) (a) Micale, N.; Vairagoundar, R.; Yakovlev, A. G.; Kozikowski, A. P. *J.Med.Chem.* **2004**, 47, 6455–6458. (b) Stevens, S. Y.; Bunin, B. A.; Plunkett, M. J.; Swanson, P. C.; Ellman, J. A.; Glick, G. D. *J. Am. Chem. Soc.* **1996**, 118, 10650–10651.

(7) (a) Berry, J. M.; Howard, P. W.; Thurston, D. E. *Tetrahedron Lett.* **2000**, 41, 6171–6174. (b) Thurston, D. E. In Molecular Aspects of Anticancer Drug-DNA Interactions; Neidle, S., Waring, M., Eds.; MacMillan: London, UK, **1993**; Vol. 1, pp 5488.

(8) Bolos, J.; Perez, A.; Gubert, S.; Anglada, L.; Sacristan, A.; Ortiz, J. A. *J. Org. Chem.* **1992**, 57, 3535–3539.

(9) De Lucca, G. V.; Otto, M. J. *Bioorg. Med. Chem. Lett*. **1992**, 2, 1639–1644.

(10) Doods, H.; Eberlein, W.; Engel, W.; Entzeroth, M.; Mihm, G.; Rudolf, K.; Ziegler, H. Condensed diazepinones, process for their preparation and compositions containing them for the treatment of the central nervous system and to enhance cerebral perfusion. EP0508370 (A1), **1992**.

(11) (a) Mariani, L.; Tarzia, G. 1,7-Dihydropyrrolo[3,4-e][1,4]diazepin-2(3H)-one derivatives, and their use as anticonvulsant and antianxiety agents. EP0102602 (A1), **1984**. (b) Mariani, L.; Tarzia, G. 3,7Dihydropyrrolo[3,4-e][1,4]diazepin-2(1H)-one derivatives. EP0066762 (A2), **1982**.

(12) Ilyn, A. P.; Trifilenkov, A. S.; Kuzovkova, J. A.; Kutepov, S. A.; Nikitin, A. V.; Ivachtchenko, A. V. *J. Org. Chem*. **2005**, 70, 1478–1481.

(13) Correa, A.; Herrero, M. T.; Tellitu, I.; Dominguez, E.; Moreno, I.; SanMartin, R. *Tetrahedron* **2003**, 59, 7103–7110.

(14) Shafiee, A.; Shekarchi, M. *J. Heterocycl. Chem.* **2002**, 39, 213–216.
(15) Deaudelin, P.; Lubell, W. D. *Org. Lett*. **2008**, 10, 2841–2844.
(16) Blanco, M. J.; Sardina, F.J. *J. Org. Chem.* **1996**, 61, 4748–4755.
(17) Marcotte, F.-A.; Lubell, W. D. *Org. Lett.* **2002**, 4, 2601–2603.
(18) (a) Amodeo, P.; Naider, F.; Picone, D.; Tancredi, T.; Temussi, P. A. *J. Pept. Sci.* **1998**, 4, 253–265. (b) Schwyzer, R.; Moutevelis-Minakakis, P.; Kimura, S.; Gremlich, H. U. *J. Pept. Sci*. **1997**, 3, 65 –81. (c) Zhan, L. X.; Chen, J. Z. Y.; Liu, W. K. *Biophys. J.* **2006**, 91, 2399–2404.
(19) (a) Bleich, H. E.; Galardy, R. E.; Printz, M.P. *J. Am. Chem. Soc.* **1973**, 95, 2041–2042. (b) Rosenstrom, U.; Skold, C.; Plouffe, B.; Beaudry, H.; Lindeberg, G.; Botros, M.; Nyberg, F.; Wolf, G.; Karlen, A.; Gallo-Payet, N.; Hallberg, A. *J. Med. Chem.* **2005**, 48, 4009–4024.
(20) (a) Cann, J. R.; London, R. E.; Stewart, J. M.; Matwiyoff, N. A. *Int. J. Pept. Protein Res.* **1979**, 14, 388–392. (b) Sato, M.; Lee, J. Y. H.; Nakanishi, H.; Johnson, M. E.; Chrusciel, R. A.; Kahn, M. *Biochem. Biophys. Res. Commun.* **1992**, 187, 999–1006.
(21) Hedenstrom, M.; Yuan, Z. Q.; Brickmann, K.; Carlsson, J.; Ekholm, K.; Johansson, B.; Kreutz, E.; Nilsson, A.; Sethson, I.; Kihlberg, J. *J. Med. Chem*. **2002**, 45, 2501–2511.
(22) Levian-Teitelbaum, D.; Kolodny, N.; Chorev, M.; Selinger, Z.; Gilon, C. *Biopolymers* **1989**, 28, 51 –64.
(23) Wynants, C.; Sugg, E.; Hruby, V. J.; Van Binst, G. *Int. J. Pept. Protein Res*. **1987**, 30, 541–547.
(24) Yuan, Z.Q.; Blomberg, D.; Sethson, I.; Brickmann, K.; Ekholm, K.; Johansson, B.; Nilsson, A.; Kihlberg, J. *J. Med. Chem.* **2002**, 45, 2512–2519.
(25) Brouillette,Y.; Rombouts, F. J. R.; Lubell, W. D. *J.Comb.Chem*. **2006**, 8, 117–126.
(26) Stazi, F.; Marcoux, D.; Poupon, J. C.; Latassa, D.; Charette, A. B. *Angew. Chem., Int. Ed.* **2007,** 46, 5011–5014.
(27) (a) Ginisty, M.; Roy, M. N.; Charette, A. B. *J.Org.Chem*. **2008**, 73, 2542–2547. (b) Poupon, J. C.; Boezio, A. A.; Charette, A. B. *Angew. Chem., Int. Ed*. **2006**, 45, 1415–1420. (c) Roy, M. N.; Poupon, J. C.; Charette, A. B. *J. Org. Chem*. **2009**, 74, 8510–8515.
(28) (a) Fridkin, G.; Lubell, W.D. *J. Comb. Chem*. **2005**, 7, 977–986. (b) Rombouts, F. J. R.; Fridkin, G.; Lubell, W. D. *J. Comb. Chem*. **2005**, 7, 589–598.
(29) Zoller, T.; Ducep, J. B.; Hibert, M. *Tetrahedron Lett*. **2000**, 41, 9985–9988.
(30) Sharma, S.; Pasha, S. *Bioorg. Med. Chem. Lett.* **1997**, 7, 2077–2080.
(31) Gisin, B. *Helv. Chim. Acta* **1973**, 56, 1476–1482.
(32) http://www.harrisonresearch.com/chromatotron/, (accessed Nov 2010).
(33) Tanaka, Y.; Hidaka, K.; Hasui, T.; Suginome, M. *Eur. J. Org. Chem*. **2009**, 1148–1151.
(34) Srinivasan, N.; Ganesan, A. *Chem. Commun*. **2003**, 916–917.
(35) Chen, J.; Chen, X.; Bois-Choussy, M. L.; Zhu, J. *J. Am. Chem. Soc.* **2005**, 128, 87 –89.

(36) Prajapati, D.; Gohain, M. *Synth. Commun*. **2008**, 38, 4426–4433.
(37) Bonnet, D.; Ganesan, A. *J. Comb. Chem*. **2002**, 4, 546–548.
(38) (a) Maryanoff, B. E.; Zhang, H.-C.; Cohen, J. H.; Turchi, I. J.; Maryanoff, C. A. *Chem. Rev*. **2004**, 104, 1431–1628. (b) Le Quement, S. T.; Petersen, R.; Meldal, M.; Nielsen, T. E. *Biopolymers* **2010**, 94, 242–256.
(39) Diness, F.; Beyer, J.; Meldal, M. *Chem. —Eur. J*. **2006**, 12, 8056–8066.
(40) Li, X. F.; Zhang, L. S.; Zhang, W.; Hall, S. E.; Tam, J. P. *Org. Lett.* **2000**, 2, 3075–3078.
(41) Still, W. C.; Kahn, M.; Mitra, A. *J. Org. Chem*. **1978**, 43, 2923– 2925.
(42) (a) Kluczyk, A.; Rudowska, M.; Stefanowicz, P.; Szewczuk, Z. *J. Pept. Sci*. **2010**, 16, 31–39. (b) Stadler, A.; Kappe, C. O. *Eur. J. Org. Chem*. **2001**, 919–925.
(43) Terrett, N. K.; Gardner, M.; Gordon, D. W.; Kobylecki, R. J.; Steele, J. *Tetrahedron* **1995**, 51, 8135–8173.
(44) (a) Wiejak, S.; Masiukiewicz, E.; Rzeszotarska, B. *Chem. Pharm. Bull.* **2001**, 49, 1189–1191. (b) Jamieson, A. G.; Boutard, N.; Beauregard, K.; Bodas, M. S.; Ong, H.; Quiniou, C.; Chemtob, S.; Lubell, W D. *J. Am. Chem. Soc*. **2009**, 131, 7917–7927.
(45) Armarego, W.; Chai, C. Purification of laboratory chemicals; Butterworth-Heinemann: Oxford, **2003**; p 219.
(46) Le Sann, C.; Abell, A. D. *Aust. J. Chem*. **2004**, 57, 355–358.
(47) Kaiser, E.; Colescott, R. L.; Bossinger, C. D.; Cook, P. I. *Anal. Biochem.* **1970**, 34, 595–598.
(48) Preparation of 0.44 M MeONa solution in THF/MeOH (9:1): a 100 mL stock solution was prepared by diluting 10 mL of a 25 wt % MeONa solution in MeOH in 90 mL of dryTHF.The solution was kept in a tightly sealed dry glass bottle under argon and was stable for several weeks. The solution was used with a dry syringe under a flow of argon.
(49) Contrary to MacroKans, MiniKans are small enough to be introduced in to a 20 mL Biotage microwave reactor. Resin is kept in the Kans to avoid grinding by the stir bar.

Annexe 2 : Partie expérimetale de la synthèse des pyrrolo[3,2-*e*][1,4]diazepin-2-ones sur résine de Wang

Experimental section

Unless otherwise specified, reagents and starting materials were obtained from Aldrich® (Saint-Louis, Missouri) and used as received. Wang resin SS (75-100 mesh, 1.2 mmol/g) was purchased from Advanced Chemtech™ (Louisville, Kentucky). Wang bromide resin was prepared from Wang resin according to reference 1.[258] IRORI MacroKans™ and MiniKans™ were from Nexus Biosystems, Inc. (Poway, California). SynPhase™ spindles and cogs (Mimotopes Pty Ltd, Clayton, Victoria, Australia) were used to identify resins in Kans by color-coding. (2*S*,4*R*)-4-Hydroxy-*N*-1-(PhF)proline was prepared from (2*S*,4*R*)-4-hydroxy-*N*-1-(PhF)proline methyl ester according to reference.[124, 259] Protected amino acids [Fmoc-Leu and Fmoc-Orn] were purchased from GL Biochem Ltd. (Shanghai, China). Anhydrous THF, MeCN, DCM, MeOH and DMF were obtained from a Seca Solvent Filtration System (GlassContour™ Laguna Beach, CA); DMSO was dried over activated 4 Å molecular sieves 24 h prior to use and stored in a tightly sealed bottle under an argon atmosphere.[260] Reactions requiring anhydrous conditions were performed under an atmosphere of dry argon; glassware was flame dried immediately prior to use and allowed to cool under argon atmosphere. Syringes and needles were dried in an oven at 100 °C overnight and were allowed to cool down in desiccators prior to use. Liquid reagents, solutions and solvents were added *via* syringe through rubber septa. The removal of solvents *in vacuo* was achieved using both a Büchi™ rotary evaporator (bath temperatures up to 40 °C) at a pressure of either 15 mm

Hg (water aspirator) and a high vacuum line (0.1 mm Hg, oil pump) at room temperature. Flash column chromatography[261] was performed using SiliaFlash®F60 silica (Silicycle, Quebec City). Glass backed plates pre-coated with silica gel (SiliaPlate TLC Extra Hard Layer 60 Angstrom F-254, Silicycle, Quebec City) were used for thin layer chromatography (TLC) and were visualized by UV fluorescence or staining with a ninhydrin or a phosphomolybdic acid solution in EtOH prior to heating. ^{1}H NMR and ^{13}C NMR spectra were recorded on Bruker spectrometers (AV400 and AV700). Chemical shift values were presented in ppm relative to residual methanol (δ_H 3.31 and δ_C 49.0) or DMSO (δ_H 2.50 & δ_C 39.52) as standards. Coupling constant *J* values are given in Hz, with splitting described as s (singlet), d (doublet), t (triplet), q (quartet) and m (multiplet). When possible, ^{1}H NMR and ^{13}C NMR signals were assigned using COSY, NOESY, HMQC, HSQC, and DEPT experiments. Infrared spectra were recorded on a Perkin-Elmer Spectrum One spectrometer. Mass spectral data and high-resolution mass spectrometry (HRMS, electrospray ionization) were obtained by the Université de Montréal Mass Spectrometry Facility. Optical rotations were determined in solution by irradiating with the sodium D line (λ= 589 nm) using a Perkin Elmer 341 polarimeter. Specific rotation, $[\alpha]_D$ values are given in units 10^{-1}•deg•cm^2•g^{-1}. Melting points were determined on a Gallenkamp digital melting point apparatus and are uncorrected. Microwave assisted reactions were preformed in a Biotage Initiator microwave apparatus (Biotage AB, Uppsala, Sweden) in glass Biotage reaction vessels containing a magnetic stirrer bar and sealed with a septum cap. Analytical RP-HPLC analyses were performed on a Gemini™ C18 column (Phenomenex® Inc., Torrance, California) (150 mm x 4.6 mm, 5 μm, column A) with a flow rate of 0.5 mL/min or on a Sunfire™ C18 column

(Waters, Milford, Massachusetts) (50 mm × 2.1 mm, 3.5 μm, column B) with a flow rate of 0.4 mL/min using a linear gradient of methanol containing 0.1% formic acid (FA) in water (0.1% FA) or acetonitrile (0.1% FA) in water (0.1% FA). Retention times (R*t*) from analytical RP-HPLC were reported in minutes. Purification as indicated was made on a Gemini™ C18 column (Phenomenex® Inc., Torrance, California) (250 mm × 21.20 mm, 5 μm, column C) using a linear gradient of MeOH (0.1% FA) in water (0.1% FA) or MeCN (0.1% FA) in water (0.1% FA), with a flow rate of 10.5 mL/min. Transfected CHO cells expressing the human urotensin II receptor (CHO-UT) were a generous gift from Drs H. Vaudry and C. Dubessy (Rouen, France). Radioactivity was counted on a 1470 Automatic Gamma Counter, Perkin Elmer (Massachusetts, USA).

General procedures.

Resin swelling in IRORI Kans

Under argon sweeping, resins in Kans and a stirring bar were placed in a flame-dried round-bottom flask, which was exposed to three cycles of vacuum (20 mm Hg) followed by argon, prior to addition of the specified amount of the appropriate dry solvent. The flask was swept with argon and sealed using a rubber septum and the resin was allowed to swell for 30 minutes under inert atmosphere.

Resin washing in IRORI Kans

The Kans were placed together in a Schott Duran glass bottle equipped with a stirring bar, and treated with solvent. The bottle was sealed with a screw cap and shaken by hand for 10 seconds. The Kans were next magnetically stirred for 5 min. The solvent was decanted through a perforated screw cap, then the bottle was shaken vigorously by hand, head down, for 10 seconds. This operation was repeated for as many times and solvents

as specified. At the end of the process, residual solvent in Kans was removed by centrifugation, or by subjecting the head of each Kan to vacuum for 1 min using a water aspirator.

(2*S*)-4-Oxo-*N*-(PhF)proline Wang Resin (74)

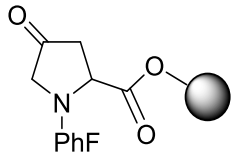

74

(2*S*,4*R*)-4-Hydroxy-*N*-1-(PhF)proline **74** was prepared as previously described[119, 124] and converted to its cesium salt (2.1 g, 5.6 mmol, 2.5 equiv) as described in reference [123] for attachment onto Wang Bromide resin[124, 258] (2.5 g, 0.9 mmol/g, 2.25 mmol) swollen in 100 mL of dry DMF in the presence of 2,3,11,12-dibenzo-1,4,7,10,13,16-hexaoxacyclooctadeca-2,11-diene (1.4 g, 3.90 mmol, 1.75 equiv) in a 500 mL Morton flask. The reaction mixture was heated to 70°C and agitated gently with a mechanical stirrer for 108 h. The beige brown resin was filtered, washed and dried under vacuum, before storage usually under argon in the refrigerator. Anchoring efficiency was evaluated by measuring a resin mass increase of 0.90 g which corresponded to a loading in (2*S*,4*R*)-4-hydroxy-*N*-1-(PhF)proline of 0.97 mmol/g (90 % conversion): IR (KBr, cm^{-1}): 3459 (OH) and 1723 (C═O) and the disappearance of a band at 594 cm^{-1}. From (2*S*,4*R*)-4-hydroxy-*N*-1-(PhF)proline Wang resin, (2*S*)-4-oxo-*N*-(PhF)proline Wang Resin **74** was prepared as described in reference [123]. To a flame-dried 100 mL round-bottom flask, under argon atmosphere, a solution of DMSO (5.6 mL, 79.2 mmol, 24 equiv) in DCM (30 mL) at −78°C was treated drop-wise with oxalyl chloride (3.4 mL,

39.6 mmol, 12 equiv). The mixture was stirred for 30 min, transferred by cannula into a 250 mL Morton flask containing (2*S*,4*R*)-4-hydroxy-*N*-(PhF)proline Wang resin (3.4 g, 0.97 mmol/g, 3.30 mmol), prepared as described in the reference [123], swollen in dry DCM (90 mL) at −78°C, and agitated gently with mechanical stirring for 4 h at −78°C. The mixture was treated drop-wise with DIEA (20.7 mL, 119 mmol, 36 equiv) over 1 h at −78°C, after which time the resin appeared brown. The cooling bath was removed and the resin suspension was allowed to warm to room temperature over 1 h. Resin 5 was filtered using a 60 mL filtration tube with a polyethylene frit, and washed with 30 mL volumes of DCM (×2), MeOH (×2), DCM (×2), MeOH (×2), DCM (×2) and Et_2O (×2). The reaction was repeated a second time to ensure complete alcohol oxidation. The resin **74** was usually stored under argon in the refrigerator; IR (KBr, cm^{-1}): 1700 and 1733 cm^{-1} (C═O) and disappearance of the OH band at 3459 cm^{-1}.

4-((4-Hydroxyphenethyl)amino)-1H-pyrrole-2-carboxylate Wang Resin (75)

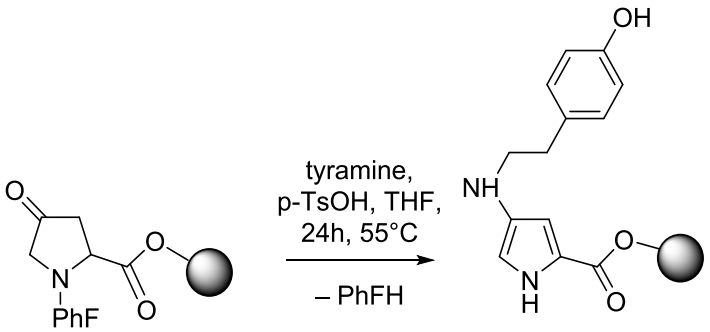

74 **75**

4-((4-Hydroxyphenethyl)amino)-1H-pyrrole-2-carboxylate Wang resin **75** was synthesized following the previously reported procedure for the synthesis of 4-aminopyrrole resins.[123] In a flame-dried 100 mL 3-neck flask possessing two IRORI MacroKans containing (2*S*)-4-oxo-*N*-(PhF)proline Wang resin **74** (0.3 g per Kan, 0.97

mmol/g, 0.58 mmol) suspended in 50 mL of THF, argon was bubbled for 30 min. The mixture was treated with tyramine (2 g, 14.6 mmol, 25 equiv), degassed by bubbling of argon for 30 min, treated with *p*-TsOH (550 mg, 0.29 mmol, 0.5 equiv) and degassed by bubbling of argon for 30 min. Under an argon atmosphere, the degassed mixture was heated to 55°C using an oil bath and stirred for 24 h. The tyramine was only partially soluble in THF at the start of the reaction and dissolved as the reaction proceeded, during which time, the resin changed color from brown to dark green. The yellow-green resin was indicative of methyl 4-((4-hydroxyphenethyl)amino)-1H-pyrrole-2-carboxylate protected again by PhF group. The IRORI MacroKans were transferred to 20 mL plastic filtration tubes, washed with 10 mL volumes of THF (×3), DCM (×3), MeOH (×3), H_2O, DCM (×2), MeOH (×2), H_2O (×2), MeOH (×3), and DCM (×3). The filtrate and washings were recovered, combined and evaporated to a residue, which was partitioned between H_2O (15 mL) and EtOAc (15 mL). Insoluble excess tyramine was removed by filtration. The organic phase was dried with sodium sulphate and evaporated to a residue, which was purified by column chromatography (2% Et_2O/hexanes). Evaporation of the collected fractions gave PhFH (0.129 g, 0.5 mmol, mp 146°C, lit.[124] mp 148°C) corresponding to a loading of 0.89 mmol/g (81 % conversion).

Methyl 4-(N-(4-hydroxyphenethyl)acetamido)-1*H*-pyrrole-2-carboxylate (81)

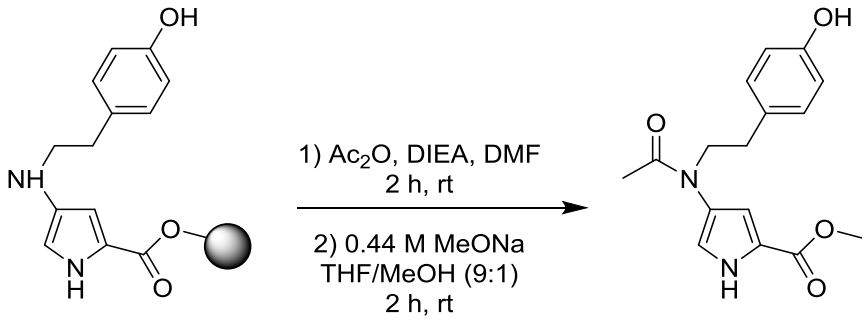

75 **81**

4-((4-hydroxyphenethyl)amino)-1H-pyrrole-2-carboxylate Wang resin (**75**, 15 mg, 0.89 mmol/g, 0.013 mmol) was removed from an IRORI MacroKan, placed into a 3 mL plastic filtration tube equipped with polyethylene frit and stopcock, treated with Ac_2O (30 µL, 0.312 mmol, 20 equiv) and DIEA (70 µL, 0.39 mmol, 25 equiv) in DMF (1.5 mL), shaken for 2 h at room temperature, filtered, washed sequentially with agitation for 1 min and filtered from DMF (3 × 1 mL), MeOH (3 × 1 mL), and DCM (3 × 1 mL). Cleavage of acetamide **81** was performed in the plastic filtration tube using a 0.44 M NaOMe solution in THF/MeOH (9:1, 1 mL) for 2 h at room temperature. The resin was filtered and washed with EtOAc (×3). The filtrate and washings were partitioned between EtOAc and saturated aqueous NH_4Cl solution. The organic layer was filtered through a Pasteur pipette containing a 5 mm layer of Na_2SO_4 and evaporated to dryness. The residue was analyzed by RP-HPLC-MS (column A, 50-90% MeOH over 10 min followed by 90% MeOH over 10 min, λ = 214 nm), which showed acetamide **81** (93% purity, Rt: 8.6; $[MH]^+$: 303.1) contaminated with 3% of (2*S*,4*R*)-4-hydroxy-*N*-1-(PhF)proline (Rt: 14.3; $[MH]^+$: 386.2). Conversion to ((4-hydroxyphenethyl)acetamido)-

1H-pyrrole-2-carboxylate Wang resin **75** was deemed complete, because no trace of (2*S*)-4-oxo-*N*-(PhF)proline-2-carboxylate was detected.

4-(2-((Fmoc)amino)-5-(Boc)amino)-*N*-((4-hydroxyphenethyl)pentanamido)-1H-pyrrole-2-carboxylate Wang Resin (76a)

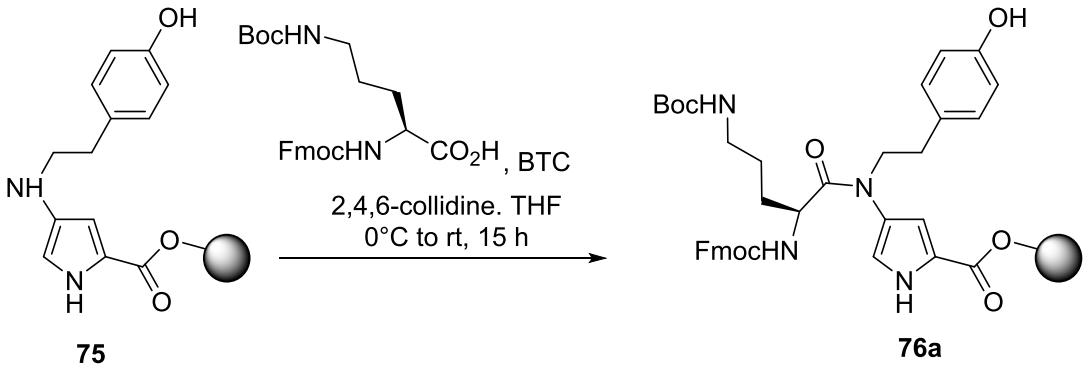

75 **76a**

4-(2-((Fmoc)amino)-5-(Boc)amino)-*N*-((4-hydroxyphenethyl)pentanamido)-1H-pyrrole-2-carboxylate Wang Resin (**76a**) was prepared by a modification of the previously described protocol for amino acylation of 4-aminopyrrole resin.[123] 4-((4-hydroxyphenethyl)amino)-1H-pyrrole-2-carboxylate Wang resin (**75**, 0.3g, 0.89 mmol/mg, 0.27 mmol) was transferred from IRORI MacroKans into a 20 mL plastic filtration tube equipped with polyethylene frit. In a 20 mL flame-dried flask at 0°C, a solution of Fmoc-Orn(Boc) (0.608 g, 1.34 mmol, 5 equiv) was activated with bis(trichloromethyl)carbonate (0.131 g, 0.44 mmol, 1.65 equiv) in THF (8 mL) and 2,4,6-collidine (0.49 mL, 3.74 mmol, 14 equiv) and stirred for 5 min under argon atmosphere. The resulting white suspension was transferred by syringe to the plastic filtration tube containing resin **76a**. After agitation at room temperature for 15 h, the

resin was filtered, and washed with volumes of DMF (×3), MeOH (×3) and DCM (×3). Resin **76a** (0.465 g, 72% conversion) was stored under vacuum.

(S)-4-(2-Acetamido-5-amino-N-((4-hydroxyphenethyl)pentanamido))-1H-pyrrole-2-carboxylic acid (82a)

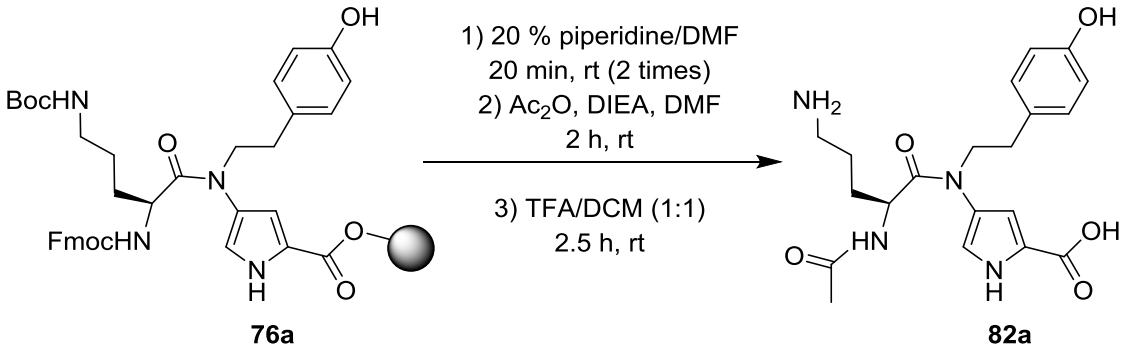

76a **82a**

(***S***)-4-(2-Acetamido-5-amino-***N***-((4-hydroxyphenethyl)pentanamido))-1H-pyrrole-2-carboxylic acid (**82a**) The degree of aminoacylation of **75** with Fmoc-Orn(Boc) was ascertained on a 15 mg aliquot of resin **76a**, which was removed from a 20 mL plastic filtration tube, placed into a 3 mL plastic filtration tube, treated twice with 20% piperidine in DMF for 20 min at room temperature to remove Fmoc protection and washed with 1.5 mL volumes of DMF (×3), MeOH (×3), and DCM (×3). A positive Kaiser test indicated qualitatively the presence of free amine. The resin was treated with acetic anhydride (30 µL, 0.312 mmol, 20 equiv) and DIEA (70 µL, 0.39 mmol, 25 equiv) in 1.5 mL of DMF as described, followed by cleavage with a 1.5 mL of a 1:1 TFA/DCM solution for 2h at room temperature. The resin was washed in a 3 mL plastic filtration tube with 1.5 mL volumes of MeOH (x3) and DCM (x3) and the filtrate and washing solution were combined and evaporated. Analysis of the residue by RP-HPLC-MS

(column A, 10-90% MeOH over 10 min followed by 90% MeOH over 10 min, λ = 254 nm) detected acid **82a** (93% purity, R*t*: 9.2, $[M+H]^+$: 403.2).

4-(2-((Fmoc)amino)-6-*N*-(Boc)amino)-*N*-((4-hydroxyphenethyl)hexanamido)-1H-pyrrole-2-carboxylate Wang Resin (76b)

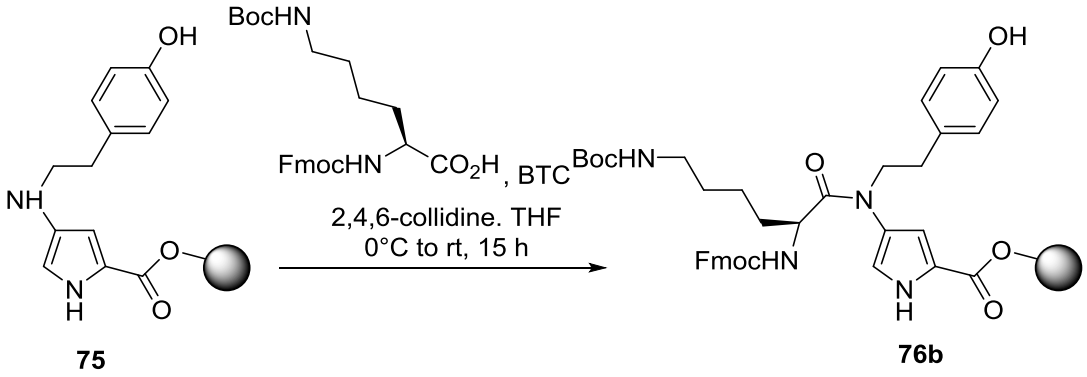

4-(2-((Fmoc)Amino)-6-*N*-(Boc)amino)-*N*-((4-hydroxyphenethyl)hexanamido)-1H-pyrrole-2-carboxylate Wang resin (**76b**) was synthesized as described for resin **76a**. The suspension from activation of Fmoc-Lys(Boc) (0.625 g, 1.34 mmol, 5 equiv) in THF (8 mL) with BTC (0.131 g, 0.44 mmol, 1.65 equiv) and 2,4,6-collidine (0.49 mL, 3.74 mmol, 14 equiv) was transferred to a 20 mL plastic filtration tube containing 4-((4-hydroxyphenethyl)amino)-1H-pyrrole-2-carboxylate Wang resin (**75**, 0.3g, 0.89 mmol/mg, 0.27 mmol). Agitation at room temperature for 15h, filtration and washings gave resin **76b** (0.450 g, 81 % conversion), which was stored under vacuum.

(S)-4-(2-Acetamido-6-amino-N-((4-hydroxyphenethyl)hexanamido)-1H-pyrrole-2-carboxylic acid (82b)

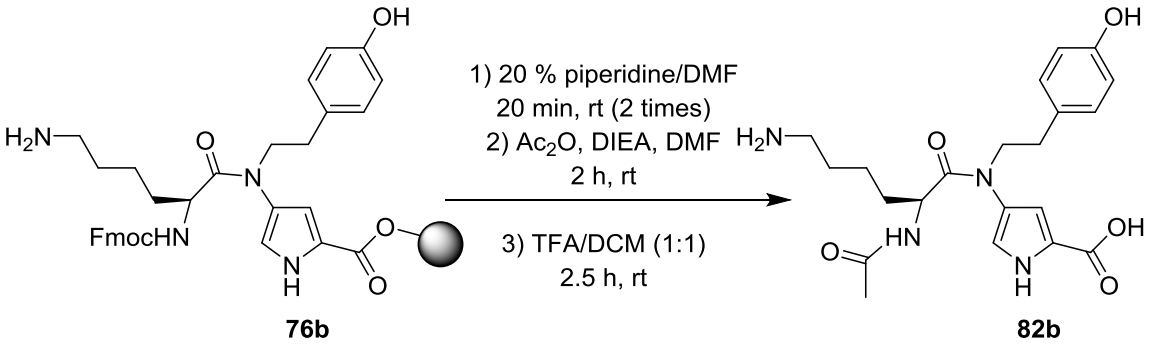

76b **82b**

The product from coupling of Fmoc-Lys(Boc) to resin **76b** was evaluated as described for the synthesis of acid **82a**. After cleavage with 1.5 mL of a 1:1 TFA/DCM solution at room temperature for 2h, analysis by RP-HPLC-MS (column A, 10-90% MeOH over 10 min followed by 90% MeOH over 10 min, λ = 254 nm) detected acid **82b** (92% purity, R*t*: 9.4, $[M+H]^+$: 417.2).

(*S*)-5-([1,1'-Biphenyl]-4-yl)-3-(3-aminopropyl)-1-(4-hydroxyphenethyl)-2-oxo-1,2,3,6-tetrahydropyrrolo[3,2-*e*][1,4]diazepine-7-carboxylic acid (77a)

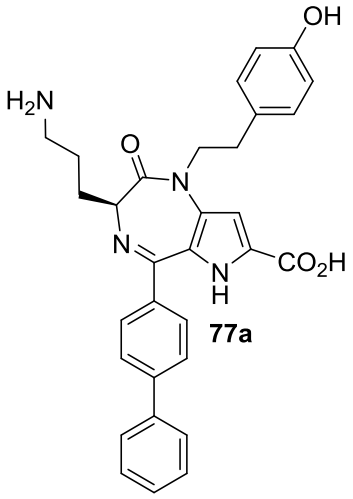

77a

The Fmoc protection was removed by twice agitating resin **76a** at room temperature with a freshly prepared solution of 20% piperidine in DMF (10 mL) in a 20 mL plastic filtration tube equipped with polyethylene frit. After washing with 6 mL volumes of DMF (×3), MeOH (×3), and DCM (×3), the orange resin exhibited a positive Kaiser test, was stored under vacuum, and transferred later into IRORI MiniKans (around 100-150 mg of resin per MiniKan). Four IRORI MiniKans (4 x 145 mg, 0.89 mmol/g, 0.13 mmol) were placed in four 5-10 mL Biotage microwave vessels, treated respectively with biphenyl-4-carboxyaldehyde (0.474 g, 2.6 mmol, 20 equiv) in 4.83 mL of DCE, follow by 0.175 mL of TFA. Each vessel was sealed with a conventional rubber septum and heated at 75°C by microwave irradiation for 3.5h. Each IRORI MiniKan was transferred into a 6 mL plastic filtration tube and washed with 3 mL of MeOH (x 3) and DCM (x 3). The filtrate and washing were combined and evaporated to dryness. The crude oil was

analyzed by RP-HPLC-MS (column A, 20-90% MeOH over 8 min followed by 90% MeOH over 6 min, λ = 254 nm), which demonstrated the residue was composed of **77a** (5%, R*t*: 9.2; $[M+H]^+$: 523.2), *S*-**79a** (11 %, R*t*: 9.8; $[M+H]^+$: 525.2) and *R*-**79a** (10 %, R*t*: 10.5; $[M+H]^+$: 525.2). The excess biphenyl-4-carboxyaldehyde was removed by dissolving the residue in 2 mL of MeOH, treating the solution with 4 mL of H_2O, letting stand overnight, and filtering the precipitate onto a filter paper in a fritted glass filter. The precipitate was washed with 1:1 MeOH/H_2O. The filtrate and washings were combined, evaporated and treated a second time with methanol and water to remove more precipitate. Evaporation of the filtrate and washings gave a residue containing 60% less aldehyde. Purification by reverse phase preparative HPLC (column C, 30-60-90% MeOH, 30-60% MeOH over 13 min, followed by 60% MeOH over 17 min and 60-90% MeOH over 1 min, followed by 90% MeOH over 9 min, λ = 254 nm) gave **77a** (13 mg), and a mixed fraction of **77a**, *S*-**79a** and *R*-**79a**. Analysis by RP-HPLC-MS (Column A, 30-50% MeOH over 8 min followed by 50% over 17 min, λ = 254 nm) demonstrated the mixed fraction contained **77a** (26%, R*t*: 10.0; $[M+H]^+$: 523.2), *S*-**79a** (6%, R*t*: 11.7; $[M+H]^+$: 525.2) and *R*-**79a** (12%, R*t*: 13.8; $[M+H]^+$: 525.2). Purification of the mixed fraction by reverse phase preparative HPLC (column C, 30-35-40% MeOH, 30-35% MeOH over 10 min, followed by 35% MeOH over 38 min and 35-40% MeOH over 1 min, followed by 40% MeOH for 21 min, λ = 254 nm) gave after freeze drying from 0.1 N HCl, acid **77a** (3 mg for a total of 16 mg of yellow oil, 0.031 mmol, 8% yield) which was shown to be of ≥98 % purity by RP-HPLC-MS [Column A, eluent 1 = 20-90% MeOH over 8 min followed by 90% MeOH over 12 min, λ = 254 nm (R*t*: 8.7 ; $[M+H]^+$: 523.2) and Column B, eluant 2 = 10-20% MeCN over 7 min followed by 20% MeOH

over 8 min, λ = 214 nm (R*t*: 6.1; $[M+H]^+$: 523,2)]: $[\alpha]^{21}_D$ –99.7 (*c* 0.22, MeOH); ^{1}H NMR (MeOD, 700 MHz) δ 1.95 (s, 2H), 2.28 (s, 1H), 2.46 (s, 1H), 2.92 (m, 1H), 3.00 (m, 1H), 3.09 (t, *J* = 8.7 Hz, 2H), 4.15 (m, 2H), 4.68 (m, 1H), 6.46 (d, *J* = 4.8 Hz, 2H), 6.86 (d, *J* = 10.6 Hz, 2H), 7.19 (s, 1H), 7.50 (t, *J* = 7.6 Hz, 1H), 7.57 (t, *J* = 7.6 Hz, 2H), 7.80 (d, *J* = 8.9 Hz, 2H), 7.83 (d, *J* = 8.4 Hz, 2H), 8.03 (d, *J* = 8.9 Hz, 2H); ^{13}C NMR (MeOD, 176 MHz) δ 23.9 (CH_2), 25.4 (CH_2), 32.0 (CH_2), 38.9 (CH_2), 48.6 (CH_2), 59.2 (CH), 106.7 (CH), 114.8 (2CH), 119.2 (C), 127.0 (2 CH), 127.7 (2 CH), 128.0 (C), 128.8 (CH), 128.9 (2 CH), 129.6 (2 CH), 132.7 (2 CH), 138.8 (2 C), 140.7 (2 C), 147.9 (C), 155.6 (C), 160.3 (C=O), 162.9 (C=N), 164.4 (C=O); HRMS calcd for $C_{31}H_{30}N_4O_4$ $[M+H]^+$: 523.2340 found: 523.2330.

(3*S*,5*R*)-5-([1,1'-Biphenyl]-4-yl)-3-(3-aminopropyl)-1-(4-hydroxyphenethyl)-2-oxo-1,2,3,4,5,6-hexahydropyrrolo[3,2-*e*][1,4]diazepine-7-carboxylic acid (*R*-79a)

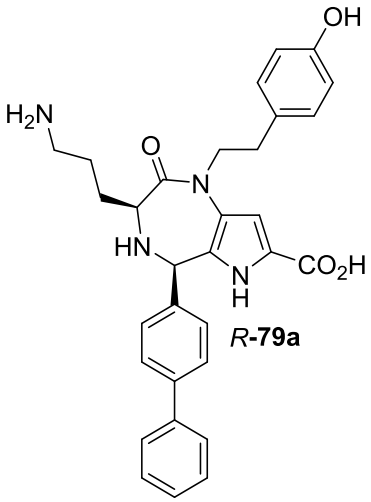

R-**79a**

(3*S*,5*R*)-5-([1,1'-Biphenyl]-4-yl)-3-(3-aminopropyl)-1-(4-hydroxyphenethyl)-2-oxo-1,2,3,4,5,6-hexahydropyrrolo[3,2-***e***][1,4]diazepine-7-carboxylic acid (*R*-**79a**) was

isolated by purification of the mixed fraction of **77a**, *S*-**79a** and *R*-**79a** by reverse phase preparative HPLC (column C, 30-35-40% MeOH, 30-35% MeOH over 10 min, followed by 35% MeOH for 38 min and 35-40% MeOH over 1 min, followed by 40% over 21 min, λ = 254 nm) which after freeze drying from 0.1N HCl, gave *R*-**79a** (yellow oil, 13mg, 0.025 mmol, 5 % yield) that was demonstrated by RP-HPLC-MS to be of ≥98% purity using column A, eluent 1 = 20-90% MeOH over 8 min followed by 90% MeOH over 12 min, λ = 254 nm (R*t*: 11.3) and 97% purity using column B, eluant 2 = 10-20% MeCN over 8 min followed by 20% MeCN over 12 min, λ = 254 nm (R*t*: 8.4; $[M+H]^+$: 525,2): $[\alpha]^{21}_D$ 4.7 (*c* 0.38, MeOH); ^{1}H NMR (MeOD, 700 MHz) δ 1.18 (s, 2H), 2.03 (s, 1H), 2.27 (s, 1H), 2.93 (m, 2H), 3.03 (t, *J* = 8.5 Hz, 2H), 4.01 (m, 1H), 4.16 (m, 1H), 4.38 (s, 1H) , 6.14 (s, 1H), 6.77 (d, *J* = 8.0 Hz, 2H), 6.90 (s, 1H), 7.14 (d, *J* = 5.7 Hz, 2H), 7.39 (m, 3H), 7.46 (t, *J* = 8.0 Hz, 2H), 7.64 (d, *J* = 8.0 Hz, 2H), 7.72 (d, *J* = 5.7 Hz, 2H); ^{13}C NMR (MeOD, 175 MHz) δ 24.0 (CH_2), 26.3 (CH_2), 32.7 (CH_2), 39.0 (CH_2), 49.6 (CH_2), 56.8 (CH), 59.1 (CH), 107.4 (CH), 115.0 (2 CH), 124.6 (3 C), 126.7 (2 CH), 127.4 (2 CH), 127.6 (CH), 128.6 (2 CH), 128.9 (2 C), 129.1 (2 CH), 129.6 (2 CH), 139.8 (2 C), 156.0 (C), 161.9 (2 C=O); HRMS calcd for $C_{31}H_{33}N_4O_4$ $[M+H]^+$: 525.2496 found: 525.2485.

(*S*)-3-(4-Aminopropyl)-1-(4-hydroxyphenethyl)-5-(naphthalen-1-yl)-2-oxo-1,2,3,6-tetrahydropyrrolo[3,2-*e*][1,4]diazepine-7-carboxylic acid (77b)

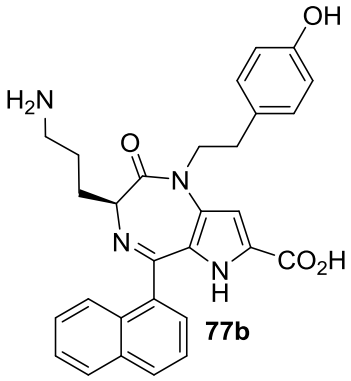

77b

(*S*)-3-(4-Aminopropyl)-1-(4-hydroxyphenethyl)-5-(naphthalen-1-yl)-2-oxo-1,2,3,6-tetrahydropyrrolo[3,2-***e***][1,4]diazepine-7-carboxylic acid (**77b**) was synthesized as described for **77a** using IRORI MiniKans containing resin (3 x 136 mg, 0.89 mmol/g, 0.12 mmol), 4.9 mL of DCE, 1-naphthaldehyde (0.33 mL, 2.4 mmol, 20 equiv), and 0.1 µL TFA. Analysis by RP-HPLC-MS RP-HPLC-MS (column A, 10-90 % MeOH over 8 min followed by 90% MeOH over 6 min, λ = 254 nm) showed the residue to possess **77b** (7%, R*t*: 10.1; $[M+H]^+$: 497.1), *S*-**79b** (6%, R*t*: 11.1; $[M+H]^+$: 499.1) and *R*-**79b** (2%, R*t*: 11.9; $[M+H]^+$: 499.1). Purification by reverse phase preparative HPLC (column C, 20-35-50% MeOH, 20-35% MeOH over 9 min followed by 35% MeOH over 21 min and 35-50% MeOH over 1 min followed by 50% MeOH for 19 min, λ = 214 nm) gave **77b** (5 mg), and a mixed fraction of **77b**, *S*-**79b** and *R*-**79b** (15 mg). Analysis of the mixed fraction of **77b**, *S*-**79b** and *R*-**79b** by RP-HPLC-MS (column A, 20-35-50% MeOH, 20-35% MeOH over 7 min, followed by 35% MeOH over 13 min and 35-50% MeOH over 1 min, followed by 50% MeOH over 9 min, λ = 214 nm) found **77b** (10%, R*t*: 10.8;

$[M+H]^+$: 497.1), *R*-**79b** (18%, R*t*: 15.0; $[M+H]^+$: 499.1) and *S*-**79b** (12%, R*t*: 27.0; $[M+H]^+$: 499.1). Purification of the mixed fraction by reverse phase preparative HPLC (column C, 20-35-50% MeOH, 20-35% MeOH over 9 min, followed by 35% MeOH over 21 min and 35-50% MeOH over 1 min, followed by 50% MeOH over 19 min, λ = 214 nm) gave after freeze drying from 0.1 N HCl, **77b** (7 mg for a total of 12 mg of yellow oil, 0.024 mmol, 8% yield), which was shown to be of ≥98 % purity by RP-HPLC-MS (Column A, eluent 1 = 10-45% MeOH over 8 min followed by 45% MeOH over 12 min, λ = 254 nm, R*t*: 13.9 and eluent 2 = 10-50% MeCN over 8 min followed by 59% MeCN over 12 min, λ = 254 nm, R*t*: 9.5; $[M+H]^+$: 497.1); 1-naphthyl analog **77b**: $[\alpha]^{21}_D$ –18.9 (*c* 0.35, MeOH); ^{1}H NMR (MeOD, 700 MHz) δ 2.01 (s, 2H), 2.32 (s, 1H), 2.51 (s, 1H), 3.03 (m, 1H), 3.07 (m, 1H), 3.13 (t, *J* = 8.1 Hz, 2H), 4.35 (m, 2H), 4.61 (m, 1H), 6.63 (d, *J* = 8.3 Hz, 2H), 7.06 (s, 2H), 7.19 (s, 1H), 7.68 (m, 3H), 7.79 (t, *J* = 7.4 Hz, 2H), 8.12 (d, *J* = 9.1 Hz, 1H), 8.37 (d, *J* =8.5 Hz, 1H); ^{13}C NMR (MeOD, 176 MHz) δ 24.0 (CH_2), 25.7 (CH_2), 32.4 (CH_2), 39.0 (CH_2), 49.4 (CH_2), 59.7 (CH), 106.1 (CH), 115.1 (2 CH), 120.2 (C), 123.3 (C), 125.0 (CH), 127.0 (2 CH), 127.1 (C), 128.1 (2 CH), 128.6 (C), 129.0 (2 CH), 129.7 (2 CH), 133.0 (C), 134.2 (C), 136.7 (C), 155.9 (C), 160.1 (C=O), 162.9 (C=N), 163.9 (C=O); HRMS calcd for $C_{29}H_{29}N_4O_4$ $[M+H]^+$: 497.2183 found: 497.2179.

(3*S*,5*S*)-3-(4-Aminopropyl)-1-(4-hydroxyphenethyl)-5-(naphthalen-1-yl)-2-oxo-1,2,3,4,5,6-hexahydropyrrolo[3,2-*e*][1,4]diazepine-7-carboxylic acid (*S*-79b)

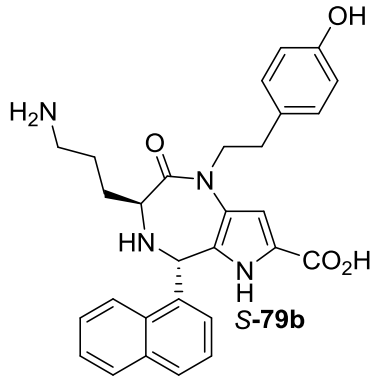

(3*S*,5*S*)-3-(4-Aminopropyl)-1-(4-hydroxyphenethyl)-5-(naphthalen-1-yl)-2-oxo-1,2,3,4,5,6-hexahydropyrrolo[3,2-***e***][1,4]diazepine-7-carboxylic acid (*S*-**79b**) The mixed fraction of **77b**, *S*-**79b** and *R*-**79b** was purified by reverse phase preparative HPLC (column C, 20-35-50% MeOH, 20-35% MeOH over 9 min, followed by 35% MeOH over 21 min and 35-50% MeOH over 1 min, followed by 50% MeOH for 19 min, λ = 214 nm). Acid *S*-**79b** was isolated as a light yellow oil (3 mg, 0.060 mmol, 2% yield), which was demonstrated by RP-HPLC-MS to be of ≥98% purity (column A, eluent 1 = 10-45% MeOH over 8 min, followed by 45% MeOH over 12 min, λ = 254 nm, R*t*: 13.5) and to be of 96 % purity (column B, eluent 2 = 10-15% MeCN over 7 min, followed by 15% MeCN over 8 min, λ = 214 nm R*t*: 8.8; $[M+H]^+$: 499.1): $[\alpha]^{21}_D$ –8.7 (*c* 0.23, MeOH); HRMS calcd for $C_{29}H_{31}N_4O_4$ $[M+H]^+$: 499.2340 found: 499.2331.

(3S,5R)-3-(4-aminopropyl)-1-(4-hydroxyphenethyl)-5-(naphthalen-1-yl)-2-oxo-1,2,3,4,5,6-hexahydropyrrolo[3,2-*e*][1,4]diazepine-7-carboxylic acid (*R*-79b)

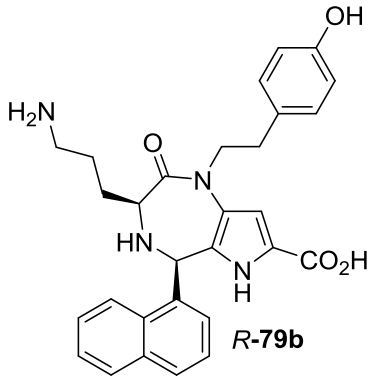

R-**79b**

Purification of the mixed fraction of **77b**, *S*-**79b** and *R*-**79b** by reverse phase preparative HPLC (column C, 20-35-50% MeOH, 20-35% MeOH over 9 min, followed by 35% MeOH over 21 min and 35-50% MeOH over 1 min, followed by 50% MeOH over 19 min, λ = 214 nm) gave a light yellow oil (2.8 mg, 0.006 mmol, 2% yield), which was demonstrated by RP-HPLC-MS to be of 97% purity (column A, eluant 1, 10-45% MeOH over 8 min, followed by 45% MeOH over 12 min, λ = 254 nm, R*t*: 16.5) and to be of 96% purity (column B, eluent 2, 10-15% MeCN over 7 min, followed by 15% MeCN over 8 min, λ = 254 nm, R*t*: 9.5): $[M+H]^+$, 499.1); $[\alpha]^{21}_D$ 3.2 (*c* 0.36, MeOH); HRMS calcd for $C_{29}H_{31}N_4O_4$ $[M+ H]^+$: 499.2340 found: 499.2345.

(*S*)-3-(4-Aminopropyl)-1-(4-hydroxyphenethyl)-5-(naphthalen-2-yl)-2-oxo-1,2,3,6-tetrahydropyrrolo[3,2-*e*][1,4]diazepine-7-carboxylic acid (77c)

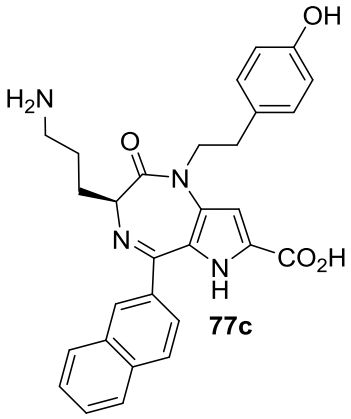

77c

(*S*)-3-(4-Aminopropyl)-1-(4-hydroxyphenethyl)-5-(naphthalen-2-yl)-2-oxo-1,2,3,6-tetrahydropyrrolo[3,2-***e***][1,4]diazepine-7-carboxylic acid (**77c**) was made as described for **77a** using IRORI MiniKans containing resin (3 x 117 mg, 0.89 mmol/g, 0.10 mmol), 4.9 mL of DCE, 2-naphthaldehyde (0.325 mg, 2.1 mmol, 20 equiv) and 0.1 μL of TFA. Analysis of the residue by RP-HPLC-MS (column A, 20-90% MeOH over 8 min followed by 90% MeOH over 7 min, λ = 254 nm) found a mixture containing **77c** (8%, R*t*: 8.9; $[M+H]^+$: 497.1), *S*-**79c** (30%, R*t*: 9.8; $[M+H]^+$: 499.1) and *R*-**79c** (25 %, R*t*: 10.5; $[M+H]^+$: 499.1). Purification by reverse phase preparative HPLC (column C, 20-80% MeOH over 36 min, followed by 80% MeOH over 14 min, λ = 254 nm) gave **77c** (3 mg), and a mixed fraction of **77c**, *S*-**79c** and *R*-**79c** (13 mg), which was ascertained by RP-HPLC-MS (column A, 20-50% MeOH over 10 min, followed by 50% MeOH over 20 min, λ = 254 nm) to contain **77c** (6%, R*t*: 10.8; $[M+H]^+$: 497.2), *S*-**79c** (15%, R*t*: 12.2; $[M+H]^+$: 499.2) and *R*-**79c** (18 %, R*t*: 14.1; $[M+H]^+$: 499.2). Purification by reverse phase preparative HPLC (column C, 20-40-50% MeOH, 20-40% MeOH over 9 min,

followed by 40% MeOH over 16 min and 40-50% MeOH over 1 min, followed by 50% MeOH over 24 min, λ = 214 nm) gave after freeze-drying from 0.1 N HCl, 7 mg of **77c** (for a total of 10 mg, 0.02 mmol, 8 % yield) of ≥98% purity by RP-HPLC-MS (column A, eluent 1, 20-50% MeOH over 8 min, followed by 50% MeOH over 12 min, λ = 254 nm, R*t*: 11.8 and eluent 2, 10-50% MeCN over 8 min, followed by 50% MeCN over 12 min, λ = 254 nm R*t*: 10.6; $[M+H]^+$: 497.1): $[\alpha]^{21}_D$ –31.5 (*c* 0.18, MeOH); ^{1}H NMR (MeOD, 700 MHz) δ 1.93 (s, 1H), 1.98 (s, 1H), 2.30 (s. 1H), 2.45 (s, 1H), 2.93 (m, 1H), 2.98 (m, 1H), 3.10 (t, *J* = 7.8 Hz, 2H), 4.16 (m, 2H), 4.66 (s, 1H), 6.44 (d, *J* = 9.3 Hz, 2H), 6.89 (d, *J* = 7.8 Hz, 2H), 7.17 (s, 1H), 7.71 (m, 2H), 7.79 (t, *J* = 7.0 Hz, 1H), 8.08 (d, *J* = 9.0 Hz, 1H), 8.18 (d, *J* = 7.9 Hz, 1H), 8.23 (d, *J* = 9.0 Hz, 1H), 8.31 (s, 1H); ^{13}C NMR (MeOD, 176 MHz) δ 23.9 (CH_2), 29.4 (CH_2), 32.1 (CH_2), 39.0 (CH_2), 48.1 (CH_2), 48.7 (CH), 106.7 (CH), 114.8 (2 CH), 126.1 (CH), 127.5 (CH), 127.7 (2 CH), 128.1 (2 C), 128.8 (C), 129.2 (CH), 129.6 (3 CH), 129.6 (CH), 132.7 (2 C), 136.3 (C), 147.6 (C), 155.7 (C), 163.8 (C=O and C=N), 164.7 (C=O); HRMS calcd for $C_{29}H_{29}N_4O_4$ $[M+H]^+$: 497.2183 found: 497.2182.

(S)-5-([1,1'-Biphenyl]-4-yl)-3-(4-aminobutyl)-1-(4-hydroxyphenethyl)-2-oxo-1,2,3,6-tetrahydropyrrolo[3,2-*e*][1,4]diazepine-7-carboxylic acid (78a)

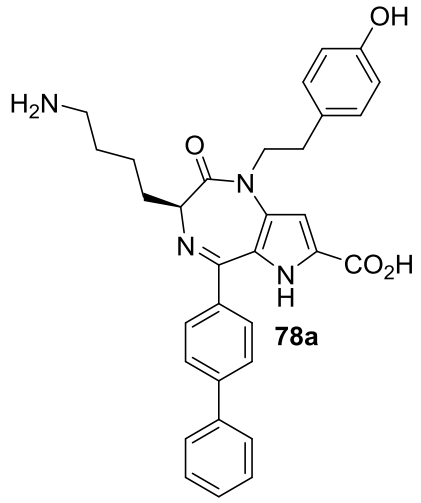

78a

(*S*)-5-([1,1'-Biphenyl]-4-yl)-3-(4-aminobutyl)-1-(4-hydroxyphenethyl)-2-oxo-1,2,3,6-tetrahydropyrrolo[3,2-***e***][1,4]diazepine-7-carboxylic acid (**78a**) was synthesized as describes for **77a** using four IRORI MiniKans containing resin (4 x 157 mg, 0.89 mmol/g, 0.14 mmol) and biphenyl-4-carboxyaldehyde (0.509 g, 2.79 mmol, 20 equiv) in 4.83 mL of DCE, on treatment with 0.175 mL of TFA. Analysis by RP-HPLC-MS (column A, 20-90 % MeOH over 8 min, followed by 90% MeOH over 6 min, λ = 254 nm) found a mixture containing **78a** (3%, R*t*: 9.1; $[M+H]^+$: 537.2), *S*-**80a** (2 %, R*t*: 9.6; $[M+H]^+$: 539.2) and *R*-**80a** (28 %, R*t*: 10.2; $[M+H]^+$: 539.2). Purification by reverse phase preparative HPLC (column C, 20-60-90% MeOH, 20-60% MeOH over 13 min, followed by 60% MeOH over 12 min and 60-90% MeOH over 1 min, followed by 90% MeOH over 14 min, λ = 214 nm) gave 8 mg of **78a**, and 85 mg of a mixed fraction containing **78a**, *S*-**80a** and *R*-**80a**, which on analysis by RP-HPLC-MS (column A, 20-

35-40% MeOH, 20-35% MeOH over 6 min, followed by 35% MeOH over 16 min and 35-40% MeOH over 1 min, followed by 40% MeOH over 12 min, λ = 214 nm) was shown to contain **78a** (15%, R*t*: 15.1; $[M+H]^+$: 537.2), *S*-**80a** (14 %, R*t*: 22.4; $[M+H]^+$: 539.2) and *R*-**80a** (26 %, R*t*: 30.1; $[M+H]^+$: 539.2). Purification by reverse phase preparative HPLC (column C, 20-35-40% MeOH, 20-35% MeOH over 9 min, followed by 35% MeOH over 60 min and 35-40% MeOH over 1 min, followed by 40% MeOH over 29 min, λ = 214 nm) gave 6 mg more for a total of 13 mg of **78a** (yellow oil, 13 mg, 0.024 mmol, 6 % yield), which was lyophilized from a solution of 0.1N HCl and shown to be of ≥ 98% purity by RP-HPLC-MS (Column A, eluent 1, 20–90% MeOH over 8 min, followed by 90% MeOH over 12 min, λ = 254 nm, R*t*: 9.0 and eluent 2, 10-50% MeCN over 8 min, followed by 50% MeCN over 12 min, λ = 254 nm, R*t*: 10.5; $[M+H]^+$: 537.1): $[\alpha]^{21}_D = -72.5$ (*c* = 0.22, MeOH); ^{1}H NMR (MeOD, 700 MHz) δ 1.65 (d, *J* = 39.9 Hz, 2H), 1.84 (t, *J* = 8.4 Hz, 2 H) , 2.25 (s, 1H), 2.37 (s, 1H), 2.90 (m, 1H), 2.93 (m, 1H), 3.05 (t, *J* = 8.3 Hz, 2 H), 4.09 (m, 1 H), 4.19 (m, 1 H), 4.67 (m, 1 H), 6.46 (d, *J* = 8.1 Hz, 2H), 6.87 (d, *J* = 9.7 Hz, 2H), 7.17 (s, 1H), 7.50 (t, *J* = 6.5 Hz, 1H), 7.57 (t, *J* = 8.9 Hz, 2H), 7.79 (d, *J* =8.1 Hz, 2H), 7.83 (d, *J* = 9.8 Hz, 2H), 8.02 (d. *J* = 8.1 Hz, 2H); ^{13}C NMR (MeOD, 176 MHz) δ 22.7 (CH_2) 27.0 (CH_2), 27.9 (CH_2), 32.0 (CH_2), 39.1 (CH_2), 48.6 (CH_2), 59.9 (CH), 106.5 (CH), 114.9 (2 CH), 119.2 (C), 127.0 (2 CH), 127.6 (2 CH), 128.0 (C), 128.7 (CH), 128.9 (2 CH), 129.6 (2 CH), 132.6 (2 CH), 138.9 (2 C), 140.6 (2 C), 147.9 (C), 155.7 (C), 160.5 (C=O), 162.8 (C=N), 164.5 (C=O); HRMS calcd for $C_{32}H_{33}N_4O_4$ $[M+H]^+$:537.2496 found: 537.2499.

(3*S*,5*S*)-5-([1,1'-Biphenyl]-4-yl)-3-(4-aminobutyl)-1-(4-hydroxyphenethyl)-2-oxo-1,2,3,4,5,6-hexahydropyrrolo[3,2-e][1,4]diazepine-7-carboxylic acid (*S*-80a)

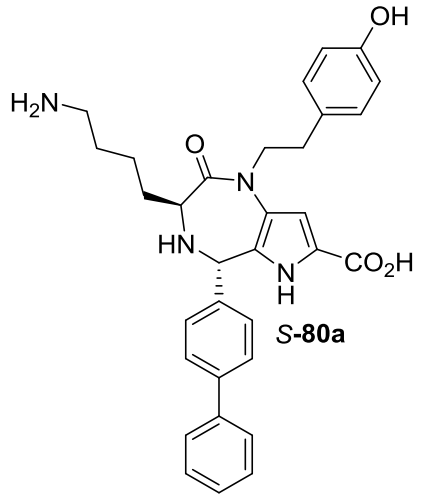

S-**80a**

(3*S*,5*S*)-5-([1,1'-Biphenyl]-4-yl)-3-(4-aminobutyl)-1-(4-hydroxyphenethyl)-2-oxo-1,2,3,4,5,6-hexahydropyrrolo[3,2-e][1,4]diazepine-7-carboxylic acid (*S*-**80a**) was obtained from purification of the above mixture (85 mg) of **78a**, *S*-**80a** and *R*-**80a** by reverse phase preparative HPLC (column C, 20-35-40% MeOH, 20-35% MeOH over 9 min, followed by 35% MeOH over 60 min and 35-40% MeOH over 1 min, followed by 40% MeOH over 29 min, λ = 214 nm), which gave *S*-**80a** (light yellow oil, 11 mg, 0.020 mmol, 5 % yield) after freeze-drying from a solution of 0.1 N HCl, and shown to be of ≥98% purity by RP-HPLC-MS (Column A, eluent 1, 20–90% MeOH over 7 min, followed by 90% MeOH over 13 min , λ = 254 nm, R*t*: 9.6 and eluant 2, 10-50% MeCN over 8 min, followed by 50% MeCN over 12 min, λ = 254 nm, R*t*: 11.0, $[M+H]^+$: 539.1): $[\alpha]^{21}_D$ = –4.3 (*c* = 0.33, MeOH); ^{1}H NMR (MeOD, 700 MHz) δ 1.34 (s, 2H), 1.68 (t, *J* = 8.96 Hz, 2H), 1.80 (s, 1H), 2.20 (s, 1H), 2.95 (m, 3H), 3.04 (m, 1H), 3.99 (d, *J* = 11.56

Hz, 1H), 4.05 (m, 1H), 4.45 (m, 1H), 5.14 (s, 1H), 6.75 (d, *J* = 5.95 Hz, 2 H), 6.94 (s, 1H), 7.08 (d, *J* = 9.45 Hz, 2H), 7.43 (t, *J* = 7.07 Hz, 1H), 7.51 (t, *J* = 7.08 Hz, 2H), 7.65 (d, *J* = 8.26 Hz, 2H), 7.72 (d, *J* = 7.07 Hz, 2H), 7.86 (d, *J* = 8.26 Hz, 2H); ^{13}C NMR (MeOD, 176 MHz) δ 22.6 (CH_2), 26.7 (CH_2), 27.3 (CH_2), 32.3 (CH_2), 39.0 (CH_2), 48.2 (CH_2), 55.7 (CH), 57.2 (CH), 107.9 (CH), 115.1 (2 CH), 121.5 (C), 124.4 (C), 126.4 (C), 126.7 (2 CH), 127.8 (3 CH), 128.5 (C), 128.7 (2 CH), 129.1 (2 CH), 129.6 (2 CH), 139.7 (C), 143.1 (2 C), 155.9 (C), 161.9 (C=O), 164.7 (C=O); HRMS calcd for $C_{32}H_{35}N_4O_4$ $[M+ H]^+$: 539.2653 found: 539.2652.

(3*S*,5*R*)-5-([1,1'-biphenyl]-4-yl)-3-(4-aminobutyl)-1-(4-hydroxyphenethyl)-2-oxo-1,2,3,4,5,6-hexahydropyrrolo[3,2-e][1,4]diazepine-7-carboxylic acid (*R*-80a)

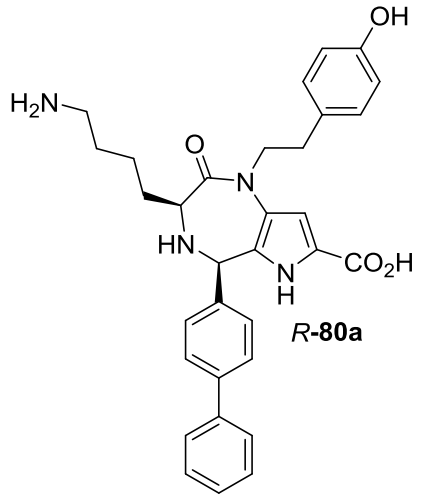

R-**80a**

(3*S*,5*R*)-5-([1,1'-biphenyl]-4-yl)-3-(4-aminobutyl)-1-(4-hydroxyphenethyl)-2-oxo-1,2,3,4,5,6-hexahydropyrrolo[3,2-e][1,4]diazepine-7-carboxylic acid (*R*-**80a**) was obtained from purification of the mixture of **78a**, *S*-**80a** and *R*-**80a** (85 mg) by reverse phase preparative HPLC (column C, 20-35-40% MeOH, 20-35% MeOH over 9 min,

followed by 35% MeOH over 60 min and 35-40% MeOH over 1 min, followed by 40% over 29 min, λ = 214 nm, λ = 214 nm), which after freeze-drying from a solution of 0.1N HCl, gave *R*-**80a** (light yellow oil, 12 mg, 0.022 mmol, 5 % yield) that was shown to be of ≥ 98% purity by RP-HPLC-MS (Column A, eluent 1, 20–90% MeOH over 8 min, followed by 90% MeOH over 12 min, λ = 254 nm, R*t*: 10.3, and eluent 2, 10-50% MeCN over 8 min, followed by 50% MeCN over 12 min, λ = 254 nm, R*t*: 11.3; $[M+H]^+$: 539.2): $[\alpha]^{21}_D$ = 10.5 (*c* = 0.67, MeOH); ^{1}H NMR (MeOD, 700 MHz) δ 1.51 (m, 2H), 1.77 (m, 2H), 1.96 (s, 1H), 2.22 (s, 1H), 2.86 (m, 2H), 3.00 (t, *J* = 8.8 Hz, 2H), 4.00 (m, 1H), 4.13 (m, 1H), 4.27 (s, 1H), 6.10 (s, 1H), 6.76 (d, *J* = 10.2 Hz, 2H), 6.89 (s, 1H), 7.12 (d, *J* = 9.4 Hz, 2H), 7.37 (t, *J* = 7.5 Hz, 1H), 7.40 (d, *J* = 6.1 Hz, 2H), 7.45 (t, *J* = 14.9 Hz, 2H), 7.63 (d, *J* = 7.8 Hz, 2H), 7.71 (d, *J* = 7.8 Hz, 2H); ^{13}C NMR (MeOD, 176 MHz) δ 22.8 (CH_2), 27.0 (CH_2), 28.8 (CH_2), 32.6 (CH_2), 38.9 (CH_2), 49.4 (CH_2), 57.1 (CH), 58.9 (CH), 107.5 (CH), 115.1 (2 CH), 123.4 (C), 124.8 (2 C), 126.7 (2 CH), 127.4 (2 CH), 127.5 (CH), 128.6 (2 CH), 128.7 (2 CH), 129.0 (C), 129.5 (2 CH), 139.9 (C), 142.5 (2 C), 155.9 (C), 161.9 (2 C=O); HRMS calcd for $C_{32}H_{35}N_4O_4$ $[M+ H]^+$: 539.2653 found: 539.2658.

(*S*)-3-(4-Aminobutyl)-1-(4-hydroxyphenethyl)-5-(naphthalen-1-yl)-2-oxo-1,2,3,6-tetrahydropyrrolo[3,2-e][1,4]diazepine-7-carboxylic acid (78b)

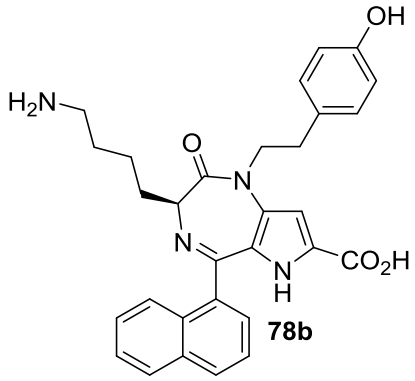

78b

(*S*)-3-(4-Aminobutyl)-1-(4-hydroxyphenethyl)-5-(naphthalen-1-yl)-2-oxo-1,2,3,6-tetrahydropyrrolo[3,2-e][1,4]diazepine-7-carboxylic acid (**78b**) The preparation of acid **78b** was performed as described for **77a**, using four IRORI MiniKans containing (4 x 127 mg, 0.89 mmol/g, 0.11 mmol) in four 5-10 mL Biotage microwave vessels, to which a solution of 1-naphthaldehyde (0.31 mL, 2.3 mmol, 20 equiv) in 4.83 mL of DCE, follow by 0.175 mL de TFA were added. The vessels were heated under microwave irradiation at 75°C for 3.5h. Analysis of the residue by RP-HPLC-MS (column A, 20-90 % MeOH over 10 min, followed by 90 % MeOH over 5 min, λ = 254 nm) indicated a composition of **78b** (4% R*t*: 7.8; $[M+H]^+$: 511.2), *S*-**80b** (9%, R*t*: 8.9; $[M+H]^+$: 513.2) and *R*-**80b** (8 %, R*t*: 9.7; $[M+H]^+$: 513.2). The mixture was purified by reverse phase preparative HPLC (column C, 10-60% MeOH over 15 min followed by 60% MeOH over 20 min, λ = 214 nm) to provide 15 mg of **2b**, and mixed fractions of **78b**, *S*-**80b** and *R*-**80b** that were combined together. The fraction of **78b** was demonstrated to be of 80 % purity by RP-HPLC-MS (column A, 10-35 % MeOH over 8 min followed by 35%

MeOH over 12 min, λ = 254 nm, R*t*: 15.2; $[M+H]^+$: 511.2), and purified by reverse phase preparative HPLC (column C, 10-35% MeOH over 15 min followed by 35 % MeOH over 30 min, λ = 214 nm) to give 10 mg of **78b**. The remaining mix fractions of **78b**, *S*-**80b** and *R*-**80b** were combined and analyzed by RP-HPLC-MS (column A, 10-35-40 % MeOH, 10-35% MeOH over 10 min, followed by 35% MeOH over 12 min and 35-40% MeOH over 1 min, followed by 40% MeOH over 12 min, λ = 254 nm), which detected a mixture of **78b** (24 %, R*t*: 15.5; $[M+H]^+$: 511.2), *S*-**80b** (15 %, R*t*: 20.7; $[M+H]^+$: 513.2) and *R*-**80b** (19 %, R*t*: 29.5; $[M+H]^+$: 513.2). Purification of the mixture by reverse phase preparative HPLC (column C, 10-35-40% MeOH, 10-35% MeOH over 13 min followed by 35% MeOH over 20 min, 35-40% MeOH over 2 min, followed by 40% MeOH over 25 min, λ = 214 nm) provided 4 mg of **78b**, for a total of 14 mg (yellow oil, 0.027 mmol, 8 % yield). After freeze-dying from 0.1N HCl, **78b** was demonstrated to be of ≥ 98% purity by RP-HPLC-MS (Column A, eluent 1, 10-35% MeOH over 8 min, followed by 45% MeOH over 12 min, λ = 254 nm, R*t*: 13.0, and column B, eluant 2, 10-15% MeCN over 7 min followed 15% MeCN over 8 min, R*t*: 9.1, λ = 254 nm, $[M+H]^+$: 511.2). Acid **78b**: $[\alpha]^{21}_D = -7.9$ (*c* = 0.92, MeOH); ^{1}H NMR (MeOD, 400 MHz) δ 1.71 (s, 2H), 1.87 (s, 2H), 2.29 (s, 1H), 2.45 (s, 1H), 3.07 (m, 4H), 4.33 (m, 2H), 4.58 (s, 1H), 6.64 (d, *J* = 7 Hz, 2H), 7.07 (d, *J* = 7 Hz, 2H), 7.19 (s, 1H), 7.67 (m, 3H), 7.78 (t, *J* = 8 Hz, 2H), 8.12 (d, *J* = 9 Hz, 1H), 8.36 (d, *J* = 9Hz, 1H); ^{13}C NMR (MeOD, 176 MHz) δ 23.0 (CH_2), 27.0 (CH_2), 28.2 (CH_2), 32.4 (CH_2), 39.3 (CH_2), 49.3 (CH_2), 60.3 (CH), 106.1 (CH), 114.9 (2 CH), 123.4 (C), 125.1 (2 C), 127.0 (CH), 128.2 (2 CH), 128.5 (2 C), 129.0 (2 CH), 129.7 (2 CH), 132.6 (C), 134.1 (2 CH), 155.9 (2 C), 160.2 (C=O), 162.7 (C=N), 164.0 (C=O); HRMS calcd for $C_{30}H_{31}N_4O_4$ $[M+H]^+$: 511.2340 found: 511.2334.

(*S*)-3-(4-Aminobutyl)-1-(4-hydroxyphenethyl)-5-(naphthalen-2-yl)-2-oxo-1,2,3,6-tetrahydropyrrolo[3,2-e][1,4]diazepine-7-carboxylic acid (78c)

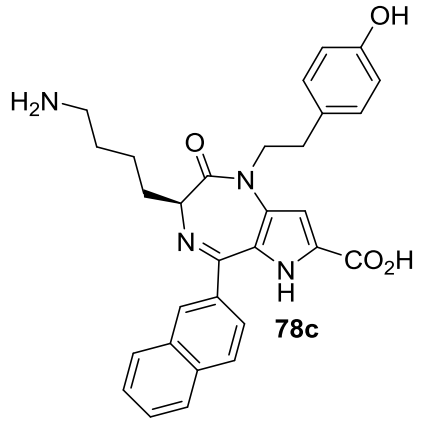

78c

(*S*)-3-(4-Aminobutyl)-1-(4-hydroxyphenethyl)-5-(naphthalen-2-yl)-2-oxo-1,2,3,6-tetrahydropyrrolo[3,2-e][1,4]diazepine-7-carboxylic acid (**78c**) was prepared as described for **77a** using three IRORI MiniKans containing (3 x 123 mg, 0.89 mmol/g, 0.11 mmol), 4.9 mL of DCE, 2-naphthaldehyde (0.343g, 2.2 mmol, 20 equiv) and 0.1 mL of TFA. Analysis by RP-HPLC-MS (Column A, 10-90 % MeOH over 8 min, followed by 90% MeOH over 7 min, λ = 254 nm) demonstrated the residue was composed of **78c** (5%, R*t*: 10.0; $[M+H]^+$: 511.1), *S*-**80c** (29%, R*t*: 10.7; $[M+H]^+$: 513.1) and *R*-**80c** (15%, R*t*: 11.5; $[M+H]^+$: 513.1). Purification by reverse phase preparative HPLC (column C, 20-35-60 % MeOH, 20-35% MeOH over 12 min, followed by 35% MeOH over 8 min and 35-60% MeOH over 11 min, followed by 60% MeOH over 29 min, λ = 214 nm) gave **78c** (4.9 mg) and 15 mg of a mixed fraction, which by RP-HPLC-MS (column A, 20-35-40 % MeOH, 20-35% MeOH over 10 min, followed by 35% MeOH over 10 min and 35-40% MeOH over 1 min, followed by 40% MeOH over 9

min, λ = 254 nm) was shown to contain **78c** (25%, R*t*: 13.9; $[M+H]^+$: 511.1), *S*-**80c** (28%, R*t*: 18.0; $[M+H]^+$: 513.2) and *R*-**80c** (30%, R*t*: 27.0; $[M+H]^+$: 513.2). Purification by reverse phase preparative HPLC (column C, 20-35-60 % MeOH, 20-35% MeOH over 12 min, followed by 35% MeOH over 8 min and 35-60% MeOH over 11 min, followed by 60% MeOH over 29 min, λ = 214 nm) gave acid **78c** (3 mg, for a total of 8 mg of yellow oil, 0.015 mmol, 6 % yield), which after freeze-drying from 0.1 N HCl, was shown to be of ≥ 98 % purity by RP-HPLC-MS (column A, eluent 1, 20-50 % MeOH over 8 min, followed by 50% MeOH over 12 min, λ = 254 nm, R*t*: 10.3 and eluent 2, 10-50% MeCN over 8 min followed by 50% MeCN over 12 min, λ = 254 nm, R*t*: 8.8; $[M+H]^+$: 511.1): $[\alpha]^{21}_D$ = –87.1 (*c* = 0.29, MeOH); ^{1}H NMR (MeOD, 700 MHz) δ 1.66 (s, 1H), 1.71 (s, 1H), 1.86 (s, 2 H), 2.30 (s 1H), 2.42 (s, 1H), 2.95 (m, 1H), 3.01 (m, 1H), 3.08 (t, *J* = 7.9 Hz, 2H), 4.13 (s, 1H), 4.23 (m, 1H), 4.68 (m, 1H), 6.45 (d, *J* = 9.2 Hz, 2H), 6.89 (d, *J* = 7.8 Hz, 2H), 7.19 (s, 1H), 7.70 (d, *J* = 9.0 Hz, 1H), 7.75 (t, *J* = 7.5 Hz, 1H), 7.81 (t, *J* = 7.5 Hz, 1H), 8.10 (d, *J* = 8.1 Hz, 1H), 8.21 (d, *J* = 8.7 Hz, 1H), 8.26 (d, *J* = 8.6 Hz, 1H), 8.33 (s, 1H); ^{13}C NMR (MeOD, 176 MHz) δ 22.8 (CH_2), 27.0 (CH_2), 27.8 (CH_2), 32.1 (CH_2), 39.0 (CH_2), 48.8 (CH_2), 58.9 (CH), 106.6 (CH), 114.9 (2 CH), 119.4 (C), 126.1 (C), 126.7 (C), 127.6 (CH), 127.7 (CH), 128.1 (CH), 129.3 (CH), 129.6 (2 CH), 129.8 (CH), 129.9 (CH), 132.6 (CH), 134.6 (C), 136.4 (C), 140.9 (C), 155.7 (2 C), 160.4 (C=O), 163.4 (C=N), 164.4 (C=O); HRMS calcd for $C_{30}H_{31}N_4O_4$ $[M+H]^+$: 511.2340 found: 511.2322.

(3*S*,5*S*)-3-(4-Aminobutyl)-1-(4-hydroxyphenethyl)-5-(naphthalen-2-yl)-2-oxo-1,2,3,4,5,6-hexahydropyrrolo[3,2-e][1,4]diazepine-7-carboxylic acid (*S*-80c)

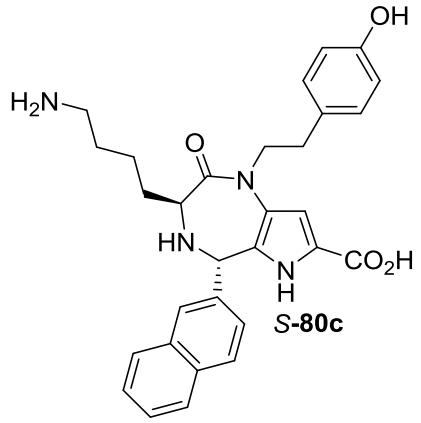

***S*-80c**

(3*S*,5*S*)-3-(4-Aminobutyl)-1-(4-hydroxyphenethyl)-5-(naphthalen-2-yl)-2-oxo-1,2,3,4,5,6-hexahydropyrrolo[3,2-e][1,4]diazepine-7-carboxylic acid (*S*-**80c**) was isolated by reverse phase preparative HPLC (column C, 20-35-60 % MeOH, 20-35% MeOH over 12 min, followed by 35% MeOH over 8 min and 35-60% MeOH over 11 min, followed by 60% MeOH over 29 min, λ = 214 nm) from the mixture of **78c**, *S*-**80c** and *R*-**80c**. Acid *S*-**80c** (light yellow oil, 2.8 mg, 0.006 mmol, 2 % yield) was shown by RP-HPLC-MS to be of 98% purity (column A, eluent 1: 20-50 % MeOH over 8 min followed by 50% MeOH over 12 min, λ = 254 nm, R*t*: 11.8) and to be of 95% purity (column B, eluent 2: 10-15% MeCN over 7 min followed by 15% MeCN over 8 min, λ = 280 nm, R*t*: 5.6, $[M+H]^+$: 513.2): $[\alpha]^{21}_D$ –11.7 (*c* = 0.014, MeOH); HRMS calcd for $C_{30}H_{33}N_4O_4$ $[M+H]^+$: 513.2496 found: 513.249.

(3*S*,5*R*)-3-(4-Aminobutyl)-1-(4-hydroxyphenethyl)-5-(naphthalen-2-yl)-2-oxo-1,2,3,4,5,6-hexahydropyrrolo[3,2-e][1,4]diazepine-7-carboxylic acid (*R*-80c)

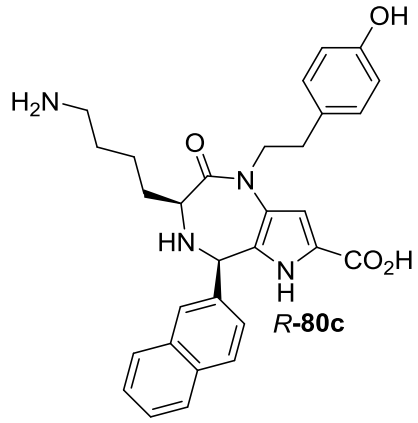

R-**80c**

(3*S*,5*R*)-3-(4-Aminobutyl)-1-(4-hydroxyphenethyl)-5-(naphthalen-2-yl)-2-oxo-1,2,3,4,5,6-hexahydropyrrolo[3,2-e][1,4]diazepine-7-carboxylic acid (*R*-**80c**) was isolated by reverse phase preparative HPLC (column C, 20-35-60 % MeOH, 20-35% MeOH over 12 min, followed by 35% MeOH over 8 min and 35-60% MeOH over 11 min, followed by 60% MeOH over 29 min, λ = 214 nm) from the mixture of **2c**, *S*-**80c** and *R*-**80c**. Acid *R*-**80c** (light yellow oil, 3.5 mg, 0.009 mmol, 3 % yield) was determined by RP-HPLC-MS to be 98% purity (column A, eluent 1: 20-50 % MeOH over 8 min followed by 50% MeOH over 12 min, λ = 280 nm, R*t*: 13.1) and 95% purity (column B, eluent 2: 10-15% MeCN over 7 min followed by 15% MeCN over 8 min, λ = 254 nm, R*t*: 6.8, $[M+H]^+$: 513.2): $[\alpha]^{21}_D$ 6.4 (*c* = 0.017, MeOH); HRMS calcd for $C_{30}H_{33}N_4O_4$ $[M+H]^+$:513.2496 found: 513.2483.

Annexe 3: Biologie des pyrrolo[3,2-*e*][1,4]diazepin-2-ones

Cell culture

Transfected CHO cells (generous gift from Drs H. Vaudry and C. Dubessy, Rouen, France) expressing the human urotensin receptor (CHO-*h*UT) were maintained in Ham-F12 medium with 10% fetal bovine serum (FBS), 2 mM L-glutamine, 100 UI/mL each of penicillin and streptomycin, and 400 μg/mL G418.[13]

Competitive binding assays

Synthetic hUII was radiolabeled with $Na^{125}I$ using the chloramine-T technique, as previously described.[170] Iodinated peptides were then purified using a C_{18} Sep-Pak cartridge (Waters Corp., Milford, MA, USA), collected and stored at -20°C until use. Binding assays were performed, as reported,[13] using CHO-*h*UT . Briefly, cells were plated at a density of 150,000 cells/well in 24-well plate, and exposed to high concentrations (10^{-4} or 10^{-5}M) of pyrrolo[3,2-e][1,4]diazepin-2-ones in the presence of 0.2 nM ^{125}I-hUII. After 90 min of incubation at room temperature, the cells were washed, lysed, and the cell-bound radioactivity was quantified using a γ-counter (1470 Automatic Gamma Counter, Perkin Elmer). Results were expressed as a percentage of the specific binding of ^{125}I-hUII obtained in the absence of competitive ligands. Non-specific binding was determined in the presence of 10 μM hUII and ranged between 10% to 15% of total binding.

Aortic Ring Contraction

Adult male Sprague-Dawley rats (Charles-Rivers, San Diego, CA) weighing 250–300 g were housed in group cages under controlled illumination (12:12h light-dark cycle), humidity, and temperature (21–23°C) and had free access to tap water and rat chow. All experimental procedures were performed in accordance with regulations and ethical guidelines from the Canadian Council for the Care of Laboratory Animals and received approvals of the institutional animal care and use committee of the Institut National de la

Recherche Scientifique-Institut Armand-Frappier.[262] On the day of the experiment, rats were killed by CO_2 asphyxiation. The thoracic aorta was cleared of surrounding tissue and excised from the aortic arch to the diaphragm. From each vessel, conjunctive tissues were removed and the clean vessel was cut into 4 mm rings. The endothelium was removed by rubbing gently the vessel intimal surface. All preparations were placed in 5 mL organ baths filled with oxygenated normal Krebs-Henseleit solution. Contractile responses to 40 mM KCl were used as control at the beginning and at the end of each experiment. Agonistic activity of pyrrolo[3,2-e][1,4]diazepin-2-ones was evaluated by adding a high concentration of KCl (10^{-4} or 10^{-5}M) in the organ chamber. For antagonist behaviour, thoracic aortic rings were first exposed to a sample of pyrrolo[3,2-e][1,4]diazepin-2-one for 15 min, to ensure that the peptide reached equilibrium and that no agonistic effect was observed,[252] and then cumulative concentration-response curves to hUII or URP (10^{-10}-3.10^{-6} M) were constructed. The amplitude of the contraction induced by each peptide concentration was expressed as a percentage of the KCl-induced contraction.

Statistical analysis

Binding and functional experiments were performed at least in triplicate and data, expressed as mean ± S.E.M, were analyzed with the Prism software (Graph Pad Software, San Diego, CA, USA). In all experiments, n represents the total number of animals studied or individual assays performed. EC_{50}, pEC_{50}, pIC_{50} as well as E_{max} values were determined from corresponding concentration-response curves obtained through a sigmoidal dose-response fit with variable slope. Non-competitive antagonist affinities (pK_B) were determined as previously described using the method of Gaddum where equally active concentrations of agonist, in the absence or presence of pyrrolo[3,2-e][1,4]diazepin-2-one **1b** and *R*-**4a**,were compared in a linear regression.[213] Statistical comparisons of binding affinities and contractile potencies were analyzed using unpaired Student's t-test and differences were considered significant when $*P < 0.05$, $**P < 0.01$, and $***P < 0.001$.

Effects of 77a on (A) hUII- and (B) URP-induced contraction of rat aortic ring

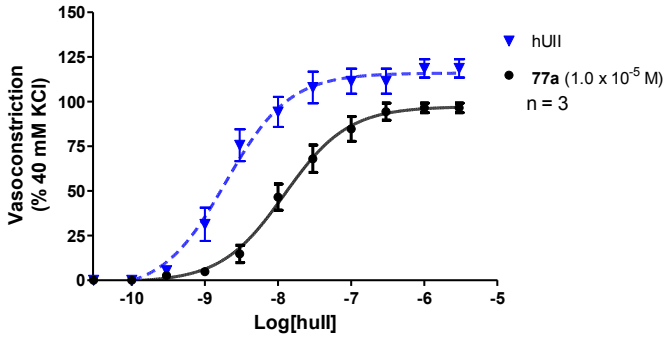

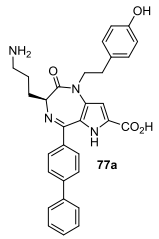

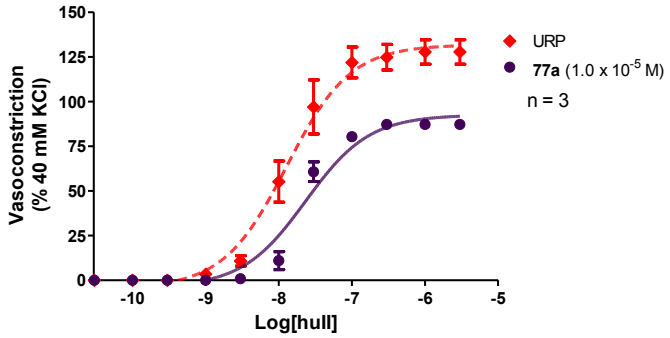

Effects of 77b on (A) hUII- and (B) URP-induced contraction of rat aortic ring

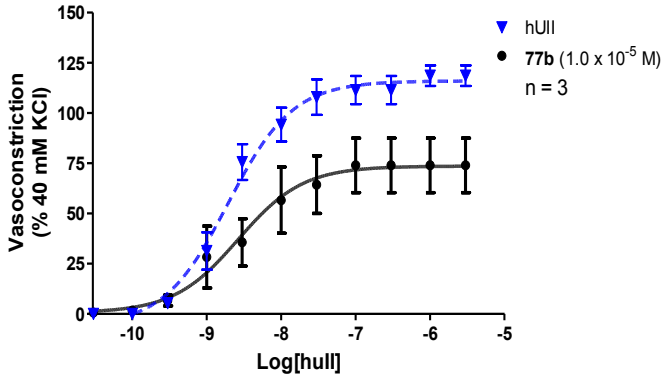

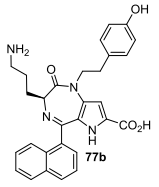

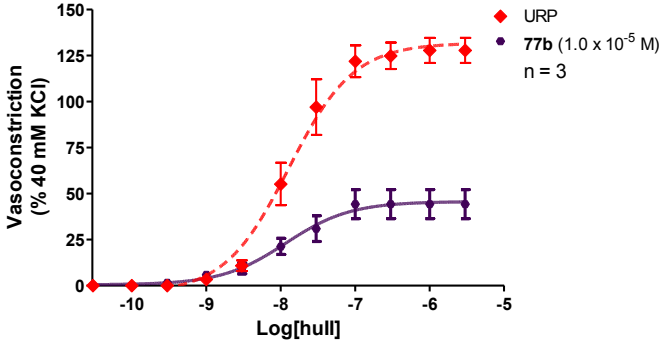

Effects of 77c on (A) hUII- and (B) URP-induced contraction of rat aortic ring

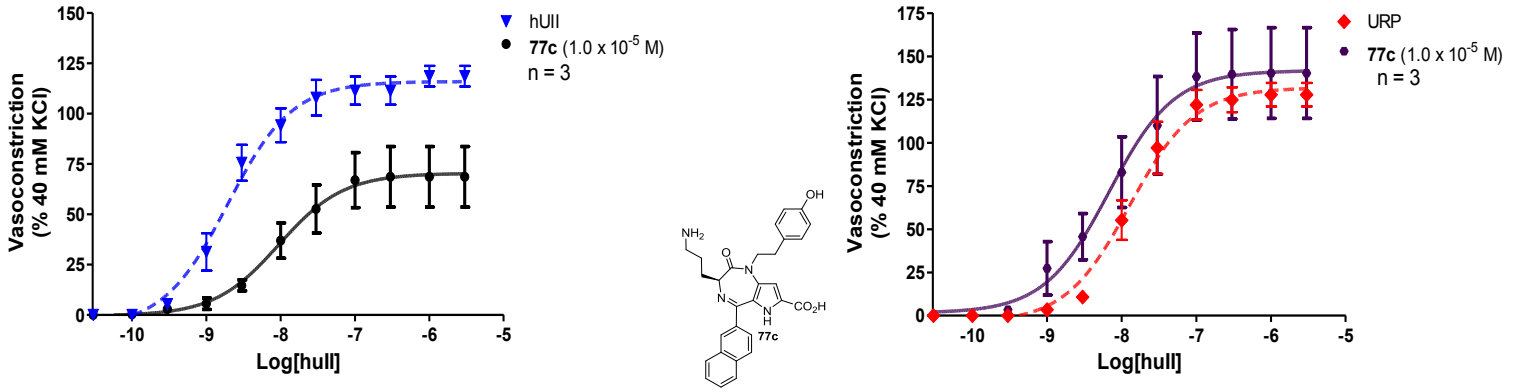

Effects of 78a on (A) hUII- and (B) URP-induced contraction of rat aortic ring

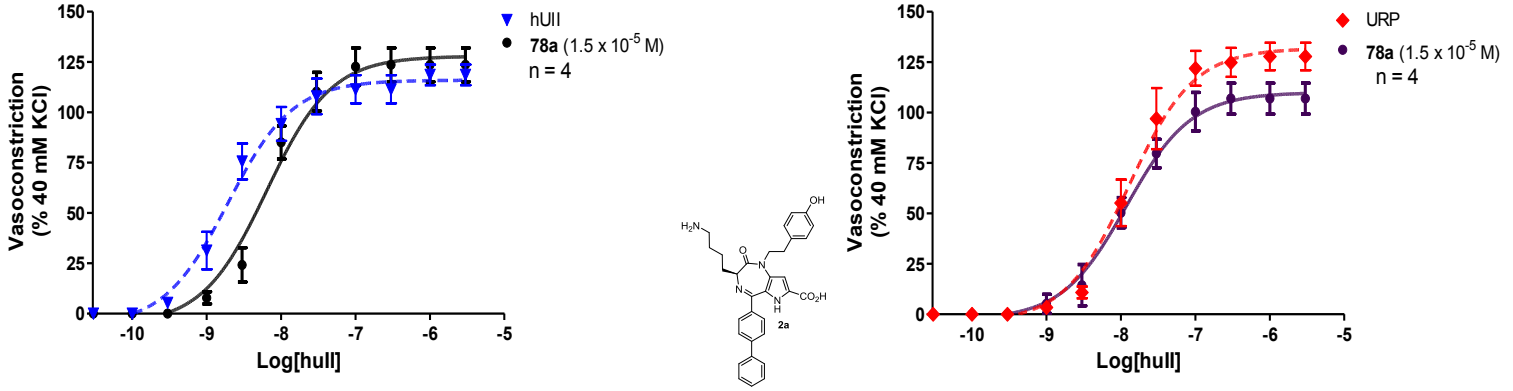

Effects of 78b on (A) hUII- and (B) URP-induced contraction of rat aortic ring

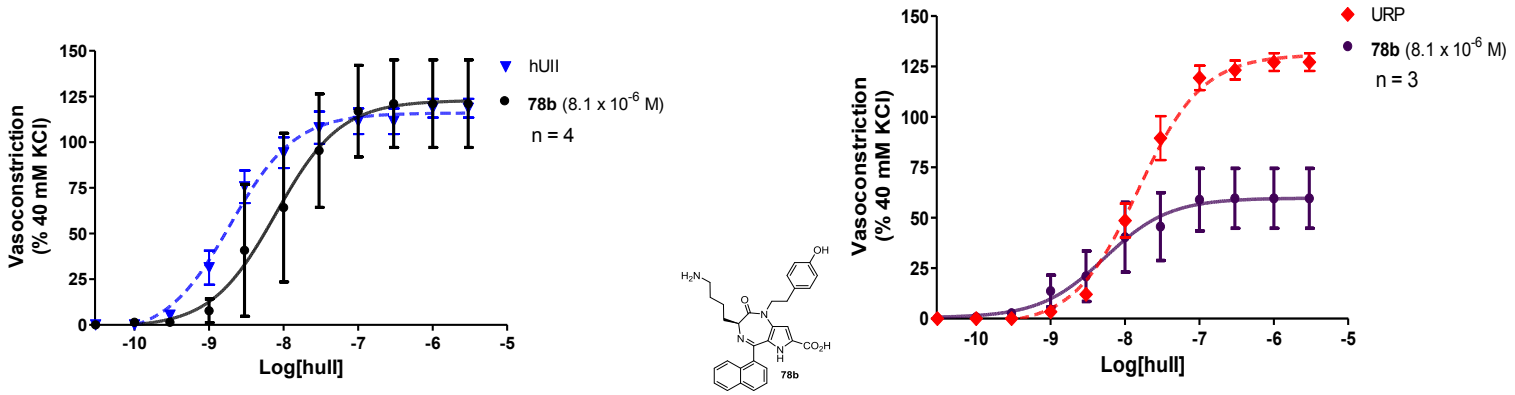

Effects of 78c on (A) hUII- and (B) URP-induced contraction of rat aortic ring

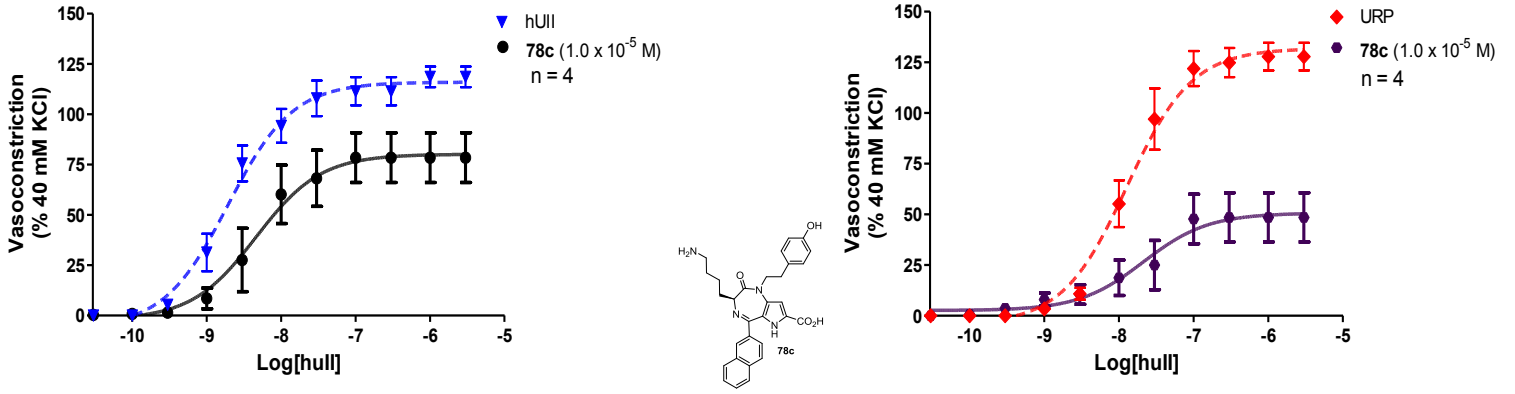

Effects of *R*-79a on (A) hUII- and (B) URP-induced contraction of rat aortic ring

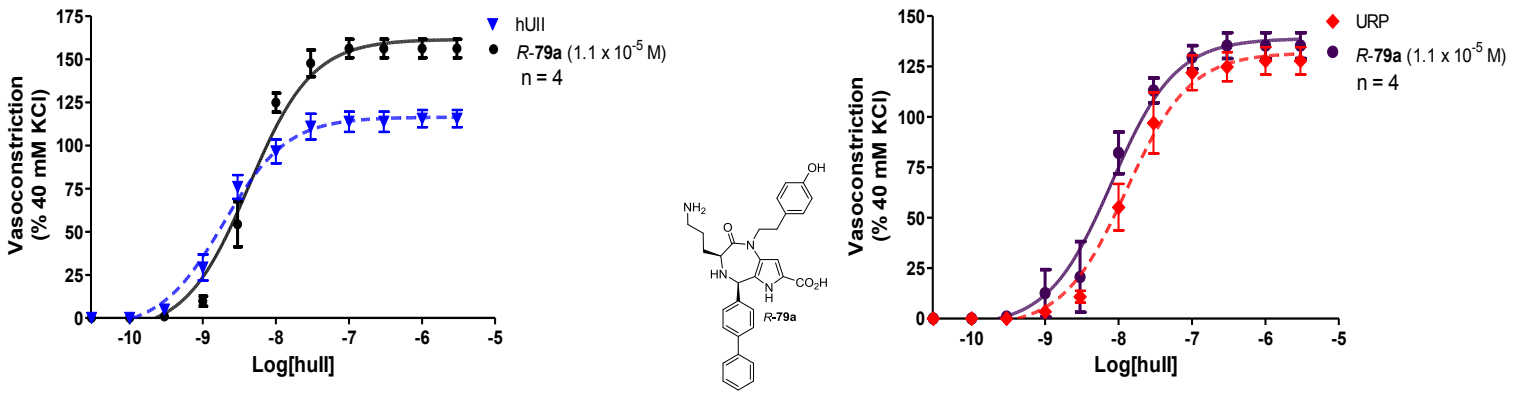

Effects of *S*-79b on (A) hUII- and (B) URP-induced contraction of rat aortic ring

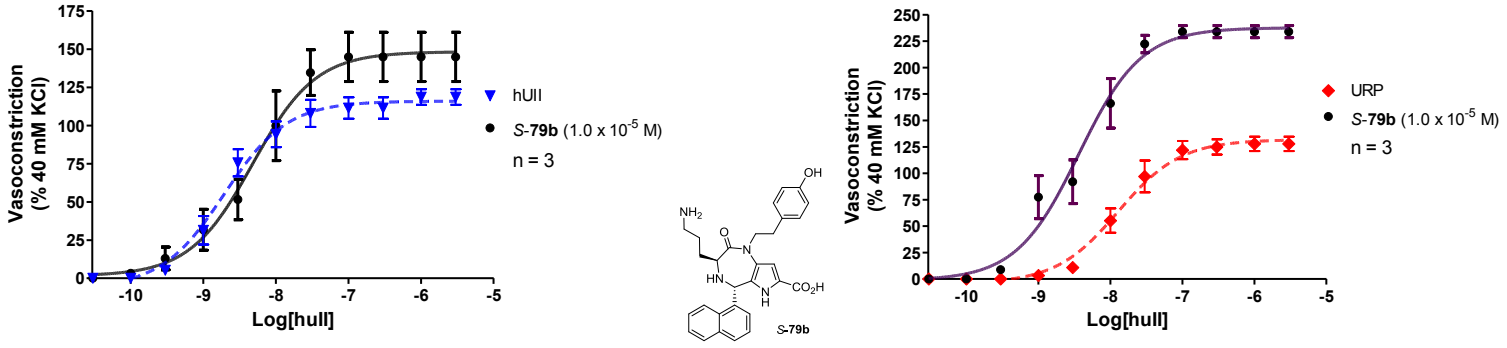

Effects of *R*-79b on (A) hUII- and (B) URP-induced contraction of rat aortic ring

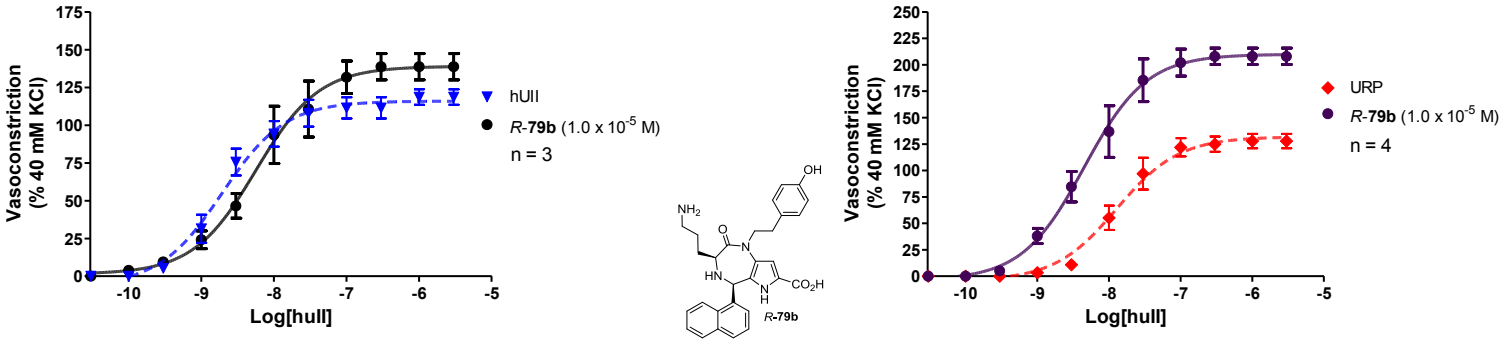

Effects of *S*-80a on (A) hUII- and (B) URP-induced contraction of rat aortic ring

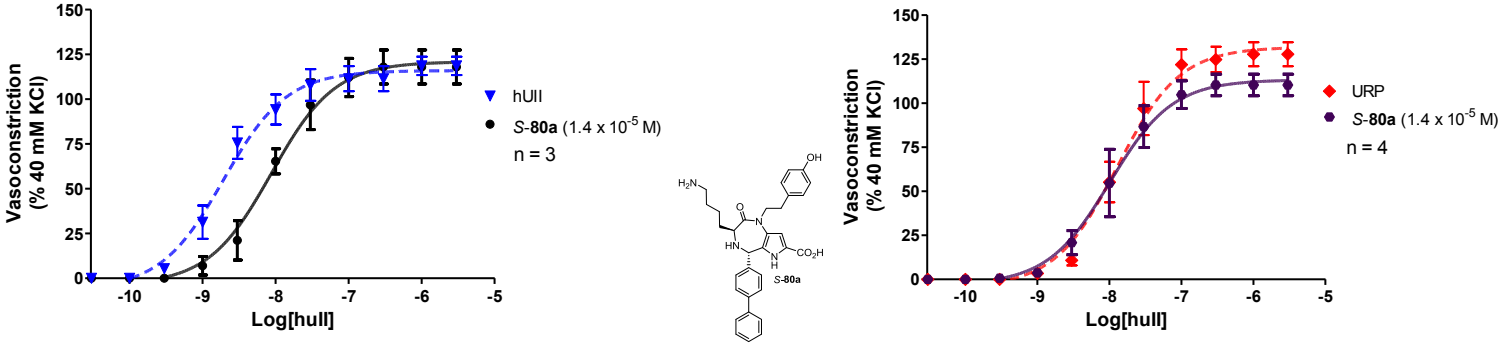

Effects of *R*-80a on (A) hUII- and (B) URP-induced contraction of rat aortic ring

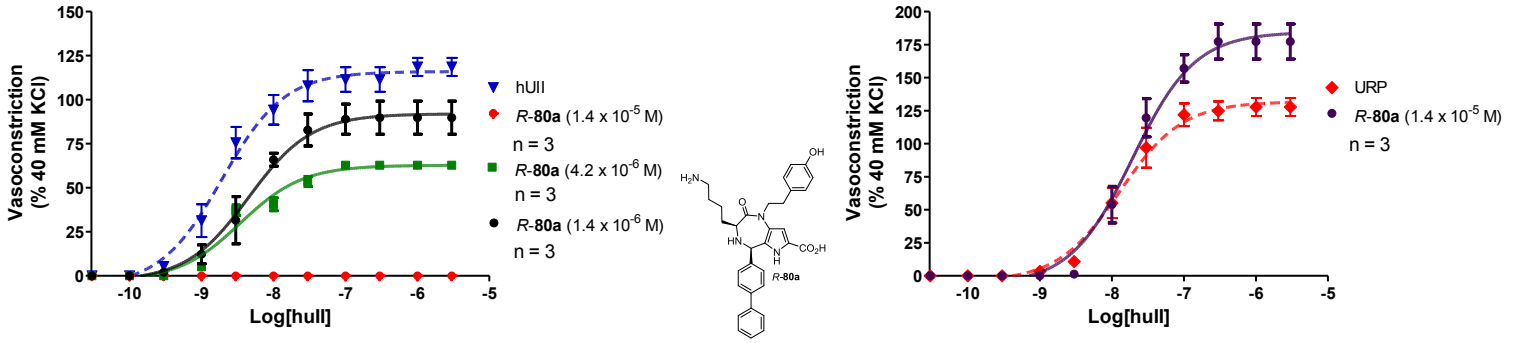

Effects of *S*-80c on (A) hUII- and (B) URP-induced contraction of rat aortic ring

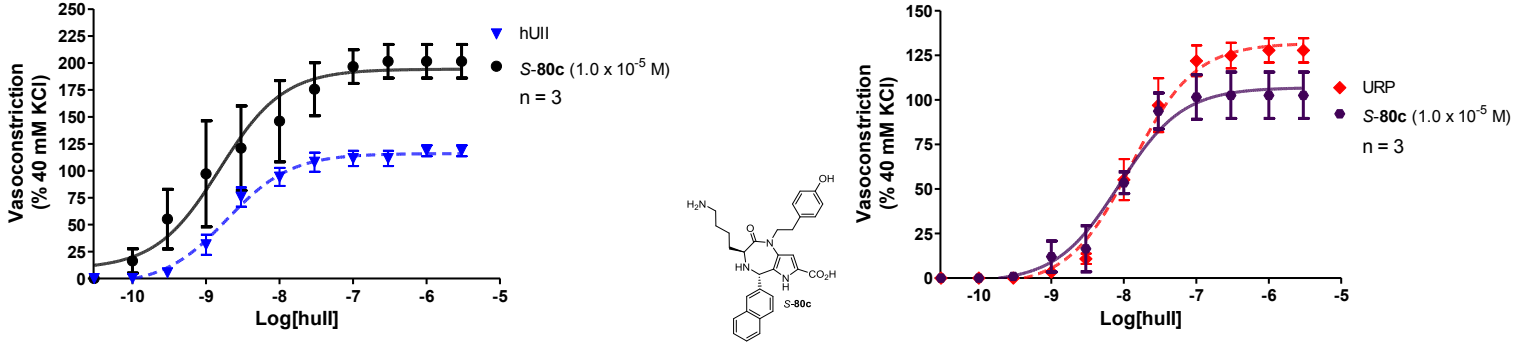

Effects of *R*-80c on (A) hUII- and (B) URP-induced contraction of rat aortic ring

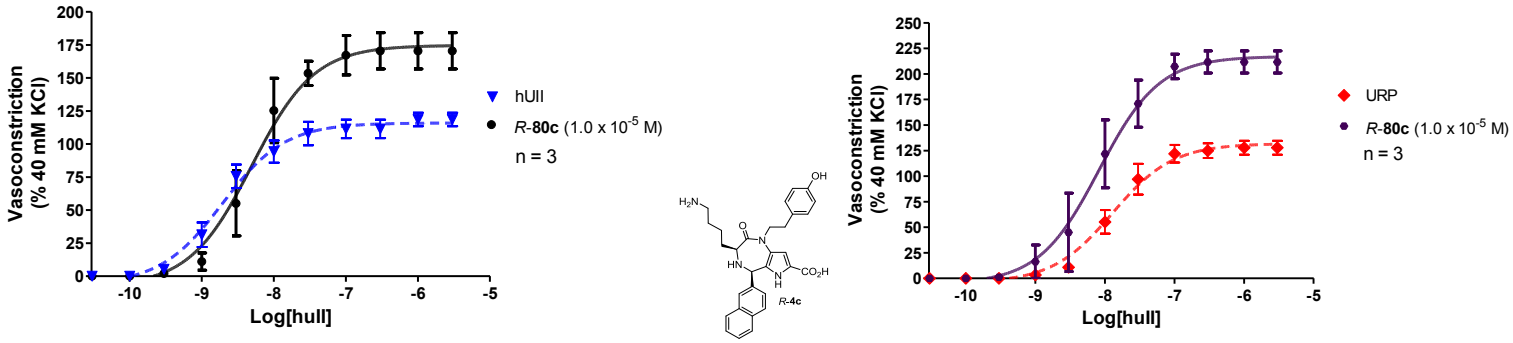

Dose response of endothelin-1-mediated contraction in the presence of *R*-80a

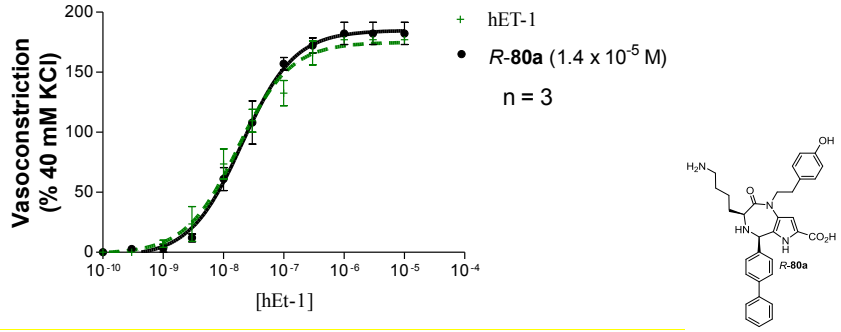

Annexe 4 : Spectres RMN des pyrrolo[3,2-*e*][1,4]diazépin-2-ones

RMN ^{1}H: (*S*)-5-([1,1'-Biphenyl]-4-yl)-3-(3-aminopropyl)-1-(4-hydroxyphenethyl)-2-oxo-1,2,3,6-tetrahydropyrrolo[3,2-*e*][1,4]diazepine-7-carboxylic acid (77a)

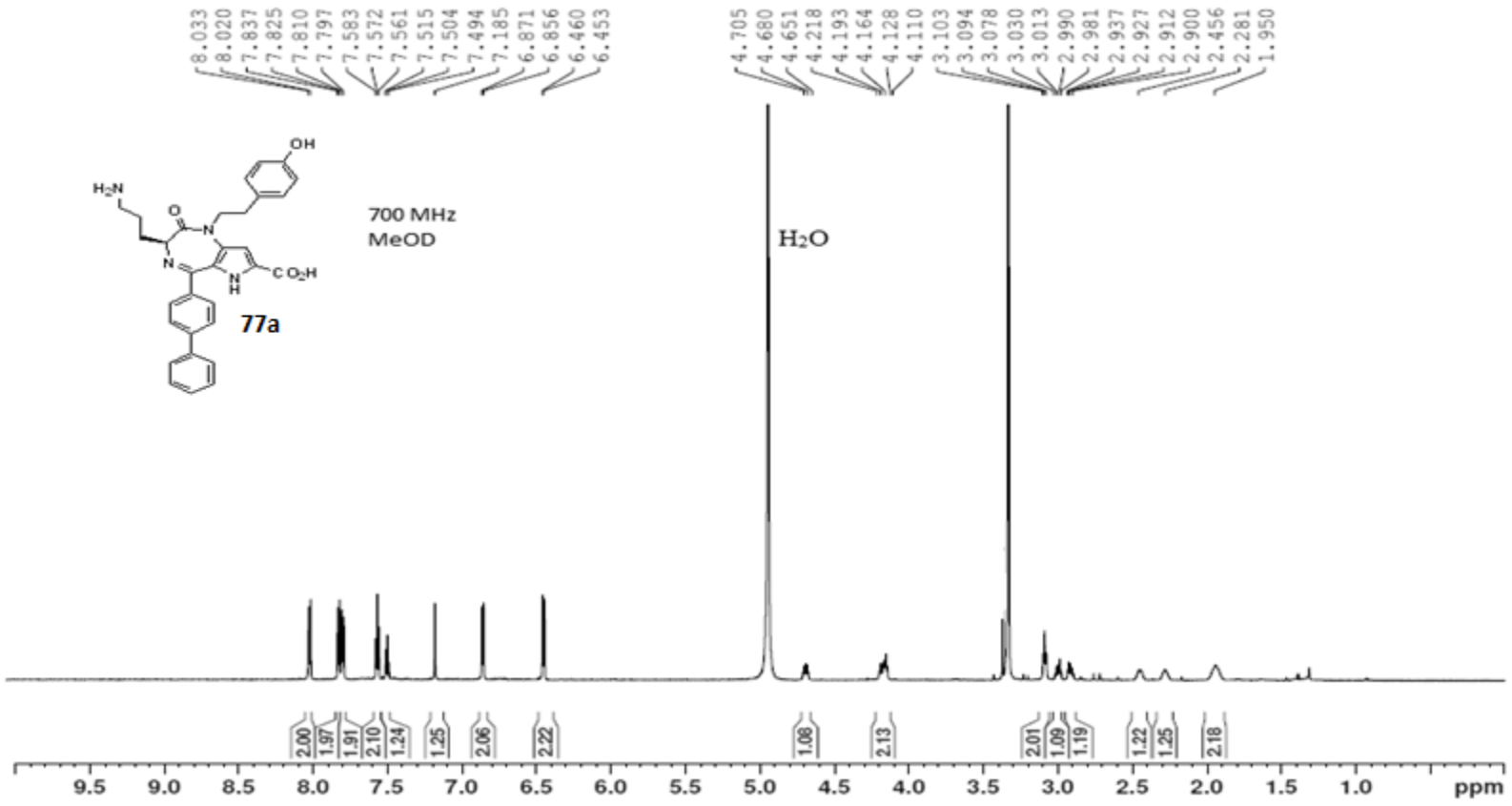

RMN ^{13}C: (*S*)-5-([1,1'-Biphenyl]-4-yl)-3-(3-aminopropyl)-1-(4-hydroxyphenethyl)-2-oxo-1,2,3,6-tetrahydropyrrolo[3,2-*e*][1,4]diazepine-7-carboxylic acid (77a)

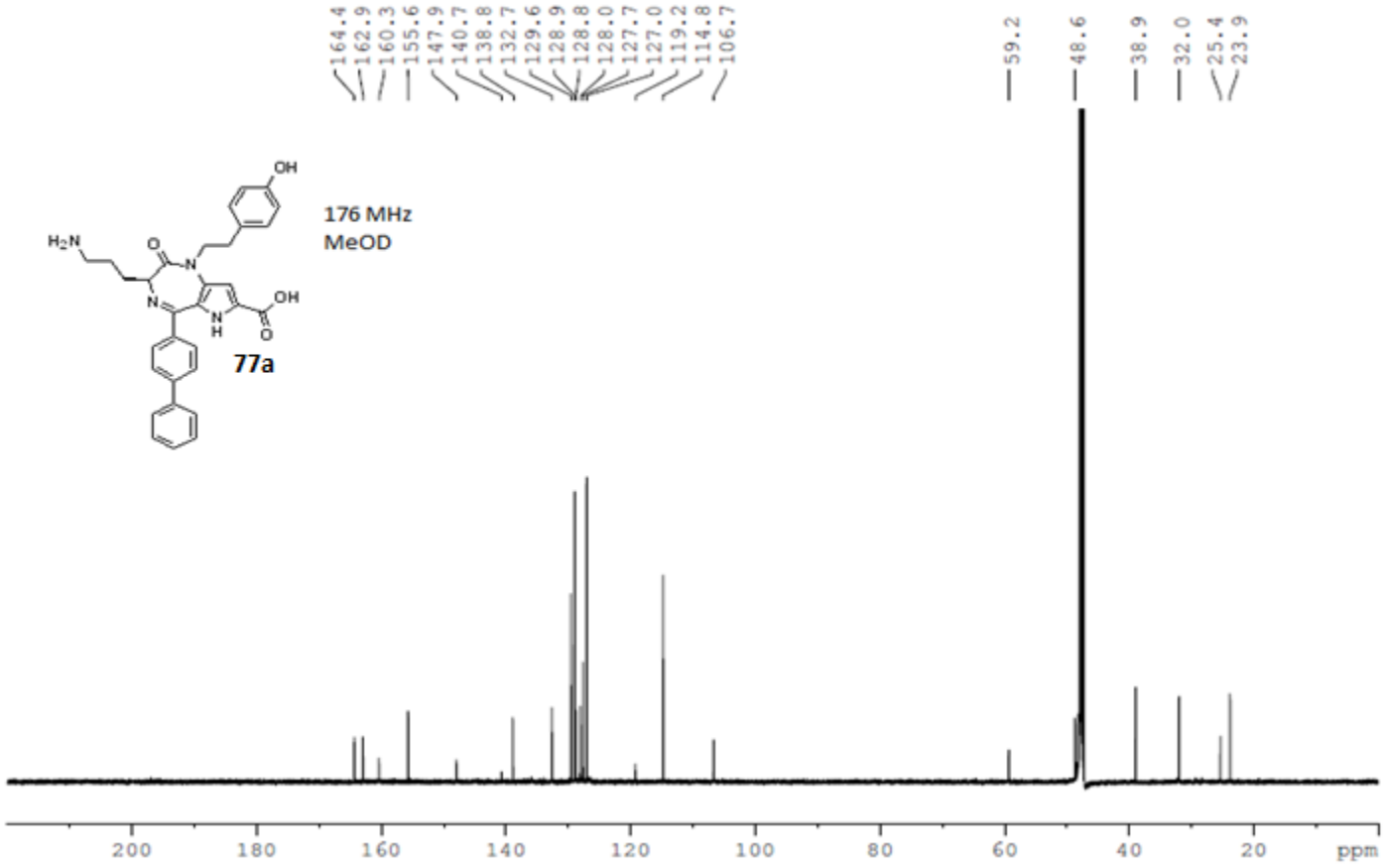

RMN ^{1}H: (*S*)-3-(4-Aminopropyl)-1-(4-hydroxyphenethyl)-5-(naphthalen-1-yl)-2-oxo-1,2,3,6-tetrahydropyrrolo[3,2-*e*][1,4]diazepine-7-carboxylic acid (77b)

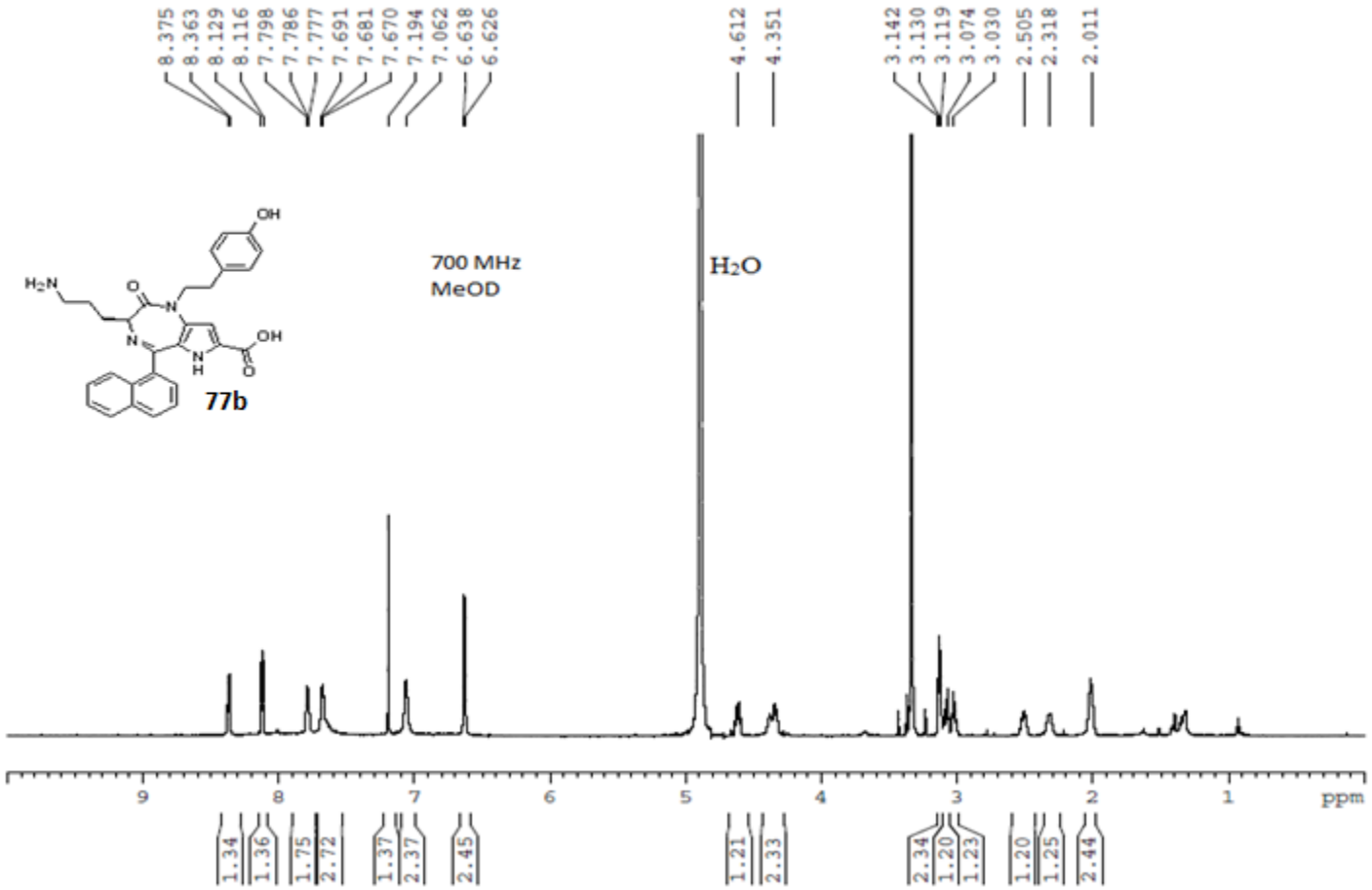

RMN ^{13}C: (*S*)-3-(4-Aminopropyl)-1-(4-hydroxyphenethyl)-5-(naphthalen-1-yl)-2-oxo-1,2,3,6-tetrahydropyrrolo[3,2-*e*][1,4]diazepine-7-carboxylic acid (77b)

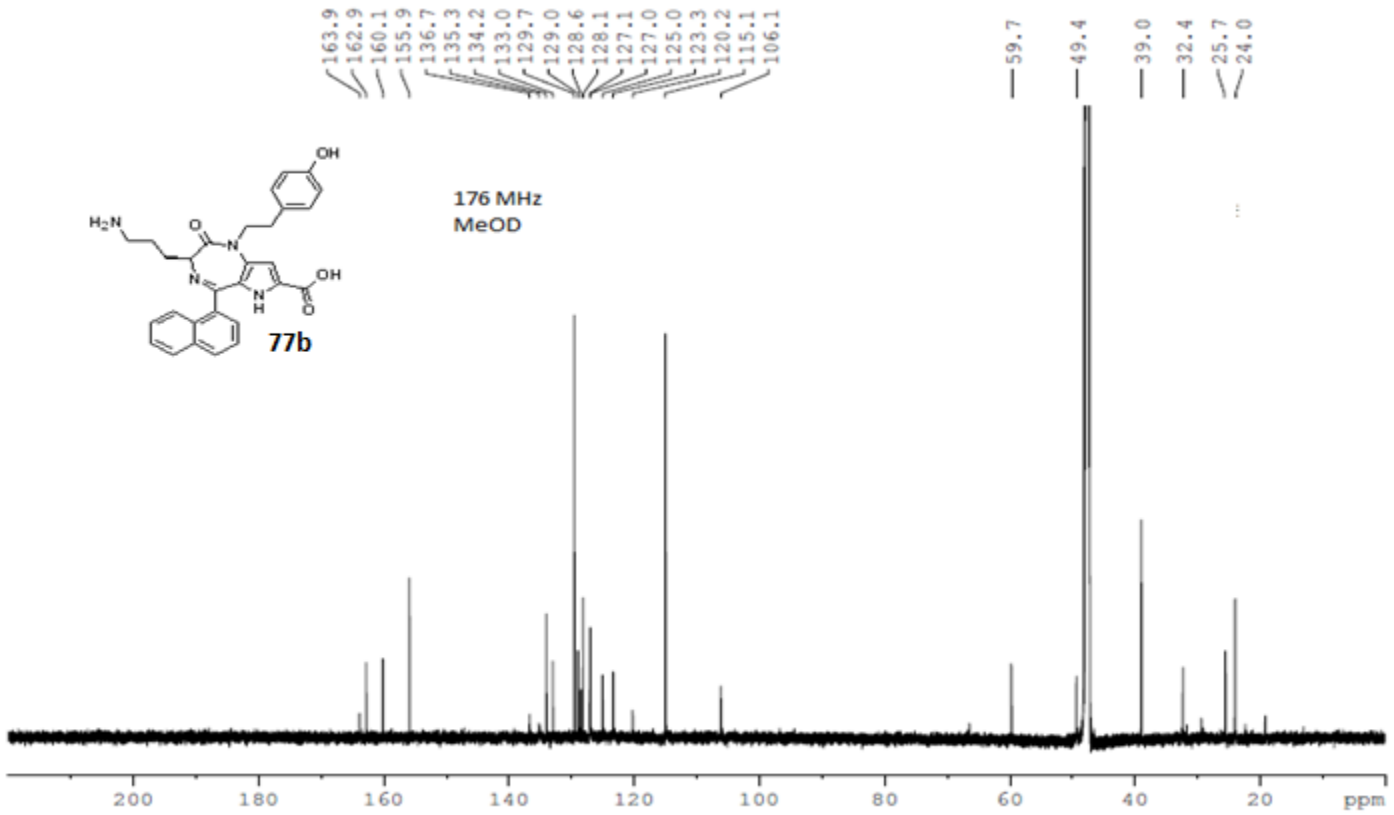

RMN ^{1}H: (*S*)-3-(4-Aminopropyl)-1-(4-hydroxyphenethyl)-5-(naphthalen-2-yl)-2-oxo-1,2,3,6-tetrahydropyrrolo[3,2-*e*][1,4]diazepine-7-carboxylic acid (77c)

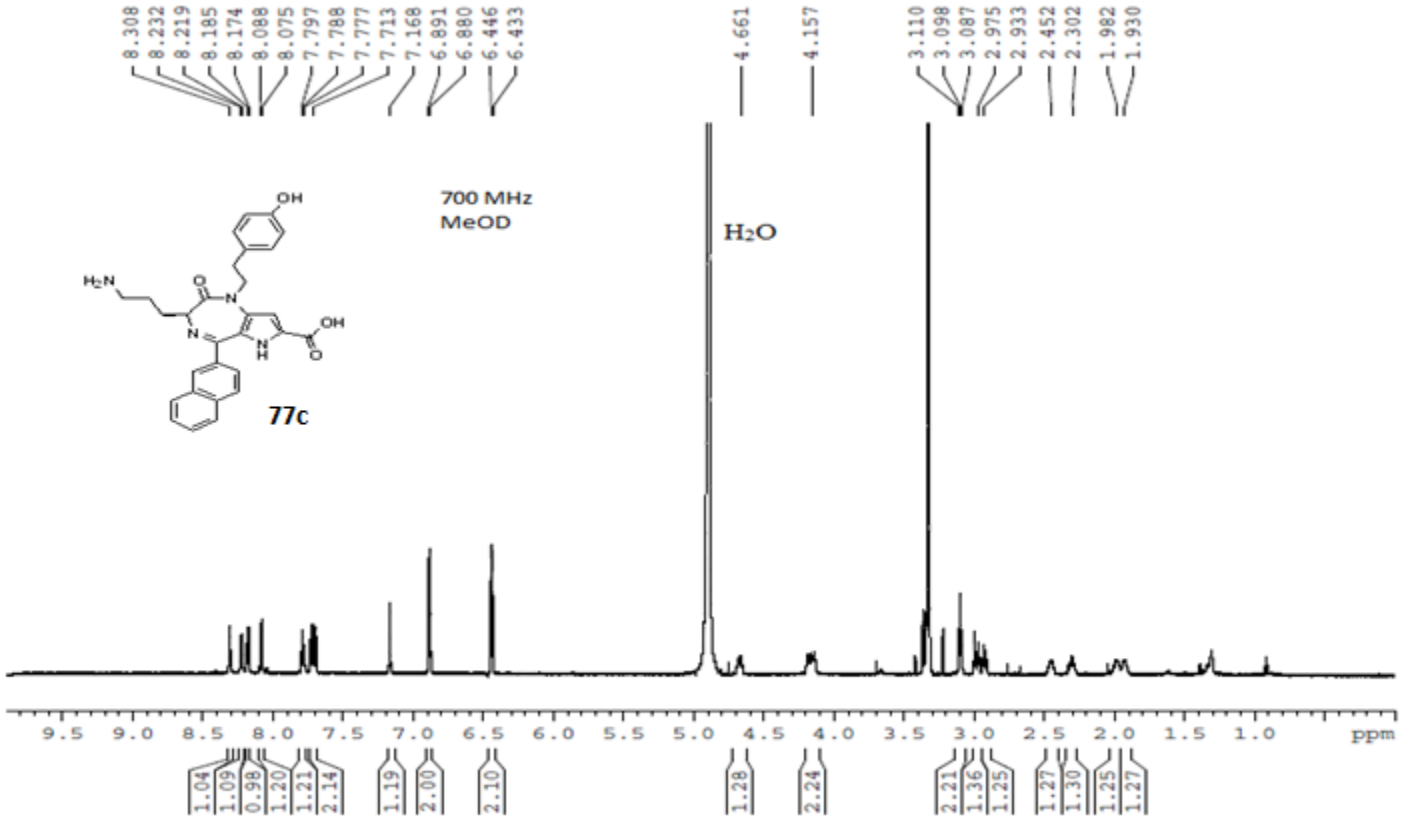

RMN ^{13}C: (*S*)-3-(4-Aminopropyl)-1-(4-hydroxyphenethyl)-5-(naphthalen-2-yl)-2-oxo-1,2,3,6-tetrahydropyrrolo[3,2-*e*][1,4]diazepine-7-carboxylic acid (77c)

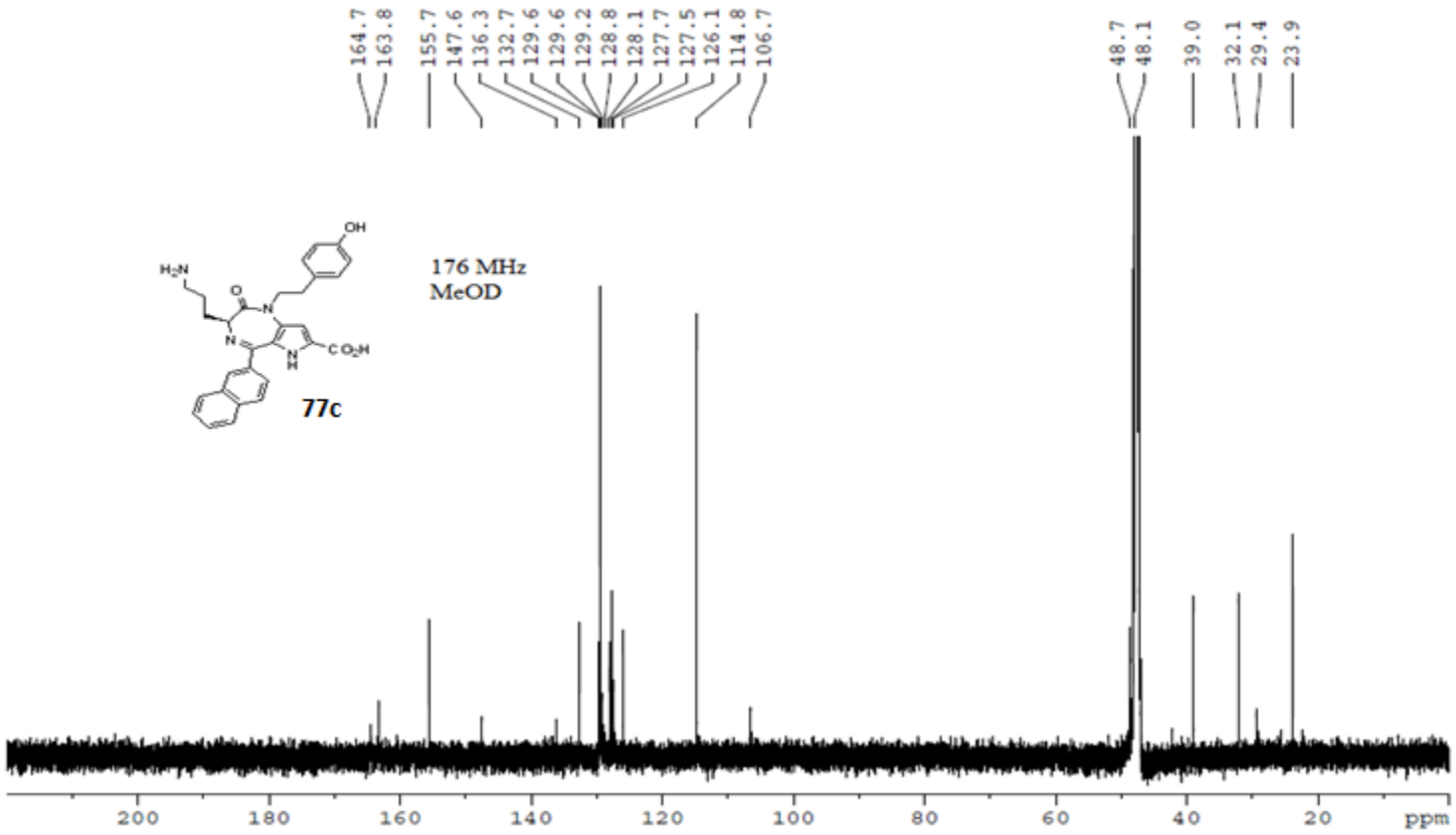

RMN ^{1}H: (S)-5-([1,1'-Biphenyl]-4-yl)-3-(4-aminobutyl)-1-(4-hydroxyphenethyl)-2-oxo-1,2,3,6-tetrahydropyrrolo[3,2-*e*][1,4]diazepine-7-carboxylic acid (78a)

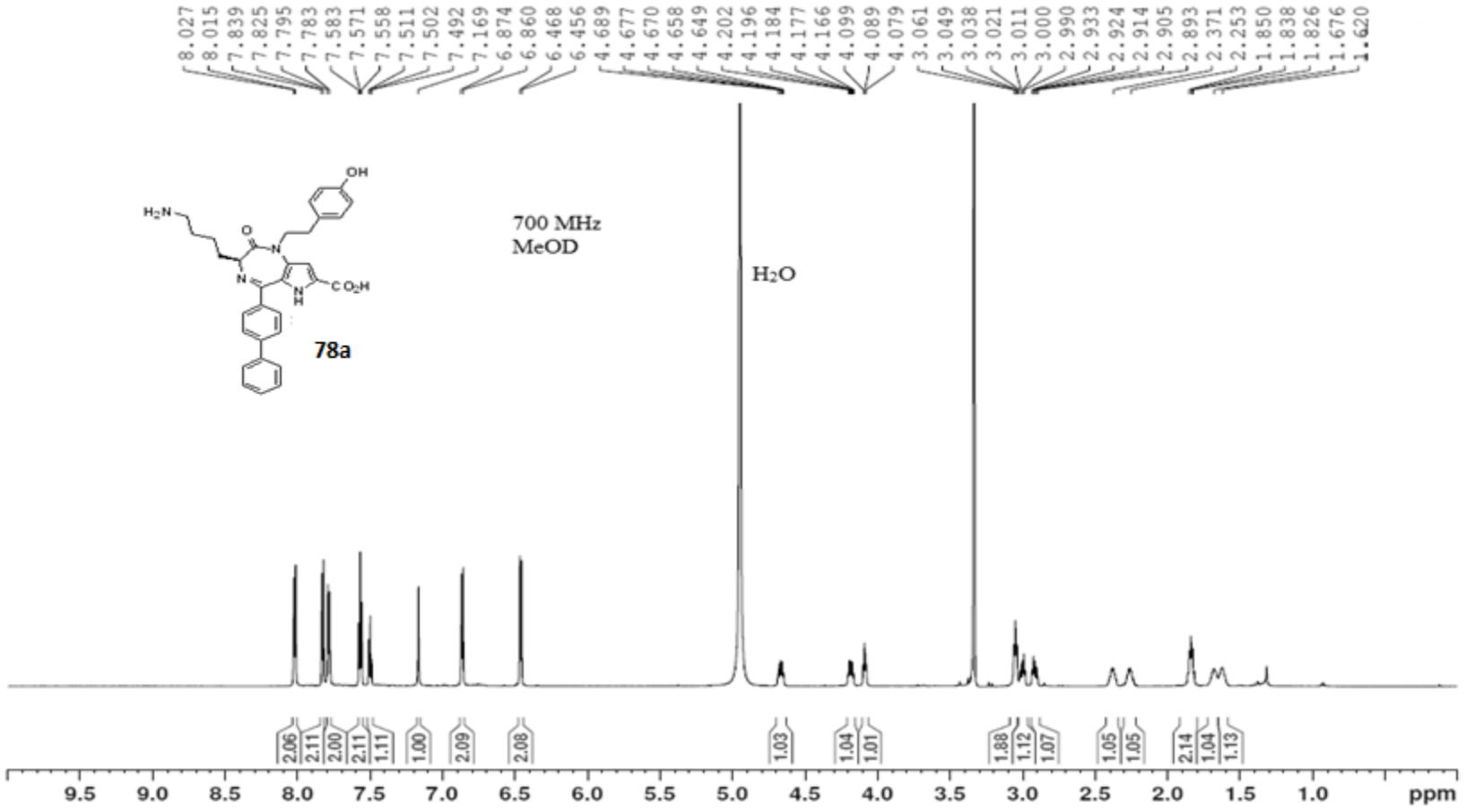

RMN ^{13}C: (S)-5-([1,1'-Biphenyl]-4-yl)-3-(4-aminobutyl)-1-(4-hydroxyphenethyl)-2-oxo-1,2,3,6-tetrahydropyrrolo[3,2-*e*][1,4]diazepine-7-carboxylic acid (78a)

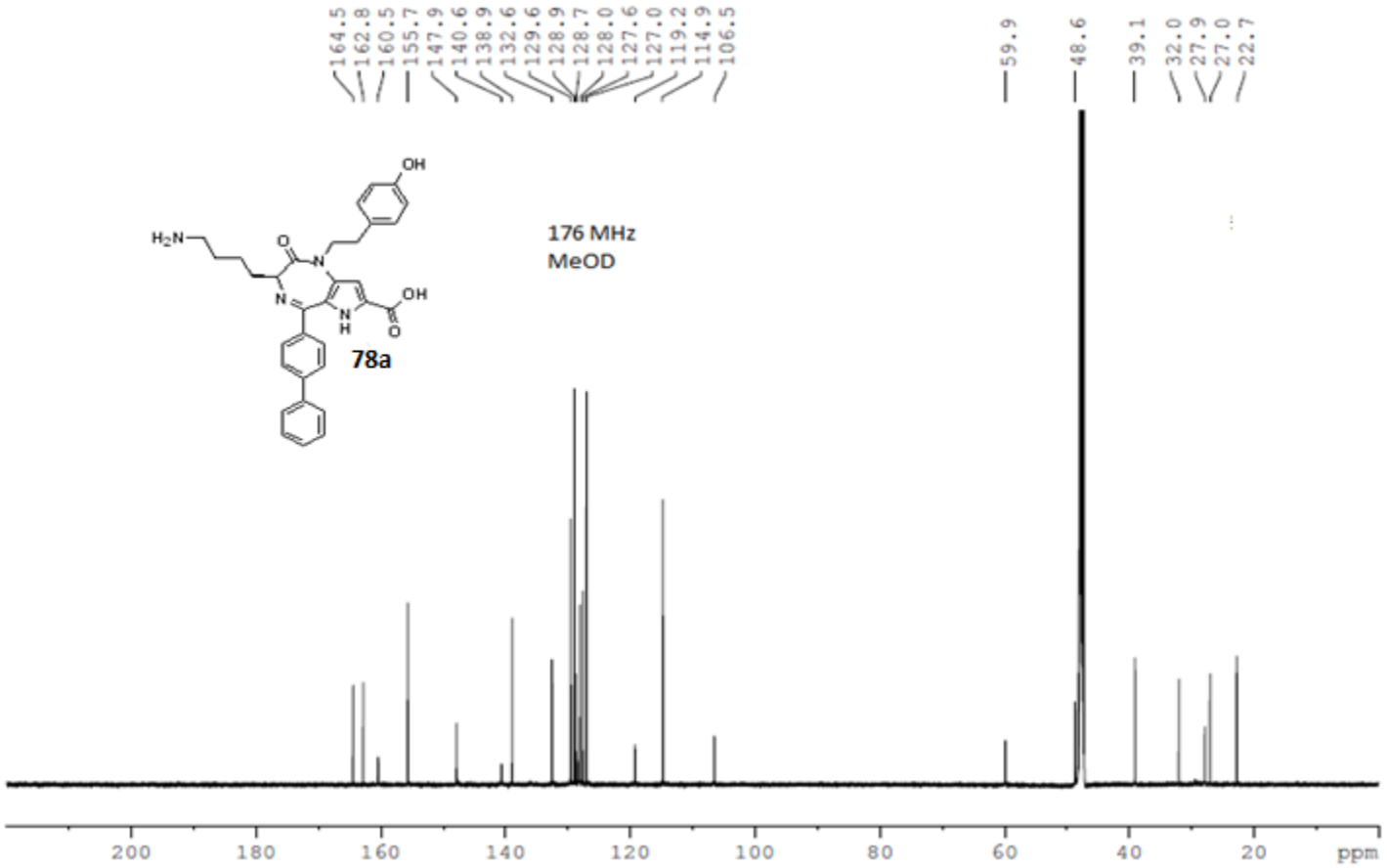

RMN ^{1}H: (*S*)-3-(4-Aminobutyl)-1-(4-hydroxyphenethyl)-5-(naphthalen-1-yl)-2-oxo-1,2,3,6-tetrahydropyrrolo[3,2-e][1,4]diazepine-7-carboxylic acid (78b)

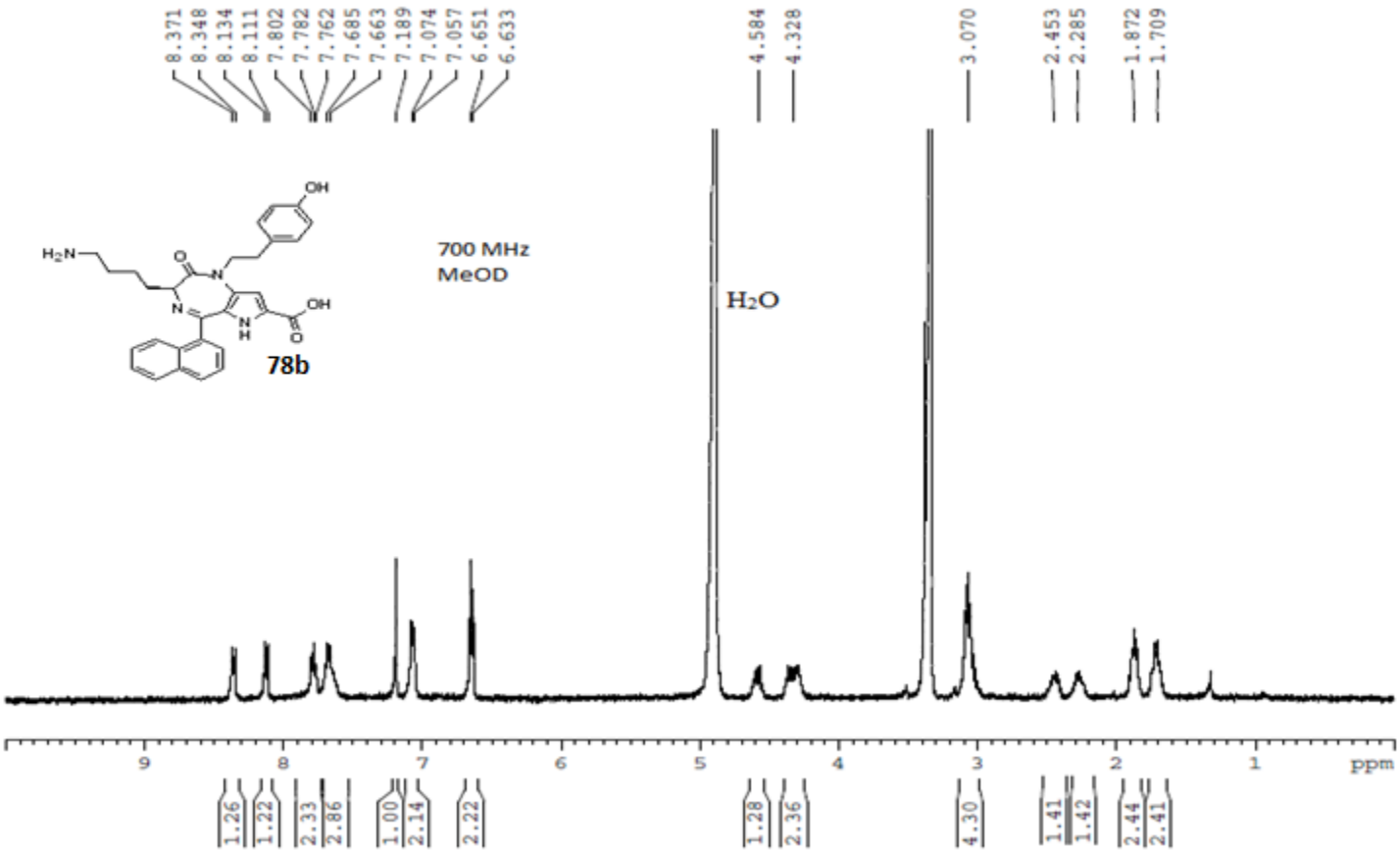

RMN ^{13}C: (*S*)-3-(4-Aminobutyl)-1-(4-hydroxyphenethyl)-5-(naphthalen-1-yl)-2-oxo-1,2,3,6-tetrahydropyrrolo[3,2-e][1,4]diazepine-7-carboxylic acid (78b)

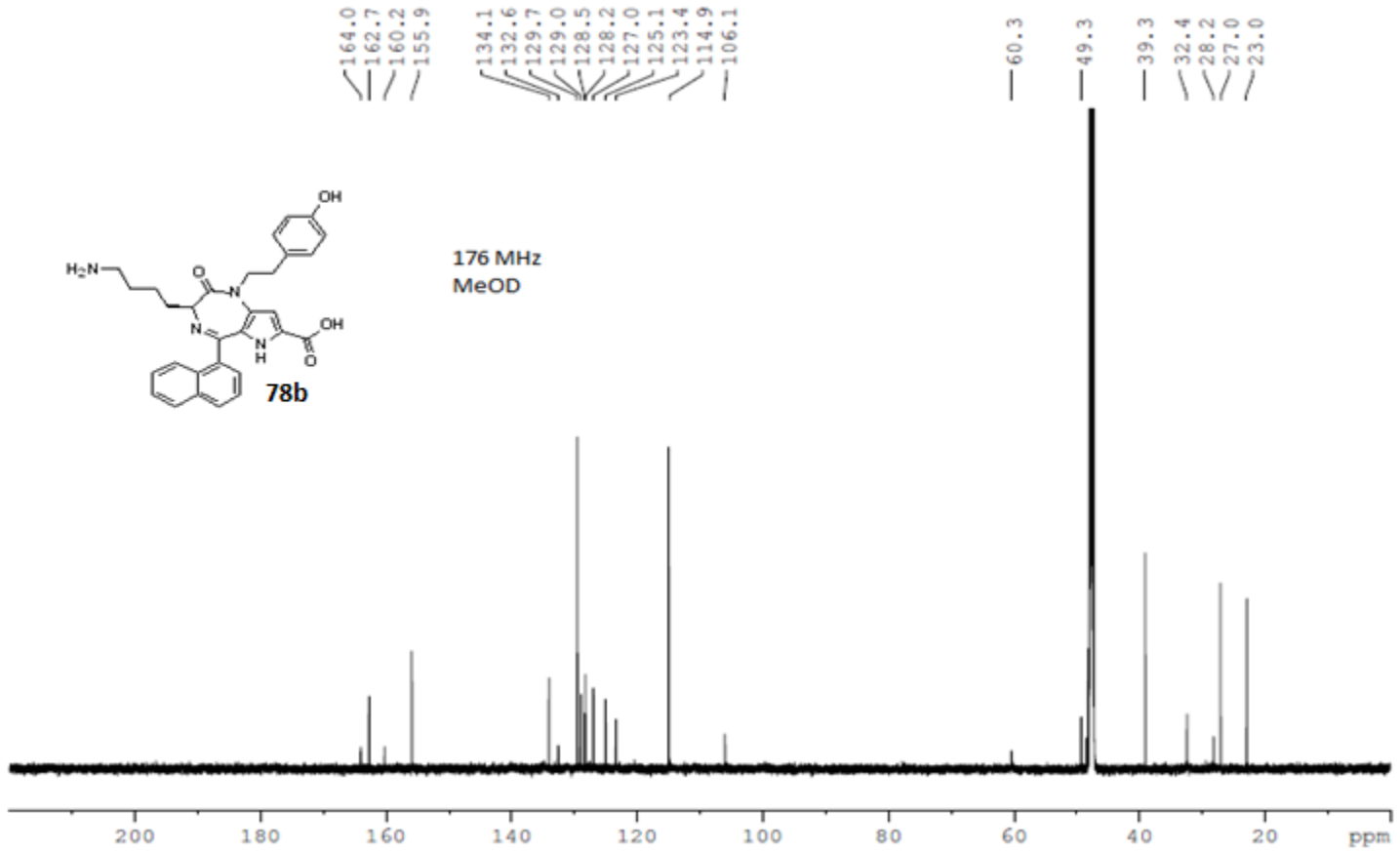

RMN ^{1}H: (*S*)-3-(4-Aminobutyl)-1-(4-hydroxyphenethyl)-5-(naphthalen-2-yl)-2-oxo-1,2,3,6-tetrahydropyrrolo[3,2-e][1,4]diazepine-7-carboxylic acid (78c)

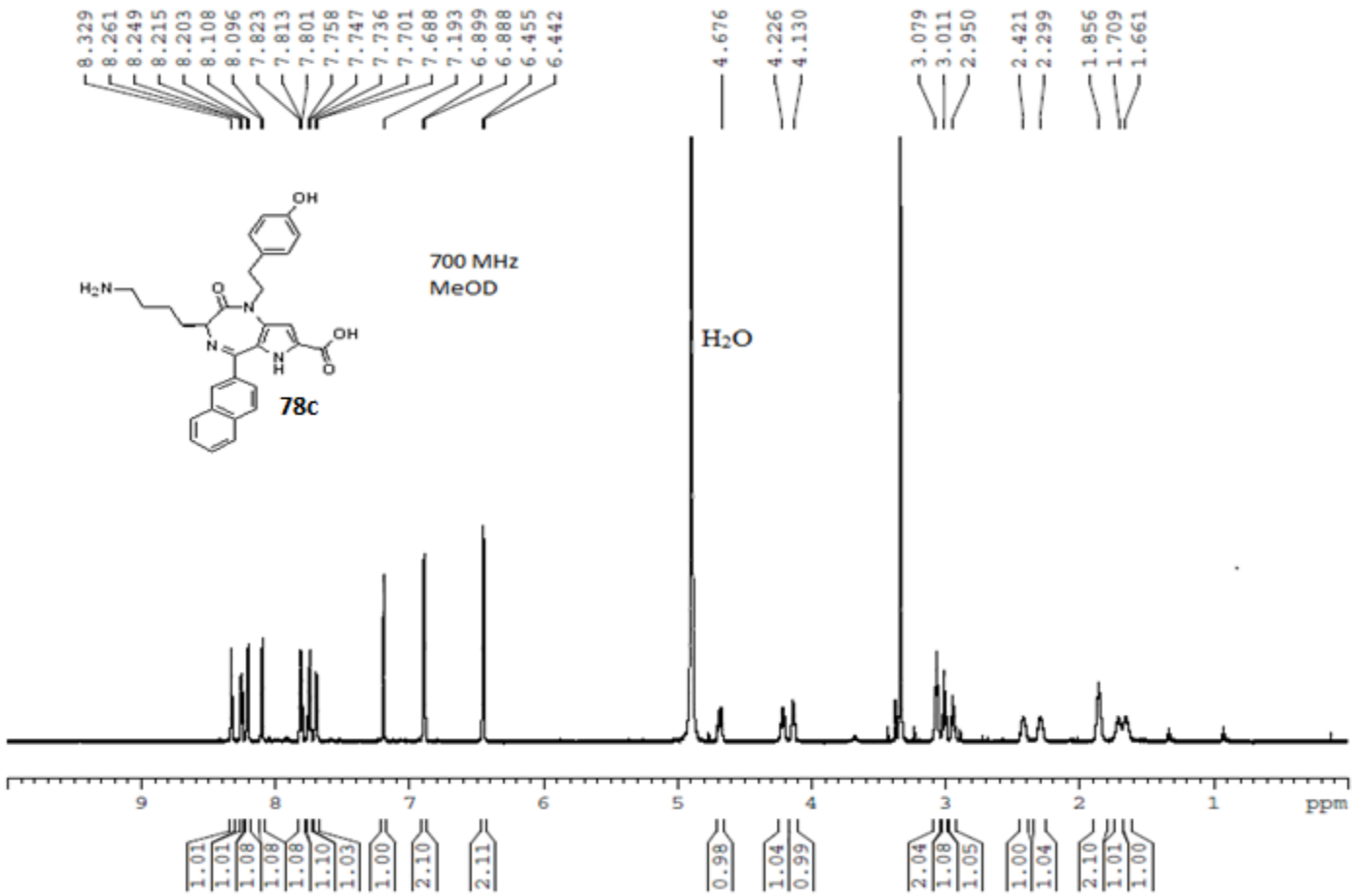

RMN ^{13}C: (*S*)-3-(4-Aminobutyl)-1-(4-hydroxyphenethyl)-5-(naphthalen-2-yl)-2-oxo-1,2,3,6-tetrahydropyrrolo[3,2-e][1,4]diazepine-7-carboxylic acid (78c)

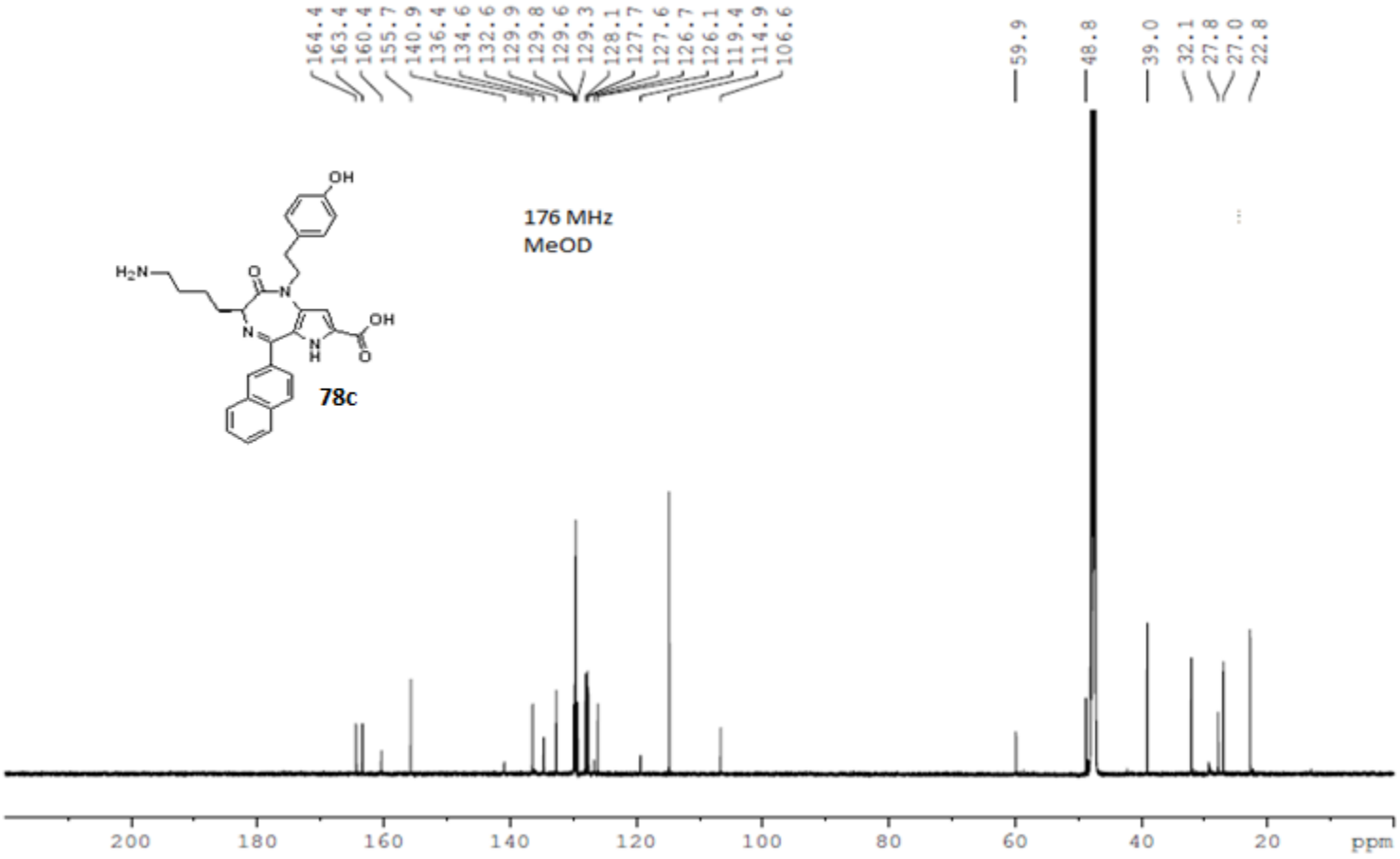

RMN ^{1}H: (3*S*,5*R*)-5-([1,1'-Biphenyl]-4-yl)-3-(3-aminopropyl)-1-(4-hydroxyphenethyl)-2-oxo-1,2,3,4,5,6-hexahydropyrrolo[3,2-*e*][1,4]diazepine-7-carboxylic acid (*R*-79a)

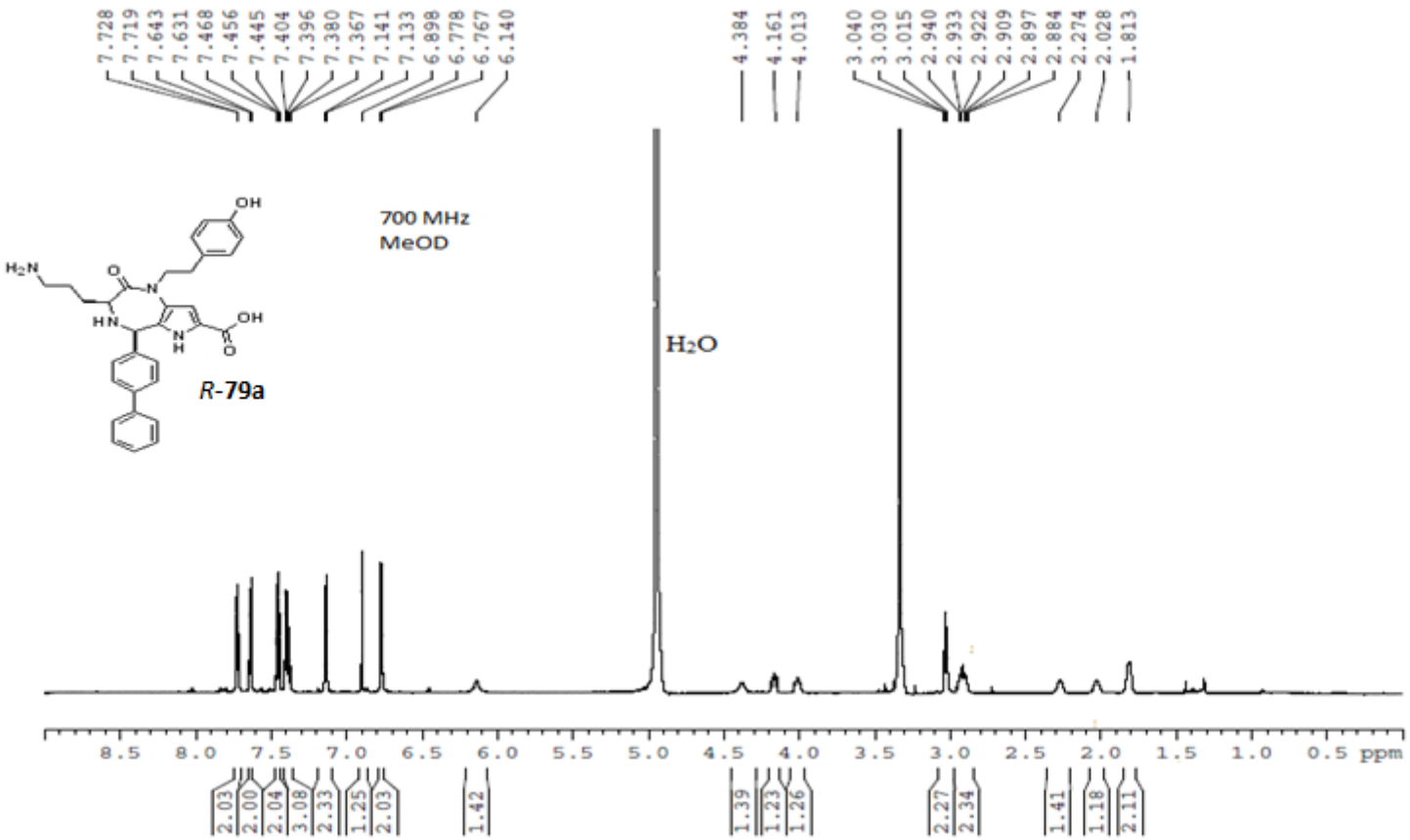

RMN ^{13}C: (3*S*,5*R*)-5-([1,1'-Biphenyl]-4-yl)-3-(3-aminopropyl)-1-(4-hydroxyphenethyl)-2-oxo-1,2,3,4,5,6-hexahydropyrrolo[3,2-*e*][1,4]diazepine-7-carboxylic acid (*R*-79a)

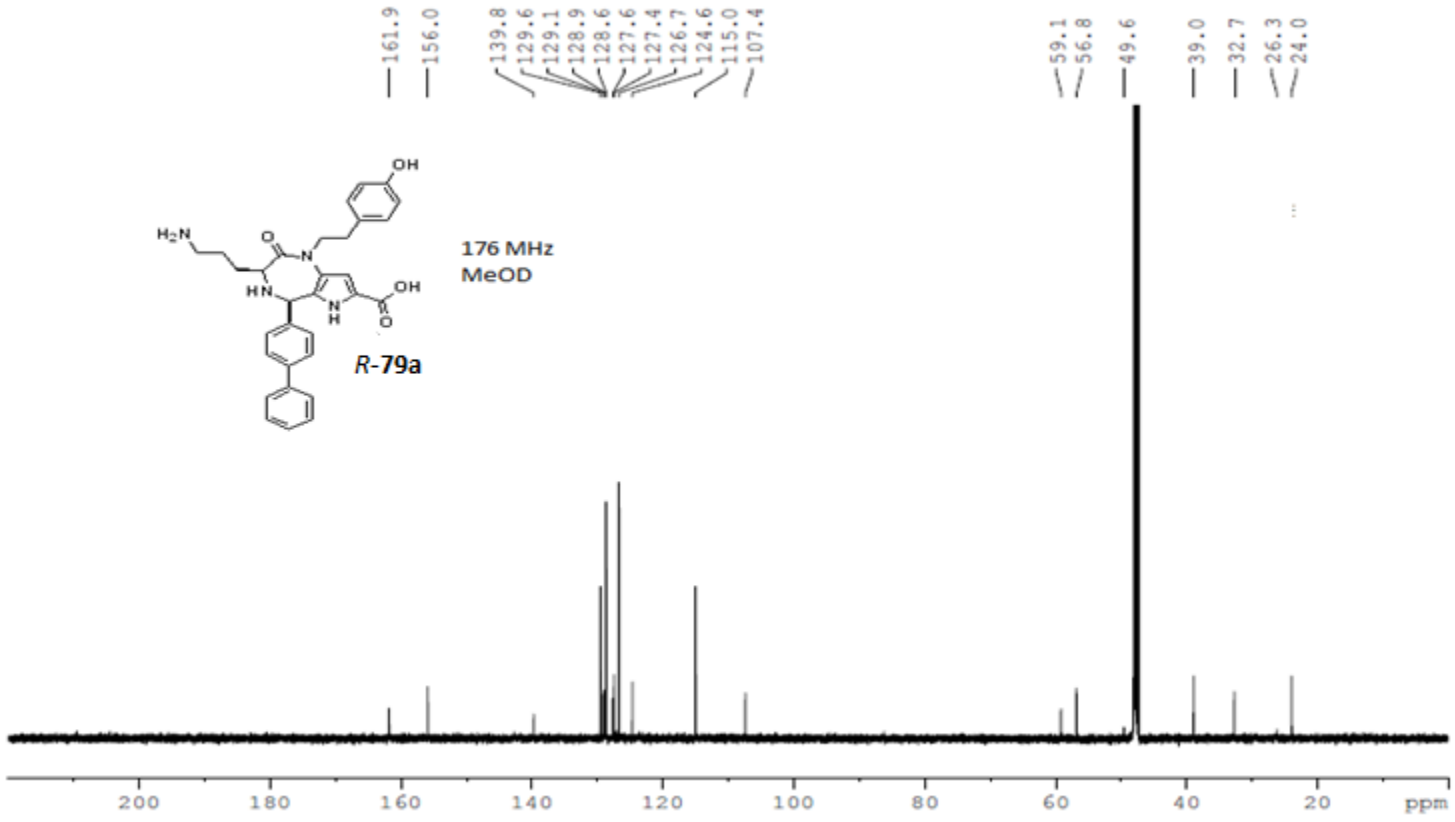

RMN ^{1}H: (3*S*,5*S*)-5-([1,1'-Biphenyl]-4-yl)-3-(4-aminobutyl)-1-(4-hydroxyphenethyl)-2-oxo-1,2,3,4,5,6-hexahydropyrrolo[3,2-e][1,4]diazepine-7-carboxylic acid (*S*-80a)

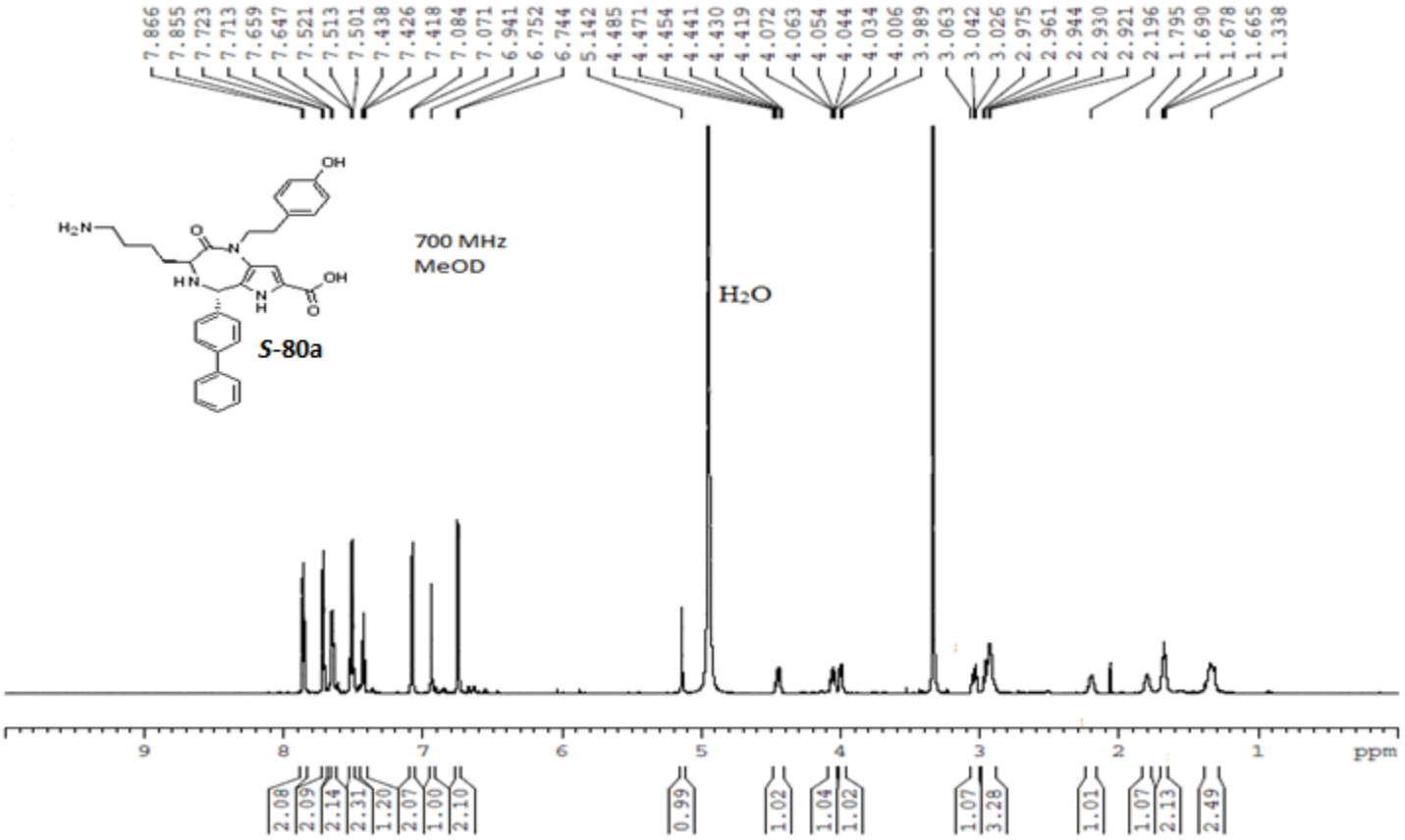

RMN ^{13}C: (3*S*,5*S*)-5-([1,1'-Biphenyl]-4-yl)-3-(4-aminobutyl)-1-(4-hydroxyphenethyl)-2-oxo-1,2,3,4,5,6-hexahydropyrrolo[3,2-e][1,4]diazepine-7-carboxylic acid (*S*-80a)

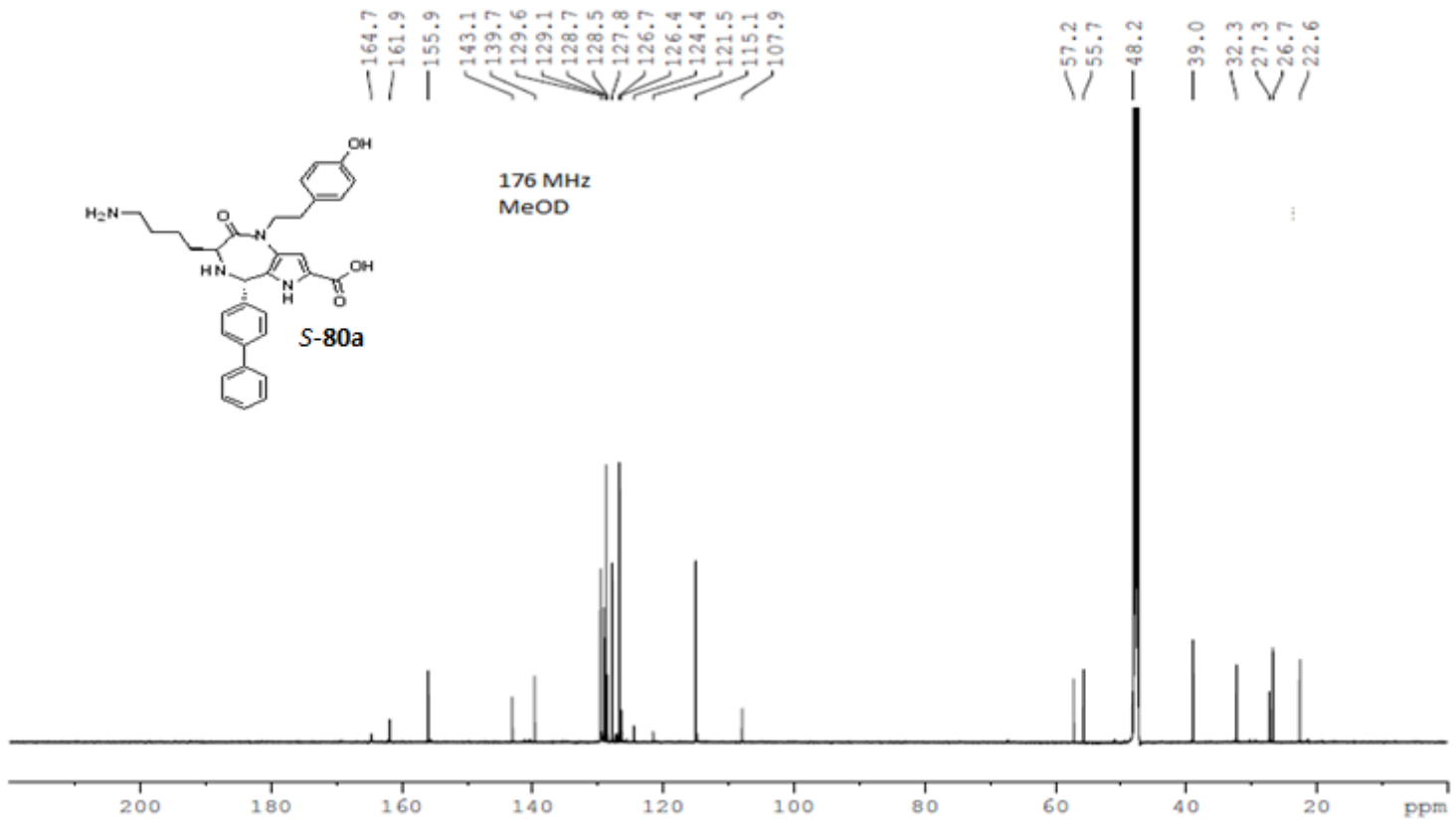

RMN ^{1}H: (3*S*,5*R*)-5-([1,1'-biphenyl]-4-yl)-3-(4-aminobutyl)-1-(4-hydroxyphenethyl)-2-oxo-1,2,3,4,5,6-hexahydropyrrolo[3,2-e][1,4]diazepine-7-carboxylic acid (*R*-80a)

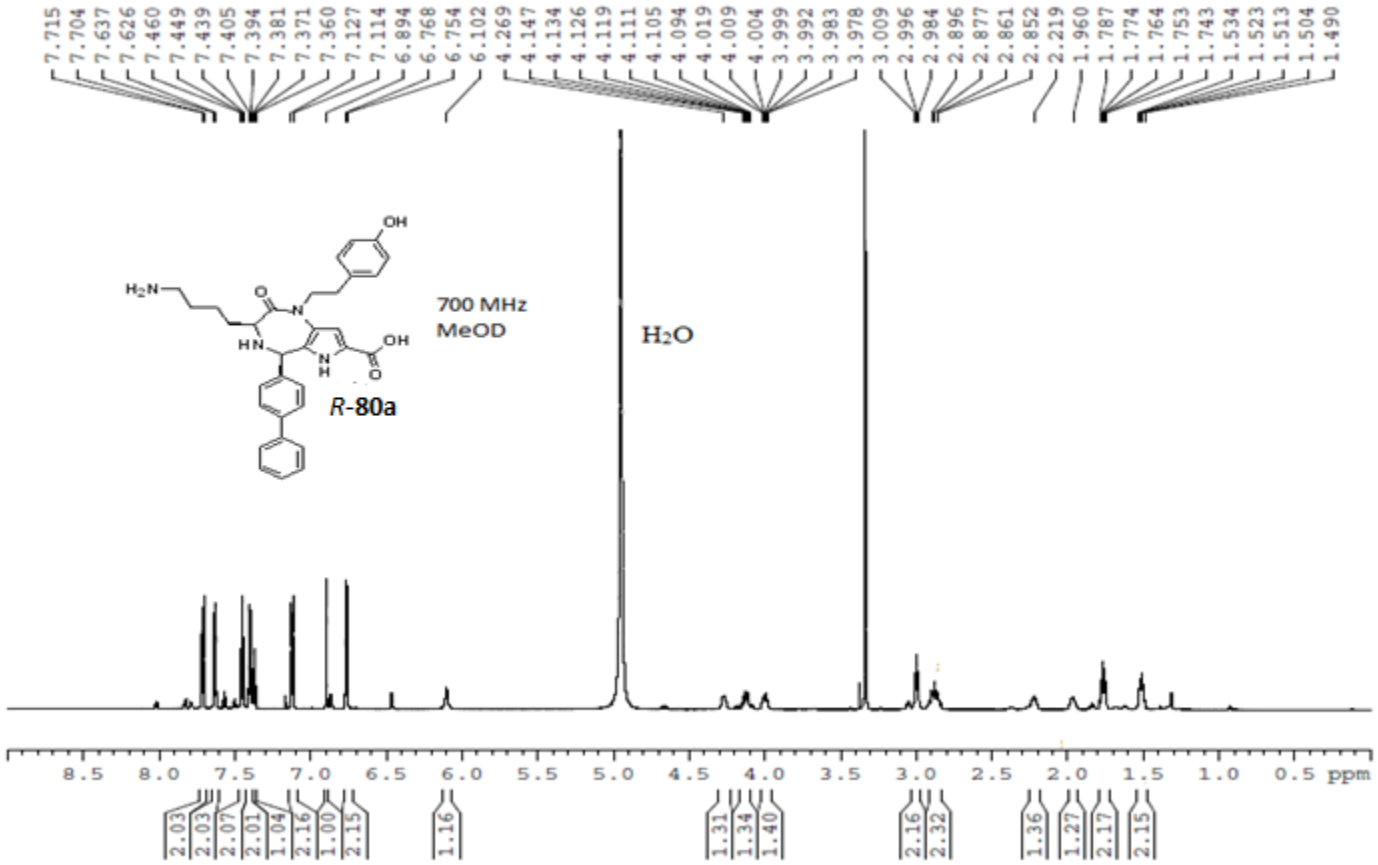

RMN ^{13}C: (3*S*,5*R*)-5-([1,1'-biphenyl]-4-yl)-3-(4-aminobutyl)-1-(4-hydroxyphenethyl)-2-oxo-1,2,3,4,5,6-hexahydropyrrolo[3,2-e][1,4]diazepine-7-carboxylic acid (*R*-80a)

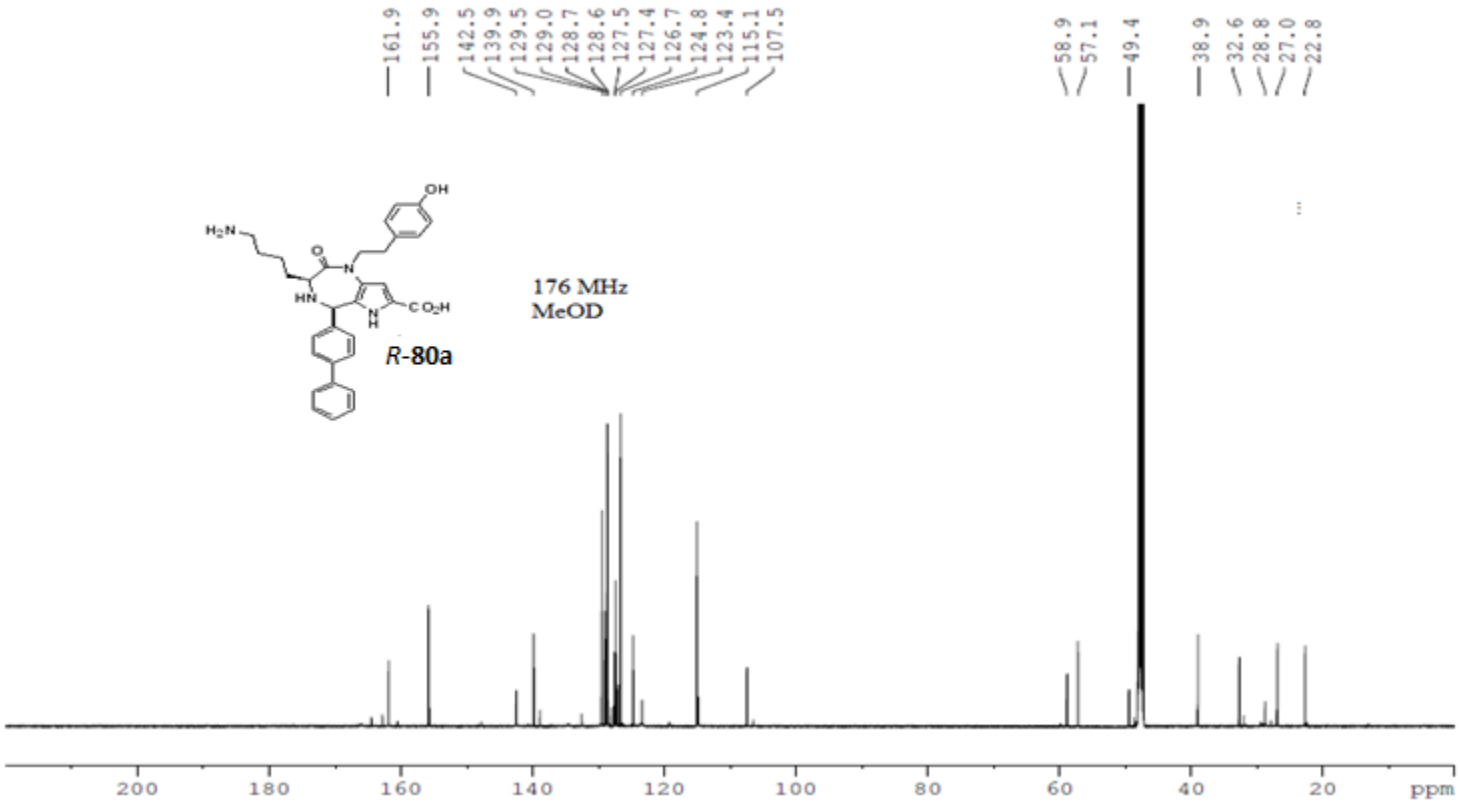

Annexe 5: Partie expérimentale de la synthèse des pyrrolo[3,2-*e*][1,4]diazépin-2-ones *N*-substitués

(*S*)-5-([1,1'-Biphenyl]-4-yl)-4-([1,1'-biphenyl]-4-ylmethyl)-3-(3-aminopropyl)-1-(4-hydroxyphenethyl)-2-oxo-1,2,3,4-tetrahydropyrrolo[3,2-e][1,4]diazepine-7-carboxylic acid 81a

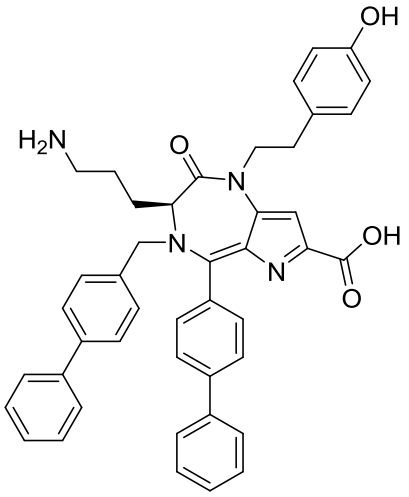

81a

The pyrrolo[3,2-e][1,4]diazepin-2-one **77a**, obtained during the Pictet-Spengler reaction with 4-biphenylcarboxaldehyde on resin **76a**, was purified by reverse phase preparative HPLC (column C, 30-60-90% MeOH, 30-60% MeOH over 13 min followed by 60% MeOH over 17 min and 60-90% MeOH over 1 min followed by 90% over 9 min, λ = 254 nm) give also 20 mg of **81a** with a purity of 71 % purity, (RP-HPLC-MS, column A, 50-60% MeOH over 10 min followed by 60% MeOH over 10 min, λ = 214 nm, R*t*: 9.4; $[M+H]^+$: 689.1). A second purification by reverse phase preparative HPLC (column C, 50-60% MeOH over 9 min followed by 60% MeOH over 21 min, λ = 254 nm) was necessary, follow by freeze-drying from 0.1 N HCl gave **81a** (15 mg, bright yellow oil, 0.029 mmol, 8% yield, 97% purity, RP-HPLC-MS, column A, eluent 1, 50-60% MeOH

over 8 min followed by 60% MeOH over 12 min, R*t*: 11.7; $[M+H]^+$: 689.1 and eluent 2, 10-50% MeCN over 8 min followed by 50% MeCN over 12 min, λ = 254 nm, (R*t*: 11.2; $[M+H]^+$: 689.1): $[\alpha]^{21}_D$ –74.9 (*c* 0.18, MeOH); ^{1}H NMR (MeOD, 700 MHz) δ 2.03 (s, 2H), 2.29 (m, 1H), 2.47 (m, 1H), 2.91 (m, 1H), 3.00 (m, 1H), 3.24 (t, *J* = 7.7 Hz, 2H), 4.18 (m, 2H), 4.32 (s, 2H), 4.71 (m, 1H), 6.45 (d, *J* = 7.3 Hz, 2H), 6.86 (d, *J* = 7.3 Hz, 2H), 7.20 (s, 1H), 7.41 (t, *J* = 7.4 Hz, 1H), 7.51 (m, 3H). 7.57 (t, *J* = 7.4 Hz, 2H), 7.66 (m, 4H), 7.77 (m, 2H), 7.82 (m, 4 H), 8.03 (d, *J* = 9.9 Hz, 2H); ^{13}C NMR (MeOD, 176 MHz) δ 22.5 (CH_2), 25.4 (CH_2), 32.0 (CH_2), 46.5 (CH_2), 48.7 (CH_2), 50.6 (CH_2), 59.1 (CH), 106.7 (CH), 114.8 (2 CH), 119.2 (C), 126.6 (2 CH), 127.0 (2 CH), 127.4 (2 CH), 127.6 (CH), 127.7 (2 CH), 128.0 (C), 128.6 (2 CH), 128.8 (CH), 129.0 (2 CH), 129.6 (2 CH), 130.0 (C), 130.3 (2 CH), 132.7 (2 CH), 138.8 (2 C), 139.9 (C), 140.9 (C), 142.5 (2 C), 148.1 (C), 155.7 (C), 160.3 (C=O), 163.0 (C), 164.2 (C=O); HRMS calcd for $C_{44}H_{41}N_4O_4$ $[M+ H]^+$: 689.3122 found: 689.3110.

(*S*)-5-([1,1'-Biphenyl]-4-yl)-4-([1,1'-biphenyl]-4-ylmethyl)-3-(3-aminopropyl)-1-(4-hydroxyphenethyl)-2-oxo-1,2,3,4-hexahydropyrrolo[3,2-e][1,4]diazepine-7-carboxylic acid 81b

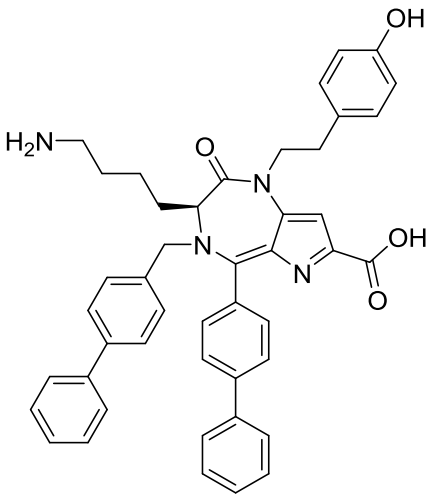

81b

The pyrrolo[3,2-e][1,4]diazepin-2-one **78a**, obtained during the Pictet-Spengler reaction with 4-biphenylcarboxaldehyde on resin **76b**, was purified by reverse phase preparative HPLC (column C, 20-60-90% MeOH, 20-60% MeOH over 13 min, followed by 60% MeOH over 12 min and 60-90% MeOH over 1 min, followed by 90% MeOH over 14 min, λ = 214 nm) give also 16 mg of **81b** with 90% purity (RP-HPLC-MS column A, 20-60% MeCN over 10 min followed by 60% MeCN over 10 min, λ = 214 nm, R*t*: 11.0; $[M+H]^+$: 703.3). Acid **81b** (yellow oil, 8 mg, 0.011 mmol, 4 % yield) was isolated by reverse phase preparative HPLC (column C, 20-60% MeCN over15 min followed by 60% MeCN over 25 min, λ = 214 nm) in 97% and 98% purity respectively (RP-HPLC-MS column A, eluent 1, 20-90% MeOH over 8 min followed by 90% MeOH over 12 min, λ=254 nm, R*t*: 11.9 and eluent 2, 20-60% MeCN over 8 min followed by 60% MeCN over 12 min, λ=254 nm, R*t*: 11.4, $[MH]^+$: 703.1): $[\alpha]^{21}_D$ = –31.2 (*c* = 0.92, MeOH); ^{1}H NMR (MeOD, 700 MHz) δ 1.58 (s, 2H), 1.90 (s, 2H), 2.59 (s, 1H), 2.66 (s,

1H), 2.81 (t, *J* = 8.1 Hz, 2H), 3.08 (t, *J* = 9.1 Hz, 2H), 4.09 (m, 1H), 4.31 (m, 1H), 4.47 (s 1H), 5.10 (d, *J* = 14.1 Hz, 1H), 5.50 (d, *J* = 16.1 Hz, 1H), 6.70 (d, *J* = 7.3 Hz, 2H), 6.92 (d, *J* = 8.5 Hz, 2H), 7.03 (d, *J* = 9.7 Hz, 3H), 7.35 (t, *J* = 7.3 Hz, 1H), 7.41 (t, *J* = 7.3 Hz, 2H), 7.51 (m, 6H), 7.56 (t, *J* = 7.9 Hz, 2H), 7.82 (d, *J* = 7.3 Hz, 2H), 7.96 (d, *J* = 8.5 Hz, 1H), 8.10 (d, *J* = 8.5 Hz, 1H), 8.22 (d, *J* = 10.9 Hz, 1H); ^{13}C NMR (MeOD, 175 MHz) δ 23.0 (CH_2), 27.1 (CH_2), 27.5 (CH_2), 32.8 (CH_2), 39.0 (CH_2), 49.7 (CH_2), 54.3 (CH_2), 65.5 (CH), 105.7 (CH), 115.0 (2 CH), 122.0 (C), 126.5 (2 CH), 127.0 (2 CH), 127.1 (2 CH), 127.5 (CH), 127.8 (CH), 128.1 (CH), 128.4 (C), 128.6 (2CH), 128.7 (2 CH), 128.9 (2 CH), 129.0 (2 CH), 129.7 (2 CH), 131.5 (C), 132.2 (CH), 133.8 (C), 138.9 (C), 139.7 (C), 141.8 (C), 142.2 (C), 147.1 (2 C), 155.9 (C)**,** 160.2 (C=O), 163.4 (C=O), 165.7 (C); HRMS calcd for $C_{45}H_{43}N_4O_4$ $[M+H]^+$: 703.3279 found: 703.3280.

(*S*)-3-(4-Aminopropyl)-1-(4-hydroxyphenethyl)-5-(naphthalen-1-yl)-4-(naphthalen-1-ylmethyl)-2-oxo-1,2,3,4-tetrahydropyrrolo[3,2-e][1,4]diazepine-7-carboxylic acid 81c

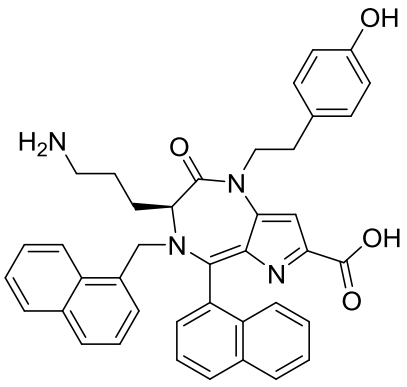

81c

The pyrrolo[3,2-e][1,4]diazepin-2-one **77b**, obtained during the Pictet-Spengler reaction with 1-naphthyladehyde on resin **76a**, was purified by reverse phase preparative HPLC

(column C, 20-35-50% MeOH, 20-35% MeOH over 9 min followed by 35% MeOH over 21 min and 35-50% MeOH over 1 min followed by 50% MeOH for 19 min, λ = 214 nm) give also as a 5:4 mixture of atropisomers of **81c** with a purity of 90% (RP-HPLC-MS, column A, 20-35% MeCN over 10 min followed by 35% MeCN over 10 min, λ = 254 nm, R*t*: 12.5 and 12.7; $[M+H]^+$: 637.1). A second purification by reverse phase preparative HPLC (column C, 25% MeCN, 35 min, λ = 254 nm) and freeze-drying from 0.1 N HCl gave a single aptomer less polar **81c** (5 mg) and a 6:4 mixture of atropisomers **81c**. (bright yellow oil, 19 mg, 0.0299 mmol, 13.8 % yield, $[\alpha]^{21}_D$ –76.0 (*c* 0.89, MeOH), HRMS calcd for $C_{40}H_{37}N_4O_4$ $[M+H]^+$: 637.2809 found: 637.2798). Aptomer less polar **81c** (bright yellow oil, 5 mg, 0.008 mmol, 3.6 % yield) was demonstrated to be of ≥ 98% purity by RP-HPLC-MS (column A, eluent 1, 40-50% MeOH over 8 min follow by 50% MeOH over 12 min, λ = 254 nm, R*t*: 13.7 and eluent 2, 10-50% MeCN over 8 min followed by 50% MeCN over 12 min, λ = 254 nm, R*t*: 11.7; $[M+H]^+$: 637.1): $[\alpha]^{21}_D$ –14.1 (*c* 0.26, MeOH); ^{1}H NMR (MeOD, 700 MHz) δ 2.11 (s, 2H), 2.33 (s, 1H), 2.51 (s, 1H), 3.00 (m, 1H), 3.04 (m, 1H), 3.37 (m, 2H), 4.30 (m, 2H), 4.60 (m, 1H), 4.80 (s, 2H), 6.62 (d, J=8.6 Hz, 2H), 7.05 (d, *J* = 10.4 Hz, 2H), 7.16 (s, 1H), 7.60 (m, 5H), 7.72 (m, 4H), 8.02 (q, *J* = 6.9 Hz, 2 H), 8.09 (d, *J* = 8.6 Hz, 1H), 8.24 (d, *J* = 8.6 Hz, 1H), 8.31 (d, *J* = 7.8 Hz, 1H); ^{13}C NMR (MeOD, 176 MHz) δ 22.6 (CH_2), 26.1 (CH_2), 29.3 (CH_2), 32.4 (CH_2), 48.4 (CH_2), 49.2 (CH_2), 60.0 (CH), 106.4 (CH), 115.0 (2 CH), 122.6 (CH), 123.5(C), 125.0 (CH), 125.2 (CH), 126.3 (2 CH), 126.8 (CH), 127.1 (2 C), 127.1 (2 CH), 128.2 (C), 128.8 (2 CH), 128.9 (CH), 129.0 (CH), 129.6 (2 CH), 130.3 (2 CH), 131.4 (2 C), 134.0 (2 C), 134.1 (2 C), 155.8 (C), 160.3 (C), 162.9 (C=O), 164.2 (C=O); HRMS calcd for $C_{40}H_{37}N_4O_4$ $[M+H]^+$: 637.2809 found: 637.2797.

(*S*)-3-(4-Aminopropyl)-1-(4-hydroxyphenethyl)-5-(naphthalen-2-yl)-4-(naphthalen-2-ylmethyl)-2-oxo-1,2,3,4-tetrahydropyrrolo[3,2-e][1,4]diazepine-7-carboxylic acid 81d

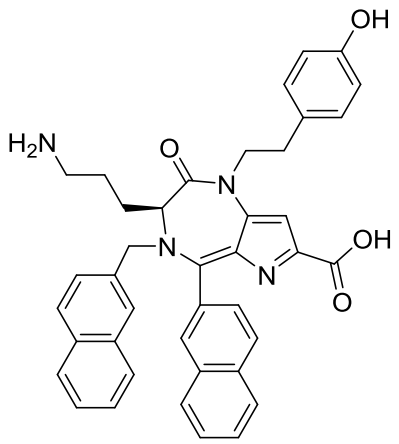

81d

The pyrrolo[3,2-e][1,4]diazepin-2-one **77c**, obtained during the Pictet-Spengler reaction with 2-naphthyladehyde on resin **76a**, was purified by reverse phase preparative HPLC (column C, 20-80% MeOH over 36 min, followed by 80% MeOH over 14 min, λ = 254 nm) give also as a 5:2 mixture of atropisomers of **81d** with a purity of 55% (RP-HPLC-MS, column A, 30% MeCN, 20 min, λ = 254 nm, R*t*: 10.2 and 12.3; $[M+H]^+$: 637.1). A second purification by reverse phase preparative HPLC (column C, 30% MeCN, 50 min, λ = 254 nm) and freeze-drying from 0.1N HCl gave 7 mg of a single atropisomer less polar **81d**, and a 5 mg of 1:1 mix of atropisomers **81d** (bright yellow oil, 0.0079 mmol, 4.2% yield, $[\alpha]^{21}_D$ –110.7 (*c* 0.25, MeOH), HRMS calcd for $C_{40}H_{37}N_4O_4$ $[M+H]^+$:637.28093 found: 637.27998)**.** Aptomer less polar **81d**: (7 mg, 0.011 mmol, 5.9% yield, ≥ 98% purity, RP-HPLC-MS, column A, 40-50% MeOH over 8 min followed by 50% MeOH over 12 min, λ = 254 nm, (R*t*: 12.5; $[M+H]^+$: 637.1) : $[\alpha]^{21}_D$ –95.3 (*c* 0.27, MeOH); ^{1}H NMR (MeOD, 700 MHz) δ 2.04 (s, 1H), 2.11 (s, 1H), 2.33 (s, 1H), 2.45 (s,

1H), 2.91 (m, 1H), 2.97 (m, 1H), 3.26 (t, *J* = 8.0 Hz, 2H), 4.16 (m, 2H), 4.45 (s, 2H), 4.66 (m, 1H), 6.43 (d, *J* = 8.1 Hz, 2H), 6.87 (d, J= 9.6 Hz, 2H), 7.16 (s, 1H), 7.58 (m, 2H), 7.67 (d, *J* = 7.8 Hz, 1H), 7.72 (m, 2H), 7.78 (t, *J* = 7.6 Hz, 1H), 7.97 (m, 2H), 8.07 (d, *J* = 9.7 Hz, 1H), 8.09 (d, *J* = 7.2 Hz, 1H), 8.09 (s, 1H), 8.17 (d, *J* = 9.0 Hz, 1H), 8.24 (d, *J* = 9.0 Hz, 1H), 8.34 (s, 1H); ^{13}C NMR (MeOD, 176 MHz) δ 22.3 (CH_2), 25.6 (CH_2), 32.0 (CH_2), 46.8 (CH_2), 48.6 (CH_2), 51.0 (CH_2), 59.8 (CH), 106.7 (CH), 114.7 (2 CH), 119.9 (C), 126.2 (CH), 126.3 (CH), 126.5 (CH), 126.8 (CH), 127.4 (CH), 127.5 (2 CH), 127.7 (CH), 127.8 (CH), 128.1 (C), 128.5 (2 C), 128.8 (CH), 129.1 (CH), 129.4 (C), 129.5 (CH), 129.6 (2 CH), 129.7 (CH), 132.7 (C), 133.3 (C), 133.6 (C), 134.3 (C), 136.3 (2 C), 155.6 (C), 160.5 (C), 163.3 (C=O), 164.6 (C=O); HRMS calcd for $C_{40}H_{37}N_4O_4$ $[M+H]^+$:637.2809 found: 637.2800.

Annexe 6: Spectres RMN des pyrrolo[3,2-*e*][1,4]diazepin-2-ones *N*-substitués

(*S*)-5-([1,1'-Biphenyl]-4-yl)-4-([1,1'-biphenyl]-4-ylmethyl)-3-(3-aminopropyl)-1-(4-hydroxyphenethyl)-2-oxo-1,2,3,4-tetrahydropyrrolo[3,2-e][1,4]diazepine-7-carboxylic acid 81a

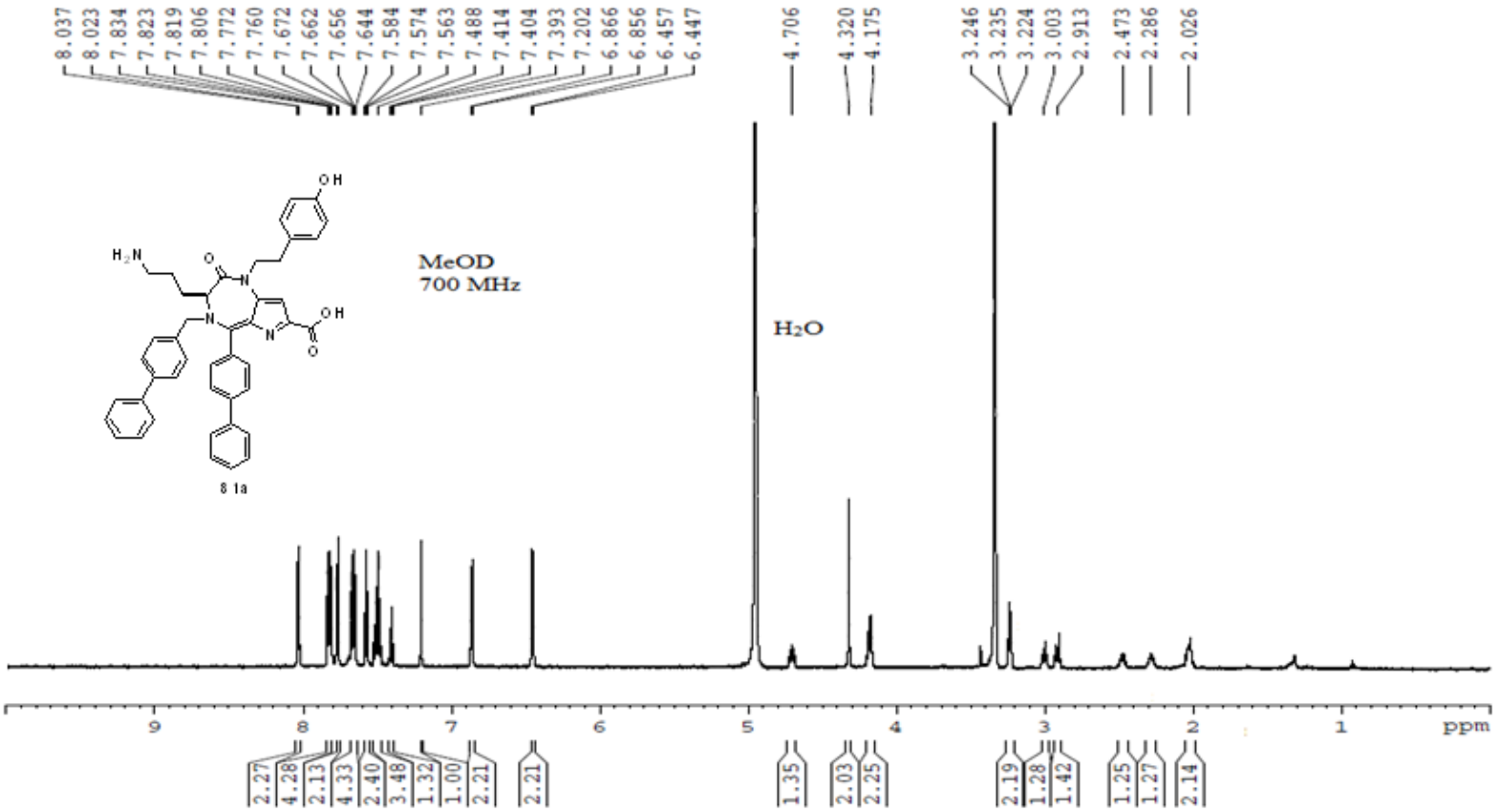

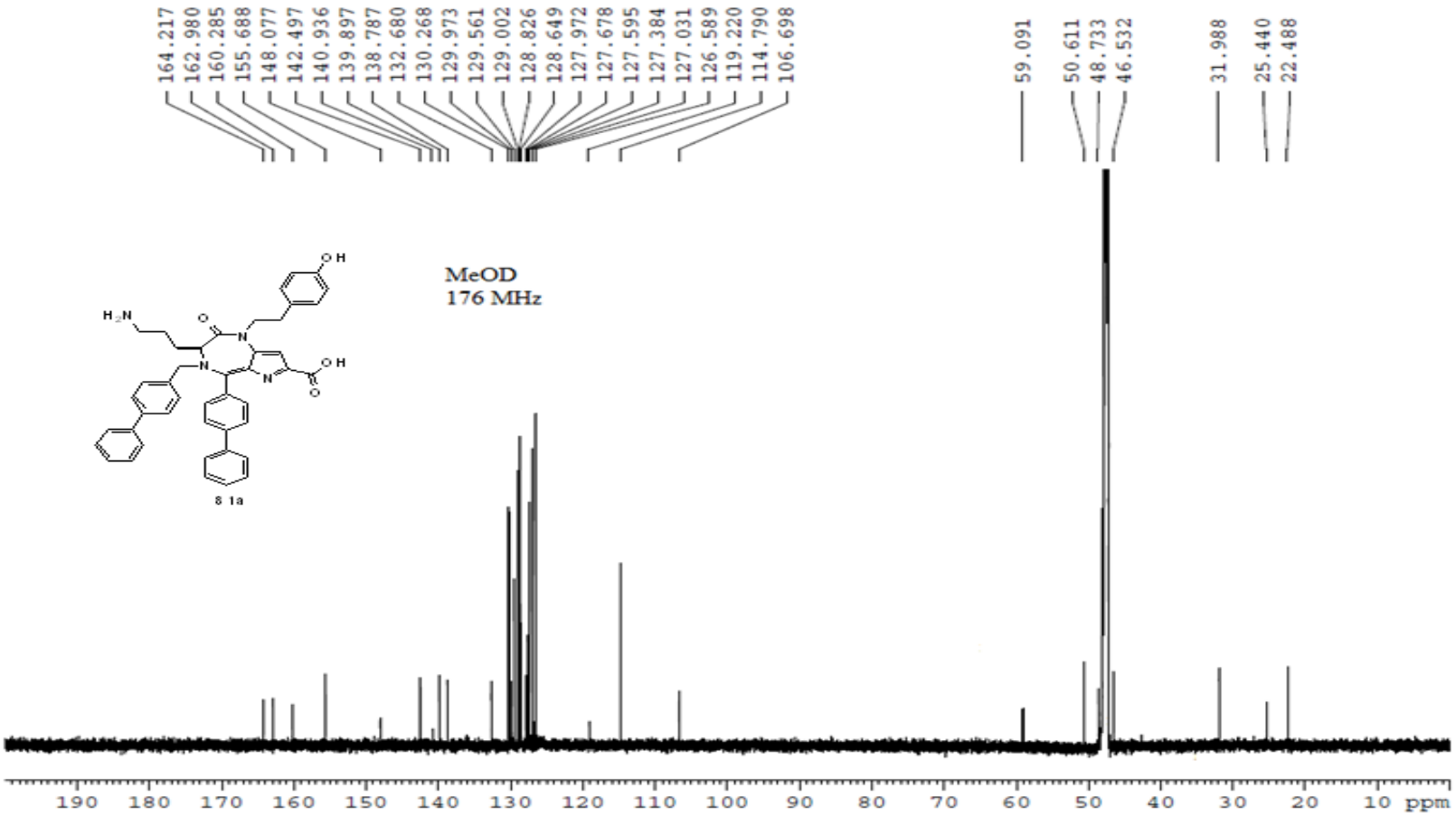
164.217
162.980
160.285
155.688
148.077
142.497
140.936
139.897
138.787
132.680
130.268
129.973
129.561
129.002
128.826
128.649
127.972
127.678
127.595
127.384
127.031
126.589
119.220
114.790
106.698
59.091
50.611
48.733
46.532
31.988
25.440
22.488
MeOD
176 MHz
8 1a
190 180 170 160 150 140 130 120 110 100 90 80 70 60 50 40 30 20 10 ppm

(S)-5-([1,1'-biphenyl]-4-yl)-4-([1,1'-biphenyl]-4-ylmethyl)-3-(3-aminopropyl)-1-(4-hydroxyphenethyl)-2-oxo-1,2,3,4-hexahydropyrrolo[3,2-e][1,4]diazepine-7-carboxylic acid 81b

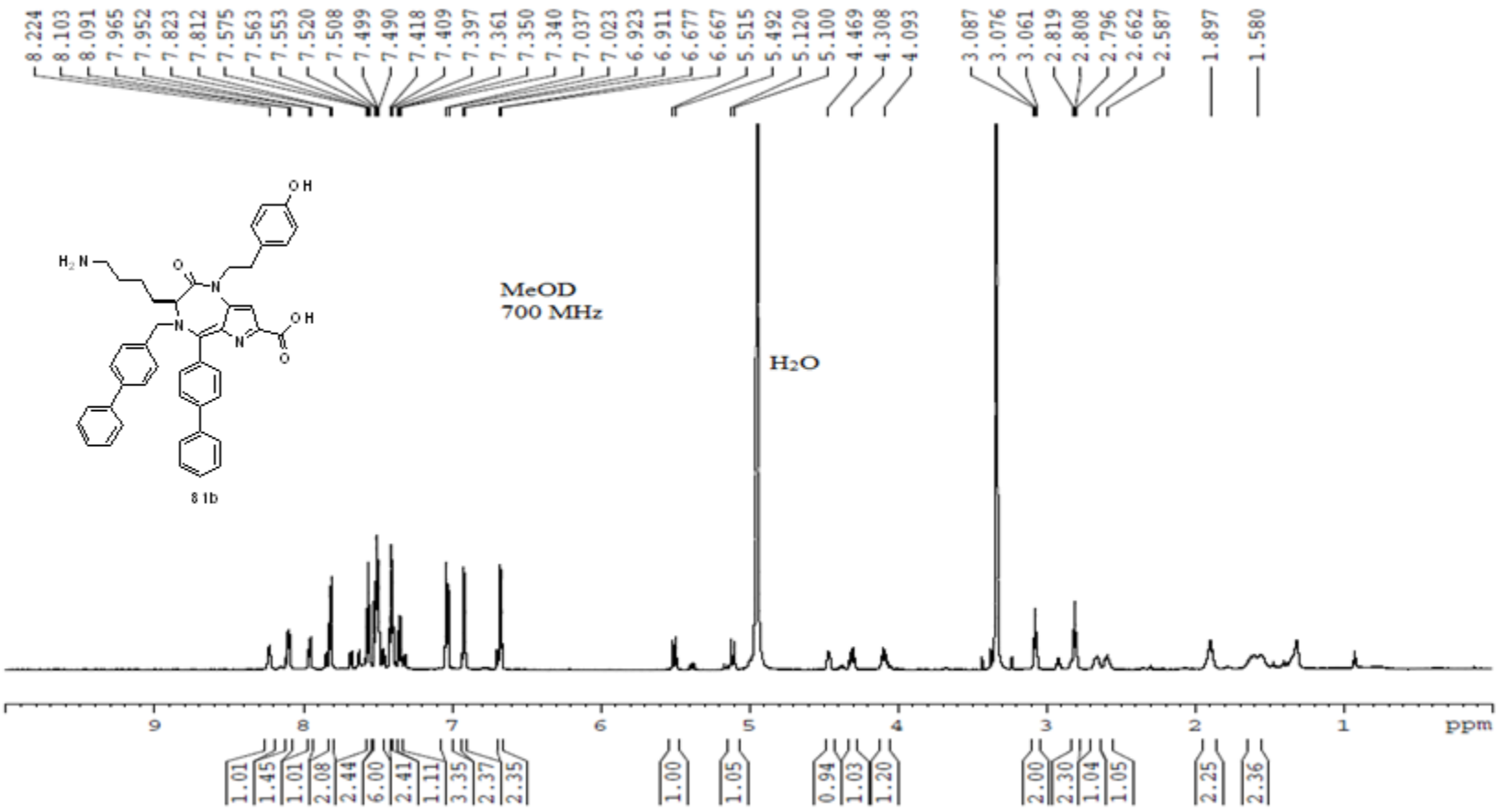

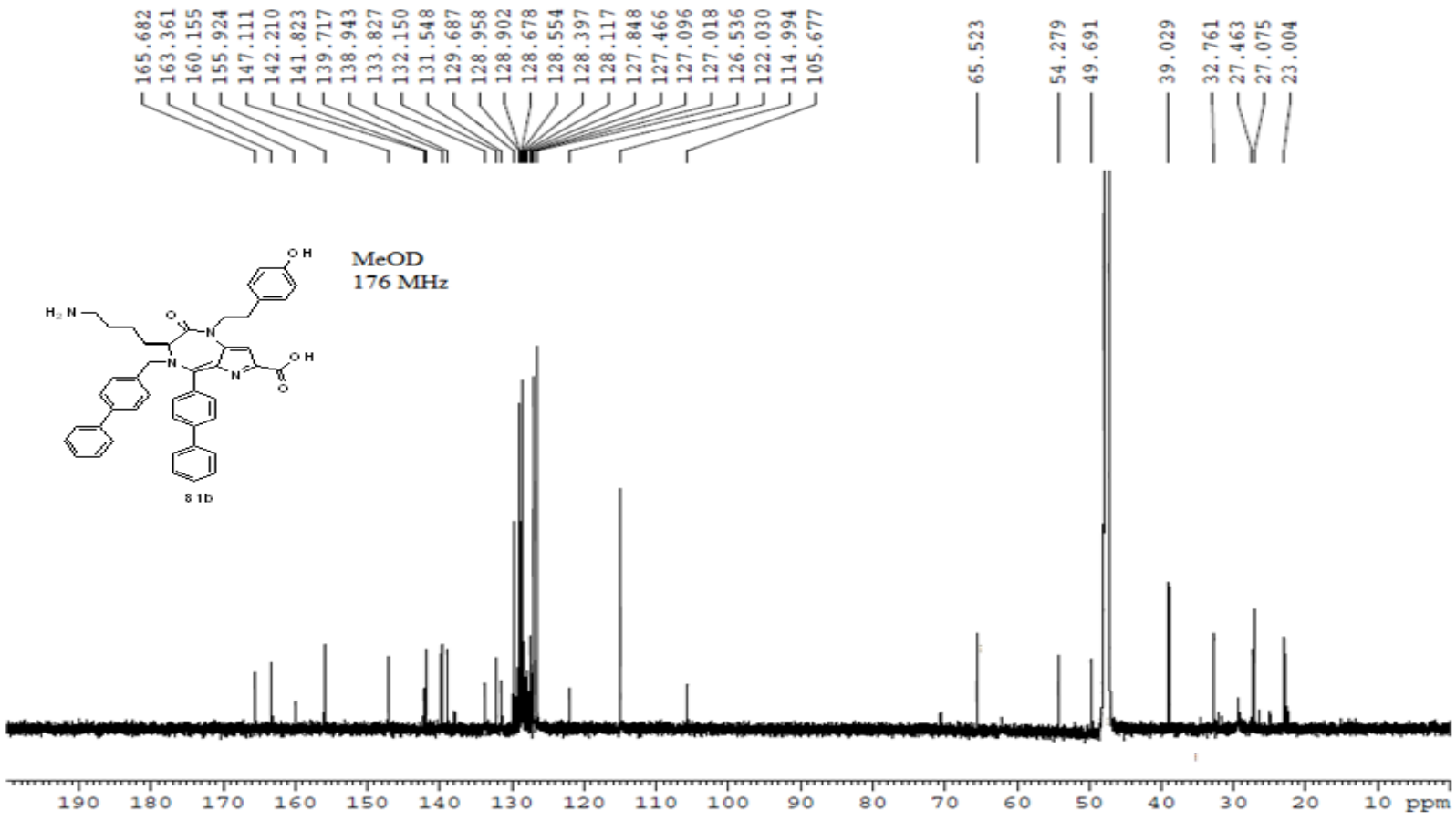
165.682
163.361
160.155
155.924
147.111
142.210
141.823
139.717
138.943
133.827
132.150
131.548
129.687
128.958
128.902
128.678
128.554
128.397
128.117
127.848
127.466
127.096
127.018
126.536
122.030
114.994
105.677
65.523
54.279
49.691
39.029
32.761
27.463
27.075
23.004
MeOD
176 MHz
81b
190 180 170 160 150 140 130 120 110 100 90 80 70 60 50 40 30 20 10 ppm

(S)-3-(4-aminopropyl)-1-(4-hydroxyphenethyl)-5-(naphthalen-1-yl)-4-(naphthalen-1-ylmethyl)-2-oxo-1,2,3,4-tetrahydropyrrolo[3,2-e][1,4]diazepine-7-carboxylic acid 81c

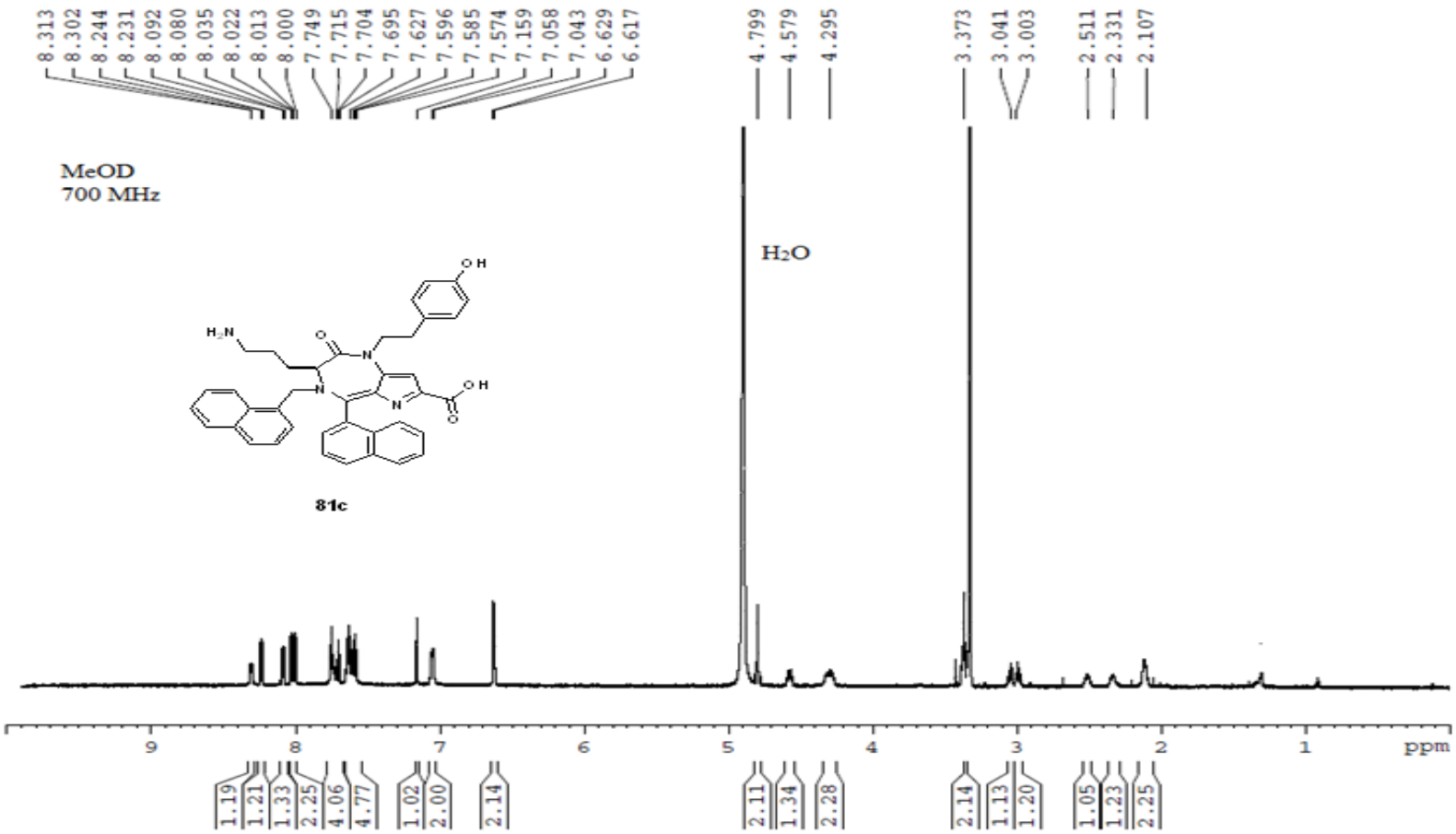

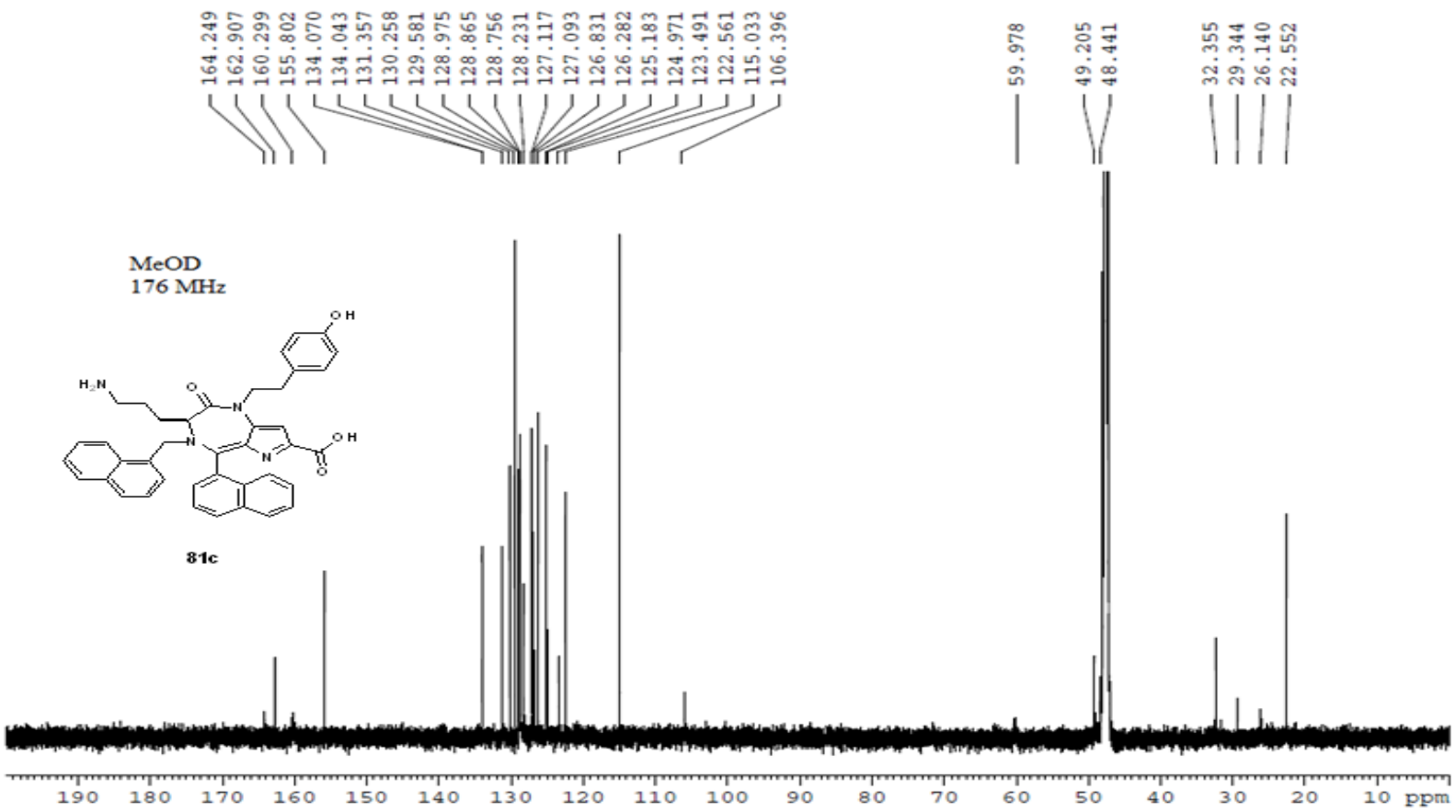
164.249
162.907
160.299
155.802
134.070
134.043
131.357
130.258
129.581
128.975
128.865
128.756
128.231
127.117
127.093
126.831
126.282
125.183
124.971
123.491
122.561
115.033
106.396
59.978
49.205
48.441
32.355
29.344
26.140
22.552
MeOD
176 MHz
81c
190 180 170 160 150 140 130 120 110 100 90 80 70 60 50 40 30 20 10 ppm

(S) -3-(4-aminopropyl)-1-(4-hydroxyphenethyl)-5-(naphthalen-2-yl)-4-(naphthalen-2-ylmethyl)-2-oxo-1,2,3,4-tetrahydropyrrolo[3,2-e][1,4]diazepine-7-carboxylic acid 81d

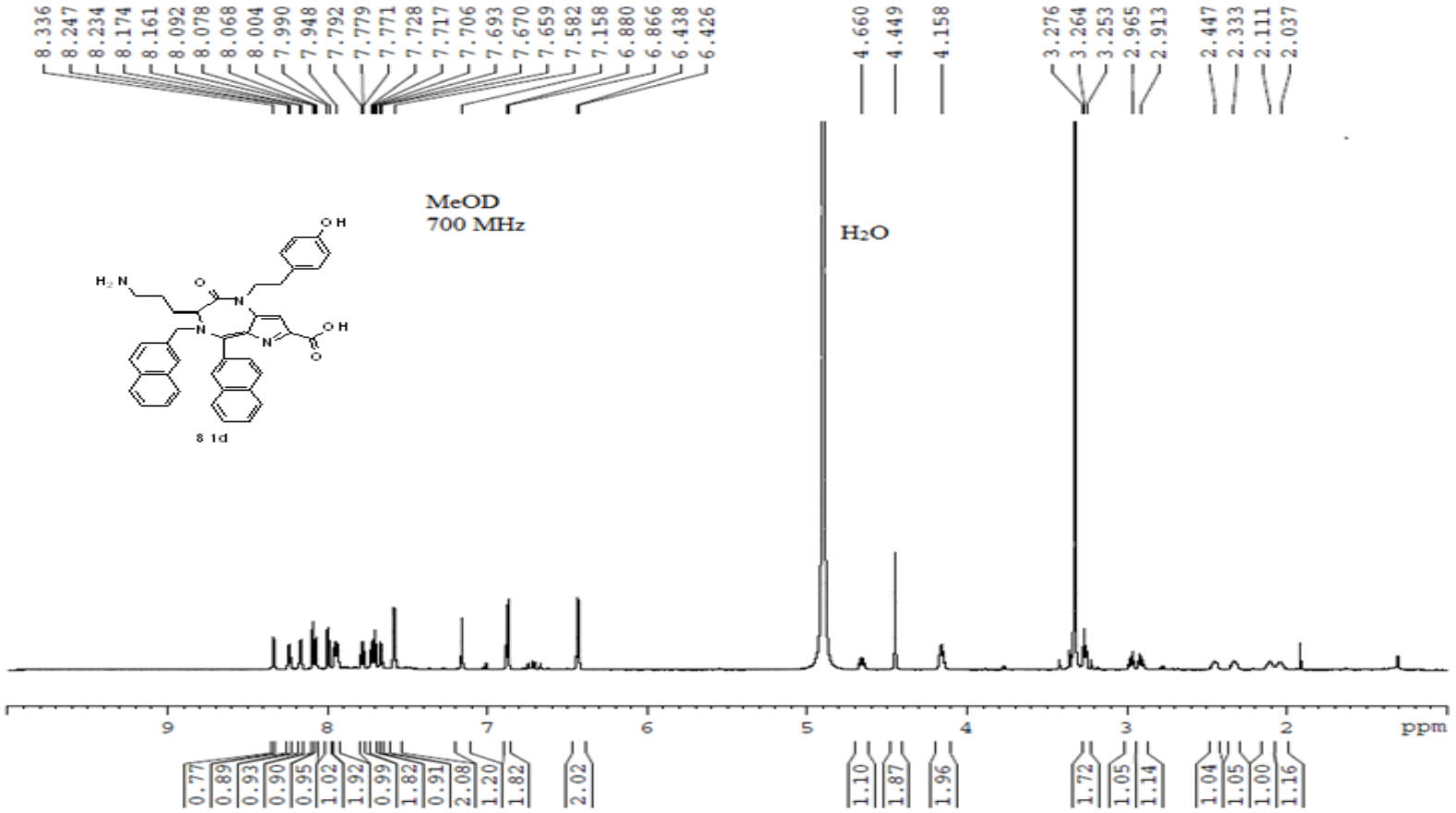

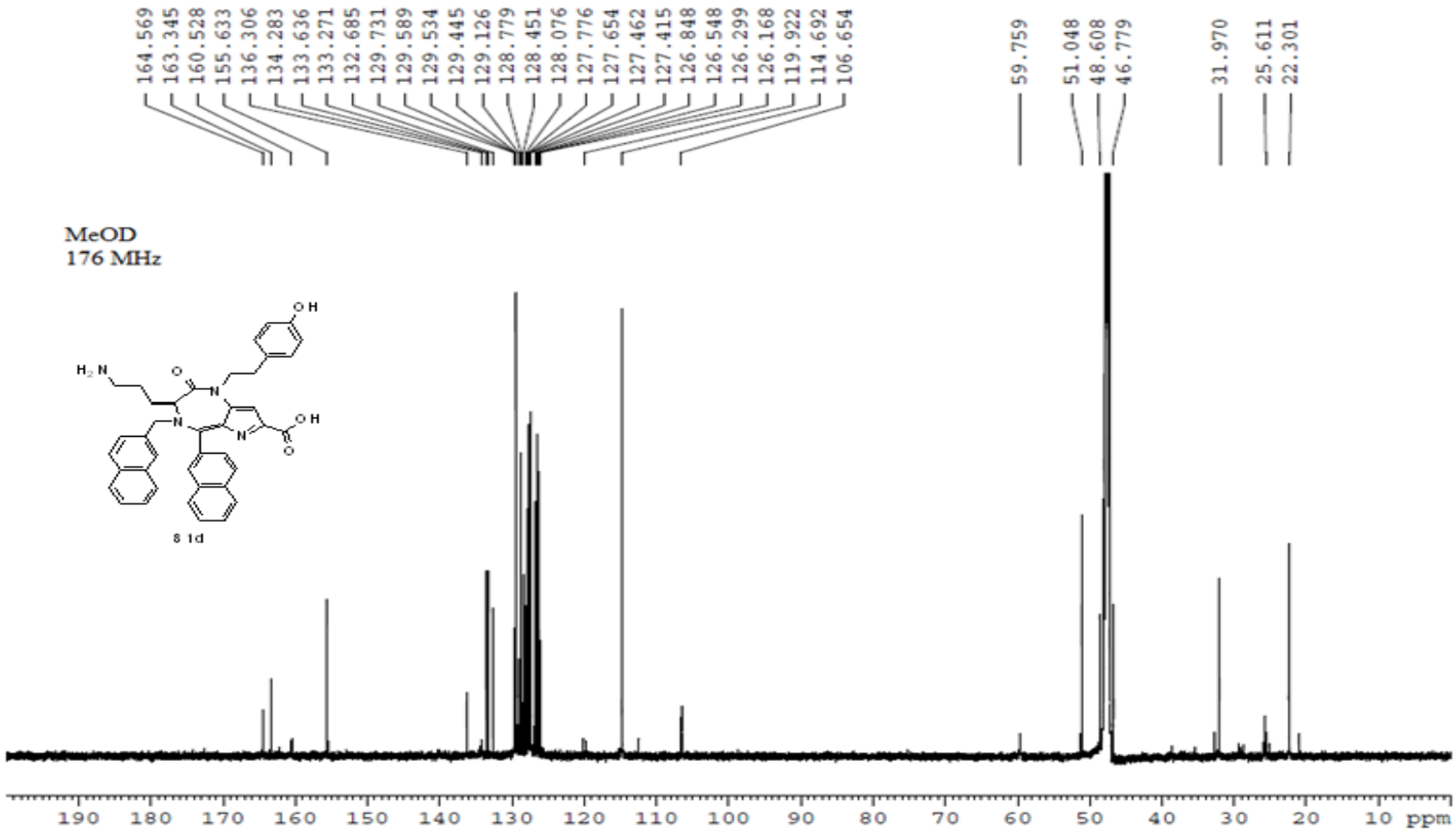
164.569
163.345
160.528
155.633
136.306
134.283
133.636
133.271
132.685
129.731
129.589
129.534
129.445
129.126
128.779
128.451
128.076
127.776
127.654
127.462
127.415
126.848
126.548
126.299
126.168
119.922
114.692
106.654
59.759
51.048
48.608
46.779
31.970
25.611
22.301
MeOD
176 MHz
8 1d
190 180 170 160 150 140 130 120 110 100 90 80 70 60 50 40 30 20 10 ppm